AN INVESTIGATION INTO THE CEREBRAL AUTOREGULATORY UPPER LIMIT: NORMAL CONTROL MECHANISMS AND CHANGES ASSOCIATED WITH AGEING

by

EMMA LOUISE THOMPSON

Student ID: 874535

A thesis submitted to the University of Birmingham for the degree of DOCTOR OF PHILOSOPHY

Supervisors: Professor Janice Marshall and Dr Andrew Coney
Institute of Cardiovascular Sciences
College of Medical and Dental Sciences
University of Birmingham
October 2017

ABSTRACT

Cerebral autoregulation (CA) is the process by which cerebral arterial vessels constrict or dilate, in order to maintain cerebral blood flow (CBF) in the face of changes in arterial blood pressure. This thesis aimed to investigate the mechanisms that normally control CA, with specific reference to the upper limit (UL); the point at which autoregulatory vasoconstriction is overcome. The UL is associated with an increase in CBF, which can potentially cause damaging cerebrovascular hyperperfusion. Ageing is associated with a general decrease in regulatory mechanisms, and an increased risk of stroke. Therefore we sought to assess whether changes in CA at the UL may predispose older rats to haemorrhagic stroke. We assessed CA by infusion of phenylephrine to increase ABP in an anaesthetised rat model, whilst measuring CBF to enable identification of the UL. This protocol was repeated in young (6-8 weeks) and old (12-15 months) rats in control conditions, or during removal of regulatory inputs. The UL in young, control rats was 168±4mmHg. Removal of nitric oxide-mediated dilatation and sympathetically-mediated vasoconstriction increased the UL. In old rats, the increase in UL was even greater. Thus we propose a new working hypothesis to explain the control of CA and the UL.

DEDICATION

I would like to dedicate this thesis to a number of people. Firstly, to my wonderful family; my parents Neil and Julie, my sister Ellen, my grandparents Pam and Malcolm, my great aunt Joyce, and my extended family, who have all supported me throughout my time at university. Secondly, to my kind and patient fiancé, Chris, who has been there for me during this challenging and amazing experience. And finally in loving memory of my grandparents Jean and Brian, who always believed in me.

ACKNOWLEDGMENTS

Firstly, I wish to acknowledge my supervisors Professor Janice Marshall, and Dr Andrew Coney, for their invaluable advice, patience, encouragement, expertise, experimental abilities, and vast knowledge. Their help and support has been instrumental throughout my PhD, and I want to express my sincere and heartfelt gratitude for their part in such a rewarding experience.

Secondly I want to acknowledge my colleagues, who have become dear friends; Professor Prem Kumar, Dr Clare Ray, Dr Andrew Holmes and Dr Clare Box. Their kindness and friendship throughout my PhD has kept me going during difficult times, brought me happiness and laughter, and created memories that will last me a lifetime.

I would also like to acknowledge Dave Westwood, for his excellent technical support during my experiments.

Finally, I would like to acknowledge the British Heart Foundation for their generous funding of this PhD. I would also like to thank the Physiological Society, the College of Medical and Dental Sciences overseas travel fund, and the Elizabeth Watson Davidson award, for travel grants that enabled me to attend national and international conferences to present my work.

TABLE OF CONTENTS

LIST OF ILLUSTRATIONS AND TABLES

Chapter 1: Introduction

Chapter 2: Methods

Chapter 3: Method Development

Chapter 4: Effect of ageing on CA and the UL

Chapter 5: Role of NO in CA and the UL

Chapter 6: Role of autonomic innervation in CA and the UL

Chapter 7: General discussion

LIST OF MAIN DEFINITIONS AND ABBREVIATIONS

7-NI – 7-Nitroindazole

ABP – Arterial blood pressure

ACA – Anterior cerebral artery

ACh – Acetylcholine

BA – Basilar artery

BBB – Blood brain barrier

CA – Cerebral autoregulation

CBF – Cerebral blood flow

CoBF – Cortical blood flow

CVR – Cerebral vascular resistance

HR – Heart rate

LL – Lower limit

L-NAME – N_w-Nitro-L-arginine methyl ester hydrochloride

MCA(v) – Middle cerebral artery (velocity)

NO – Nitric oxide

NOS – Nitric oxide synthase

NPY – Neuropeptide Y

$PaCO_2$ – Partial pressure of carbon dioxide in arterial blood

PaO_2 – Partial pressure of oxygen in arterial blood

PCA – Posterior cerebral artery

PE – (R)-(-)-Phenylephrine hydrochloride

PPG – Pterygopalatine ganglia

RCF – Red cell flux

SCG – Sympathetic cervical ganglia

SMTC – S-Methyl-L-Thiocitrulline acetate

SympX – Sympathectomy

UL – Upper limit

VIP – Vasoactive intestinal polypeptide

CHAPTER 1: GENERAL INTRODUCTION

Cerebral autoregulation (CA) is the term used to describe the ability of the cerebral vasculature to maintain constant blood flow in the face of changes in arterial blood pressure (ABP). This concept implies that as ABP rises, cerebral arterial vessels constrict, or show an increase in cerebral vascular resistance, and *vice versa*.

The mechanisms that underlie CA, particularly in response to rises in ABP, and the factors that determine the upper limit (UL) of autoregulation, are not only important, but incompletely understood. Investigating the interrelation between the factors that might contribute to CA, and the effects of ageing upon it, were the main aims of the present study. Therefore, the sections that follow consider the various methods that are used to record cerebral blood flow and monitor cerebral vascular responses, and the various factors that are considered to contribute to regulation of cerebral blood flow, with particular emphasis on those that might contribute to CA and the UL.

1.1 The Cerebral Circulation

The brain receives its constant blood supply via the internal carotid and vertebro-basilar arteries. These arteries join to form the Circle of Willis, a collateral blood flow system first described by Thomas Willis in 1664 (see Figure 1a). The Circle of Willis gives rise to three major pairs of cerebral arteries supplying the cerebral hemispheres; the anterior, middle and posterior cerebral arteries (ACA/MCA/PCA), as shown in Figure 1b.

From the major cerebral arteries, pial arteries branch off to supply the surface of the brain. Branches of the pial arteries then form penetrating arteries, arterioles and eventually capillaries, supplying the brain internally (see Figure 2, also reviewed by Cipolla, 2009).

Despite accounting for only ~2% of total body weight, the brain is highly perfused, accounting for 15-20% of cardiac output at rest. This reflects its dense vascularity and the high metabolic demand of the brain; it has a low capacity for glycogen storage, and is dependent upon oxidative energy production. In addition, cerebral blood flow (CBF) must increase in discrete brain regions to meet the metabolic demand associated with increased neuronal activity, by a process known as flow-metabolism coupling (also known as neurovascular coupling, discussed by Filosa & Iddings, 2013). Any compromise in cerebral blood supply leaves brain tissue vulnerable to damage. Loss of consciousness can occur within seconds of CBF stopping, and any longer leads to permanent neuronal damage (Cipolla, 2009).

Although the brain requires a high and constant blood flow, which must be able to adapt to changing demands, the fixed volume of the rigid cranium in which the brain is contained restricts changes in CBF. As defined by the Monro-Kellie hypothesis, if blood flow increases locally, this must be matched by an increased venous drainage or a reduction in the space taken up by cerebrospinal fluid (CSF), in order to avoid an increased intracranial pressure (ICP) (Mokri, 2001).

For this reason, changes in ABP must also be buffered against in the cerebral circulation. If the increases in ABP that occur throughout a typical day, for example during exercise or periods of stress, led to increases in CBF with no regulation, the result could be a haemorrhagic stroke and/or a damaging increase in ICP. However, it is widely agreed that CBF is controlled, across a wide range of physiological ABP values, by the process of CA. This concept requires that if ABP increases, CBF remains relatively constant until the UL of autoregulation is reached, the point at which the regulatory mechanisms are overcome (see 1.3.1).

1.2 Methods for Investigation of Cerebral Autoregulation

Measurement of CBF and assessment of CA can be performed in numerous ways. There are limitations associated with many of them, and there are reasons to argue that the method chosen may influence the results obtained. Thus, the various methodologies that have been most widely used are considered below. It is important to consider these methods here, as they are referred to when discussing the current literature on the regulation of CBF in section 1.3.

1.2.1 Cerebral blood flow measurements in humans

The first method that allowed quantitative measurement of CBF in man was the Kety-Schmidt method, developed in 1945. The method works on the Fick principle; the amount of a diffusible tracer substance carried in the blood to an organ of interest i.e. the brain, is equal to the product of blood flow to the organ and the arterio-venous concentration difference, within a defined time. The original tracer used was nitrous oxide, although many inert tracers have been applied since then. The gas is inhaled in low concentrations for 10 minutes and serial arterial and venous blood samples are taken throughout. This allows saturation curves (concentration of tracer against time) to be plotted and global CBF to be determined mathematically (Kety & Schmidt, 1948). Alternatively, tracer administration can be stopped and clearance curves can be generated, also allowing determination of gross CBF in the region perfused by the vessels used for sampling.

Radioactively labelled tracers have also been used; these are typically dissolved in saline and injected intra-arterially (via the carotid artery), but can also be inhaled. Arterio-venous sampling can then be carried out as described above, or alternatively the radioactivity can be measured extracranially by one or more scintillation detectors, which may be placed, for

example, on either hemisphere, to allow a more regional assessment of cerebral tissue perfusion (Hoedt-Rasmussen *et al*, 1966).

Although the CBF values determined by this methodology can be global or more localised, the volume and area being investigated is difficult to define with accuracy. There is also potential for contamination by extracerebral blood in the venous samples, or radioactivity in extracerebral tissues. Further, these techniques require fairly invasive cannulations if arterio-venous sampling is done. Another limitation of tracer methods is that the calculations assume complete diffusibility of the tracer, which may not have been achieved, and assume steady-state CBF over the time of measurement, even though there is no way of checking whether this is so. Generally, only one measurement is made under any given condition. Nevertheless, multiple measurements can be made within the same individual over time or under different conditions (Madsen *et al*, 1993). The technique can also be applied to laboratory animals.

More recent technological advancements have brought about the use of functional imaging techniques such as positron emission tomography (PET). The principle of this technique is similar to the tracer methods discussed above, as it uses a radionuclide attached to a biologically active molecule (inhaled or injected) to assess cerebral tissue perfusion. However 3D images can also be produced using a complementary technique such as magnetic resonance imaging (MRI), in order to assess the concentration of the molecule via the detected emissions, and allow more precise localisation. The tracer may be radiolabelled water for detection of regional CBF (rCBF), or radiolabelled glucose/glucose analogues which can be used to indicate cerebral O_2 or glucose metabolism, and reflect coupling between CBF and metabolism (Baron *et al*, 1982).

fMRI (arterial spin labelling) is a specific MRI imaging technique which, rather than giving a labelled tracer, uses a magnetic field to excite the protons present in water molecules in tissues, causing them to spin and generate a signal based on the relaxation of this spin (Singer & Crooks, 1983). The water in arterial blood can therefore be used as an endogenous tracer, by exciting the protons in the water in blood as it enters the brain. As the labelled water flows into the brain and mixes with the non-labelled blood already present, it changes the contrast of the images based on the relaxation time of the protons. These data are then used in mathematical models to calculate a quantitative cerebral tissue perfusion value, based on the changes in the water concentration in the region of the brain being imaged. The short half-life of the labelled water means that the measurement can be repeated multiple times, and has been applied to both humans and laboratory animals including rats to assess CBF (Muir *et al*, 2014). Phase contrast MRI is another MRI technique that can be used specifically to measure blood flow velocity. For example, Geurts *et al* (2018) have used 2D phase contrast imaging MRI to assess cerebrovascular reactivity to increases in end tidal PCO_2, in the MCA and penetrating arteries in the semioval centre and basal ganglia.

Both PET and MRI techniques tend provide an index of CBF within a specific brain region, rather than simply an assessment of global CBF. This is important because cerebrovascular reactivity or CA may vary between brain regions.

Another commonly used method for assessment of CBF in humans is the Transcranial Doppler (TCD) technique, which measures blood flow velocity at the macrovascular level. TCD probes emit ultrasonic waves at a particular frequency (usually 2MHz). Flow of blood in the path of this wave causes a phase shift, changing its frequency, and this change correlates with blood flow velocity. To be valid, the TCD probe must be positioned at a specific angle for detection of blood flow in the cerebral artery of interest, typically the MCA. However, the

Duplex Doppler technique, which combines traditional and Doppler ultrasound, can also be used to measure velocity in the ICA, PCA, and venous vessels such as the internal jugular vein (Ogoh *et al*, 2011). Doppler probes must be placed in an appropriate position where the skull bone is thinner, known as the insonation window, in order to allow more of the ultrasound wave to be transmitted. Drawbacks of using TCD include the assumption that diameter of the insonated vessel remains constant. This can be a problem because TCD measures velocity rather than flow (Markus, 1999), and velocity does not change proportionally with flow if the diameter changes. In fact, a comparative study between TCD and a radioactive tracer clearance method showed poor correlation for basal CBF, but a strong correlation for cerebral reactivity to a hypercapnic stimulus (Bishop *et al*, 1986). However, diameter can be measured simultaneously using the Duplex Doppler technique, which therefore enables a measurement of flow, rather than velocity (Ogoh *et al*, 2011).

Near Infrared Spectroscopy (NIRS) is becoming more widely used to measure CBF. The technique is based on the fact that the transmission and absorbance of near infrared light in human tissues is influenced by the concentration of haemoglobin (Hb) and its oxygenation status. Cerebral oxygenation can thus be taken as an indirect indication of CBF (Jobsis, 1977). Alternatively, a brief inhalation of 100% oxygen to produce a sudden increase in oxygenated haemoglobin (HbO_2) can be used as a tracer as described above, allowing a more accurate CBF calculation (Owen-Reece *et al*, 1996). The disadvantage of NIRS is that its use is restricted to superficial regions of brain tissue. The probe is usually placed on the forehead, over the frontal cortex. The probe contains fibre optic bundles, through which near infrared light is emitted in pulses. The transmitted light is then detected and passed via a photomultiplier tube, to be compared with the emitted light. The data are analysed to detect

the different transmission by Hb and HbO_2. Assuming a constant haematocrit (HCT), the total Hb signal can be taken to reflect cerebral blood volume (CBV) (Wagner *et al*, 2011).

The more recently developed imaging techniques tend to be less invasive than the tracer methods and technically easier, with better temporal resolution. However they all provide indications or indices of cerebral perfusion, or blood flow velocity, rather than direct measurements of flow. Therefore, even though studies conducted in humans may be more clinically relevant, the use of animals allows for application of more invasive techniques under anaesthetic, which can provide more direct measurements of CBF as outlined below.

1.2.2 CBF measurement in animals

1.2.2.1 Tracer techniques

The saturation and clearance tracer techniques described above, can be applied to laboratory animals as well as humans. The major difference is that in an animal model it is possible to use invasive intracerebral probes that are precisely placed at a specific locus in the brain, by the experimenter. For example, platinum electrodes polarised by hydrogen are a commonly used technique in animals, the resultant signal correlating with the concentration of the tracer in a known sphere of brain tissue, and therefore representing local CBF at the microvascular level by Fick's principle (see Sadoshima *et al*, 1985). Further, chronic implantation of probes allows multiple studies to be repeated within the same animal without anaesthetic. However, a limitation of such techniques is the invasiveness of the initial surgery. This can cause trauma-associated phenomena such as cortical spreading depression, which is associated with prolonged constriction or dilatation in cortical parenchymal arterioles, and can therefore affect CBF values (Brennan *et al*, 2007).

Administration of radiolabelled or fluorescently-labelled microspheres is another widely used technique. A bolus of microspheres is given intra-arterially and they circulate until, due to their diameter (15μm), they become trapped within small arterioles and capillaries. The concentration of microspheres, indicated by the level of detected radioactivity or fluorescence, is therefore indicative of the blood flow supplying that region. In order to use this technique, blood samples are withdrawn from an arterial vessel at a known rate, before and during administration and distribution of the microspheres, so as to generate reference blood flow and radioactivity values, which the region of interest within the brain can then be compared to. This technique allows for multiple, instantaneous measurements to be taken under different conditions, by using a succession of microspheres labelled with different isotopes or fluorescent labels. Therefore the number of measurements possible depends on the ability to discriminate between different radioactive or fluorescent labels, which is generally limited to 3-4 radioactive labels, and 4-5 fluorescent labels (Deveci & Egginton, 1999).

This technique also allows for assessment of rCBF; the animals are euthanized, and the brain removed and dissected into different anatomical regions, such that the radioactivity can be counted and compared in different brain tissue regions (Gross *et al*, 1979). The limitations of this technique include the fact that invasive catheterisation of the left atrium or ventricle is generally used as the means of delivering the microspheres. Also, the number of microspheres that need to be given is relatively large, because the amount of trapped radioactive label must be large enough to allow accurate measurement, and therefore allow accurate determination of rCBF measurements. This is more likely to be a problem in smaller laboratory animals, which are more likely to suffer side effects of blocked microvessels. However the technique has been used successfully in rats; for example Hoffman *et al* (1991) measured regional cerebral and spinal blood flow in rats using radioactive microspheres. The technique also rests on a

number of assumptions; that the microsphere solution has been thoroughly mixed before administration, that complete mixing occurs once in the blood, that all the microspheres become trapped in the capillaries during the first pass through the circulation, and therefore that the radioactivity or fluorescence levels are directly proportional to blood flow.

1.2.2.2 Measuring flow in a supplying artery

Whilst the saturation and microsphere techniques described above (1.2.2.1) directly reflect tissue perfusion, they are limited by the fact that the measurements made of CBF are not continuous. When investigating, for example, the gross CBF response to a gradual increase in ABP, a method that allows continuous measurement of CBF is more suitable, such as the TCD technique used in humans. In animals, this can be achieved by isolating a major vessel supplying the brain, such as a carotid or vertebral artery, and using vascular flowmetry. Transonic flow probes have been used previously in our laboratory to assess CBF at the level of the common carotid artery (Omar & Marshall, 2010a), and offer direct volumetric blood flow measurements. The vessel rests in a V-shaped trough between two ultrasonic transducers and an acoustic reflector. An ultrasonic wave passes through the vessel and the transit time taken for the wave to travel between the two transducers is calculated for both upstream and downstream directions, giving a measurement of actual volume flow. Unlike TCD used in humans which only measures blood flow velocity, Transonic flow probes use wide beam illumination, which accounts for both velocity of blood flow, and also the length of the measurement path i.e. vessel diameter. The output is therefore given in $ml \cdot min^{-1}$ and can be applied to the major arteries supplying the brain, giving an excellent index of CBF (see 2.3.1 for more information).

1.2.2.3 Laser Doppler and Laser Speckle techniques

Another technique, which provides a direct and continuous recording of perfusion in the cerebral cortex, is Laser Doppler flowmetry. This works by applying a laser beam to the tissue of interest and detecting the reflected light using a photodetector. The reflected light is scattered by red blood cells moving within the vessels in the tissue, causing a Doppler shift (change in wavelength). Both the fraction of light shifted (representing concentration of red blood cells) and the frequency of the shift (proportional to the blood flow velocity) can be detected, and the product of these two is recorded as red cell flux (RCF) on the principle of mean transit time described above (Perimed AB, Laser Doppler Monitoring guide, 2015). Providing that HCT is constant, RCF is proportional to blood flow. This method involves using a small probe which is carefully placed on the surface of a tissue, for example on the surface of the cerebral cortex, to monitor local microcirculatory tissue perfusion, as opposed to global or regional blood flow. A disadvantage is that RCF is recorded only in a hemisphere of ~0.8mm diameter, and the output cannot be calibrated to give a volume flow per unit time, but is given as a voltage which is standardised against a calibration signal equivalent to a set flow rate i.e. 10 $ml \cdot min^{-1}$. Further, the laser beam penetrates to a depth of only ~1mm, therefore thinning of the cranium or a cranial window is required before it can be used in assessment of cortical blood flow. This method was used by Euser & Cipolla (2007) to assess CA during pregnancy in anaesthetised rats, and was adopted for some of the experiments in the present study.

Laser Speckle imaging is a newer development of this technique, and is also utilised for measurement of cortical blood flow. It involves using a laser source to illuminate the tissue, while a camera captures the resulting speckle pattern. This pattern is varied by movement of particles i.e. red blood cells in the tissue, and the level of this variation can be quantified to

show regions of high and low perfusion (see section 2.3.2). This technique also penetrates to a depth of ~1mm in skin, and so also requires thinning or removal of the cranium as described above. However, it has a major benefit over the use of a laser probe, in that it enables resolution of several individual vessels and tissue perfusion at the capillary level, which is continuous and covers a much wider area, typically an area of 10 x 8mm. As such, this technique has been used in flow-metabolism coupling studies, and during clinical neurological procedures in humans (Kazmi *et al,* 2015). It was employed in some of the studies in this thesis.

1.2.2.4 Measurement of vessel diameter

Another technique that is commonly used in studies on cerebral vascular responses is that of directly observing cerebral vessel diameter via an open or sealed cranial window. The anaesthetised animal is secured in a stereotaxic frame, the parietal bones are exposed and removed by drilling. The dura is removed and the exposed brain tissue is then generally superfused with gassed and heated artificial CSF. A camera can then be used to image cortical (pial) blood vessels, and image analysis software can be used to assess changes in vessel diameter in response to experimental conditions. For example, Bauser-Heaton & Bohlen (2007) used this technique to investigate the role of nitric oxide (NO), in cerebral dilatation (increase in vessel diameter) induced by decreasing $pO_{2,}$ or hypotension. This method has also been used to assess cerebrovascular responses to *increasing* ABP (Paternò *et al*, 2000, see 3.1.3).

However, whilst measurement of vessel diameter allows continuous and direct observation of cortical microvessel behaviour, enabling specific investigation of surface vessel responses during CA, it cannot be assumed that changes in diameter in single vessels are proportional to CBF. Indeed, because the images are limited to a defined local area or a select number of

vessels on the surface of the brain, this technique may be more valuable when used in combination with a method that allows more global assessment of CBF. The technique also requires delicate surgical procedures to remove skull bone and dura, rather than just thinning of the bone. This can alter the CSF pressure, has the potential to induce trauma, and requires superfusion of the brain surface to maintain physiological conditions. Nevertheless this does allow for easy topical application of pharmacological agonists or antagonists, or alteration of CSF composition.

Measurement of vessel diameter has been used in conjunction with measurement of pial vessel pressure, which is performed by insertion of a glass micropipette, connected to a pressure transducer, into the vessel lumen. This allows for assessment of vascular resistance in different size vessels in the cerebrovasculature. Such measurements have provided evidence that large cerebral arterial vessels make a significant contribution to total cerebral vascular resistance (CVR) and therefore to the pressure transmitted to the cortical microvasculature: a major contrast with other vascular beds, where the main resistance lies in medium and small arterioles (Faraci & Heistad, 1990). This combination of techniques has also been used by Kontos *et al* (1978), who similarly demonstrated an important role for the larger cerebral arteries in the autoregulatory vasoconstriction observed between ABPs of 110-160mmHg, whilst smaller cerebral vessels did not respond until pressures reached 170-200mmHg (see 4.4). They used measurements of pressure in vertebral arteries and pial arterioles, direct visualisation of vessel diameter, and assessment of CBF using the hydrogen clearance technique, and calculated CVR (ratio of the pressure drop divided by CBF) across the different segments of the cerebral circulation. Their results suggested that the cerebral circulation demonstrates segmental vascular resistance; at 120mmHg, the large, extracranial vessels (aorta to the Circle of Willis) accounted for 17% of total CVR, the large cerebral

surface arteries (Circle of Willis to pial vessels) for 26%, the small surface, intracerebral arterioles, and precapillary vessels for 32%, and around 25% from the capillaries and veins. The reason for the high level of contribution of the larger cerebral arteries to resistance when compared to other vascular beds, may be the relative diameter and length of the vessels, as well as the vascular branching patterns in the brain (Faraci & Heistad, 1990).

Given that vessels of different resting diameters and pressures may behave differently during the same stimulus, analysis of multiple vessels is required to build up a general picture of the behaviour of cortical vessels to a given stimulus. These techniques are therefore also restricted to use on cortical vessels that can be visualised.

1.2.2.5 In Vitro methods

Finally, *in vitro* methods can be used to study the behaviour of isolated cerebral arteries from all levels of the vascular tree, from supplying arteries such as the carotid artery and MCA, down to arterioles isolated from the cortex. The most common method is that of myography, where a segment of vessel is mounted between two wires, which are connected to a transducer to detect contraction or relaxation of the vascular smooth muscle. The vessels undergo a normalisation procedure to ensure they are representative of the vessel *in situ*, under an appropriate amount of transmural pressure (Mulvany & Halpern, 1977). This set-up can then be used to assess the reactivity of the vessel to specific drugs, for example the use of phenylephrine to investigate cerebral vessel reactivity to α-adrenoreceptor agonists. Alternatively, and more relevant to the current aims of investigating autoregulatory changes in ABP, a pressure myograph system can be used. In this set-up, the vessel segments are cannulated and perfused to replicate an *in vivo* pressurised vessel. The flow rate, and/or perfusion pressure, can then be altered and the constrictor or dilator response measured. For example, New *et al* (2003) tested the autoregulatory responses of MCA segments to changes

in both flow and pressure, from uremic hypertensive Wistar-Kyoto (WKY) rats, spontaneously hypertensive rats (SHRs) and normotensive controls. They found that the uremic hypertensive rats displayed a reduced myogenic constriction, whilst SHRs displayed increased constriction to changes in flow.

Although a useful addition, *in vitro* myography methods are limited by the fact that they show only the behaviour of the isolated vessel, whether larger vessel or arteriole, and this does not necessarily represent the behaviour that would be seen in all vessels, in an intact animal, where multiple regulatory factors are present. In the present study, the decision to develop a whole animal model, in the rat, was influenced by the ability to use more invasive and direct measurements of CBF, whilst accepting the potentially confounding issue of the influence of anaesthetic. A novel aspect of the work described in this thesis is the use of two measurement methods simultaneously; a Transonic flow probe on the carotid arterial supply to the brain to assess gross CBF, and either a Laser Doppler probe or Laser Speckle imaging to assess cortical CBF concurrently (see 2.3.1 and 2.3.2 for methodological details). As discussed above, these techniques enable direct and continuous assessment of CBF *in situ*, and allow an attempt to be made to characterise the responses at different levels of the cerebral vasculature. This is important as the mechanisms underlying CA in response to rises in ABP, even in young, healthy adults, are incompletely understood (see 1.3). This also improves the ability to investigate the impact of other factors, such as ageing, on CA (1.4), which was the secondary focus of this thesis.

1.3 Mechanisms involved in the control of cerebral blood flow

Due to the dependence of the brain on an intact blood supply, and the restricted intracranial volume, CBF is efficiently regulated to maintain a constant and sufficient flow by four main control mechanisms:

1.3.1 Autoregulation

The term 'autoregulation' was first used to describe the cerebral circulation by Lassen (1959). It is the phenomenon by which CBF is maintained at a relatively constant level over a physiological range of ABPs, or more specifically cerebral perfusion pressures (CPP = ABP – intracranial pressure (ICP), the latter of which tends to be stable at 10-15mmHg (Dunn, 2002)).

According to this hypothesis, if ABP decreases, cerebral vasodilatation occurs and CBF is maintained. In humans, if ABP falls below ~60mmHg, known as the lower limit (LL), autoregulation begins to fail and CBF will drop steeply. If ABP increases, cerebral vasoconstriction occurs and CBF is maintained. If ABP rises above ~160mmHg, known as the UL, CBF will increase (reviewed by (Paulson *et al*, 1990 and Cipolla, 2009). A diagrammatic representation of CA, with a distinct plateau, LL and UL, is shown in Figure 3.

Therefore, according to this hypothesis, at ABPs beyond the UL, the risk of small vessel rupture is high, as they are exposed to both high arterial pressure and increased flow. This would be expected to lead to disruption of the blood brain barrier (BBB), endothelial damage and cerebral haemorrhage or stroke (see section 1.3), and is supported by the strong link between hypertension and stroke (Endres *et al*, 2011).

Further to this definition, CA can be split into two categories; dynamic and static. Dynamic CA describes the CBF response to rapid changes in ABP. It is often described as a high-pass

filter, whereby the cerebral vessels cannot respond quickly enough to autoregulate against high frequency oscillations in ABP, and therefore rapid changes in CBF are seen. Static CA refers to the relationship between CBF and steady-state ABP changes, which are typically well-counteracted by the cerebral vasculature (Tiecks *et al*, 1995). Whilst data from studies of static CA is generally analysed by directly plotting ABP against CBF to generate an autoregulatory curve, dynamic CA is usually assessed by calculating the gain between ABP and CBF. Gain is calculated by plotting mean CBF as a function of mean ABP, performing linear regression analysis, and calculating the slope of the resulting curve. Thus, gain is an indicator of the effectiveness of CA i.e. how well the cerebral vasculature is buffering against changes in ABP. Despite these differences in analysis, both static and dynamic CA are not different in terms of the underlying mechanisms, only in the time over which they act.

1.3.1.1 Myogenic mechanisms

Traditionally, a critical mechanism involved in CA is considered to be the Bayliss myogenic response. First described by Sir William Bayliss (1902), the Bayliss response is a specialised version of the myogenic reflex that occurs in arteries and arterioles, whereby the vascular smooth muscle contracts when stretched, and *vice versa*.

In 1938, Fog demonstrated myogenic mechanisms in the pial cerebral circulation. He showed pressure-dependent changes in the vessel diameter of cat pial arteries. The arteries dilated when ABP decreased, and constricted when ABP increased, independently of the sinus, aortic, cervical sympathetic and vagi nerves, demonstrating an intrinsic, pressure-sensitive vasomotor mechanism, which assists in keeping blood flow to the brain constant (Fog, 1938). Further, Harder (1984) showed a positive correlation between cat MCA intracellular membrane potential and transmural pressure *in vitro*, which was dependent upon extracellular calcium. It is now known that cerebral and other arterioles are sensitive to transmural pressure

changes, such that increases in ABP stretches smooth muscle cells, activating phospholipase C. This leads to opening of stretch-activated K^+ channels, causing depolarisation, Ca^{2+} release and, subsequently, vasoconstriction (Tan *et al*, 2013).

1.3.1.2 Shear stress

As well as pressure-dependent mechanisms, the flow of blood, independent of changes in pressure, can cause changes in vessel diameter, mediated by changes in shear stress-induced release of vasoactive substances. In most vascular beds, shear stress causes vasodilatation via the release of vasoactive substances from the endothelium, such as NO (see 1.3.4), prostaglandins and endothelium-derived hyperpolarising factor (EDHF). This shear stress-induced release of vasoactive substances, particularly NO, is exploited by researchers investigating endothelium-dependent flow-mediated dilatation, for example by performing a reactive hyperaemia test (Pyke & Tschakovsky, 2005). However, a number of studies (reviewed by Koller and Toth, 2012) have shown that in rats, whilst dilatation was seen in the vertebrobasilar arteries in response to an increase in flow, constriction was seen in the intracerebral arteries arising from the internal carotid arteries, such as the MCA, and biphasic responses were seen in cerebral arterioles branching off the MCA.

For example, Bryan *et al* (2001) isolated vessels from male Long-Evans rats, mounted them in a tissue bath and pressurised them using input and output reservoirs, which were raised or lowered to achieve pressures close to those seen *in vivo*. Flow through the vessels was then induced using a syringe pump; the input reservoir was clamped and, as flow rate was increased, the output reservoir was lowered, to maintain the pressure within the vessels. This ensured that changes in flow, independently of pressure, were being imposed on the vessel segments. They found that, whilst isolated cremaster muscle arterioles dilated to increases in flow, the MCA and cerebral penetrating arterioles constricted. This constriction was

accompanied by an increase in [Ca^{2+}] in vascular smooth muscle cells (VSMCs). They saw similar responses when viscosity of the solution was increased by adding dextran, and passed through the lumen at a constant rate, demonstrating that the vessel responses were shear-stress induced. Flow-mediated constriction persisted in MCA and penetrating arteriole segments, even after the endothelium was removed by passing air through the lumen of vessel segments. Further, Bryan *et al* (2001) demonstrated that integrins were involved in the mechanism of constriction to shear-stress. When an integrin binding antagonist, specifically of the β_3-integrin, was applied to endothelium-denuded MCA segments, the constriction response to a single level of shear stress was inhibited. They therefore hypothesised that, due to the function of integrins to bridge the extracellular matrix and actin filaments, and recent evidence of their role in affecting vascular tone via changes in Ca^{2+} currents, integrin binding may be altered by shear stress, and produce increases in Ca^{2+} in VSMCs. This shear-stress-induced constriction may be a contributory mechanism for the maintenance of basal cerebrovascular tone, from which dilatation to increase flow in activated brain regions can occur (see 1.3.2).

A number of other factors are known to regulate CBF, and may contribute to autoregulation. These are discussed below (1.3.2-1.3.4).

1.3.2 Metabolic/chemical control of cerebral blood flow

Metabolic, or chemical, regulation is a dominant CBF control mechanism. Local changes in interstitial pCO_2 (partial pressure of CO_2), which may be due to changes in metabolism or $PaCO_2$ (arterial partial pressure of CO_2), have substantial effects on CBF. Even a small increase in pCO_2 leads to a large cerebral vasodilatation, and *vice versa*. For example, a 1mmHg increase in pCO_2 can cause a 2-3% increase in CBF in humans (Raichle & Plum, 1972).

These changes in CBF appear to be independent of the associated changes in arterial pH, as it has been shown that metabolic acidosis and alkalosis have no effect on CBF. For example, Harper & Bell (1963) held $PaCO_2$ constant in anaesthetised dogs by adjusting a respiratory pump, whilst changing *intraluminal* arterial pH, by infusion of lactic acid or sodium bicarbonate, and saw no change in cerebral cortical blood flow.

However, CO_2 is able to easily diffuse across the BBB and equilibrate with the CSF, and the change in extravascular pH *is* thought to be important. Increased or decreased CSF pH can then act directly on the cerebral vascular smooth muscle to alter CBF, consistent with the idea that pCO_2 only affects CBF via its action on CSF pH. This is supported by Kontos *et al* (1977), who used a cranial window technique in anaesthetised cats to directly measure pial arteriolar diameter. The area under the cranial window was perfused with artificial CSF, in which the pH and/or pCO_2 was varied, to alter the local, extravascular conditions. They found that changing extravascular pH *did* change vessel diameter, and this occurred independently of pCO_2. In contrast, changing pCO_2 did not change arteriolar diameter when pH was held constant.

In terms of transduction of the pH signal, it is thought that H^+ ions, associated with the decrease in pH caused by increased CO_2, can act to alter vascular smooth muscle tone and therefore CBF. Several mechanisms have been proposed; Loutzenhiser *et al* (1990) showed that altered pH can cause vasodilatation of rat aorta *in vitro*, via direct effects on contractile proteins and Ca^{2+} entry, specifically an increased Ca^{2+} sequestration into intracellular stores. Alternatively, H^+ ions may elicit the release of NO to cause vasodilatation. Iadecola (1992) superfused cranial windows in rats, and saw an increase in CBF with increased pCO_2 levels. Subsequent superfusion with NO synthesis inhibitors reduced or abolished the vasodilation.

The source of this NO may be perivascular nerves innervating the vessels (see 1.3.3.2), vascular smooth muscle, or glial cells (for further discussion of NO see section 1.3.4).

By contrast, one study does support a role for pCO_2 independently of pH. Harder & Madden (1985) studied isolated sections of cat MCA. They exposed the vessel segments to a reduction in pCO_2, from 37 to 14mmHg, whilst maintaining a pH of 7.4, and measured membrane depolarisation and tension development. Reducing pCO_2 caused a graded depolarisation and an increased tension i.e. a vasoconstriction. Increasing pH from 7.4 to 7.6 had a similar effect. However restoring pCO_2 from 14 to 37mmHg caused only a transient vasodilatation, followed by a constriction. However, the interpretation of this study, in relation to whether pCO_2 is acting extra- or intravascularly, is difficult due to the preparation used. Further, the majority of the evidence supports the hypothesis of pCO_2 acting via a change in CSF pH.

Severe changes in pO_2 (partial pressure of O_2) can also affect CBF, but to a lesser extent than CO_2; hypoxia causes a vasodilatation via activation of Ca^{2+}-activated K^+ channels in the smooth muscle cell membranes. Various substances have been implicated in the mechanism of hypoxia sensing and subsequent K^+ channel activation, for example, 20-HETE (Gebremedhin *et al*, 2008). Further, roles for substances that are released in proportion to local metabolism, such as K^+ itself, lactic acid and adenosine have also been suggested (reviewed by Mchedlishvili, 1980, and Cipolla, 2009). Coney & Marshall (1998) showed that in anaesthetised rats, the increase in cortical RCF and cortical vascular conductance induced by hypoxia (8% O_2), was mimicked by topical application of adenosine to the cortex. Further, both the non-selective adenosine receptor antagonist 8-PT, as well as an A_{2A}-specific antagonist, reduced these responses.

It is this flow-metabolism coupling which forms the basis for a number of functional neuroimaging techniques such as PET (see 1.2.1).

As well as direct effects on CVR and CBF, CO_2 and O_2 can influence CA. For example, Querido *et al* (2013) assessed dynamic CA (regulation of CBF to rapid changes in ABP), by using squat-stand manoeuvres to change MABP (5 secs standing, followed by 5 seconds squat, repeated for 5 minutes), and measuring MCA blood flow velocity (MCAv) using a Transcranial Doppler probe in healthy volunteers. They plotted mean MCAv as a function of MABP, and calculated the linear regression of the slope. This was taken to represent gain; the change in MCAv for a given change in ABP, or, in other words, the extent to which changes in ABP are transmitted through to the cerebral vasculature to cause changes in CBF. Experiments were performed in normocapnia, isocapnic hypoxia, and poikilocapnic hypoxia. They found that the increases in ABP during the squat-stand manoeuvres caused a significant increase in MCAv during isocapnic hypoxia compared to normocapnia, i.e. impaired dynamic CA. But when PCO_2 was allowed to fall, due to the hyperventilation caused by hypoxia (poikilocapnia), there was no significant change in MCAv, demonstrating the strong influence of CO_2 on dynamic CA.

Further, hypercapnia has also been shown to impair static CA (CBF regulation to more prolonged changes in ABP). Perry *et al* (2014) induced increases in MABP by lower body positive pressure (LBPP) over periods of 5 minutes, and measured MCAv using a Transcranial Doppler probe. Subjects were exposed to two levels of LBPP (20 and 40mmHg), with and without hypercapnia (breathing 5% CO_2 in air). They found that, whilst during the LBBP in eucapnia, MCAv was well maintained (i.e. CA was intact), hypercapnia with the 40mmHg LBPP caused an increase in MCAv (i.e. CA was impaired).

1.3.3 Autonomic control of cerebral blood flow

The cerebral circulation is richly innervated by both sympathetic vasoconstrictor fibres, which are primarily noradrenergic and originate from the superior cervical ganglia (SCG) (Arbab *et al*, 1986), and parasympathetic vasodilator fibres, which are primarily cholinergic and originate from the pterygopalatine ganglia (PPG, also known as sphenopalatine), otic and internal carotid ganglia (Walters *et al*, 1986) (see Figure 4). These fibres run in the vessel adventitia.

This innervation is thought to be mainly ipsilateral (Arbab *et al*, 1986), although there is evidence for some bilateral and contralateral innervation in specific regions, more commonly in species larger than the rat (Hardebo *et al*, 1996). It is also thought to be confined mostly to the larger cerebral vessels, as shown by Figure 2, a diagrammatic representation of the neurovascular unit in the cerebral cortex (Filosa and Iddings, 2013). It shows the arrangement of such a network, where innervation from extrinsic ganglia i.e. sympathetic fibres from the SCG, are present to the level of the pial arteries. Once these arteries branch to form penetrating arterioles, this innervation decreases and is replaced by a close association with astrocytes. This coupling of cerebral arterioles with astrocytes is known as the neurovascular unit, and allows for control of vascular tone and local CBF based on the needs of the surrounding neurons i.e. flow-metabolism, or neurovascular, coupling (Filosa and Iddings, 2013).

1.3.3.1 The influence of sympathetic innervation on cerebral blood flow and autoregulation

Traditionally, the functional role for the sympathetic nervous system in the control of CBF is thought to be minimal. A review by Heistad & Marcus (1978) considered studies using isolated cerebral vessels to assess sympathetic innervation, and responsiveness to electrical

stimulation and α-agonists, as well as *in vivo* studies using radiolabelled microspheres, and flowmeters on the common carotid artery after ligation of the external carotid branch.

They concluded that, despite the rich sympathetic innervation of cerebral vessels, there was no convincing evidence for a neural control of CBF. Studies they reviewed included Bevan *et al* (1975), who found that BA rings from rabbits were minimally responsive to noradrenaline when compared to saphenous artery rings. *In vivo* studies utilising the microsphere technique also produced results suggesting a minimal CBF response to sympathetic stimulation. For example, Heistad *et al* (1977) found that stimulation of the SCG in anaesthetised dogs did not alter cerebral, cerebellar, or brainstem blood flow. The studies, all performed in the 1960s and 70s, that did show an effect of cerebral sympathetic innervation, used techniques to measure CBF that were deemed to have methodological limitations. For example, James *et al* (1969) stimulated or sectioned the cervical sympathetic nerve in anaesthetised baboons. They saw a decrease in blood flow in response to stimulation, and an increase following denervation. However, they measured CBF using the xenon clearance method, the limitations of which are discussed in 1.2.1.

Further, Heistad *et al* (1978) themselves found that sympathetic denervation at the level of the SCG did not affect CBF (measured using microspheres) in monkeys or cats, suggesting a minimal role in controlling basal cerebrovascular tone. When they stimulated the SCG, CBF significantly decreased in monkeys, but not cats. When severe, acute hypertension was induced, the decrease in CBF to stimulation was augmented in cats and dogs, but was similar to control conditions in monkeys. Disruption to the BBB caused by hypertension alone, was reduced by sympathetic stimulation.

Thus, Heistad & Marcus (1978) concluded that sympathetic nerves were unlikely to significantly influence flow under normal physiological conditions, and suggested they may play another role, such as in affecting the surface area of capillaries.

However the ideas around the role of the sympathetic nervous system in controlling CBF has evolved; whilst older papers, such as those cited above, suggest little or no role, more recent papers do show an effect. For example, Sadoshima *et al* (1986) assessed CBF by the hydrogen clearance method, in anaesthetised WKY and SHRs, and showed that bilateral sympathetic denervation at the level of the SCG had no effect on basal CBF. However, when they raised ABP with an i.v. infusion of PE, sympathetic denervation did lower the UL of CA. Moreover, in humans, cholinergic ganglionic blockade was shown to reduce ABP and MCA blood flow velocity. When ABP was restored and normalised, the effect on MCA velocity persisted, suggesting a tonic autonomic drive to cerebral vessels supplied by the MCA (Zhang *et al*, 2002).

Interestingly, a study by Cassaglia *et al* (2008) in lambs, showed that sympathetic nerve activity in the SCG was *increased* in response to imposed increases in ABP induced by systemic infusion of phenylephrine. This provided direct evidence for sympathetically-mediated vasoconstriction helping to maintain constant CBF during rises in ABP i.e. autoregulation. More recently, it was shown that superior cervical sympathectomy disrupts CA at high ABPs in two-week-old lambs, but not preterm lambs (Czynski *et al*, 2013).

Thus, these studies suggest that there is some role for sympathetic innervation in determining resting CBF, and contributing to CA when ABP rises.

Finally, evidence was obtained that suggests that sympathetic vasoconstriction of larger extracranial arteries not only helps to maintain a constant CBF, but also protects downstream

arteries from exposure to higher pressures. Tuor (1992) unilaterally electrically stimulated the SCG in anaesthetised rats, during moderate or severe hypertension induced by i.v. infusion of angiotensin II, and measured local CBF via autoradiography. During moderate hypertension, CBF was fairly constant, and sympathetic stimulation induced small decreases in ipsilateral flow. During severe hypertension, hyperaemia was seen throughout the brain. Under these conditions, sympathetic stimulation had an increased effect and reduced the volume of the hyperaemia, suggesting a protective action against hyperperfusion in cortical tissue. Further, it has been shown that sympathetic stimulation can cause a rightwards shift in the autoregulatory curve, raising the UL, protecting against rises in CBF, and therefore limiting BBB damage (Heistad & Marcus, 1979). Thus, despite the negative evidence arguing that sympathetic innervation plays little functional role in regulating CBF, on the basis of studies just described, it can be hypothesised that sympathetic vasoconstriction protects the cerebral circulation against rises in ABP, making it important at the UL.

1.3.3.2 The influence of parasympathetic innervation on cerebral blood flow and autoregulation

Regarding the functional role for parasympathetic nerves in controlling CBF, Ishii *et al* (2014) studied the ability of parasympathetic fibres to induce cerebral vasodilatation by stimulating the lingual nerve. They recorded the effect on internal carotid artery blood flow using an ultrasonic flow probe, and on parietal cortex perfusion by Laser Speckle imaging (see 1.2.2.3). They observed an increase in internal carotid flow in response to stimulation, which was significantly reduced by both i.v. hexamethonium (a nicotinic, ganglionic ACh receptor antagonist) and atropine (a muscarinic ACh receptor antagonist). Interestingly, increases in cortical perfusion were only seen with a combination of stimulation and administration of a $GABA_A$ antagonist; this increase in cortical flow was also reduced by

hexamethonium and atropine. These data suggest a parasympathetic cerebral vasodilator input, modulated by $GABA_A$ receptors, which could be involved in the control of gross CBF, specifically cortical blood flow.

Modin *et al* (1994) investigated the potential roles for NO and vasoactive intestinal polypeptide (VIP) as mediators of parasympathetic vasodilatation. They stimulated the parasympathetic nerves projecting from the submandibular ganglion at 1Hz and 10Hz, and measured submandibular gland blood flow (which is supplied by the facial artery; a branch of the external carotid artery), using a Transonic flow probe. They repeated this protocol after i.v. administration of the NO synthase inhibitor N^G-Nitro-*L*-Arginine (L-NA, see 1.2.4), alone and in combination with atropine, and also after milrinone (a phosphodiesterase inhibitor, to increase levels of cAMP, which is the primary second messenger system for VIPergic signalling). Parasympathetic stimulation elicited a large vasodilatation, graded with stimulation frequency. 10Hz stimulation also caused a significant increase in neuropeptide Y (NPY)-like immunoreactivity, which was taken as an indication of VIP release due to reported co-localisation in parasympathetic nerves. The nitric oxide synthase (NOS) inhibitor L-NA significantly reduced not only basal blood flow, but also the absolute increases in flow, and the NPY overflow to stimulation. Moreover, atropine significantly reduced the response to 1Hz stimulation, whereas the 10Hz response was only reduced by around 23%, and NPY overflow was only slightly reduced. Thus, the stimulus-evoked vasodilator response could be divided into atropine-sensitive and atropine-resistant components. A combination of atropine and L-NA almost abolished the response to 1Hz stimulation, and significantly reduced the response to 10Hz, but had no further effect on NPY overflow. These effects of L-NA suggest an important role for NO in the cholinergic component of parasympathetic dilatation. Milrinone, which was used to increase the VIP second messenger signal, slightly reduced the

inhibitory effect of L-NA on the parasympathetic dilatation, suggesting that NO may contribute to, or modulate the VIP component.

Considering the role of parasympathetic nerves in CA, Morita *et al* (1995) measured cortical blood flow using a Laser Doppler probe placed over small holes made in the parietal cortex, whilst stepwise decreases in ABP were induced by controlled withdrawal of blood. This protocol was carried out in sham operated Sprague-Dawley rats, as well as in a group that had previously undergone bilateral parasympathetic denervation at the level of the ethmoid foramen. In the sham animals, CBF significantly decreased at ~50mmHg, indicating the LL of CA had been reached. In denervated animals, CBF was seen to decrease at ~60mmHg, suggesting that the lower limit was shifted towards higher ABPs.

Talman & Dragon (2000) also investigated the role of the parasympathetic nerves projecting from the PPG, but focused on the UL of CA. They also transected the nerves at the level of the ethmoid foramen, in anaesthetised, male Sprague-Dawley rats, and measured cortical blood flow using a Laser Doppler probe via a cranial window over the parietal lobe. An i.v. infusion of phenylephrine was used to gradually raise ABP, either until ABP would increase no further, or until breakthrough of autoregulation was seen i.e. the UL was exceeded. Parasympathetic denervation significantly attenuated the increase in CBF beyond the UL compared to sham animals, suggesting that breakthrough of autoregulation is dependent upon cerebral parasympathetic innervation, and that breakthrough includes an active dilatation. This group had also previously shown that inhibition of NOS (Talman & Dragon 1995, see 1.3.4.2), and interruption of the baroreflex pathway (Talman *et al*, 1994), both had similar effects on the UL of CA (see Chapter 5 for further discussion). Therefore, they hypothesised that release of NO, from parasympathetic nerves innervating the cerebral vessels, are involved in the increase in CBF beyond the UL, and are anatomically linked to the baroreflex.

1.3.3.3 Histological detection of cerebral autonomic fibres

1.3.3.3.1 Detection of sympathetic fibres and receptors

Sympathetic fibres have been detected, primarily by the glyoxylic acid method (Furness and Costa, 1975), or via immunohistochemical staining of enzymes involved in catecholamine synthesis, on the larger cerebral vessels. Specifically, sympathetic fibres have been detected on the internal carotid, rostral, vertebral, Circle of Willis and pial cerebral arteries in rats (for example, Hill *et al*, 1986), as well as other laboratory species including rabbits and guinea pigs (Luff & McLachlan, 1989), cats (Tsai *et al*, 1985), dogs (Kawai & Ohhashi, 1986) and baboons (Edvinsson & Owman, 1977). Sympathetic nerves have been shown to mainly use the transmitter noradrenaline (reviewed by Lincoln, 1995).

Kawai & Ohhashi (1986) studied the major cerebral arteries of dogs. Using the glyoxylic method, they demonstrated adrenergic innervation in the internal carotid, ACA, MCA and PCA, posterior communicating artery and BA, although there was regional variation in the density of innervation, which tended to decrease in the more distal arteries.

Nielsen & Owman (1967), who used an immunohistochemical staining technique to study adrenergic innervation of the cerebral vessels of cats, similarly observed innervation in the vessels named above, but also in pial vessels down to 15-20 microns in diameter. They observed some nerve fibres following the arterial branches entering the parenchyma.

In our lab we have demonstrated a perivascular network of noradrenergic, sympathetic fibres in rat MCA and BA, using the glyoxylic acid method (Omar & Marshall, 2010b).

It has been shown that both α- and β-adrenoreceptors are present on cerebral vessels (Purkayastha *et al*, 2013, Kobayashi *et al*, 1982), but that catecholamines do not easily pass through the BBB (Edvinsson *et al*, 1978). Edvinsson *et al* (1979) assessed rCBF using the

hydrogen clearance technique in rats. Interestingly, they showed that *i.v.* noradrenaline and adrenaline both caused a decrease in CBF in most brain regions, an effect which was blocked by the α-antagonist phentolamine. The noradrenaline infusion was associated with an increase in ABP, whilst the adrenaline infusion caused no significant change in ABP. The authors suggest that any effect on ABP should be compensated for by CA, and therefore the changes in CBF are due to direct effects on the cerebral vasculature. However noradrenaline increased ABP to 174±7mmHg, which is at the upper end of the CA range, if not above the UL. The same group carried out similar experiments after the BBB was opened by intracarotid injection of urea to induce hyperosmotic shock. Infusion of noradrenaline then caused an *increase* in CBF, which was unaffected by phentolamine (Edvinsson *et al*, 1978). Therefore the authors appear to suggest that the decrease in CBF is occurring via direct vasomotor effects, but also via an intraluminal mechanism (as they acknowledge poor penetration of catecholamines across the BBB, and different results if the BBB is opened). However the location of the α-receptors is not discussed.

Further, these data are in contrast with a number of studies that suggest low adrenergic receptor density on cerebral vessels, and poor responsiveness of cerebral vessels to catecholamines and sympathetic stimulation (e.g. Bevan *et al*, 1998), which provide a basis for the use of adrenergic agonists, such as phenylephrine, in studies on CA (see 3.1.2.1).

The co-transmitter NPY is also commonly present in sympathetic nerves (Hardebo *et al*, 1996). Edvinsson *et al* (1987) showed the presence of perivascular nerve fibres containing NPY in numerous species including rats, as well as in the cell bodies of the SCG, which was co-localised with dopamine-β-hydroxylase (a marker for catecholamines). Removal of the SCG resulted in a reduction of the detected NPY in pial vessels, but exogenously applied

NPY was still able to produce concentration-dependent contractions *in vitro* in rat cerebral arteries.

1.3.3.3.2 Detection of parasympathetic fibres and receptors

Detection of fibres projecting from the PPG has been carried out largely via immunohistochemical localisation or radioenzyme activity assays of choline acetyltransferase (ChAT), an enzyme involved in the synthesis of acetylcholine (ACh). For example, Florence & Bevan (1979) assayed the activity levels of ChAT and the uptake of radiolabelled choline. They found evidence of cholinergic innervation in the Circle of Willis and the major cerebral arteries, in dogs, cats and rabbits. Chédotal *et al* (1994) used double immunofluorescence staining to assess ChAT and VIP (a major non-cholinergic parasympathetic transmitter) co-localisation in the cortical cerebral vessels of Wistar rats. They found that both cholinergic, VIPergic, and also fibres positive for both transmitters, were associated with intracortical blood vessels. This suggested two distinct methods of neuronal vascular regulation, as both ACh and VIP are vasoactive. ACh produces vasodilatation in many vascular beds, including cerebral vessels, via M_3 muscarinic receptor-mediated production of NO (Dauphin & Hamel, 1990). It is also known that cerebral vessels express M_5 receptors, which when knocked out in M_5 receptor-/- mice, almost completely abolished the vasodilator response to ACh. This makes them a potential therapeutic target for conditions such as Alzheimer's and vascular dementia, in which reduced M_5 receptors have been implicated (Yamada *et al*, 2001). Csati *et al* (2012) found that, in addition to ACh and VIP, both human and rat PPGs also contain pituitary adenylate cyclase-activating protein (PACAP; so named because it activates the cAMP signalling pathway) and NOS (a group of enzymes responsible for production of NO), as well as their respective receptors. All of these substances are known to be potent vasodilators, including in cerebral vessels.

1.3.4 Endothelial mediators affecting cerebral blood flow: Nitric oxide

Endothelial cells lining blood vessels release vasoactive substances when stimulated by agonists or shear stress. The primary substance released is NO, which is a diffusible, lipophilic molecule that plays a key role in vertebrates as a transmitter. It is constitutively generated by endothelial and neuronal nitric oxide synthase enzymes (eNOS and nNOS) found in endothelial cells, autonomic 'nitrergic' nerves and brain neurons (not exclusively, i.e. eNOS can be found in nerves, and *vice versa*). The effects of constitutively produced NO are vasodilatation, hypotension, and increased blood flow, as well as inhibitory actions on platelets, reduced proliferation of smooth muscle cells and antioxidant effects. The main signalling pathway for NO is via activation of guanylate cyclase, which catalyses conversion of guanosine triphosphate (GTP) to cyclic guanosine monophosphate (cGMP). cGMP acts as a secondary messenger for NO signalling, with some of its main actions being to decrease intracellular Ca^{2+} levels, activate K^{+} channels to cause hyperpolarisation, and to cause dephosphorylation of myosin, all of which facilitate smooth muscle relaxation (reviewed by Toda *et al*, 2009). It also has a role as a neurotransmitter in the cerebral and other circulations as indicated above (Toda *et al*, 2009). The 3rd isoform of NOS is known as inducible or iNOS, and is typically only expressed during inflammation (reviewed by Toda *et al*, 2009, and Cipolla, 2009).

NOS enzymes catalyse production of NO by the conversion of L-arginine to L-citrulline, and require the presence of oxygen as well as various cofactors including BH_4 (tetrahydrobiopterin) and nicotinamide adenine dinucleotide phosphate (NADPH, reviewed by (Alderton *et al*, 2001).

NOS inhibitors have been used to investigate the role of NO in regulating CBF and, more recently, the contribution of specific NOS isoforms have been investigated, for example; L-

NA is non-selective between the isoforms; 7-Nitroindazole (7-NI) and S-Methyl- *L*-Thiocitrulline (SMTC) are used as nNOS specific inhibitors, while aminoguanidine and 1400W are iNOS selective. There are no eNOS inhibitors recognised as selective and effective (see Alderton *et al*, 2001).

1.3.4.1 Evidence for cerebral blood flow regulation by nitric oxide

Most of the investigations into the role of NO in the cerebral circulation have involved its contribution to basal CBF, or on the LL of autoregulation, studied by using graded or simulated haemorrhage.

For example, Faraci (1990) implicated NO in basal CBF by measuring BA diameter through a cranial window in anaesthetised rats. Application of L-NMMA constricted the artery and abolished the vasodilator response to topical ACh, suggesting a role for an eNOS-mediated source of NO in controlling basal CBF.

Joshi *et al* (2000) inhibited NO in humans using an intracarotid infusion of L-NMMA, and assessed CBF using a ^{133}Xe injection technique (see 1.3.1 and 1.3.2 for methodological details), with probes placed over the MCA to detect washout of the tracer. L-NMMA caused an increase in ABP and a decrease in CBF, which was reversed by infusion of the NOS substrate, L-Arginine. The effect on CBF was not replicated by infusion of PE, which produced systemic constriction and mimicked the rise in ABP, therefore suggesting a role for NO in the control of basal CBF.

Montécot *et al* (1997) showed an important role for neuronally-derived NO in basal CBF. They measured CBF by Laser Doppler flowmetry in awake rats. An i.p. injection of the selective nNOS inhibitor 7-NI caused a 27% decrease in basal CBF, without changing ABP, and addition of L-Arginine reversed the change in CBF.

As discussed in sections 1.3.3.1 and 1.3.3.2, it has been shown that the cerebral vasculature is richly innervated by both sympathetic and parasympathetic nerves. However, Okamura *et al* (2002) discussed the presence of a non-adrenergic, non-cholinergic innervation of the cerebral vasculature, and hypothesised that NO was the main neurotransmitter. They found that addition of L-Arginine analogues (NOS inhibitors), such as L-NMMA, could inhibit the vasodilatation caused by transmural stimulation of the nerve innervating the wall of isolated canine cerebral artery strips, and that high concentrations of L-Arginine could restore the effect (Toda & Okamura 1990). 7-NI was also shown to inhibit neurogenic vasodilatation, induced by stimulation of perivascular nerves in cerebral artery strips isolated from monkeys (Ayajiki *et al*, 2001). Further, methylene blue, an inhibitor of soluble guanylate cyclase, inhibited the cerebral vasodilatation evoked by electrical stimulation of perivascular nerves in dog and monkey MCA strips. This suggests that the dilatation is mediated by a transmitter that causes an increase in cGMP in smooth muscle cells (Toda, 1988). Taken together, these data indicate that NO, specifically of neuronal origin, mediates a cerebral vasodilatation via increasing cGMP in smooth muscle cells.

In terms of a functional role for this proposed NO-positive innervation, it has been shown that injection of L-NNA directly into the subarachnoid space causes constriction of the BA. Addition of phentolamine, in the presence of L-NNA, increased the magnitude of the vasoconstriction, suggesting a basal NO input to the cerebral vessels. In contrast, hexamethonium reduced the vasoconstriction, consistent with the NO input being from a neuronal source, involving nicotinic, cholinergic receptors, as found in autonomic ganglia. Further, injection of nicotine into the vertebral artery also dilated the BA, and this was abolished by L-NA. These data therefore suggest that, at least in the BA, there is a tonic release of NO from nerves innervating cerebral vessels, in addition to a basal endothelial NO

release (Toda *et al*, 1993). It seems likely that at least one source of these nerves is the parasympathetic neurones of the PPG.

1.3.4.2 Nitric oxide and autoregulation

Regarding NO and autoregulation, it has been shown that inhibition of NO synthesis, by suffusing L-NA directly into a cranial window in rats, increases the LL of CA, from ~75 to ~90mmHg. This was seen only in the group in which L-NA was suffused for 105 minutes, and not when it was suffused for only 35 minutes. It was therefore argued that the time taken to see an effect, reflected the time taken for L-NA to diffuse to a distant source of NOS i.e. eNOS in the vascular wall (Jones *et al*, 1999).

Further, White *et al* (2000) inhibited NOS with an i.v. infusion of L-NMMA in healthy humans, and studied the response to rapid falls in ABP, induced by inflation and sudden deflation of thigh cuffs. They recorded MCAv using a transcranial Doppler probe, and calculated the autoregulatory index (rate of rise of MCAv compared to ABP). They found that NOS inhibition impaired autoregulation (i.e. caused a decrease in autoregulatory index). Their results therefore suggested that NO has a role in the dynamic autoregulatory response to rapid falls in ABP in humans. As L-NMMA is a non-selective NOS inhibitor, the authors were unable to determine whether the effects were due to inhibition of endothelial or neuronal NOS. However the haemodynamic effects of L-NMMA (an increase in CVR and ABP) were consistent with inhibition of eNOS.

On the other hand, in a study on rats, a cranial window was used to study the diameter of cortical microvessels, as well as to assess NO concentration and pO_2 using microelectrodes. Hypotension was induced by gradual withdrawal of blood. As ABP was progressively reduced, cerebral NO levels increased. Moreover, selective inhibition of nNOS, using N4S

(an NMDA receptor antagonist; as NMDA receptors are involved in the uncoupling of nNOS from its scaffolding protein, allowing NO to be produced), attenuated this response. This suggested that nNOS is the important source of NO at the LL of dynamic CA (Bauser-Heaton & Bohlen, 2007).

By contrast, other studies have shown no effect of NOS inhibition on autoregulation. For example Thompson *et al* (1996) demonstrated, in anaesthetized monkeys, that intracarotid administration of L-NMMA or L-NA caused a 15% decrease in basal cortical CBF, but had no effect on CA at pressures ranging between 50-140mmHg. However, in the same animals, changes in CBF evoked by CO_2 were affected by NOS inhibition, suggesting that NO did play a role in this aspect of cerebrovascular regulation.

The role of NO at the UL of CA has not been widely studied. Talman & Dragon (1995) inhibited NOS using L-NA, before increasing ABP to identify the UL in anaesthetised rats. They found that NOS inhibition prevented an increase in CBF from occurring, even at ABPs >180mmHg, and therefore suggested that the 'breakthrough' of autoregulation is an active process involving NO. Further studies by the same group suggested that this active dilatation is mediated by NO released from nitrergic nerves (see 1.3.3.2).

1.3.4.3 Histological detection of nitric oxide synthase in the cerebral vasculature

Histologically, NOS has been detected in perivascular nerve fibres in the cerebral arteries of rats (Bredt *et al*, 1990), dogs (Yoshida *et al*, 1993) and monkeys (Yoshida *et al*, 1994). The fibres are located in the adventitia and media of cerebral vessels, suggesting that NO released from here acts on smooth muscle cells.

As discussed previously, NOS immunoreactivity has also been detected in the PPG. For example, Minami *et al* (1994) detected nNOS staining throughout the major cerebral arteries, including the Circle of Willis. They then used axonal transport to trace these neurons to the PPG, showing that projections from this ganglion innervate the cerebral arteries bilaterally, and that the fibres contain NO (co-localised with VIP). This has been confirmed by Toda *et al* (2000), who used arterial angiography to show that electrical stimulation of the PPG caused ipsilateral cerebral vasodilatation, which was abolished by L-NA, whilst denervation at the level of the PPG caused cerebral vasoconstriction. Stimulation of the greater petrosal nerve, the parasympathetic, pre-ganglionic fibres that run from the brainstem, and are upstream of the PPG, also caused cerebral vasodilatation, which was abolished by L-NA and hexamethonium. This suggests that the greater petrosal nerve synapses with the nerve that innervates the cerebral vessels. They therefore concluded that postganglionic, nitrergic nerves projecting from the PPG provide a tonic dilatory input to cerebral arteries (Okamura *et al*, 2002).

This so called nitrergic innervation of the cerebral vasculature could therefore be responsible for a tonic vasodilatation which helps to maintain CBF, and could also play a role in CA.

In summary, it has been shown that NO plays a role in tonic dilatation of the cerebral vasculature and several studies suggest it contributes to CA when ABP is lowered. Thus it

seems a reasonable hypothesis that NO sets the basal level of dilatation from which autoregulatory vasoconstriction occurs when ABP is raised. Whether it is involved in determining the level at which the UL is reached has not been tested, but it does seem to be involved in dilatation beyond the UL.

1.3.5 Regional differences in cerebral autoregulation

It has been shown that different regions of the brain may autoregulate within different ranges of ABPs, although data seems to vary depending on the experimental techniques used. Considering anaesthetised animal preparations, Sadoshima *et al* (1986) used the hydrogen clearance method to measure CBF in the parietal cortex and the thalamus, in anaesthetised WKY rats. Basal CBF was not different between the brain regions. However, when i.v. PE was infused to raise ABP, the ULs were different, with the thalamus having a significantly higher UL than the cortex (158±4 vs 142±3mmHg). Similarly, Baumbach & Heistad (1985) found that the autoregulatory response to acute decreases and increases in ABP were different between different regions of the brain in cats and dogs, with the brain stem showing less of a change in CBF in response to pressure compared to the cerebrum.

Smeda *et al* (1999) used Laser Doppler probes to assess CA to increases in ABP in the domains of the MCA and PCA. They showed that, in stroke-prone SHRs, both regions showed a reduced ability to autoregulate, such that CBF rose with ABP, prior to incidence of stroke. However, only the MCA showed a reduced ability to constrict to changes in pressure *in vitro*, whilst PCA function was maintained.

Hoffman *et al* (1991) studied both awake and anaesthetised Sprague-Dawley rats. They measured CBF in the cerebral cortex, subcortex and midbrain, as well as the spinal cord, using the radiolabelled microsphere technique. ABP was increased or decreased, using i.v.

PE, or trimethaphan (ganglionic antagonist) in combination with controlled blood withdrawal respectively. In awake rats, CA was seen between 50-170mmHg in all tissues, suggesting no regional variation. However, when the rats were anaesthetised with isoflurane, autoregulatory efficiency was reduced, such that blood flow increased to a greater extent with ABP. This loss of autoregulatory efficiency was different in the different regions studied, the largest changes being seen in the midbrain and spinal cord, suggesting a vulnerability of these regions that have previously been found to autoregulate to higher ABPs.

These studies raise the possibility that the deeper brain structures, the hindbrain and the brain stem, have better autoregulatory efficiency than forebrain structures, autoregulating to higher ABPs, and therefore providing greater protection from hyperperfusion in the brain regions responsible for the control of vital processes. They also highlight the important effect of using anaesthetised preparations, specifically using isoflurane, on CA.

Considering studies conducted in conscious humans, Ogoh *et al* (2015) measured blood flow in the internal carotid and vertebral artery using Doppler ultrasonography in healthy volunteers, whilst ABP was reduced using lower body negative pressure (LBNP). As ABP decreased, internal carotid blood flow also decreased, however vertebral artery blood flow was unchanged. They concluded that the maintenance of vertebral blood flow may contribute to orthostatic tolerance, and that preservation of posterior cerebral blood flow ensures a constant blood supply to the medulla. On the other hand, Horsfield *et al* (2013) used MRI, specifically a gradient-echo EPI sequence, to assess dynamic autoregulatory efficiency during a rapid decrease in ABP induced by sudden deflation of bilateral thigh cuffs, enabling assessment of regional, dynamic CA in healthy volunteers. They calculated autoregulatory efficiency as the time taken for CBF to recover to baseline, after the initial drop in CBF in response to the rapid decrease in ABP, and observed no differences between the frontal,

parietal, occipital and temporal cortices. They did see a greater signal drop in the cortices compared to the cerebellum, although the cortices exhibited a significantly faster recovery i.e. a greater autoregulatory efficiency. This is in contrast to the suggestion that the hindbrain can autoregulate more efficiently, although this study only looked at dynamic CA to rapid decreases in ABP.

In conclusion, whilst a number of studies suggest a regional heterogeneity in CA, the data tends to vary depending on the species studied and whether an anaesthetic was used. Further, studies conducted using animals tend to study static CA, which is in contrast to studies in human volunteers, which usually utilise rapid fluctuations in ABP. Therefore it is difficult to reach a consensus on whether regional differences in CA exist, or whether it is an experimental artefact.

1.3.6 Summary: Mechanisms involved in the control of cerebral blood flow

In an attempt to assess relative importance of various contributions to CA, Hamner & Tan (2014) carried out a retrospective analysis of their data from studies using oscillatory LBNP to induce changes in ABP, and TCD ultrasonography to measure MCAv in healthy volunteers. The combined studies included data before and after pharmacological blockade using phentolamine, glycopyrrolate and nicardipine, enabling investigation of the contributions of sympathetic, cholinergic and myogenic mechanisms respectively, to the cerebral pressure-flow relationship. They found that these three mechanisms accounted for 62% of the overall pressure-flow relationship.

When looking at the different phases of the pressure-flow relationship using projection pursuit regression, the falling and rising slopes outside of the autoregulatory range, as well as the LL itself, were influenced mostly by myogenic mechanisms. However the active, autoregulatory

phase was mostly controlled by sympathetic mechanisms, with some input from both cholinergic and myogenic mechanisms. Of most interest to the current study, the UL was mostly dependent upon the sympathetic and cholinergic mechanisms (see Chapter 8 for further discussion).

Despite assessments of the combined influence of all of the factors discussed above on CA, many recent studies have shown that CBF is not regulated as perfectly as the original proposal of Lassen (1959). Lassen's original proposal was that CBF was held constant in a 'plateau' over a wide range of ABPs, from around 60-160mmHg. If ABP went below or above these values (the LL and UL), CBF would decrease or increase respectively. This original model of CA, as shown in Figure 3, is still the basis of many classical 'textbook' representations of CA.

This is despite the fact that this classical curve is based on a combination of data from several patient populations.

Since this classical study by Lassen, Heistad & Kontos (2011, originally published 1983) made some incremental updates to the original model. They took the data from the Lassen paper, and removed data from patients with potentially confounding pathologies or medications. The resulting autoregulatory curve showed a trend for CBF to slightly increase with ABP, and *vice versa*, within the autoregulatory range, as opposed to the flat plateau originally proposed by Lassen.

More recent studies have now significantly evolved the model of CA. For example, Lucas *et al* (2010), used NIRS to study cortical oxygenation, which has been used clinically to assess CA, in parallel with TCD assessment of MCAv. They produced stepwise increases or decreases in ABP using i.v. infusions of PE or sodium nitroprusside (SNP), holding the ABP at each step for up to 1 minute 30 seconds. In contrast to the traditional model of CA, they

found that changes in MCAv were positively correlated with ABP, i.e. as ABP increased, so did MCAv (see Figures 5a and d). This was despite an increase in CVR, and a decrease in CVC, as ABP increased (Figure 5b), which indicated that autoregulatory vasoconstriction was occurring. These data suggest that, in healthy humans, a slope exists in what is typically thought to be the 'plateau' region of CA, and that this does not reflect a pathology. As such, a pressure-passive relationship may exist between CBF and ABP.

Interestingly, cortical oxygenation showed an inverse relationship to both ABP, and MCAv (Figure 5c). The authors hypothesised that this may reflect pressure- and flow-mediated changes in extracranial-intracranial collaterals, or possible changes in sympathetic nerve activity distal to the MCA.

Lending further support to this evolving concept of a more pressure-passive model of CA, Numan *et al* (2014) performed a literature review of 40 studies, with the aim of providing an up-to-date picture of static CA. They included studies consisting of healthy subjects, aged 18-65, who underwent protocols to measure CBF or MCAv, with at least one step change in MABP, but were not exposed to hypo/hyperoxia, or hypo/hypercapnia. Figure 5e shows the data extracted from the literature review, where the thin lines represent the 40 individual studies, and the thick line represents the mean. In agreement with the findings of Lucas *et al* (2010), and in contrast to the classical Lassen curve, they also observed a pressure-passive relationship between CBF and ABP. These data also suggested that CA is more efficient to increases in ABP, indicated by a smaller slope, although this difference was lost when the authors corrected for changes in P_aCO_2.

A review by Willie *et al* (2014) lends further support to this idea, and includes a representation of the classical Lassen curve, alongside a more contemporary version of a CA

curve, based on reanalysis of various studies. The contemporary curve demonstrates a very small plateau region, with pressure-passive slopes either side as ABP increases or decreases.

Therefore, CA may not be accurately described by a curve containing a flat plateau over the physiological range of ABPs. As well as a complete paradigm shift compared to the original proposal by Lassen, the papers described above may also have implications for investigation of the upper and lower limits of CA. A pressure-passive relationship could confound identification of the ABP at which CA is overcome. In particular, the paper by Willie *et al* (2014) suggests that upper and lower limits may be incorrectly identified at either side of the small plateau region.

1.4 Ageing

1.4.1 The ageing population

According to Age UK (Later life in the UK fact sheet, 2015), as of October 2015, there were 11.4 million people aged 65 years or older in the UK, and 1.5 million aged 85 years or older. These numbers are expected to steadily rise to 16 million and 3.5 million respectively over the next 20 years. It is also known that 35% of people older than 65 live alone, which is relevant in terms of the increase in health problems generally associated with ageing. A major health issue associated with ageing is the development of hypertension, which is a risk factor for a multitude of cardiovascular diseases, as well as events affecting cerebral blood flow, such as stroke. Only 30-40% of over 65s have normal blood pressure compared to around 80% of those under 65. Of the rest of the population aged over 65, only around 20% are being treated for hypertension, whilst the rest have uncontrolled or untreated high blood pressure. Another of the most prevalent issues in the ageing population is the increased risk of falls. Annually, over 3 million people over 65 years old have a fall, the risk of which is increased after

suffering a stroke, accounting for the majority of emergency hospital admissions for older people. Many falls in the elderly result in fractures or other long-term health issues requiring both immediate medical and longer-term social care. For example, hip fractures are estimated to cost the NHS around £2 billion a year.

Age-related medical and social issues, including hypertension, stroke and falls, have been linked with changes in CBF and the efficiency of CA. For example, hypertension has been shown to be associated with a rightward-shift in the CA curve, and therefore a raised UL (e.g. Sadoshima *et al*, 1985). This is initially protective, preventing forced dilatation of the cerebral vessels in response to increases in ABP. However it is also linked with vascular hypertrophy and increased CVR, which can increase risk of future cerebrovascular events (see 1.4.3.1).

In the stroke-prone SHR model, CA has been shown to fail prior to stroke occurring, such that CBF increased linearly with MABP, and no UL could be identified. Further, isolated MCA segments from pre-stroke rats showed a reduced constriction in response to increases in pressure, which was completely abolished after stroke (Smeda *et al*, 1999). Such a loss of CA in elderly people could pre-dispose them to cerebral hyperperfusion and stroke, as well as an increased risk of future haemorrhage after a stroke.

Reduced mobility and increased incidence of falls in the elderly have also been shown to be associated with changes in cerebrovascular reactivity and CA efficiency. For example, Sorond *et al* (2010) carried out a prospective study of around 400 subjects aged 70 or older. They found that those individuals with impaired cerebrovascular responsiveness to CO_2 had a slower gait, and also tended to report a higher incidence of falls. However CA, assessed by a sit-to-stand procedure to induce orthostatic hypotension (OH), was not found to be associated with gait speed or reported number of falls. Shaw *et al* (2015) performed a cross-sectional

study of 55 subjects aged 65 or older. They used a passive seated orthostatic stress test, and recorded changes in ABP, the cerebrovascular haemodynamic response using a Transcranial Doppler probe, and also collated any history of falls. They found that those who had a history of falls showed a larger delayed drop and a slower recovery in systolic ABP in response to orthostatic stress, as well as a larger drop in CBF velocity. They suggested that this reflected compromised CA in these individuals. They hypothesised that impaired CA could be a link between OH and the increased risk of falls in the elderly. Cerebral hypoperfusion, which is often a consequence of OH, can cause dizziness, reduced cognitive function and loss of balance, which all increase the risk of a fall. OH can also lead to a syncopal episode; a 'fall-like event' involving loss of postural tone. A reduced ability to autoregulate CBF in response to falls in ABP (such as in OH), would therefore increase the risk of cerebral hypoperfusion and a fall.

1.4.2 The use of animal models to study ageing

While it is clear that ageing is associated with a general decrease in cardiovascular and overall health, it is often challenging to assign a reduced function to ageing alone, as opposed to diseases that are commonly seen in older people. For example, ageing arteries show many of the changes seen in atherosclerotic arteries (Lakatta & Levy, 2003). This is compounded by the fact that ageing is not associated with a predictable, homogeneous deterioration of function. These issues mean that the study of age-related changes to a body system in humans can be problematic. However the use of animal models of ageing can be beneficial, as invasive surgical techniques, and use of pharmacological agonists and antagonists, can be implemented to allow isolation of different aspects of the system of interest, which would not be possible in humans.

The rat is particularly useful in studies of ageing as it is not prone to developing certain age-related cardiovascular diseases such as atherosclerosis (Leong *et al*, 2015), and hypertension-prone strains, such as SHRs, must be used to study age-related hypertension (Chamiot-Clerc *et al*, 2001). Therefore the use of standard, healthy rat strains enable the study of ageing in isolation, and thus the rat was the species chosen for the present studies.

On the other hand, when using an animal model with the aim of translating findings to human ageing, the age of animal to use, and the equivalence of ages in the rat and human, is difficult to determine. A review by Ferrari *et al* (2003) gives a minimum age of 65 years old for the study of advanced ageing in humans, which is equivalent to an age of at least 18 months in rats.

Interestingly, studies have shown a steady decline in a variety of cells and functions in the brain after 12 months of age in rats, with neural changes such as a reduced density of dendritic spines in cortical pyramidal neurons (Feldman & Dowd, 1975), a general decrease in neurotransmitter enzyme activity (McGeer *et al*, 1971), and a decrease in β-adrenergic receptors in the striatum and cerebellum (Weiss *et al*, 1979).

It has also been reported that brain functional activity, as assessed by local cerebral glucose utilisation (an index of metabolism), decreases significantly between the ages of 3 and 12 months in Fischer-344 rats (which can live for up to 3 years), but is maintained beyond 12 months (London *et al*, 1981).

Ohata *et al* (1981) studied this further by measuring rCBF, which correlates strongly with changes in cerebral metabolism, using a radiolabelled tracer method, in conscious Fischer-344 rats at ages between 1-34 months. They saw a rise or no change in rCBF between 3-12 months, but a 17% decrease in rCBF between 12-24 months. There were no significant

changes in rCBF between 24-36 months, although there was a trend towards an increase. They suggested that the change in the relationship between metabolism and CBF seen between 12-24 months may reflect a resetting of the normal flow-metabolism coupling, possibly due to an increased sensitivity of the responsible mechanisms.

Balbi *et al* (2015) carried out a similar study in mice, in an attempt to define the age at which dysfunction of the cerebral vessels, and therefore compromised flow-metabolism coupling, begins. They used intravital microscopy and a Laser Doppler probe to assess the pial microcirculation response to a CO_2 challenge, or stimulation of the forepaw, in 6-week, 8-month and 12-month old mice. They found no global CBF changes in mice up to 12 months of age, but they did see a reduction in CO_2 reactivity and flow-metabolism coupling from the age of 8 months. This suggests that, at least in mice, age-related cerebrovascular dysfunction does not occur across all cerebral vessels in parallel, but may affect the pial microcirculation several months before any global CBF changes are seen.

Fischer-344 rats are commonly used as models of ageing. Whilst data from Fischer-344 rats can be drawn on in relation to the current studies, which use Wistar rats (see Chapter 2, General Methods & Materials), it may be difficult to extrapolate between the two strains, as they have been shown to exhibit differences in basal CBF and cerebrovascular reactivity to hypercapnia with ageing (Lartaud *et al*, 1993). No similar studies have been performed in Wistar rats. This strain difference adds to the difficulties of studying ageing and CA, which also include differing techniques for measuring CBF, the use of anaesthetic, whether static or dynamic CA is assessed, and comparing across species (e.g. between mouse, rat and human).

In our laboratory, we have previously used Wistar rats of 4-5, 10-12 and 42-44 weeks of age, to represent juvenile, sexually mature and middle-aged humans respectively (Omar &

Marshall, 2010a & b). These ages were based on a review by Folkow & Svanborg (1993), which considers the effects of ageing on cardiovascular physiology and the usefulness of animal models of ageing. They compared the average lifespan of laboratory rats (2.5-3 years) and humans (70-80 years) to assess relative ages. Based on this, the 42-44 week old rats are equivalent to 40-45 year old people (Omar & Marshall, 2010a & b).

Sengupta (2013) reviewed the various methods used to correlate rat and human ages, which include using eye lens weight, growth of molar teeth, counting endosteal layers of the tibial bone, and comparing rates of bone growth, specifically looking at the appearance of ossification centres and the closure of epiphyseal plates. Both humans and rats progress through similar 'phases' of mammalian life, however the rates of change in the above indicators can vary. Compounding this issue is the fact that the length of, and relative age at which each of these phases are experienced, differs between the species. Therefore the author concluded that a simple correlation of average life span may not be sufficient. Rather, researchers should consider the phase of life being studied. For example, whilst a comparison of whole life span gives a correlation of 1 human year to 14 rat days, considering the pubescent phase gives a correlation of 1 human year to 3 rat days, and the phase after reproductive senescence, in which an animal might be considered 'aged', gives 1 human year as 17 rat days (Sengupta, 2013).

Recognising the difficulties of direct comparison between animals and humans during ageing, the following sections attempt to summarise the general cardiovascular effects of ageing, as well as the specific effects on various aspects of the cerebral circulation.

1.4.3 The effects of age on the cardiovascular system and cerebral vasculature

1.4.3.1 Age-related changes in the cardiovascular system

The general effects of ageing on the cardiovascular system are summarised in Table 1, adapted from Ferrari *et al* (2003). Cardiac changes include an increase in heart weight, indicating a hypertrophy which occurs in the absence of any afterload-increasing disease (Gerstenblith *et al*, 1977). This hypertrophy is driven by a loss of cardiomyocytes and a resulting compensatory increase in myocyte volume (Webb & Inscho, 2005, Oxenham & Sharpe, 2003). There is also a decreased cardiac responsiveness to sympathetic stimulation, accompanied with a decrease in cardiac sympathetic innervation (McLean *et al*, 1983), and a decrease in heart rate and cardiac output during exercise (Fleg *et al*, 1995).

Vascular changes in the large arteries include an increase in the thickness of the arterial wall, mainly in the intima and media (Virmani *et al*, 1991), a thickened basement membrane (Donahue *et al*, 1967), an increase in inflammatory markers (Challah *et al*, 1997), increased subendothelial collagen, increased migration of vascular smooth muscle cells, and reduced levels of elastin (Hajdu *et al*, 1991). Ageing arteries therefore show a reduced distensibility (Roach & Burton, 1959, Hajdu *et al*, 1990), although this is not solely due to reduced levels of elastin, but also due to the age-related reduction in endothelial-mediated, NO-dependent vasodilatation (Taddei *et al*, 1995).

These general age-related changes manifest as an increased total peripheral resistance, which leads to an increased systolic pressure. This increased pressure drives arterial wall and left ventricular hypertrophy, and so a cycle is formed. An increased systolic blood pressure and pulse pressure then predispose for development of further cardiovascular diseases, including an increased risk of cerebrovascular events. In fact, ultrasound of the carotid artery to

examine intima-media thickening can be predictive for the risk of heart attack and stroke (O'Leary *et al*, 1999).

The arterial baroreceptor reflex is also known to change with ageing. The parasympathetic, baroreceptor-mediated decrease in heart rate, in response to a PE-induced increase in blood pressure, is reduced in old (75-90 weeks) compared to young (5-6 weeks) rats. However the sympathetic branch of the reflex (assessed by bilateral common carotid artery occlusion), which acts to regulate peripheral resistance, tends to be well maintained with age (Ferrari *et al*, 1991). A reduced baroreceptor reflex with age, particularly the sympathetic branch, would be significant for CA, as it may expose older individuals to increased fluctuations in blood pressure.

1.4.3.2 Age-related changes in the cerebral vasculature

The cerebral vasculature shows age-related changes similar to the vascular changes seen in the cardiovascular system as a whole.

Cox (1977) showed that circumferential stress-strain (a function of pial pressure, diameter and wall thickness) was left-shifted, and tangential elastic modulus vs stress responses (reflecting tissue stiffness) were increased in segments of internal carotid arteries, from aged male rats. There was also an increase in the collagen/elastin ratio, suggesting a decreased distensibility of the carotid artery with age.

Nagasawa *et al* (1979) undertook a similar study using human vertebral and basilar arteries, and also saw an increased wall thickness, increased collage/elastin ratio, due to increased collagen levels, and decreased distensibility with ageing. In the microvasculature, the most commonly reported morphological change with ageing is an increased thickness of the

basement membrane, which may be accompanied by a thinning of the endothelium (Burns *et al*, 1979).

Hajdu *et al* (1990) assessed pial arteriole pressure and diameter, in anaesthetised, adult (9-12 months) and old (24-27 months) Fischer-344 rats. Using an open cranial window, pressure measurements were made using a micropipette inserted into the lumen of a pial arteriole, and arteriolar diameter was recording using a microscope and camera system. Haemorrhage was induced to assess pressure-diameter relationships. Arterioles were then restored to *in vivo* pressures, fixed, dissected and sectioned to assess luminal and total cross-sectional area. As shown in Figure 6, the diameter responses to changes in pressure were downwards shifted in the old rats. Stress-strain curves were leftward shifted, and the slope of the tangential elastic modulus vs strain curve was increased with age. The cross-sectional areas of smooth muscle, elastin and endothelium were reduced with age, as was the total cross-sectional area of the vessel wall. Due to the decrease in elastin levels, the collagen/elastin ratio was increased in the aged rats (see Figure 6). Therefore pial arterioles appear to undergo atrophy with ageing, and this is associated with a decrease in distensibility, which might be expected to affect CA.

1.4.4 The effects of ageing on cerebral endothelial structure and function

In normal, healthy vessels, the endothelium is in a state of balance between endothelium-derived vasoconstrictor and vasodilator factors. Ageing cerebral vessels are known to undergo endothelial changes, both structural and functional, which result in this balance being disrupted.

1.4.4.1 Age-related changes in endothelial structure

The number of mitochondria in endothelial cells have been shown to decrease in the cerebral cortex of aged monkeys (Burns *et al*, 1979), although the area taken up by mitochondria in the

capillaries of aged rats appears to be increased, in association with a thinning of the capillary endothelium, and thickening of the basement membrane (Topple *et al*, 1990). It has also been shown that there is a decrease in endothelial area, and an increase in endothelial permeability due to a loss of pericytes, which normally maintain the integrity of the BBB (Stewart *et al*, 1987). This could potentially leave aged individuals more vulnerable to leaks across the BBB.

1.4.4.2 Age-related changes in endothelial function: Release of and response to vasoactive substances

As well as structural changes, release of and response to endothelial-derived, vasoactive substances have also been shown to be affected by age. Amrani *et al* (1996) showed that, in isolated heart preparations from rats at 1, 5, 15, and 26 months of age, the NOS inhibitor L-NMMA caused a decrease in coronary flow, whilst 5-HT (5-hydroxytryptamine, an endothelium-dependent vasodilator) caused an increase. The magnitude of both of these responses was significantly reduced with increasing age. They also directly measured NO release in the coronary effluent, and saw a significantly decreased NO release with age. Perfusion with 5-HT increased NO release in all groups, but the trend for a significantly reduced release with age persisted. These data suggest, at least in coronary endothelium, that ageing decreases both basal and stimulated NO release. However, Paterno *et al* (1994) studied the ACh-induced release of endothelial-derived relaxing factor (EDRF) from carotid 'donor' arteries from rats aged 6-8, 24-26 and 30-32 months, and the ability of the donor arteries to induce dilatation in aortic 'detector' vessels. They found that, whilst vasodilatation of the donor vessels themselves was reduced with ageing, release of EDRF from the donor vessels to induce vasodilatation in the detector vessels was unaffected. This suggests that ACh-induced, endothelium-dependent vasodilatation is impaired with ageing, but that the release of EDRF is not.

Mayhan *et al* (1990) used a cranial window preparation to assess the diameter response in cerebral arterioles of 6-8 month old and 22-24 month old Wistar rats. They found that ACh and bradykinin-induced vasodilatation was reduced in aged rats, whilst the response to nitroglycerin was maintained. The vasoconstrictor response to thromboxane was similar between the adult and aged rats. Further, infusion of indomethacin to inhibit production of cyclooxygenase (COX) vasoconstricting products, did not increase the response to ACh in aged rats. These data suggest an age-related impairment in endothelial function, specifically a reduced vasodilatation which is not associated with an increase in COX products.

Similar data was seen in experiments by Eisenach *et al* (2014), who studied young (18-38 years old) and older (55-73 years old) healthy volunteers. They gave ACh intra-arterially and measured forearm vascular conductance, before and after COX-2 inhibition, and during NOS inhibition. Forearm dilatation to ACh was significantly reduced in the older group, and was attenuated by NOS inhibition in both age groups. COX-2 inhibition had no effect on the response to ACh in either group.

However, other studies have shown that, as well as changes in the release or response to vasodilatory substances, ageing may also be associated with an increase in vasoconstrictor substances, such as an increased contribution by COX-derived vasoconstrictor products. For example, Heymes *et al* (2000) found that the response to ACh in aortic rings from aged Wistar rats (24 months old) was biphasic, showing relaxation to low doses, but constriction to higher doses, in comparison to consistent relaxation in aorta from young rats (4 months old). The response in aorta from young rats was unaffected by indomethacin, by specific COX-1 and COX-2 inhibitors, or by a thromboxane receptor antagonist. By contrast, the COX inhibitors all reduced the 1st phase of ACh-mediated relaxation in aorta from aged rats, and

both the COX and thromboxane inhibitors reduced the 2nd phase of constriction. Further, in both young and aged rats, high-dose ACh-induced release of prostaglandins and thromboxane in an endothelium-dependent manner, but this was significantly increased in the preparations from aged rats. Similarly, Denniss *et al* (2011) found that relaxation in segments of common carotid arteries in response to a cumulative ACh dosing protocol, was similar between adult and old rats at lower doses. However, dilatation was reduced in old vs adult rats at higher doses; a difference which was attenuated by COX inhibition, but was unaffected by NOS or reactive oxygen species (ROS) inhibition, suggesting an increase in COX-mediated constriction in the carotid arteries of older rats.

Lee *et al* (1987) assessed the response of cerebral arteries from young and aged rats, to various vasodilating agents, including NO donors, as well as to 8-bromo-cGMP, an activator of the cGMP signalling pathway. The relaxation seen in response to vasodilators was reduced with age and experimentally-induced hypertension. However this age-related reduction was only seen in cerebral vessels with an intact endothelium, but not in denuded preparations. Moreover, the response to 8-bromo-cGMP was unaffected by removal of the endothelium, and also by age and hypertension. This suggests that the vasodilator capacity of the vascular smooth muscle is not reduced with age, and that the reduced responsiveness to vasodilators is a result of dysfunction of the endothelium.

A reduced ability to vasodilate might be expected to cause an imbalance in the control of cerebrovascular tone with ageing, tipping the balance towards an increasingly vasoconstricted state, reducing CBF and potentially causing ischaemia (Mayhan *et al*, 1990). One of the major contributory factors to decreased endothelial function with ageing is an increase in ROS, which disrupt the production of, and responsiveness to NO (see 1.4.5).

1.4.4.3 Age-related changes in NOS expression and function

As well as alterations in the vascular response to endothelial-derived vasoactive substances, there is also evidence for age-related changes in NO production and NOS expression, which varies between the different NOS isoforms.

Some studies have observed excessive NO production in the ageing brain, and this has been hypothesised as a contributory factor in the ageing process (McCann *et al*, 1998). This is supported by several studies showing an increase in NOS-containing neurones in the CNS, detected by histological staining for NADPH-d (the electron donor in NO synthesis), and has been linked with neurodegenerative diseases (reviewed by Jung *et al*, 2012).

Siles *et al* (2002) investigated NOS expression using a Western blot, and NO production by assaying the amount of tissue nitrite and nitrate, in the brains of 2-, 4- and 30-month old rats. They found no significant change in nNOS, eNOS or iNOS levels in the aged rats, or in levels of NO in brain tissue.

On the other hand, some studies have shown a decrease in NO with ageing, which has been linked with a reduction in memory and learning capacity. For example, Yamada & Nabeshima (1998) showed that NADPH-d staining was reduced in the striatum and cortex of aged rats, but unchanged in the hippocampus.

Specifically focussing on NOS activity, Chalimoniuk & Strosznajder (1998) assayed NOS and guanylate cyclase activity in brain slices of adult (3 month old) and aged (28 month old) rats, and found a decrease in basal cGMP (the secondary messenger in the NO signalling pathway), but a significantly increased NOS activity in the aged brain. NMDA-induced increases in cGMP were also reduced in the hippocampus and cerebellum of aged rats. Jesko *et al* (2003) followed up this study to assess the expression and activity of specific NOS

isoforms, in 4- (adult), 14- (old adult), and 24-month old (aged) male Wistar rats. Brain homogenate preparations were used to detect iNOS and nNOS mRNA levels, as well as NOS activity via production of radiolabelled citrulline, in the presence or absence of the nNOS inhibitor 7-NI, and constitutive NOS inhibitor L-NNA. They found that NOS activity was higher in all parts of the aged brain, whilst nNOS mRNA levels were reduced. iNOS mRNA was not detected in adult or aged rat brains. L-NNA inhibited NOS activity in both adult and old brains, whereas 7-NI reduced NOS activity to a greater extent in the aged brain. They therefore suggested that a specific increase in nNOS activity was responsible for the apparent increase in NOS activity with age, possibly due to the observed altered nNOS phosphorylation state. They also suggested that the paradoxical decrease in nNOS mRNA may be a feedback response to the increased NOS activity, and therefore increased NO release. Such a negative feedback loop has been demonstrated, both by NO binding to the heme-iron bond in NOS to reduce enzyme activity, and by NO-mediated inhibition of eNOS and iNOS expression (decreasing mRNA levels), by inhibition of the transcription factor NF-κβ (reviewed by Kopincová *et al*, 2011).

The same group also investigated the expression and activity of eNOS in 4- (adult) and 24-month old (aged) male Wistar rats, using the same techniques as the study above. They found that eNOS mRNA was significantly increased in the brains of aged rats, although the level of eNOS protein was not different between adult and aged rats. In the presence of 7-NI, the resistant NOS activity was significantly lower in cerebellum from aged rats. These data suggest possible age-related changes in translation, post-translational modifications, or a decrease in the ability of the NOS protein to synthesise NO, possibly due to oxidative-stress induced damage (Strosznajder *et al*, 2004).

In conclusion, the majority of studies indicate that NOS expression is increased with ageing. This could either lead to excessive production of NO, or, due to the potential for NOS to become uncoupled with ageing, result in the production of reactive oxygen and nitrogen species. These free radicals cause cellular damage and further drive the endothelial dysfunction associated with ageing (as discussed in 1.4.5.2).

1.4.5 Ageing and oxidative stress

1.4.5.1 Molecular mechanisms of oxidative stress

Oxidative stress is one of the biological hallmarks of ageing. It is caused by reactive free radicals, such as oxygen and nitrogen species, damaging cellular components including proteins, lipids, DNA and telomeres. This damage is associated with a number of age-related pathologies and can alter gene regulation, resulting in cell senescence and apoptosis (reviewed by Venkataraman *et al*, 2013). An accumulation of this oxidative damage underpins the free radical theory of ageing proposed by Harman (1956). The theory suggests that free radicals, and the resulting gradual increase in oxidative damage to cellular components, is the common mechanism underlying the effects of both irradiation, which can cause dissociation of water molecules to produce free radicals, and ageing.

Free radicals are produced endogenously, the majority during aerobic respiration in the mitochondria. They are formed as a by-product of the electron transport chain, whereby the electrons bind with oxygen molecules to form superoxide (O_2^-) (Matsuzaki *et al*, 2009). O_2^- is itself a damaging free radical species, although it cannot easily leave the mitochondria. It can, however, react with water, or be converted via superoxide dismutase (SOD), to produce hydrogen peroxide (H_2O_2), which can more easily cross the mitochondrial membrane into the cell. It can also be converted to peroxynitrite ($ONNO^-$) via a reaction with NO, effectively

blocking NO's normal vasodilatory action (Castro *et al*, 2011). Once in the cell, both H_2O_2 and $ONOO^-$ are highly reactive with a variety of cellular components. Damage caused by free radicals includes DNA damage, particularly to mitochondrial DNA, degradation and functional impairment of proteins, damage to cell membranes and therefore a potential compromise in cell integrity (reviewed by Venkataraman *et al*, 2013).

In relation to the brain, it has been shown that free radicals are a key factor in the functional impairment seen in the brain during ageing (Poon *et al*, 2004).

Free radicals are usually buffered by the body's antioxidant system, which includes enzymes such as SOD, and non-enzymatic antioxidants such as vitamin C. In fact OH^- (hydroxide ion) and NO^- play a role in signalling to increase the level of antioxidants (Matsuzaki *et al*, 2009). In contrast, $ONOO^-$ can cause oxidation of antioxidants themselves, and can also oxidize the eNOS cofactor BH_4, causing uncoupling of the enzyme (Kuzkaya *et al*, 2003), as shown in Figure 7. In turn, uncoupled NOS produces O_2^-, and the O_2^- species produced by uncoupled eNOS has been implicated in various cardiovascular diseases (Luo *et al*, 2014).

A state of oxidative stress occurs when endogenous antioxidants can no longer cope with the level of free radicals, and the balance is tipped in the direction of oxidative damage.

1.4.5.2 Functional consequences of oxidative stress

Reduced endothelium-dependent dilatation (EDD) is often seen in the systemic circulation with ageing, due to reduced eNOS-derived NO bioavailability (Eskurza *et al*, 2005). This decrease in NO bioavailability is caused by a decline in NO synthesis (see 1.4.2), as well as increased levels of oxidative stress, particularly increased levels of O_2^-, which is known to degrade NO to form $ONNO^-$ (see 1.4.3.1).

Age-related declines in NOS expression or activity have not been reported in cerebral tissue (e.g. Jesko *et al* 2003, see 1.4.2), thus the likely explanation for decreased NO synthesis is a decrease in levels of a NOS cofactor, such as BH_4. BH_4 is known to be sensitive to oxidative damage by free radicals, which leads to formation of the oxidized forms BH_3 or BH_2 (Kuzkaya *et al*, 2003). Further, BH_4 synthesis may be decreased with ageing due to a reduction in the levels or activity of the enzyme GTPCH I, which is the rate limiting enzyme in the synthesis of BH_4 from GTP (Werner-Felmayer *et al*, 2002). Ultimately, reduced BH_4 levels can lead to uncoupling of eNOS, and an increased production of O_2^- (Kuzkaya *et al*, 2003, see Figure 7).

Eskurza *et al* (2005) measured the diameter of the brachial artery in humans using an automatic vascular wall-tracking system, and assessed flow-mediated dilatation (FMD) in response to brachial artery occlusion, to assess EDD, as well as the response to a sublingual dose of the NO donor nitroglycerine. Studies were performed in young adults and sedentary older adults, before and after oral administration of a single, high dose of BH_4. Control FMD was significantly lower in the older subjects, and was restored to levels close to those seen in the young group by BH_4. The response to nitroglycerine was not different between the young and old groups, and was unaffected by BH_4. This study suggests that the impaired EDD seen with ageing is contributed to by a reduction in BH_4 bioavailability, whilst endothelium-independent dilatation is unaffected.

On the other hand, Santhanam *et al* (2007) demonstrated that reduced EDD with ageing may be due to a decrease in the levels of the NO precursor L-Arginine, caused by an increased activity of the enzyme Arginase I. They showed that Arginase I increasingly competes with NOS for the substrate L-Arginine in the tail artery and thoracic aorta of aged rats, due to an

NO-mediated post-translational modification of Arginase I. They also demonstrated that inhibition of Arginase I increased NO production and EDD in vessels from aged rats.

Delp *et al* (2008) used myography to observe the diameter response to changes in flow in skeletal muscle arterioles from young (6 months old) and old (24 months old) rats, in order to investigate age-related decline in EDD. In contrast to the hypothesis put forward by Santhanam *et al* (2007), they found that administration of an Arginase I inhibitor or exogenous L-Arginine did not improve EDD in arterioles from old rats. They also found no difference in the levels of L-Arginine in the arterioles of the young and aged rat groups. However, they did find a decrease in the levels of vascular BH_4, and that administration of a BH_4 precursor significantly improved EDD in arterioles of old rats. This improvement in EDD was significantly reduced by L-NAME, demonstrating that the improvement was mainly mediated by an increase in NO. The differences between these studies may lie in the different vessels studied, and suggests that the mechanisms underlying the age-related decrease in EDD may vary across the vascular tree.

Regarding the effects of oxidative stress in aged cerebral vessels, Mayhan *et al* (2008) studied the role of oxidative stress in the changes in responsiveness of aged cerebral arterioles. They used a cranial window preparation to measure diameter responses of pial arterioles, and found that ACh-induced dilatation was reduced in vessels from aged (22-24 month), compared to adult (2-3 months) Fischer rats. Application of the antioxidants tempol, apocynin and DPI, all reduced the age-related impairment. A Western blot demonstrated an increase in the expression of NADPH oxidase subunits (an enzyme responsible for producing physiological superoxide used by neutrophils, but which is also implicated in the pathology of atherosclerosis) and a decrease in the antioxidant SOD-1 in aged cortical tissue. They also used a chemiluminescence technique, and detected an increased superoxide production in

aged rats, both basally and in response to stimulation by NADPH. Further, Santhanam *et al* (2014) showed that GTPCH-1 (an enzyme involved in BH_4 synthesis) deficient mice demonstrated increased O_2^- levels and decreased endothelial NO in cerebral microvessels, and that treatment with EPO, to restore BH_4 levels, restored NO bioavailability.

As well as its essential role in NO synthesis, BH_4 is also a cofactor for the enzyme tyrosine hydroxylase (TH). This enzyme catalyses the rate-limiting step of the synthesis of catecholamines, including noradrenaline (Nagatsu & Nagatsu, 2016). Therefore age-related decreases in BH_4, either due to oxidative damage or decreased synthesis, may also have implications for noradrenaline content in sympathetic nerves, and therefore for the role of cerebral sympathetic innervation in CA (see 1.3.3.1). Kapatos *et al* (1992) examined the effect of inhibiting BH_4 on TH activity and levels of noradrenaline in cultured sympathetic neurones from the SCG of neonatal rats. When BH_4 synthesis was inhibited, causing a 95% decrease in BH_4 levels, TH activity was also decreased by 75%, and noradrenaline content declined gradually over 4 days, to around 25% of the control levels. Interestingly, acute BH_4 supplementation has been shown to reduce sympathetically-mediated vasoconstriction, in both resting and contracting skeletal muscle in rats. It is hypothesised that NO, which would have been increased by administration of BH_4, is responsible for the blunting of sympathetic vasoconstriction, which is particularly important in exercising skeletal muscle (Jendzjowsky *et al*, 2014). This could indicate that BH_4 supplementation improves NO bioavailability to a greater extent than it increases levels of catecholamines.

In conclusion, ageing, and the oxidative stress associated with it, appears to decrease the synthesis and/or release of NO in cerebral vessels, as well as other vascular beds, and is manifested as a decrease in endothelium-dependent vasodilatation.

1.4.6 The effects of age on autonomic control of the cerebral vasculature

1.4.6.1 Age-related changes in cerebral innervation

As discussed in 1.3.3, it has been shown that large cerebral arteries, arterioles, and at least the outermost portion of parenchymal vessels, are innervated by both sympathetic and parasympathetic fibres. Several studies have shown that there is an age-related decrease in this innervation.

1.4.6.1.1 Changes in sympathetic innervation and nerve activity

Mione *et al* (1988) reported a reduction in noradrenergic innervation density between 8-27 months of age, and serotonergic innervation density between 4-27 months of age, on vessels in the Circle of Willis, and its branching arteries, in male Wistar rats. Saba *et al* (1984) demonstrated that both glyoxylic acid staining for noradrenergic fibres, and histochemical staining for acetylcholinesterase, were reduced in the MCA of aged rabbits (3 years old). Cowen & Thrasivoulou (1990) studied the accumulation of 5-HT (serotonin) in noradrenergic, sympathetic nerves, using immunohistochemistry, as well as the density of nerve fibres using the neuronal marker PGP9.5. They incubated the MCA, PCA and internal carotid arteries of rats, at 3-4 months old compared to 24-30 months old, with exogenous 5-HT for 30-60 mins. 5-HT was used as an indicator of sympathetic nerve density, as the 5-HT transporter, a type of monoamine transporter, is responsible for uptake of 5-HT into sympathetic nerve fibres. Densitometric image analysis revealed significantly lower immunofluorescence in nerve fibres in all vessels in the aged animals. Nerve density was also lower in the MCA and PCA of the old animals, showing that cerebrovascular nerve fibres are generally lost with ageing.

In our lab, Omar & Marshall (2010b) demonstrated age-related changes in sympathetic innervation in the MCA and BA of male Wistar rats, using glyoxylic acid staining.

Innervation density was increased from juvenile (4-5 weeks) to mature rats (10-12 weeks), but was decreased by middle-age (42-44 weeks) (see Figure 8). In contrast, innervation density in the femoral artery and caudal ventral tail artery appeared to increase with age, suggesting possible differences between tissues and organs across the vascular tree.

In contrast, others have shown that NPY and substance P-containing fibres appear to be unchanged with ageing, as innervation was not significantly reduced in rats up to the age of 27 months old (Mione *et al*, 1988). This raises the possibility that NPY, which is generally thought of as a co-transmitter associated with noradrenaline, must also be located in fibres other than noradrenaline-containing fibres.

Despite the apparent decrease in innervation with ageing, resting sympathetic nerve activity has widely been reported to increase with age, in both humans (Iwase *et al*, 1991) and rats (Ito *et al*, 1986).

1.4.6.1.2 Age-related changes in parasympathetic innervation and nerve activity

Cholinergic nerves have also been studied in ageing, and have been shown to be differentially affected across different brain regions. For example, Hamel *et al* (1990) showed that accumulation of choline was decreased by 25%, and ChAT significantly increased by 187% in the major cerebral arteries of 22 month old Fischer-344 rats. However, looking at the same markers in the small pial arteries revealed no age-related change. They also showed a maintained response of the BA to ACh and noradrenaline, as well as other vasoactive drugs. Further, Mione *et al* (1988) showed a significant increase in the levels of nerve fibres containing the vasodilator neurotransmitters calcitonin gene-related peptide (CGRP) and VIP in aged rats (from 4-8 months of age), and VIP has been shown to be co-localised with ACh in nerve fibres originating from the PPG (Hara *et al*, 1985).

There is little data on the effect of ageing on parasympathetic nerve activity, however vagal function has been shown to decrease with ageing. For example, a reduced parasympathetic contribution to heart rate variability has been reported in healthy humans aged 50 years and older (Korkushko *et al*, 1991). Further, the decreases in HR induced by atropine, and the M_1 ACh receptor antagonist pirenzepine, were reduced in healthy, older subjects (60±2 years) compared to younger subjects (26±2 years) (Poller *et al*, 1997).

1.4.6.1.3 Age-related changes in neurotransmitters and receptors

It is possible that there are also age-related changes in neurotransmitter content and release, and in adrenergic and cholinergic receptor density and/or sensitivity. For example, although α1-adrenoreceptor-mediated vasoconstriction appears to be maintained with age in the dorsal hand veins of healthy male volunteers, α2-adrenoreceptor responses are reduced (Pan *et al*, 1986). Since pre-junctional α2 receptors are involved in negative feedback to reduce noradrenaline release, the decrease in α2-mediated responses, coupled with reduced noradrenaline reuptake, may explain the increase in plasma levels of noradrenaline seen with ageing (Ziegler *et al*, 1976). β-adrenoreceptors are also affected by ageing. Kobayashi *et al* (1982) showed that, in brain microvessel preparations from 3- and 24-month old male Sprague-Dawley rats, ageing was associated with a decrease in the density of β-adrenoreceptors.

Catecholamine content and release from nerve terminals has also been shown to decrease with age in rats (Daly *et al*, 1988), as has neuronal noradrenaline uptake in the cardiovascular system (Borton & Docherty, 1989). There are contrasting reports regarding the effects of ageing on catecholamine synthesis. As discussed previously, age-related oxidative stress can cause a decline in BH_4, a cofactor for catecholamine synthesis, leading to a decrease in TH activity and therefore noradrenaline content (see 1.4.3.2). However, increased TH and ChAT

activity have also been reported in the aged rat SCG and adrenal gland respectively (Partanen *et al*, 1985), which may be compensatory for the decreased content.

Regarding cholinergic receptors, Nordberg *et al* (1992) showed in post-mortem human brains, that ageing is associated with regional changes in ACh receptor density. Both muscarinic and nicotinic receptors were decreased in the cortex, but increased in the thalamus with age. Araujo *et al* (1990) assessed the density of cholinergic receptors using radioligand binding, and found that nicotinic and muscarinic (M_2) binding sites were decreased in the thalamic, striatal, hippocampal and cortical tissue of aged rats, whereas M_1 receptor levels were maintained.

1.4.6.2 Functional implications of age-related changes in cerebral innervation

1.4.6.2.1 Functional implications of sympathetic changes

As discussed in 1.3.3.1, the role of sympathetic innervation of the cerebral vasculature in the control of CBF is controversial. Some studies have shown no effect of sympathetic stimulation or denervation on basal CBF, whilst others have suggested a role in maintaining basal vascular tone, and also in the autoregulatory constriction in response to increases in ABP. As sympathetic innervation, receptor density, and catecholamine synthesis all decrease with ageing, it is reasonable to expect that this may cause an altered basal cerebrovascular tone, and a compromised ability to vasoconstrict.

This has been investigated by Hervonen *et al* (1990), who measured cortical CBF by Laser Doppler flowmetry, and stimulated cervical sympathetic trunks in adult (4-6 months) and aged (28-32 months) anaesthetised rats. They saw an initial increase, followed by a decrease in cortical CBF, which was frequency-dependent, and was similar between the adult and aged rats, suggesting that sympathetic control of cortical CBF is not affected by ageing.

In some contrast, Shiba *et al* (2009) investigated the effect of stimulation of the cervical sympathetic trunks, which innervate the olfactory bulb as well as the cerebral vasculature, on olfactory bulb blood flow, measured by Laser Doppler flowmetry. They found that stimulation at 30Hz caused a ~30% decrease in blood flow in young (4-6 months), anaesthetised Wistar rats, but in aged rats (18-21 months) the largest decrease in blood flow was ~15% at 20Hz. When stimulation was repeated after i.v. administration of phenoxybenzamine (an α-adrenergic antagonist), the decrease in blood flow was abolished in both age groups. If the cerebral vasculature behaves in the same way as the olfactory bulb, these data suggest that sympathetic nerve fibres produce an attenuated α-adrenoreceptor-mediated vasoconstriction in old relative to young rats.

1.4.6.2.2 Functional implications of parasympathetic changes

The cerebral vasculature is also innervated by parasympathetic nerves, which have been shown to cause cerebral vasodilatation (see 1.3.3.2). The effect of ageing on this innervation seems to be selective, with decreases in innervation in some cerebral vessels, and regional decreases in specific types of ACh receptor in the brain. In terms of implications for CBF control, Biesold *et al* (1989) studied the Nucleus Basalis of Meynert (NBM), an area of the basal forebrain rich in acetylcholine and ChAT, which has been shown to contain cholinergic neurones that project to the cerebral cortex, and terminate on cerebral blood vessels. Stimulation of the NBM, either electrically or by microinjection of L-Glutamate, increased cortical CBF in the parietal cortex of anaesthetised, adult Wistar rats, independently of any pressor effects. The muscarinic antagonist atropine (administered i.v.) reduced the vasodilatation by around 40%, and subsequent administration of the nicotinic antagonist mecamylamine abolished the remainder of the increase in cortical CBF. These data suggest that cholinergic projections from the NBM release ACh to cause vasodilatation in the cortex,

and show a classical parasympathetic distribution of cholinergic receptors. Further, the muscarinic antagonist methylatropine, which cannot cross the BBB (in contrast to atropine and mecamylamine), had no effect on the cortical vasodilatation. The authors suggested that this reflected an extraluminal location of these cholinergic receptors, i.e. located on the brain side of the BBB, rather than the luminal side. This is supported by Araujo *et al* (1990), who showed, by staining for ChAT, that both muscarinic and nicotinic autoreceptors (pre-ganglionic) are present in hippocampal, cortical and cerebellar tissue in rats, and that both were decreased in the forebrain with ageing.

Uchida *et al* (2000) extended these findings to include the effect of ageing on this cholinergic cortical vasodilatation. Stimulation of the NBM caused similar increases in cortical CBF in young adult rats (4-7 months) and old rats (24-25 months). However, in very old (32-42 months) rats, the response was significantly attenuated. Further, they demonstrated that i.v. injection of nicotine (which can cross the BBB, and alter its permeability) produced a dose-dependent increase in cortical CBF in young rats, which was reduced by ~50% by lesion of the NBM. The dose of nicotine required to increase CBF in old rats was significantly higher than in young, and the increase in CBF was significantly attenuated in very old rats (Uchida *et al*, 1997). On the other hand, the response to a muscarinic ACh receptor agonist, arecoline, was well maintained between the age groups, suggesting that the decrease in cholinergic vasodilatation in very old rats is due to a loss of cortical nicotinic ACh receptors (Uchida *et al*, 2000).

In contrast to the above studies, Araujo *et al* (1990) observed that, functionally, it was primarily muscarinic receptors that were compromised with ageing. However, these results were tissue specific, emphasising that different types of cholinergic receptor appear to be differentially affected by ageing depending on the brain region studied.

1.4.7 The effects of ageing on cerebral blood flow and autoregulation

1.4.7.1 The effects of ageing on basal CBF

It is generally agreed that ageing is associated with a decrease in CBF and cerebral blood volume, and a decrease in the cerebral metabolic rate of oxygen ($CMRO_2$) and oxidation of glucose in humans with no other age-related condition (Burns & Tyrrell, 1992, Leenders *et al*, 1990).

For example, Claus *et al* (1998) studied rCBF in 60 people aged between 65-84 years, using SPECT (single photon emission computed tomography). They assessed age-related changes in rCBF, as well as any relationships between rCBF and cerebrovascular risk factors in the study population. Health status, medical history including any cerebrovascular event, drug prescriptions and use, smoking status, blood pressure, cholesterol level, intima-media wall thickness and presence of atherosclerotic plaques in the carotid artery (assessed by ultrasonography), and cortical atrophy or cerebral white matter lesions (assessed by an MRI scan) were considered as risk factors. By using multiple linear regression analysis, they found that increasing age was associated with decreased rCBF in all cortical regions studied (frontal, temporal, parietal and temporo-parietal). When the majority of the cerebrovascular risk factors were added to the regression analysis, the relationship between age and rCBF was still statistically significant. The only risk factor that altered the relationship was the indicator of carotid atherosclerosis, which greatly reduced the strength of correlation between age and rCBF in all regions, particularly the temporo-parietal region.

The authors suggested that the observed age-related increase in atherosclerosis, which attenuated the relationship between age and rCBF, contributes to the reduced elasticity and contractility seen in ageing cerebral arterial vessels, and the lower CBF. They also showed

that this reduced elasticity is associated with a rightwards-shift in the LL of autoregulation to a higher ABP; the UL was not investigated.

Similarly, Amin-Hanjani *et al* (2015) assessed CBF in healthy adult volunteers aged 18-84 years old, and found that CBF declined with age by around 2.6ml·min^{-1} per year. When 3 age ranges were defined, CBF was lowest in the oldest group (61-80 years).

Considering rats, Berman *et al* (1988) studied rCBF, and the ability to learn a maze for a food reward, in male, Sprague-Dawley rats at 6-, 12- and 24-months of age. The 24-month old animals demonstrated a significantly decreased ability to learn the maze, which was strongly correlated with a decrease in basal cortical blood flow.

However, similar findings have not been made in other studies on rats, which often show no change in CBF with age. For example, Ohata *et al* (1981) measured CBF in 14 brain regions using a radiolabelled tracer technique, in awake Fischer-344 rats at 5 ages; 1, 3, 12, 24 and 34 months. rCBF rose between 1-3 months in all studied brain regions, a slight rise or no change in rCBF was seen between 3-12 months, and an average 17% decrease in rCBF was seen between 12-24 months. There were no significant changes in rCBF between 24-36 months, although there was a trend towards an increase. When the rCBF data was compared with reported local cerebral glucose utilisation levels over the same age ranges, it was revealed that there was not a direct coupling between the two parameters. Local cerebral glucose utilisation increases between 1-3 months, but shows a large decrease between 3-12 months, and then remains stable after 12 months. This suggests a possible change in cerebral oxidative metabolism between 3-12 months, which resets the functional coupling between rCBF and cerebral metabolism.

1.4.7.2 The effects of ageing on CBF responses and cerebral autoregulation

As well as changes in basal CBF, ageing has been associated with changes in CBF responses, for example to CO_2, and CA. For example, Springo *et al* (2015) investigated the effect of ageing on myogenic tone in isolated MCAs of young (3 months) and aged (24 months) mice. As discussed in 1.3.1.1, myogenic tone is considered to play a vital role in the maintenance of CBF in the face of ABP fluctuations, as well as in the adaptation to pulse pressure waves, protecting the cerebral microcirculation from haemorrhagic injury. They mounted MCA segments on micropipettes, and vessel diameter was recording during exposure to static, stepwise increases in intraluminal pressure (20-140mmHg), as well as pulsatile intraluminal pressure changes (450 pulses per minute, amplitude of 40mmHg). The MCAs from young mice showed myogenic constriction across the range of static pressures. However, MCAs from aged mice showed a decrease in myogenic tone at the higher pressures, and an increase in vessel diameter. In response to pulsatile pressure, young MCAs displayed effective myogenic constriction, whilst the constriction seen in aged MCAs was significantly reduced. This suggests that myogenic activity is attenuated with ageing.

Yam *et al* (2005) investigated the effects of ageing on dynamic CA in humans. They measured bilateral MCAv using TCD, in young (28+/-5 years) and old (54+/-8 years) healthy human subjects, in response to spontaneous ABP fluctuations. They calculated a dynamic cerebral autoregulatory index (Mx), indicating how well the blood flow velocity autoregulated to rapid ABP changes, and compared this between the two age groups. They found no correlation between age and Mx, and no statistically significant differences between the two groups in terms of Mx, basal ABP or MCAv.

The effect of ageing on static CA has been studied in rats. Lartaud *et al* (1993) used the hydrogen clearance technique to assess CBF responses in the frontal cortex of 2-, 14- and 23-

month old Wistar and Fischer-344 rats, in response to hypercapnia, and hypotension caused by haemorrhage. They found that cerebrovascular reactivity to hypercapnia was reduced in the 14- and 23-month old Wistar rats, but not in the Fischer-344 rats, demonstrating differences between the rat strains. Further, the LL of autoregulation, assessed by haemorrhagic hypotension, was significantly increased in the 14- and 23-month old rats of both strains.

Similar findings were made by Toyoda *et al* (1997), who investigated autoregulation in the brain stem of anaesthetised adult (4-6 months) and aged (24-26 months) Sprague-Dawley rats. They measured brain stem CBF using Laser Doppler flowmetry, and measured the diameter of the BA, as well as a large and small branch off the BA, via a cranial window during controlled haemorrhage. The LL was shifted to significantly higher ABPs in the aged rats. Further, the dilatation seen in the BA, and its branches, were significantly smaller in aged rats. These data suggest that ageing is associated with an increased risk of brain stem ischaemia during hypotension.

Fujishima *et al* (1984) studied young (3 months) and aged (20 months) SHRs, and showed that haemorrhage-induced hypotension produced a larger decrease in CBF in the aged rats, indicating a rightwards-shift in the LL of autoregulation. They hypothesised that this was due to the effects of chronic hypertension on cerebral vessels, but it may simply have reflected the effect of ageing.

Generally, the studies on the effect of ageing on CA have focused on the LL, which is particularly relevant with respect to age-related postural hypotension and falls or fainting, issues that are prevalent in the elderly, and contribute a large cost to the NHS (see 1.4.1).

1.4.8 Ageing and the upper autoregulatory limit: Clinical implications for haemorrhagic stroke

Stroke is the 3rd most common cause of death and the most common cause of physical disability in the UK, affecting 150,000 people each year, around 60,000 of which are emergency hospital admissions (Age UK, 2015). In total, stroke is thought to cost the UK around £9 billion per year, accounting for around 5% of total NHS costs (Saka *et al*, 2008). Ageing is one of the major risk factors for having a stroke, with ¾ of all victims being 65 and older. Stroke is caused by interruption of the blood supply to the brain, either due to blockage by a clot (ischaemic, accounting for ~80% of cases) or due to rupture of a blood vessel (haemorrhagic) (NHS choices website). The risk of the latter is highly associated with hypertension (Endres *et al*, 2011) making efficient autoregulation at the UL important.

Despite this, the UL is much less widely studied than the LL, or dynamic CA. This may be due to the risk of causing cerebral hyperperfusion and haemorrhagic injury when experimentally raising ABP, making it particularly difficult to address in either young or aged humans. Assessment of the UL is therefore limited to studies using young adult animal models (see 3.1.2.2, 3.1.3 and Chapter 4). To our knowledge, no attempt has been made to assess the effects of ageing on the UL of CA in animals or humans. However, the link between ageing, hypertension, and the risk of stroke, means that this area warrants further research, and therefore forms the basis for the research conducted in this thesis.

1.5 Aims and Hypotheses

The aim of the first set of experiments was to develop an anaesthetised rat model for the assessment of the autoregulatory UL. This involved establishing an appropriate dosage and infusion protocol using PE, to generate reproducible autoregulatory curves, and identifying a method of analysis which facilitated quantitative identification of the UL. This protocol was then used to assess the autoregulatory UL of young male Wistar rats under control conditions, and also to identify the relative contribution of tonic NO-mediated dilatation (from both neuronal and endothelial sources) and sympathetically-mediated vasoconstriction (primarily from the SCG) to CA. Experiments were then repeated in older rats to assess the effect of ageing upon these normal control mechanisms, and therefore upon autoregulation at the UL.

Our hypotheses were as follows:

- The control UL would be lower in old rats compared to young, due to age-related degradation of normal control mechanisms.
- NOS inhibition would decrease the UL in young rats, due to removal of a tonic vasodilatory influence. NOS inhibition would have a reduced effect on the UL in old rats, due to age-related decrease in NO bioavailability.
- Stimulation of the autonomic innervation of cerebral vasculature would alter basal CBF in young rats. The magnitude of this response would be reduced in old rats, due to an age-related decline in innervation and function.
- Removal of the autonomic innervation to the cerebral vasculature would alter basal CBF, and the UL, in young rats, due to removal of a vasoactive input. The magnitude of this effect would be reduced in old rats, due to an age-related decline in innervation and function.

a)

b)

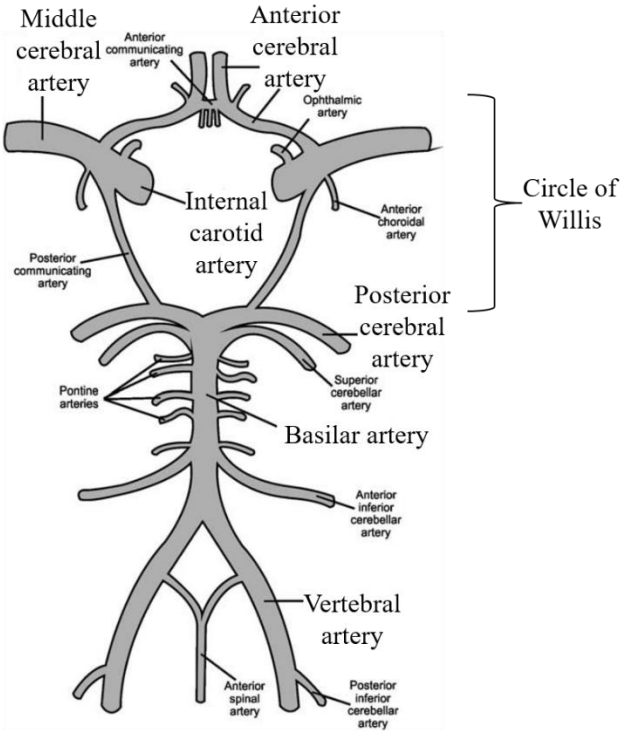

Figure 1: a) A copy of the original illustration of the cerebral circulation from the text 'Cerebri Anatome' published by Thomas Willis in 1664 (taken from Goodrich (2012), *Principles of Neurological Surgery* (3rd Ed), Chpt 1; 3–36), and b), a diagrammatic representation of the cerebral blood supply (adapted from Vrselja *et al* (2014), *J Cereb Blood Flow Metab*, 34: 578-584). The internal carotid arteries and the vertebro-basilar arteries run from extracranially to form the intracranial Circle of Willis, which was named after Thomas Willis posthumously. The major cerebral arteries branch bilaterally from the circle of Willis.

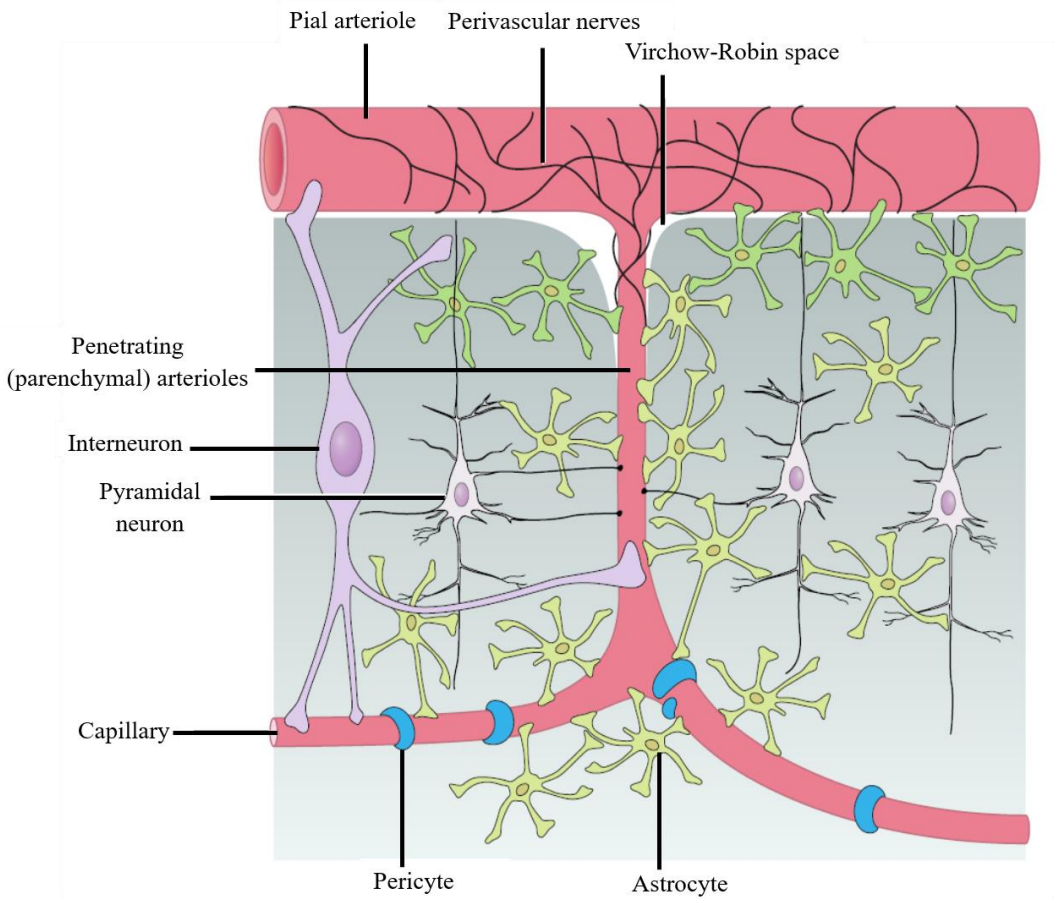

Figure 2: A diagram showing the neurovascular unit in the cerebral cortex. The pial arteries are richly innervated by extrinsic nerves. This innervation decreases as penetrating arteries branch off to supply the deeper structures, and is replaced by close apposition with astrocytes, forming the basis of neurovascular coupling. Adapted from Filosa and Iddings (2013).

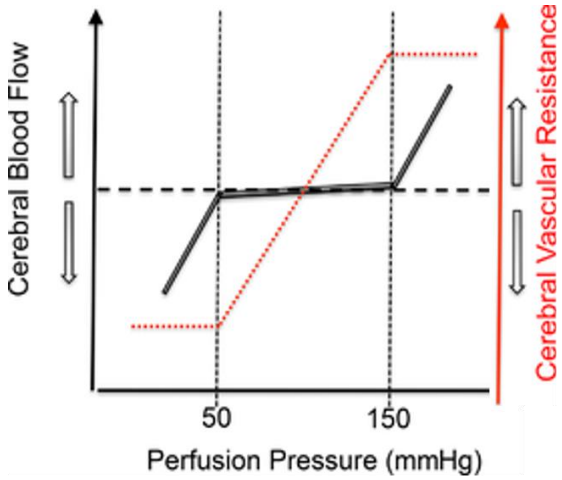

Figure 3: An example of the traditional view of an autoregulatory curve. CBF is maintained at a constant level over a wide range of perfusion pressures (~50-150mmHg), before autoregulation fails at the upper and lower limits, leading to an increase or decrease in CBF respectively. Adapted from Willie *et al* (2014).

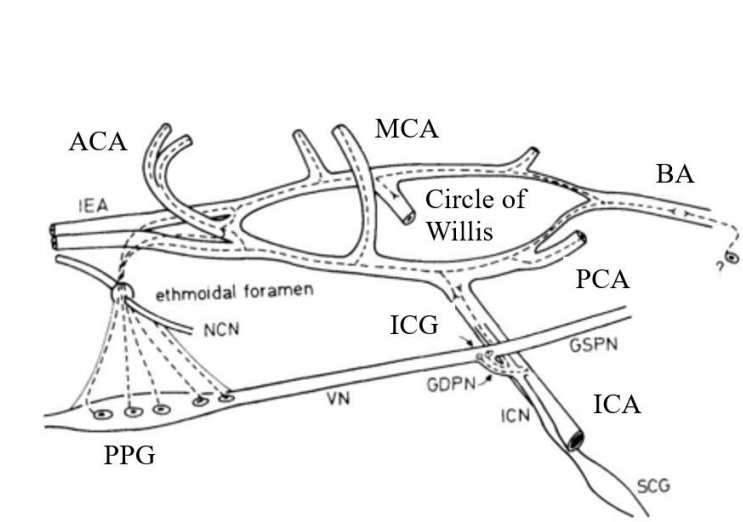

Figure 4: A diagrammatic representation of the location of, and projections from, the pterygopalatine ganglion (PPG) and superior cervical ganglion (SCG). Parasympathetic, ACh- and VIP-positive, nerve fibres project from the PPG, via the ethmoidal foramen, to innervate the Circle of Willis and its branches. Parasympathetic fibres also project from the internal carotid ganglia (ICG) to innervate the internal carotid artery (ICA). Sympathetic, noradrenergic- and NPY-positive, nerve fibres project from the SCG, to innervate the ICA, Circle of Willis and its branches. Adapted from Suzuki *et al* (1988).

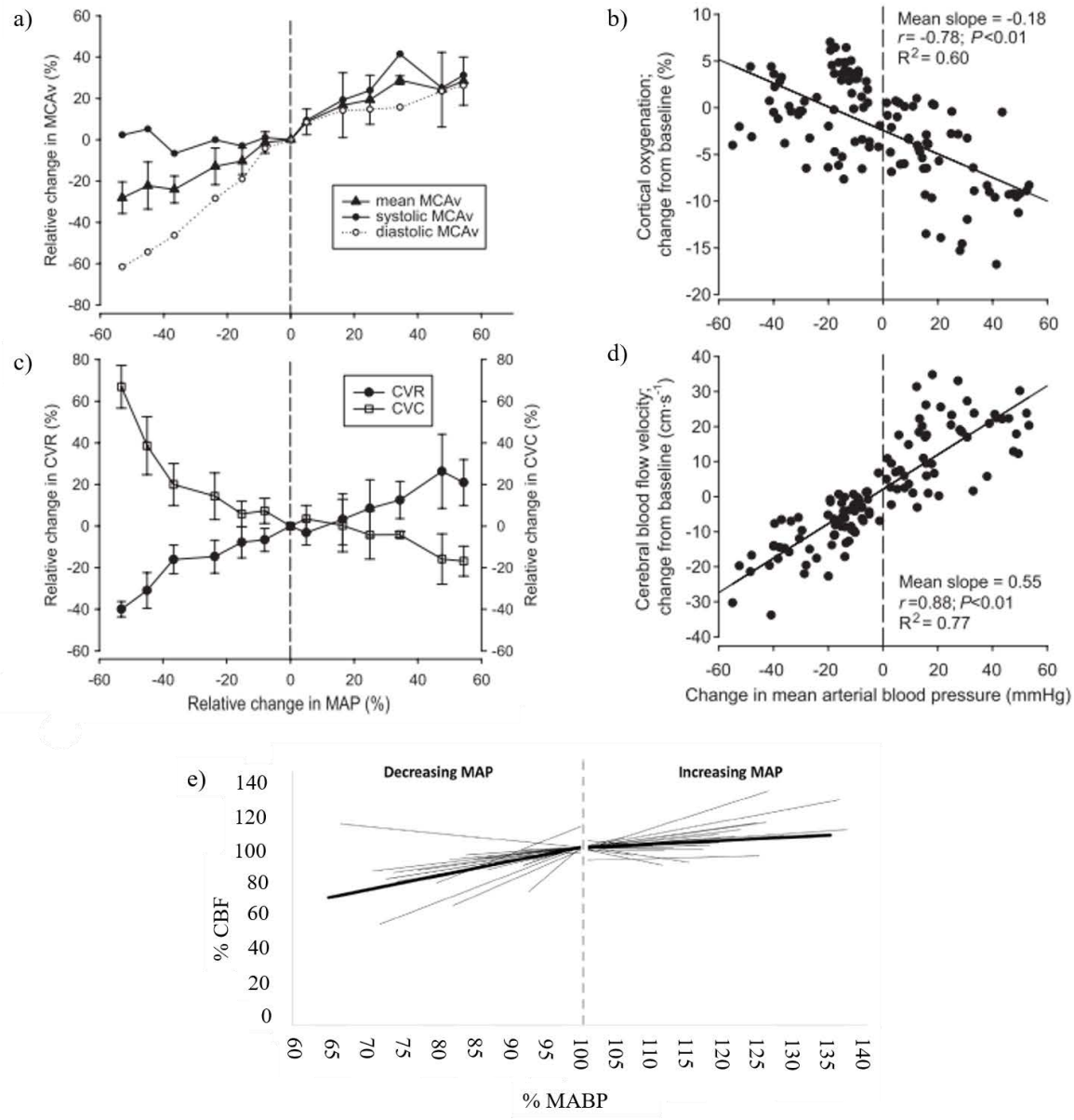

Figure 5: Graphs adapted from Lucas *et al* (2010), showing the change in a) MCAv, b) cortical oxygenation (measured by NIRS), c) CVR, and d) CBFv in response to a range of pharmacologically-induced changes in ABPs. In contrast to the classical representation of CA, with a flat plateau region representing perfect autoregulation of CBF over a range of ~90mmHg, these data indicate an almost linear relationship between MCAv/cortical oxygenation and ABP, despite autoregulatory changes in CVR/CVC.
e) is a graph taken from Numan *et al* (2014) showing the relationship between the change in CBF and MABP, across a range of increasing and decreasing ABPs. The thin lines show data reanalysed from 40 individual studies, and the thick lines show the mean. These data also support the idea of a more pressure-passive relationship between CBF and ABP i.e. no plateau region. They also show that autoregulation appears to be more efficient to increases in ABP.

Cardiac changes		Vascular changes	
Heart weight	↑	Arterial wall thickness	↑
Cardiomyocyte dimensions	↑	Subendothelial collagen	↑
Cardiomyocyte number	↓	Elastin	↓
Collagen in cross-linking	↑	Elastin fragmentation	↑
Ejection fraction	=	Proteoglycans	↑
Stroke volume	=	Matrix metalloprotease activity	↑
Cardiac output	=	Intimal migration/proliferation of vascular smooth muscle cells	↑
Early diastolic filling	↓	Arterial distensibility	↓
End-diastolic filling	↑	Pulse wave velocity	↑
Chronotropic responsiveness to β-adrenergic stimuli/catecholamines	↓	Total peripheral resistance	↑
Ionotropic responsiveness to β-adrenergic stimuli/catecholamines	↓	Endothelial permeability	↑
Ionotropic responsiveness to digitalis glycosides	↓	Endothelial nitric oxide release	↓
Peak cardiac output to maximal effort	↓	Inflammatory markers & mediators	↑
Lusitropic function	↓	Superoxide dismutase activity	↓
Release of natriuretic peptides	↑	β-adrenergic-mediated vasodilatation	↓

Table 1: A table adapted from a review by Ferrari *et al* (2003), summarising the major structural and functional cardiovascular effects of ageing. Of most relevance to the current study are the vascular changes, which include an increased arterial wall thickness, with increased levels of collagen and reduced elastin, resulting in reduced distensibility, a reduction in endothelial NO release, increased inflammation, decreased activity of the major antioxidant superoxide dismutase (SOD), and a decreased vasodilator response to β-adrenergic stimulation.

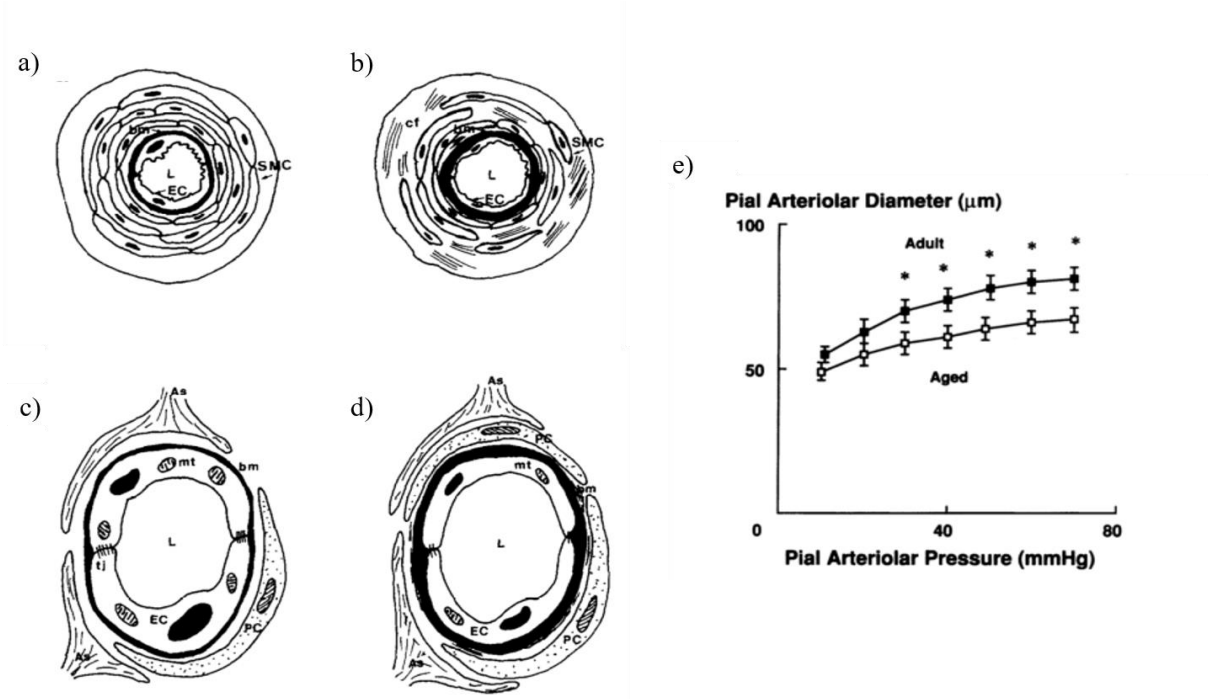

Figure 6: A cross-sectional diagram of a normal (a) and aged (b) cerebral arteriole, and a normal (c) and aged (d) cerebral capillary, adapted from Kalaria *et al* (1996). Ageing is associated with a dilated lumen, thinned endothelial cells, thickened basement membrane, reduced numbers of smooth muscle cells, and increased levels of collagen in cerebral arterioles. In cerebral capillaries, ageing causes thinning of endothelial cells, decreased numbers of mitochondria, and modified pericytes and tight junctions. The capillary structural changes may lead to increased endothelial permeability, which could compromise the integrity of the BBB. The arterial structural changes lead to reduced vascular distensibility and increased stiffness. The graph in e), adapted from Hajdu *et al* (1990), demonstrates a functional consequence of age-related changes in cerebral arterioles; pial arteriolar pressure-diameter curves are downwards-shifted in aged Fischer-344 rats.

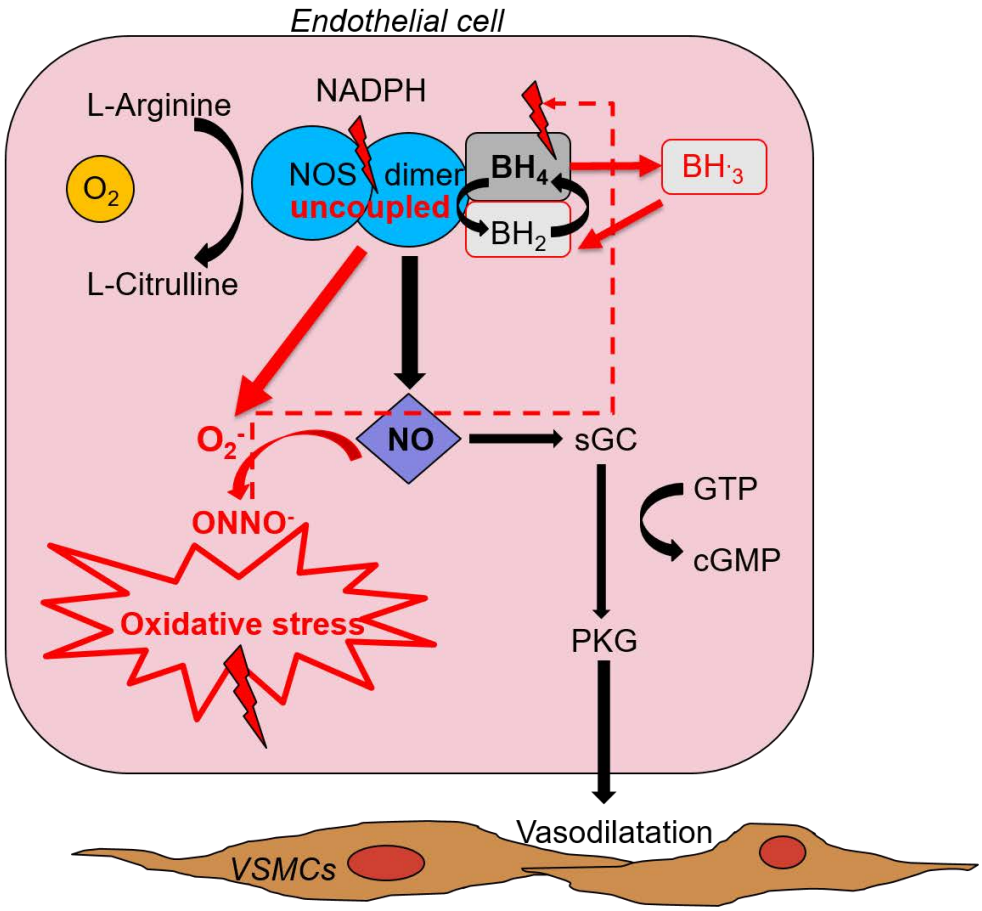

Figure 7: Based on a diagram from Kietadisorn *et al* (2011). The normal pathway of a coupled NOS dimer producing NO, and causing relaxation of vascular smooth muscle cells (VSMCs), is shown in black. The red text and arrows indicate the effects of oxidative stress; uncoupling of NOS dimers leading to production of O_2^-, oxidation of BH_4, to BH_3 or BH_2, which further compromises NOS coupling and NO production, and reaction of O_2^- with NO to produce $ONNO^-$, a free radical that further oxidizes BH_4. Therefore oxidative stress impairs regulation of vascular tone by NO, and underlies the endothelial dysfunction seen in ageing, as well as other diseases such as atherosclerosis.

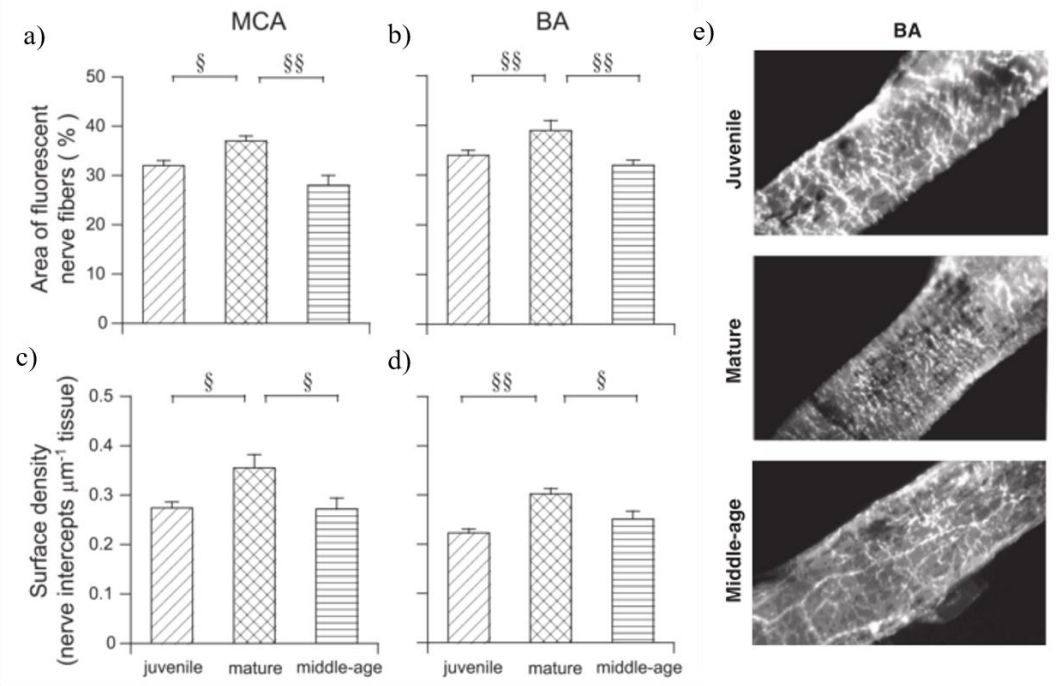

Figure 8: Omar and Marshall (2010b) used glyoxylic acid staining to detect sympathetic nerve fibres in cerebral vessels of juvenile (4-5 weeks), mature (10-12 weeks) and middle-aged (42-44 weeks old) male Wistar rats. The graphs show a) area of fluorescence in the MCA, and b) BA, and c) surface density of the detected nerve fibres in the MCA and d) BA, as well as e) photomicrographs of sympathetic nerve fibres in the BA. Innervation fluorescence and surface density significantly increased from juvenile to mature rats, and then significantly decreased by middle-age, suggesting a decrease in sympathetically-mediated, cerebral vascular tone with age.

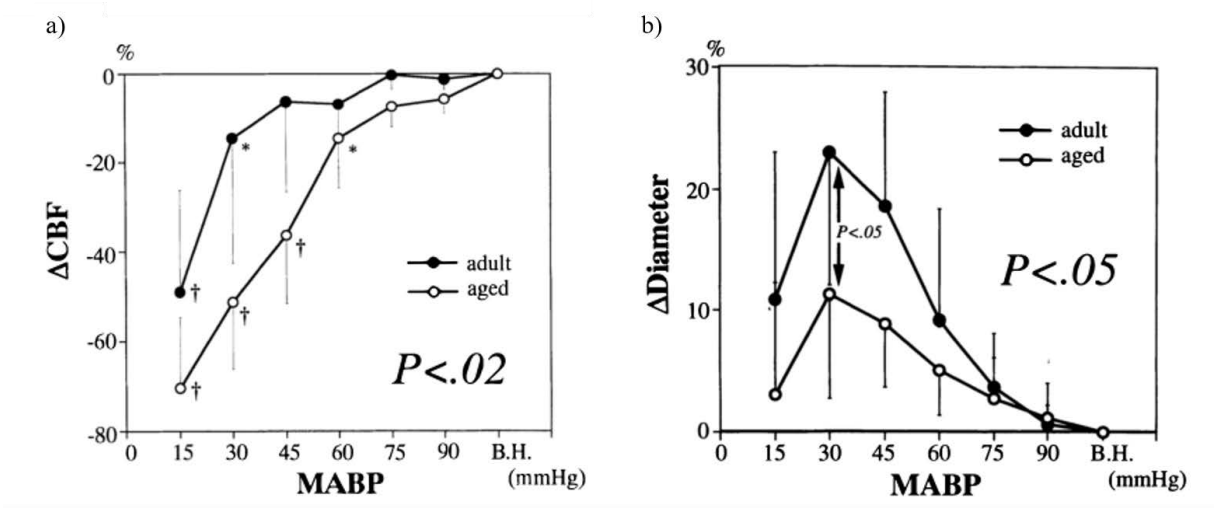

Figure 9: A figure adapted from Toyoda *et al* (1997). Hypotension was induced by haemorrhage, and brain stem blood flow was assessed by a) Laser Doppler flowmetry and b) vessel diameter measurements in the BA. As ABP decreased, adult, Sprague Dawley rats (4-6 months) autoregulated to around 45mmHg, whereas aged rats (24-26 months) only autoregulated to around 75mmHg, indicating that the LL was rightwards-shifted by ageing. The change in BA diameter in response to decreasing ABP was also significantly reduced in aged rats.

CHAPTER 2: GENERAL MATERIALS AND METHODS

2.1 Animals

All experiments were performed on Male Wistar rats sourced from Charles River Laboratories and housed in single sex groups at 21±1°C and 40-45% humidity, under a 12-hour light/dark cycle (lights on at 7:00am). Food and water was available *ad libitum*.

Wistar rats are the standard strain used in our lab, and have been used in relevant studies on cerebral blood flow and ageing e.g. Thomas & Marshall, 1994, Coney & Marshall, 1998, and Omar & Marshall, 2010a. Further, despite many studies of ageing using Fischer-344 rats, in general the rat is species which can be readily utilised to study ageing, as they are not prone to potentially confounding age-related diseases (see 1.4.2).

Rats comprised two age groups: young sexually mature rats (Y) at 6-8 weeks of age, and older, late middle-aged rats (O) at 12-15 months old, with body weights of 300-380g and 650-1200g respectively on the day of the terminal experiment. These ages were chosen to correspond to around 20 and 55 years old respectively in humans (Folkow & Svanborg 1993), and also to align with previous work in our laboratory (Omar & Marshall, 2010a & 2010b, see 1.4.2 and 1.4.4).

Care of the animals and all procedures were approved under current UK Home Office legislation, the University of Birmingham Ethical Review Sub-Committee and according to ARRIVE guidelines.

2.2 Anaesthesia and surgery

2.2.1 General surgery

Anaesthesia was induced with 4% isoflurane in O_2 at 4 $L \cdot min^{-1}$ (Merial Animal Health Ltd, Surrey, UK). The animal was prepared as shown in Figure 10: the left jugular vein was isolated and cannulated (cannula inner diameter (ID) 0.5mm, and outer diameter (OD) 1.5mm). Isoflurane anaesthesia was then withdrawn and replaced gradually with 2-3 boluses of Alfaxan® (Vétoquinol UK Ltd, Buckingham, UK, (0.1ml boluses at $5mg.ml^{-1}$), and then maintained with a 17-30 $mg.kg^{-1}.hour^{-1}$ infusion using a syringe driver (Perfusor® securaFT, B. Braun Medical Ltd, Sheffield, UK). The trachea was isolated and cannulated with a custom-made stainless steel T-piece cannula, to allow maintenance of a patent airway and supply of oxygen if necessary (see below).

The left brachial artery was then isolated from the brachial plexus and cannulated (ID 0.4mm, OD 0.8mm) to allow samples to be taken for blood gas analysis. The left femoral artery and vein were isolated from the femoral sheath and cannulated (ID 0.58mm, OD 0.96mm, and ID 0.5mm, OD 1.5mm respectively) to allow arterial blood pressure (ABP) and heart rate (HR) to be recorded and for drug infusion respectively. The right common carotid artery was isolated and cleared distally up to its bifurcation. The external carotid, as well as occipital, facial and lingual branches (if positioned distal to the cleared section of common carotid artery) were ligated, so as to achieve vascular isolation of the internal carotid artery and its distribution to the right side of the brain (as described by Thomas & Marshall, 1994 - see 3.4.1). Subsequently, blood flow recorded through the common carotid artery under these conditions, was used as an index of gross cerebral blood flow (CBF, see below). In some subgroups, the left common carotid artery was also isolated as described above, but all its branches were left intact to provide a sham control for the effect of ligation on CA. In other subgroups, the right

femoral artery was separated from the femoral vein and sciatic nerve to allow femoral artery blood flow (FBF) to be recorded.

All cannulae were filled with heparinised saline (20 units.ml^{-1} Heparin, LEO® Pharma, Berkshire, UK) and sourced from Portex™, Smiths Medical (Kent, UK). Suture was from Look®, Surgical Specialities Corporation (Pennsylvania, US) and needles (0.5x25, 0.6x30mm and 0.8x40mm, Microlance™) and syringes (1, 2, 5 and 10ml, Plastipak™) were from BD (Oxford, UK).

The depth of anaesthesia was monitored at regular intervals throughout surgery by determining whether there was any increase in ABP or HR and/or pedal withdrawal reflex to a strong paw pinch. If so, a 0.05-0.1ml bolus of Alfaxan® (5mg.ml^{-1}) was given and the infusion rate was increased. If ABP or HR fell over time, the infusion rate was decreased until the infusion rate enabled ABP to remain stable, but with no pedal withdrawal reflex to a strong paw pinch. Core body temperature was monitored and maintained at 37°C throughout, via a rectal temperature probe linked to a homeothermic heat pad system (Harvard Apparatus, Cambridge, UK).

At the end of each experiment the animals were killed by overdose of Euthatal® (pentobarbital sodium 200mg.ml^{-1}, Merial Animal Health Ltd.), which was confirmed by cervical dislocation.

2.2.2 Additional surgery

In addition to the general surgery described above, in some groups, surgery was performed to allow cortical cerebral blood flow (CoBF) to be followed as well as gross CBF. This was achieved with the animal placed in a stereotaxic frame fixed in position via ear and nose bars.

An incision was then made down the midline of the scalp and the skin and muscle retracted to reveal the skull. The cranial bone was thinned using a dental drill (model RS 549-006, R&S, Paris, France) until only a thin layer was left through which cerebral vessels were visible. In some animals, a stainless steel, angled Laser Doppler probe (Perimed UK Ltd, Bury St. Edmunds, UK) was held in a micromanipulator stand and positioned on the bone surface over the right cortex, avoiding large visible vessels, to record right cortical red cell flux (RCoRCF see Figure 11).

In others, a Laser Speckle Contrast imager (MoorFLPI-2, Moor Instruments Ltd, Axminster, UK) was mounted on a microstand at a height of 10-15cm from the thinned bone, to image the dorsal surface of both the right and left cortices and record cortical tissue perfusion (perfusion units – PU, see Figure 12).

Cranium thinning was preferred to complete removal of the bone and preparation of a cranial window, as this avoided the complication of swelling due to cerebral oedema and the need for continuous perfusion of the exposed tissue, and allowed the animals to be maintained in a more intact, physiological state.

2.3 Equipment and data acquisition

A pressure transducer (Capto, HJK, Merching, Germany) was attached to the left femoral artery cannula to monitor arterial blood pressure (ABP) (via a MacLab Bridge Amp, ADInstruments, Oxford, UK), from which mean ABP (MABP) and HR were derived beat-by-beat. All animals spontaneously breathed room air and blood samples were taken at intervals via the left brachial artery cannula to monitor arterial blood gases and pH (150µl capillary tubes and Gem® 4000 premier analyser, Instrumentation Laboratory Ltd, Warrington, UK, see section 2.5 below for further details).

The cannula in the left femoral vein was used to give drug infusions, as required for each experimental protocol, using syringe drivers (KD Scientific, Massachusetts, US).

2.3.1 Using flow probes to measure global CBF

The isolated right common carotid artery was placed in the trough of a V-shaped flow probe (Transonic Systems Inc, Elsloo, Netherlands) to record right carotid blood flow. As only the internal carotid branch remained intact, minimising extra-cranial flow, right carotid artery flow was used as an index of gross, right cerebral blood flow (RCBF).

Transonic flow probes consist of two ultrasonic transducers, one upstream and one downstream relative to the blood flow through the vessel, positioned on one side of the vessel within the probe body. On the opposite side of the vessel there is an acoustic reflector. The vessel rests in the V-shaped trough between the transducers and reflector, so that when the downstream transducer is electrically activated to emit an ultrasonic wave, this passes through the vessel and is reflected by the acoustic reflector. This causes the wave to pass back through the vessel and be detected by the upstream transducer. This signal is used to calculate the transit time taken for the wave to travel between the two transducers. This is then repeated in the opposite direction, with the upstream transducer emitting the ultrasonic wave and the downstream transducer receiving the reflected wave. From these two signals, the transit time is calculated for the wave in both an upstream (against the flow of blood, taking a longer time) and downstream (with the flow of blood, taking a shorter time) direction. The software subtracts the downstream from upstream transit times and the difference between the two is a measurement of volume flow. The flow probes use wide beam illumination, which takes into account both the shift in transit time caused by the velocity of the blood flow, and also the length of the path in which this shift is encountered. The receiving transducer integrates these factors (average velocity x cross sectional area) to give an actual flow measurement which

takes into account vessel diameter (Transonic Systems Inc. Rodent Workbook Rev A, 2011). These flow probes therefore produce continuous beat-by-beat assessment of blood flow in $ml \cdot min^{-1}$.

In some subgroups as indicated above, a second flow probe was placed either around the intact left common carotid artery to record left carotid blood flow (LCBF), or the right femoral artery to measure right femoral blood flow (RFBF), as an index of hind limb skeletal muscle blood flow.

Mean blood flow (MBF), vascular conductance (MVC=MBF/MABP) and resistance (MVR=MABP/MBF) were computed online for RCBF and LCBF or RFBF. Data was recorded at sampling frequencies of 100-1000 samples/second, using a PowerLab and Labchart software (ADInstruments) on a Mac OS X computer. The RCoRCF recordings from the Laser Doppler probe were also collected via the PowerLab.

2.3.2 Using Laser Doppler/Laser Speckle imaging to measure cortical CBF

The Laser Speckle imager works by illuminating tissue with an infra-red laser beam, producing a speckle pattern; a high contrast random interference effect. Blood cells flowing through the illuminated region cause variation in the speckle pattern, causing it to become blurred and therefore reducing contrast. Images are captured with a CCD camera, and passed to image processing software which exploits the fact that areas of high perfusion, where the number of blood cells is greater, produces fast variation of the laser speckle pattern and greater blurring, and therefore an area of low contrast. Tissue regions with lower perfusion cause less change in the speckle pattern, less blurring and therefore a region of high contrast. These contrast differences are then quantified to give Flux values which are similar to the RCoRCF output of the Laser Doppler probe, as well as to produce a real-time, colour-coded

perfusion map, representing superficial (1mm depth penetration) cortical blood flow (CoBF). Blue to green colours represent areas of no or low perfusion, whilst yellow to red colours represent higher perfusion, as shown in Figure 13. In the present study, Laser Speckle images were taken once every 4 seconds, at a resolution of 752 x 580 pixels.

2.4 Drugs and solutions

(R)-(-)-Phenylephrine hydrochloride (PE, P6126, Sigma-Aldrich, Dorset, UK), Acetylcholine chloride (Ach, A6625, Sigma), S-Methyl-L-Thiocitrulline acetate (SMTC, M5171, Sigma), N_w-Nitro-L-arginine methyl ester hydrochloride (L-NAME, N5751, Sigma), Phentolamine hydrochloride (P7547, Sigma), *N*-Acetyl-L-cysteine (NAC, A7250, Sigma), BIBP 3226 trifluoroacetate (BIBP, 2707, Tocris, Abingdon, UK) and Evans Blue (EB, E2129, Sigma) were all dissolved in 0.9% saline for intravenous infusion. 7-Nitroindazole (7-NI, N7778, Sigma) was dissolved in 75% Dimethyl sulfoxide in saline (DMSO, W387509, Sigma) and given intraperitoneally. Phosphate Buffered Saline (PBS, P4417, Sigma) was prepared from tablets, dissolved at a ratio of 1 tablet per 200ml of deionised water. Formaldehyde (47608, Sigma) was diluted to 4 or 0.5% in PBS.

2.5 Stabilisation

After surgery and before the experiment proper began, equilibration was allowed until all variables were stable. A 20-min period of baseline recordings was then made, during which blood gas samples were taken to ensure P_aO_2, P_aCO_2 and pH values were of acceptable values. The baseline values typically seen in this study were 73±2mmHg, 43±1mmHg, and 7.44±0.01 respectively.

Normal ranges in humans are 75-100mmHg, 38-42mmHg, and 7.38-7.42 respectively (Medline Plus, NIH, US National Library of Medicine, https://medlineplus.gov/ency/article/003855.htm, last updated 21/08/2016).

In rats, arterial blood gas values are similar to humans. For example Stout *et al* (2001) reported a mean P_aO_2 of 81±0.1mmHg and P_aCO_2 of 35±0.1mmHg in adult Sprague-Dawley rats breathing 2% isoflurane in room air. Thomas & Marshall (1994) and Coney & Marshall (1998) used a similar anaesthetic regime and surgical set-up to the current study, in male Wistar rats, and reported P_aO_2 values of 87-95mmHg, P_aCO_2 values of 41-44mmHg, and a mean pH of 7.24±0.02. However both studies used a lighter level of anaesthesia during the experiment proper compared to the current study.

The mean P_aO_2 in the current study was at the lower end of the normal, clinically-accepted range, whilst the P_aCO_2 and pH were slightly raised. This may be accounted for by the higher anaesthesia rate, and lack of artificial ventilation or continuous supplementation of controlled gas mixtures.

Blood samples were taken every 5-10 minutes throughout each experiment, aligning with administration of each drug/increasing dose. If the blood gas values deviated from the mean, or breathing appeared laboured, the airway was aspirated. If P_aO_2 fell below the mean, supplemental O_2 was given as needed. Close attention was paid to P_aCO_2 levels, as the cerebral circulation is particularly sensitive to changes in CO_2, as demonstrated by Willie *et al* (2012). If P_aCO_2 levels rose above 45mmHg and could not be corrected by aspiration, adjustment of the level of anaesthesia, or by allowing a longer stabilisation period, the data was discarded.

2.6 Experimental protocols

The details of the protocols used in specific groups of animals are described in the Methods sections of Chapters 4-7. The description below covers standard protocols used widely in several different experimental groups.

2.6.1 Assessment of the cerebral autoregulatory upper limit (UL)

In a number of groups, PE was infused at doses of 0.1–200µg.kg^{-1}.min^{-1} at 6-12ml.hr^{-1} in order to progressively increase MABP. Approximately 2 minutes was allowed at each dose for the effects to stabilise. When an increase in the recorded RCBF or LCBF was seen, accompanied by a fall in R or LCVR, with a rising or stable MABP, this was indicative of reaching the UL. One further dose of PE was given before the infusion was stopped. Variables were then allowed to recover back to basal levels.

2.7 Data analysis

2.7.1 Cardiovascular and blood flow data

The cardiovascular, CBF and CoRCF (cortical red cell flux) data recorded via the PowerLab were exported using the DataPad function of LabChart. Sections of data (60 seconds) representing stable baseline just prior to the start of the protocol (i.e. before starting an infusion), or the final minute of the response to each PE infusion step (i.e. each increasing dose), were exported as a mean value for each variable computed over this time. The DataPad file was then saved as a text file and opened in Excel (Office 2013, Microsoft, Reading, UK) allowing data to be further analysed.

2.7.2 Laser speckle data

Laser Speckle contrast files were opened in MoorFLPI Full-Field Laser Perfusion Imager Review software (V4.0, Moor Instruments Ltd), to allow specific regions of interest (ROIs) to be selected. Typically, a clearly defined arterial and venous vessel were traced using a freestyle selection tool (see Figure 14). In addition, a tissue region with no obvious arterial or venous vessels was selected using a rectangular selection tool, to represent tissue capillary perfusion (equivalent to the tissue perfusion measured by the laser Doppler probe, and therefore used as an index of CoCBF). The selection of the ROIs was aided by the colour photograph automatically taken by the imager at the start of each experiment (see Figure 14).

These data compiled as graphs over time, exported as such, were saved as text files and opened in Excel. This allowed the Laser Speckle data to be aligned with the LabChart data with respect to time, by using markers added to each data file during recording. The measurement made by the Laser Speckle imager is given as Flux, which is related to the speed and concentration of red blood cells moving in the tissue, similar to the RCF output of the Laser Doppler probe (although differences may be seen due to the difference in depth of penetration). These Flux measurements are expressed in arbitrary 'perfusion units' (PU). Although the size of the ROIs selected was not equal between the different vessels and tissue regions, or between experiments, this did not impact on the data output from the ROIs, as Flux is expressed as a mean, relative to area selected, and the subsequent analysis focused on the relationship between Flux and MABP, or the change in Flux from the immediately preceding baseline, rather than the absolute Flux values.

The imager is supplied pre-calibrated. The calibration is based on the Flux signal generated using a reference solution of polystyrene microspheres suspended in water, undergoing thermal motion at room temperature. Automated calibration checks were carried out

periodically during the group of experiments, using a calibration block comprised of a compartment containing the microsphere solution for a Flux reference, and a static reflector surface for a zero reference.

The imager review software was also used to generate videos of each experiment. Frames representing 60 second sections of data, aligned with the selections from LabChart for the corresponding experiment, were averaged and joined to generate a video. Lines were then added to these averaged frames, intersecting the vessels in the ROIs, generating a profile view of Flux (PU) against number of pixels, as shown in Figure 15. The points at which Flux plateaued either side of the peak were taken to represent the edges of the vessel. Therefore vessel diameter could be determined: image resolution and image size (mm) was recorded for each experiment, making it possible to calculate the size in mm of one pixel and therefore the diameter of the vessel of interest by counting the number of pixels across and converting to mm. This was done for each averaged frame, allowing vessel diameter to be tracked throughout an experimental protocol, and to compare the responses of different sized vessels.

2.7.3 Analysis of Gross and cortical UL

Autoregulatory curves were generated by plotting mean CBF, RCoRCF, or arterial, venous or capillary perfusion units (A/V/CPU), against MABP at each PE dose. Dual-line linear regression analysis (as described by Samsel & Schumacker, 1988, and used previously in our laboratory by Edmunds & Marshall, 2001) was then used to calculate the autoregulatory UL. As shown in Figure 16, to achieve this, data points were divided into two groups, representing the ‘plateau’ and ‘rising’ phases of the curve, in every possible combination i.e. ranging from just 2 points in the plateau group and the remainder in the rising group, and *vice versa*. Linear regression lines were fitted to each combination, for each animal. The UL for each animal was

then defined as the point of intersection of the two regression lines with the best fit and the smallest standard deviation of residuals (Sy.x; calculated from the sum-of-squares and degrees of freedom, another indication of goodness of fit). A group mean UL was then calculated from these individual values.

2.8 Statistical analyses

All data are presented as the mean ± SEM and/or as the change from the immediately preceding baseline. Graphs and statistics were generated using GraphPad Prism® 5. Data was analysed using t-tests (paired or unpaired as appropriate) and one-, two-way or repeated measures ANOVAs with post-hoc Dunnett's or Bonferroni (as appropriate). $P<0.05$ was taken as significant. Specific statistical analysis is discussed in the Methods of Chapters 4-7.

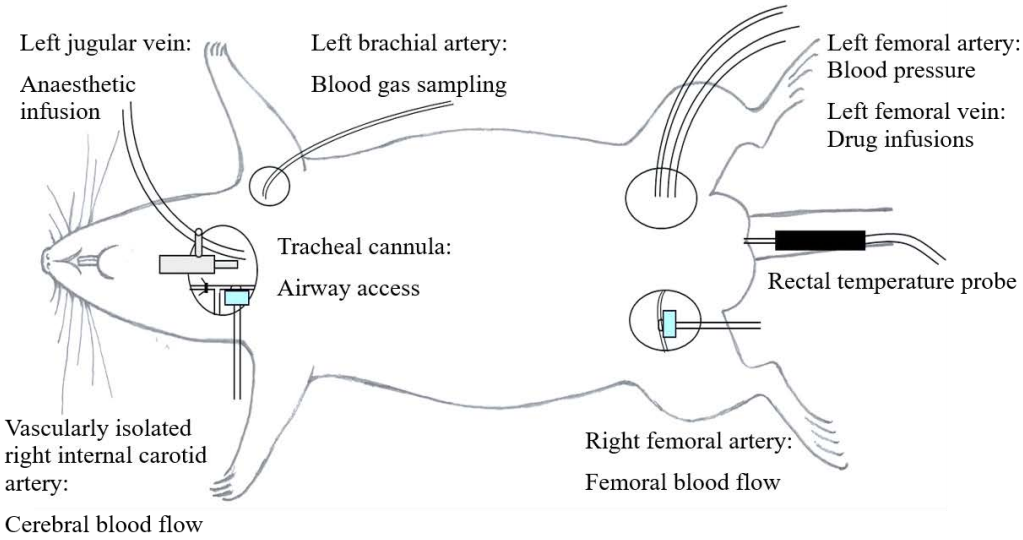

Figure 10: A diagram showing the general surgical set-up. Subgroups additionally had the intact left common carotid artery isolated to provide a sham control for the effect of ligation on cerebral blood flow recording.

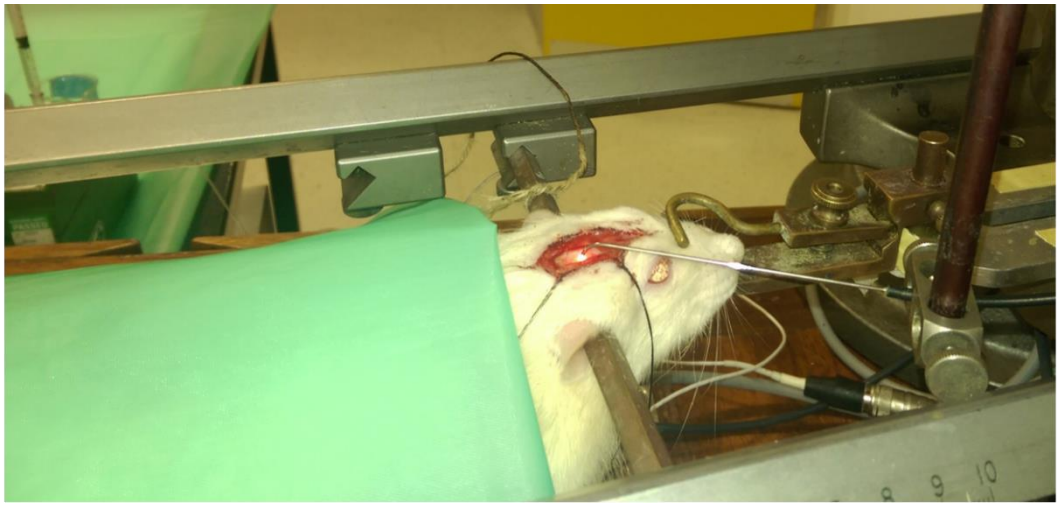

Figure 11: A photograph showing the surgical set-up used to record right cortical CBF. The rat was positioned in a stereotaxic frame, and the cranial bone exposed and thinned. A Laser Doppler probe was positioned on the bone surface, enabling measurement of cortical red cell flux.

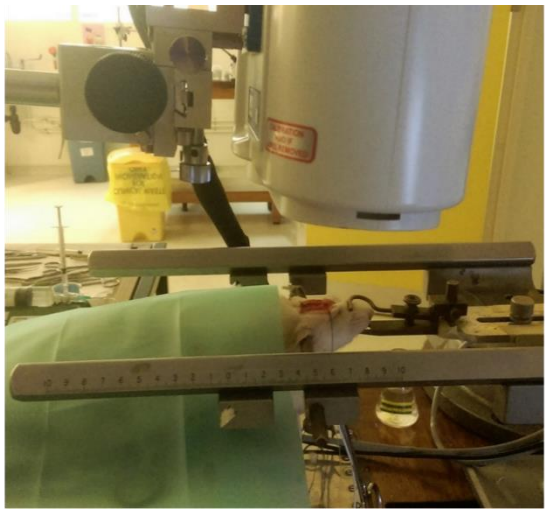

Figure 12: A photograph showing the surgical set-up used to perform Laser Speckle Contrast imaging of cortical tissue perfusion. The rat was positioned in a stereotaxic frame, and the cranial bone exposed and thinned. The imager was positioned 10-15cm away from the bone surface, enabling imaging of the dorsal surface of both the right and left cortices.

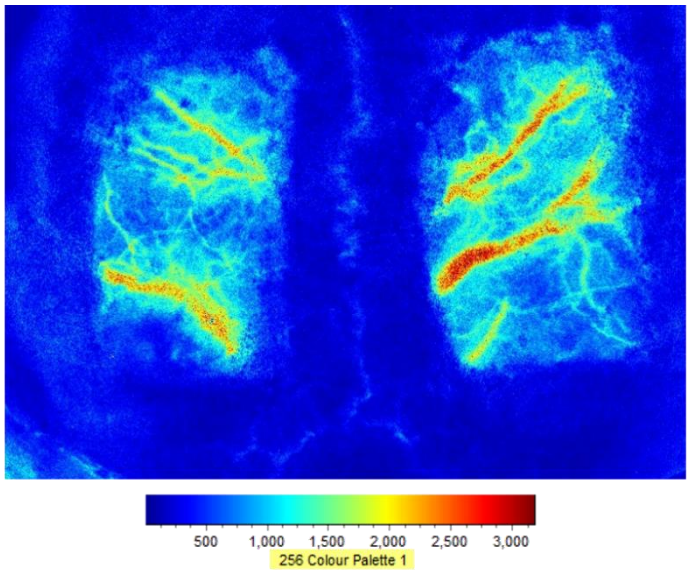

Figure 13: An example of a colour-coded perfusion map obtained from Laser Speckle Contrast imaging of cortical tissue perfusion. The outlines of cortical vessels can be seen clearly. Blue to green colours indicate areas of low perfusion, and yellow to red colours indicate higher perfusion. The scale indicates the flux values associated with the colour range. As the absolute flux values were not taken to represent a specific CBF value, the scale was set to produce the best visualisation of vessels in each experiment.

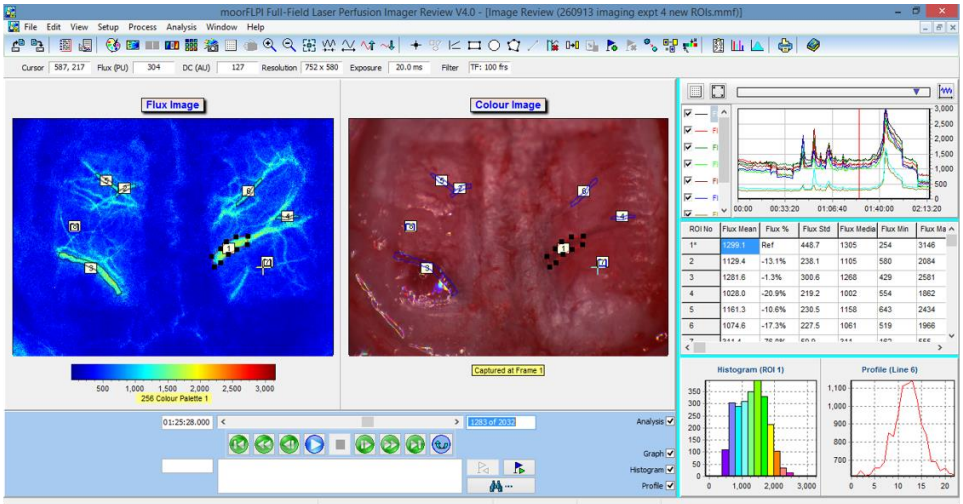

Figure 14: A screenshot of the MoorFLPI Full-Field Laser Perfusion Imager Review software (V4.0, Moor Instruments Ltd). Flux; the output of the Laser Speckle imager, which is related to the speed and concentration of red blood cells moving in the tissue, is shown in the left-hand window as a colour-coded perfusion map. Regions of high flux are shown in yellow to red colours, and low flux in blue to green colours. On this flux image, drawing tools have been used to define regions of interest (ROI) representing arterial, venous and capillary vessels, and to insert lines intersecting the vessels. The middle window is a colour photo taken automatically at the beginning of each experiment, which was used to help with identification of the different vessel types for analysis. The top right-hand panel shows the average Flux values of all the ROIs as a line graph with respect to time, as well as giving Mean, %, SD, Median, Min and Max values. The bottom right-hand panel shows a histogram of the Flux values of the currently selected ROI, and the cross-sectional Flux profile of the currently selected line.

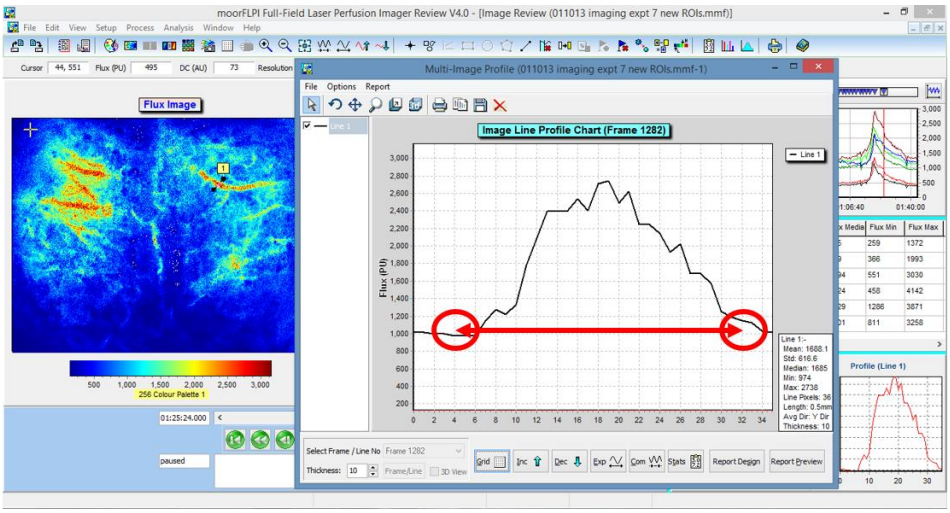

Figure 15: An enlarged window showing a line profile graph generated by the MoorFLPI Full-Field Laser Perfusion Imager Review software (V4.0, Moor Instruments Ltd). A line can be drawn to intersect a vessel on the Flux image, from which a profile view of Flux (in arbitrary perfusion units), against the number of pixels the line covers, is generated. The points at which Flux plateaued either side of the peak, shown by the red circles, represent the edges of the vessel. As the size in mm of one pixel could be calculated, the diameter of the vessel was estimated by counting the number of pixels between the plateaus, as shown by the arrows, and converting to mm. This allowed vessel diameter to be tracked throughout an experiment, and to compare the responses of different sized vessels.

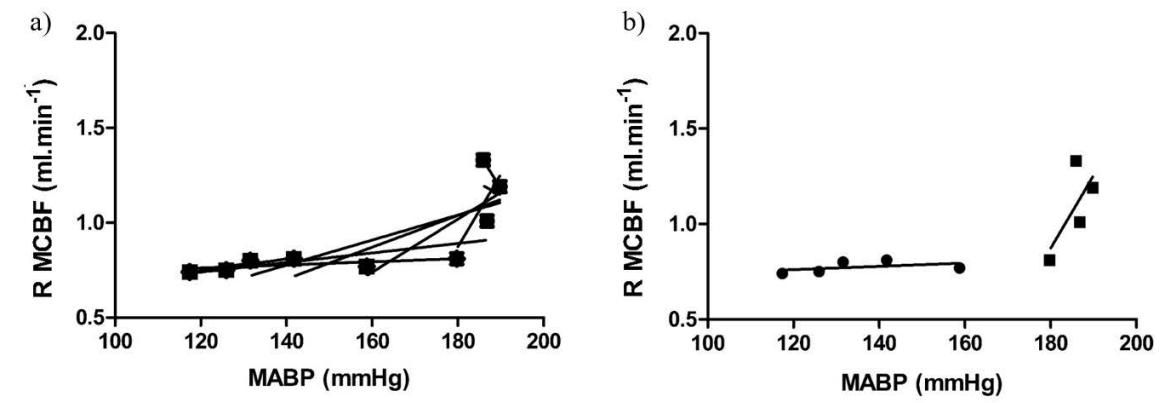

Figure 16: An example of the linear regression analysis applied to calculate the autoregulatory UL. a) The R MCBF vs MABP data points generated from a single experiment were divided into two groups, representing the 'plateau' and 'rising' phases of the autoregulatory curve. Linear regression lines were fitted to every possible combination, from 2 points in the plateau group and the remainder in the rising group, and *vice versa*. b) The UL was then defined as the point of intersection of the two regression lines with the best fit and the smallest standard deviation of residuals, which, in this experiment, gave an UL of 178mmHg.

CHAPTER 3: METHOD DEVELOPMENT

3.1 Introduction

This chapter describes the development of a protocol to investigate the UL of cerebral autoregulation. Development of this protocol required selection of a suitable model for study of the UL, a technique for measurement of cerebral blood flow and a method for raising ABP to reach the UL.

3.1.1 Measurement of cerebral blood flow

The ways in which cerebral blood flow can be measured to allow for the study of cerebral autoregulation and the pros and cons of using a rat model are discussed in detail in Chapter 1 (1.3.1 and 1.3.2).

Briefly, experiments in humans tend to use either tracers (e.g. Kety-Schmidt method), imaging techniques (e.g. MRI) or, most commonly, a Transcranial Doppler (TCD) probe. The output of all of these techniques give an indication of cerebral perfusion or blood flow velocity, rather than a direct measurement of flow.

Techniques in animals can be applied under anaesthetic and therefore be more invasive, providing more direct measurements. For example intracerebral probes, radiolabelled microspheres and direct observation of cerebral blood vessel diameter or pressure. The main method chosen for this study was vascular flowmetry using Transonic flow probes, due to the fact that this technique offers direct measurement of blood flow rather than velocity. Additionally, Laser Speckle Contrast imaging was used in parallel with flowmetry to allow assessment of both gross and cortical cerebral blood flow simultaneously. The use of animals

also facilitates assessment of the UL, which requires blood pressure to be raised to potentially damaging levels.

3.1.2 Methods for assessment of cerebral autoregulation

3.1.2.1 Validation for the use of catecholamines

Various methods have been used to induce changes in ABP in order to assess cerebral autoregulation. Many of these allow assessment of *dynamic* cerebral autoregulation i.e. the effect of rapid fluctuations in ABP on CBF. For example, this can be achieved by beat-to-beat analysis of random variations in ABP (Diehl *et al*, 1998), small bolus doses of pharmacological agents (Wagner *et al*, 2011), the use of a tilt table (Jordan *et al*, 2000), rapid inflation and deflation of pressure cuffs (White *et al*, 2000), or positive/negative lower body pressure (as used by Tan, 2012).

When studying *static* cerebral autoregulation - the CBF response to longer, more gradual changes in ABP - the most commonly used method to raise or lower ABP is a pharmacological agent. In many studies, ABP is raised by infusion of catecholamines, such as adrenaline, noradrenaline, or the sympathomimetic phenylephrine (PE). Catecholamines increase ABP by peripheral vasoconstriction, but evidence suggests they cause minimal direct cerebral vasoconstriction.

Firstly, it is known that the blood brain barrier (BBB), created by closed tight junctions between endothelial cells of cerebral vessels, prevents free passage of solutes into the brain (Reese & Karnovsky, 1967), limiting access to the vascular smooth muscle of cerebral blood vessels. As well as this physical blockade, the BBB possesses enzymatic mechanisms which prevent passage of specific substances, including catecholamines, into the brain. Thus, the endothelial cells and pericytes of cerebral microvessels, and the smooth muscle cells in larger

vessels, contain DOPA decarboxylase, which prevents passage of L-DOPA and other amine precursors (Hardebo *et al*, 1979a), and monoamine oxidases, and catechol-O-methyl transferases, which specifically catalyse the breakdown of catecholamines (Hardebo *et al*, 1979b).

Bevan *et al* (1998) performed resistance artery myography on freshly isolated human pial arteries, as compared with middle meningeal and superficial temporal arteries (branches from the external carotid). They showed that the vasoconstrictor response of the pial arteries to exogenous noradrenaline was poor, reaching only 21% of the possible tissue maximal (as defined by the response to high KCl), compared to 34% and 90% in the meningeal and superficial temporal respectively. Various explanations for the poor responsiveness of the pial artery were investigated, including possible concurrent release of NO or other endothelial factors, β-adrenoreceptor activation by the noradrenaline, release of dilator prostanoids or an effect of the level of basal tone in the vessel segment. Experiments which accounted for each of these factors did not alter the response of the pial vessels to exogenous noradrenaline or to an electrical field stimulation (see Chapter 6 for further details). Therefore the limited responsiveness of the vascular smooth muscle to noradrenaline in this study is suggestive of a low density of α-adrenoreceptors on cerebral vessels, at least in human pial arteries, lending support for the use of catecholamines in studies of cerebral autoregulation.

Further support comes from Oleson (1972), who showed that, in conscious, neurological patients, direct intra-carotid infusions of adrenaline, noradrenaline ($2\mu g.ml^{-1}$) or angiotensin ($1\ \mu g.ml^{-1}$) caused no significant changes in CBF, as assessed by ipsilaterally placed scintillation detectors and intra-arterial injection of ^{133}Xe. The dose of adrenaline they used had no significant effects on ABP or CVR, despite the selected doses being higher than the normally occurring concentrations of endogenously circulating catecholamines (De

Champlain *et al* (1976) reported combined noradrenaline, adrenaline and dopamine serum levels of 0.2±0.01ng.ml^{-1} in healthy subjects in a supine position). However both noradrenaline and angiotensin increased ABP and CVR. Therefore Oleson (1972) also administered adrenaline, noradrenaline and angiotensin intravenously for comparison. This route of administration caused larger increases in ABP and corresponding greater increases in CVR. They therefore concluded that the evoked changes in CVR represented autoregulatory changes in resistance to buffer against the increase in pressure, rather than any local vasoconstrictor effect of the infused drugs, further validating their use in studies of autoregulation.

Data from studies that *have* shown cerebral vasoconstrictor effects of catecholamines can probably be explained by lack of correction for the accompanying decrease in P_aCO_2 which is sometimes observed (Greenfield & Tindall, 1968). CO_2 itself is a potent vasoactive molecule, causing vasodilatation when levels increase, and vasoconstriction when levels decrease. Further, catecholamines stimulate respiration (e.g. Barcroft *et al*, 1957), and so the resulting hypocapnia could induce cerebral vasoconstriction. Additionally, the external carotid artery and its branches are known to be highly responsive to noradrenaline (Greenfield & Tindall, 1968), and so a decrease in blood flow may be seen if this vascular bed has not been isolated or accounted for. Denison & Green (1956) used a canine preparation in which the intra- and extra-cerebral circulations were completely isolated from one another, but retained their ability to respond to changes in pressure. When a direct arterial infusion of adrenaline or noradrenaline was given, they had no effect on CBF. Therefore, providing potential changes in arterial blood gasses and extracerebral contamination are taken into consideration or avoided, the use of catecholamines to study cerebral autoregulation is justifiable.

3.1.2.2 The use of phenylephrine in autoregulatory studies

Phenylephrine (PE) is commonly used in autoregulatory studies, as it is a readily available and cheap sympathomimetic, which does not carry the associated issue of light sensitivity and oxidation seen with adrenaline (see Material Safety Data Sheets, Sigma-Aldrich®). Studies in rats which have used PE to investigate the autoregulatory upper limit (UL) include several studies by Sadoshima *et al*. For example, they increased ABP in anaesthetised spontaneously hypertensive rats (SHRs) in step changes of 10mmHg, up to a maximum of ~220mmHg, using i.v. PE. They maintained each level for 5 minutes to record the effects on CBF, as measured by intracerebral probes and a hydrogen tracer (methods for measurement of CBF are discussed in detail in the introduction, see 1.2). This allowed investigation of autoregulatory capacity during the development of hypertension in SHRs (Sadoshima *et al*, 1985), although the use of stepwise increases in ABP precludes the precise determination of the UL.

On the other hand, Mayhan & Heistad (1986) gave a continuous 10µg.min^{-1} PE i.v. infusion for 5 minutes to cause acute hypertension in male Sprague-Dawley rats. Arterial pressure increased from 100 to 175mmHg within 1.5 minutes, and they assessed sites of leakage in the BBB, as well as pial arterial and venous pressure, to investigate the contribution of increases in cerebral venous pressure to BBB disruption seen during hypertension. The use of a continuous infusion to gradually raise ABP would have allowed for a more precise definition of the UL, although no measurement of CBF was made.

Talman & Dragon (1995) used anaesthetised Sprague-Dawley rats to investigate the role of the arterial baroreceptor reflex and NO in cerebral autoregulation. PE was continuously infused, i.v. at 0.5µg.µl^{-1} in increasing volumes, to raise ABP to ~170-190mmHg in order to assess 'breakthrough' of autoregulation. CBF was measured by Laser Doppler flowmetry via

a cranial window. This method allowed for an accurate determination of the UL, with a gradual and continuous increase in ABP and a direct assessment of CBF.

Paterno *et al* (2000) gave 4-80mg.min^{-1} of PE by an i.v. infusion to anaesthetised Sprague-Dawley rats, to increase MABP from a basal level of ~100mmHg to 130, 150, 170 and 200mHg. A steady state MABP was reached by 2 minutes and then maintained for a further 3 minutes, allowing monitoring of pial arteriolar diameter, and the effects of potassium channel inhibition on the diameter response to the induced pressure changes. As above, the use of stepwise increases in ABP limits the usefulness of this approach for the study of autoregulation.

Euser & Cipolla (2007) gave i.v. PE to anaesthetised female Sprague-Dawley rats, starting at 0.5µg.min^{-1} and increasing at regular intervals to produce a steady rise in ABP, up to ~180-210mmHg. The resultant autoregulatory curves, which were determined from Laser Doppler flowmetry traces, were compared between rats in the late stages of pregnancy and non-pregnant controls, to investigate pregnancy-induced changes in autoregulation which may predispose to eclampsia.

PE has also been used to assess autoregulation in humans; Joshi *et al* (2000) infused PE i.v. at 10-40µg.min^{-1} to patients undergoing cerebral angiography, and assessed CBF using a Xenon tracer and extracerebral detector probes. They investigated the effect of NO on vascular tone, and the infusion of PE was given to control for the effect of the increase in ABP seen upon NO inhibition (~15mmHg increase). Despite the clinical applicability of carrying out a study in patients, the relatively small increase in ABP induced by PE would not allow an assessment of the UL.

Zhang *et al* (2009) gave i.v. infusions at 0.5, 1 and 2 $\mu g.kg^{-1}min^{-1}$ to healthy volunteers, allowing 5 minutes to reach a steady state, before recording a further 6 minutes of data at each dose. They achieved stepwise increases in ABP, raising it 11, 23 and 37% from baseline and inducing steady-state increases in CVR, whilst monitoring the relationship between spontaneous blood pressure changes and CBF velocity in the middle cerebral artery using a transcranial Doppler probe. As mentioned above, relatively small increases in ABP don't allow for study of the UL. In addition, study of spontaneous oscillations in ABP and the effects on CBF enables assessment of dynamic autoregulation rather than static.

Jansen *et al* (2000) studied autoregulation in healthy volunteers at sea level, compared to Sherpas and newcomers to an altitude of ~4000m. PE was given via a slow i.v. infusion at $0.2mg.ml^{-1}$, increasing ABP by ~20mmHg over 10-15 minutes, whilst assessing CBF by transcranial Doppler. Whilst the use of human volunteers is an advantage for translatability of the data, it limits the extent of ABP increases that can be imposed, due to the risk of inducing vascular damage.

Despite the limitations, taken together these studies demonstrate that PE is widely used to raise ABP in order to assess CA in both laboratory species such as rats, as well as humans.

3.1.3 Defining the autoregulatory curve and upper limit

As discussed previously, the relationship between ABP and CBF can be described by an autoregulatory curve. The traditional model of CA (e.g. Lassen, 1959) suggests that if ABP falls or rises within the physiological range of ~60-160mmHg, CBF is maintained by either vasodilatation or vasoconstriction respectively, in a so-called plateau. If ABP exceeds this LL or UL, the vascular autoregulatory mechanisms are overcome and CBF will fall or rise respectively. More recent studies have provided an updated view of CA, suggesting a much

narrower plateau range, and a more pressure-passive relationship between CBF and ABP (Lucas *et al*, 2010, Willie *et al*, 2014) (see 1.3.6 for a more extensive discussion).

As the aim of this study was to assess the mechanisms governing the control of CBF towards the upper end of the autoregulatory range, it is pertinent to consider methods for defining an autoregulatory curve and assessing the UL.

Sadoshima *et al* (1985) defined the UL as the point at which CBF increased without a further increase in ABP. They reported that CBF remained fairly constant during initial step increases in ABP, although they did see a 15-20% increase in CBF above baseline resulting in a gradually rising slope, until a level of ABP was reached at which CBF rose 'passively', indicating breakthrough of autoregulation. However a precise ABP at which the UL was exceeded could only be estimated due to the use of a stepwise increase in ABP.

Mayhan & Heistad (1986) did not directly define the UL, but instead identified the increase in ABP required to increase pial venous pressure and cause disruption of the venous BBB (indicated by extravasation of FITC-labelled dextran from the venules; Evans Blue dye has also been used to the same effect (Euser *et al*, 2008)). As the resultant rise in CBF beyond the UL may be associated with an increased risk of BBB disruption, the point at which they observed the damage could be taken to indicate the breakthrough of autoregulation and therefore the ABP at which the UL is reached, but they made no measures of flow.

Talman & Dragon (1995) simply defined the UL as the ABP at which CBF rises and CVR falls, when expressed as a percentage of baseline values. In contrast to Sadoshima *et al* (1985), they reported no significant increases above baseline during the initial increases in ABP, and thus the autoregulatory curves were flat until the UL was reached. This may be due to differences in the technique used to measure CBF (platinum electrodes stereotaxically

placed in the cortices, vs. Laser Doppler probe over a cortical window) or in the method of PE infusion (10mmHg steps in ABP vs. a smooth, progressive infusion, see above 3.1.2.2).

Paterno *et al* (2000) monitored pial arteriole diameter, and took an increase in diameter to indicate a 'breakthrough of autoregulation' i.e. exceeding the UL. However, similar to Sadoshima *et al* (1985), they followed a protocol of predefined steps in ABP, meaning an exact ABP at which the UL was exceeded could not be identified.

By contrast, Euser & Cipolla (2007) plotted pressure vs. flow curves from experiments in which 'evidence of breakthrough' had occurred. They then defined the UL as the point at which this curve showed a sudden steep rise, indicating that autoregulation had been overcome.

Study of the UL in humans is hampered ethically by the risk of inducing microvascular damage. Thus the increases in ABP induced in published studies tend to be moderate and do not allow identification of the UL. For example, Zhang *et al* (2009) saw an 11% increase in CBF velocity at the top dose of PE given, which had raised ABP by 37% and was associated with a 23% increase in CVR. They stated that this reflected an intact steady-state autoregulation and did not define an UL, but rather used the protocol to investigate the effects of the acute rises in ABP and CVR upon dynamic autoregulation to spontaneous ABP fluctuations. Similarly, Jansen *et al* (2012) elevated ABP by just 20mmHg from baseline, and assessed autoregulation by plotting CBF velocity in the MCA at baseline and during the induced hypertension, against the respective ABPs. This allowed evaluation of whether autoregulation was intact (i.e. no change in CBF velocity between baseline and hypertension) or compromised (i.e. if CBF velocity had increased with ABP), but did not allow them to assess the UL.

The discussed studies highlight the advantages and disadvantages of the use of animals vs. human volunteers. Whilst research conducted in humans may be more clinically relevant and translatable, the study of the UL of autoregulation, and the associated risks of raising ABP to the point of potential BBB damage, justifies the use of an animal model. None of the published studies using humans have attempted to reach the UL, and none of the above described studies have precisely defined a quantitative method for identifying the UL. These studies have relied either on qualitative assessment of the point at which CBF started to rise, seeing a specific characteristic in the ABP vs CBF curve e.g. a certain % rise above baseline/a steep increase in CBF, or used pre-defined steps in ABP, precluding a precise definition. It is also worth considering the findings of studies such as Lucas *et al* (2010), which have evolved the traditional model of CA. They demonstrated a much more pressure-passive relationship between CBF and ABP than originally described, with a much narrower plateau range. This could impair identification of an UL.

As such, we sought to define a method for a quantitative, reproducible and precise determination of the UL. To do this we developed an analysis method based on previous work in our laboratory by Edmunds & Marshall (2001), and originally described by Samsel and Schumacker (1988). Autoregulatory curves were plotted for each individual experiment and dual-line linear regression analysis was applied to subsets of data representing the 'plateau' and 'rising' phases of the curve. The UL was achieved by calculating the point of intersection of the two regression lines with the best fit (see 2.6.3 for further details). Using this mathematical approach removed the issue of any qualitative judgement.

In initial experiments on n=25 young rats (mean weight (± SEM) of 330±5g), of which 17 were subsequently included in the young (Y) control group, various methods and surgical set-ups were tested to identify a protocol which reliably measured CBF, induced a smooth and

progressive increase in MABP and resulted in a consistent identification of the autoregulatory UL. The results obtained are described below (see 3.3).

3.2 Methods and protocols

3.2.1 Group 1: Pharmacological assessment of cerebral autoregulation and the UL

In n=16 young male Wistar rats (338±5g), basic surgery was carried out as described in 2.2.1. In this group only the right common carotid artery was isolated, allowing vascular isolation of the right internal carotid artery. Flow was then measured at the level of the right common carotid artery, and was taken as an index of gross RCBF. In n=8 of these animals, a second flow probe was placed on the right femoral artery to record hind limb skeletal muscle blood flow. Once baseline variables were stable, the PE infusion protocol was carried out as described in 2.5.1, with variations to identify the most suitable method. At the end of the protocol, ABP was allowed to recover back to basal levels and, if all variables stabilised, the protocol was repeated (see Results 3.3.1).

3.2.2 Group 2: The effect of vascular isolation on cerebral autoregulation and the UL

In order to validate recording from a vascularly isolated internal carotid artery as an index of gross CBF, n=5 young rats (324±8g) underwent the protocol described above. However CBF was recorded bilaterally from both the right and left common carotid arteries, with the external carotid and other branches ligated on the right side only (see Results 3.3.2).

In addition, at the end of the experiment in 3 young rats (337±4g), the right common carotid artery was cannulated in the direction of the brain, with all ligations still intact. A vessel clip was placed on the left jugular vein (the right jugular vein having already been cannulated – see 2.2.1) to prevent cerebral venous drainage, and a 2% Evans Blue solution was injected. Immediately following this the rat was killed as described in 2.2.1. The rat was then examined for regions of the face and brain showing blue staining, and photos were taken (see 3.3.2).

3.2.3 Group 3: The effect of position on cerebral autoregulation and the UL

As discussed in 2.2.2, some subgroups of animals underwent an advanced surgical procedure, which involved them being placed in a prone position, with the skull being held in a stereotaxic frame, as opposed to a supine position for the basic procedure. The effect of this postural difference upon the assessment of CA and the UL was investigated in 4 young rats (297±14g). These animals underwent an identical surgical set-up to 3.2.2, but were then placed prone in the stereotaxic frame before the PE infusion protocol commenced (see Results 3.3.3).

All data are presented as the mean ± SEM, and was analysed as described above in section 3.1.3 and General Methods sections 2.6.1 and 2.7.3. The statistics carried out were paired or unpaired t-tests as appropriate, and one-way ANOVAs with either post-hoc Bonferroni or Dunnett's tests.

3.3 Results

3.3.1 Group 1: Refining a protocol to allow PE-induced increases in ABP to be used to investigate cerebral autoregulation and the upper limit

Various methods of PE infusion were tested. First, a continuous infusion of gradually increasing dose was achieved by increasing the infusion rate between 6ml.hr^{-1} to 12ml.hr^{-1} to increase the dose from, for example, 0.3 to 0.6µg.kg^{-1}.min^{-1}. A switch was then made to a syringe containing a higher concentration, which was infused at 6ml.hr^{-1}, before increasing the rate and so on. Each dose was infused for 5 minutes with the intention of achieving a smooth progressive increase in ABP with no recovery between doses.

This method produced autoregulatory curves of M RCBF against MABP that were different from expected in several animals (Figure 17a); the initial increase in MABP caused a slight increase followed by a decrease in M RCBF, indicating a cerebral vasoconstriction beyond that required to maintain a constant CBF. M RCBF then returned towards the original baseline before increasing as the UL was exceeded. For comparison, Figure 17b shows the classical view of an autoregulatory curve, taken from a review by Willie *et al* (2014), where CBF is held constant over a wide range of MABPs, only increasing or decreasing at the upper and lower limits respectively.

The second method tested involved giving shorter PE infusions, continued only until the effect on MABP had plateaued, after which ABP was allowed to recover before a higher dose was given. This was to assess whether the initial decrease in M RCBF seen with the first method (in Figure 17a) was an effect of continuous infusion of PE. An example of the data generated is shown in Figure 18. Again an initial decrease in M RCBF was seen, but this persisted across the range of doses tested and the UL was apparently not reached. This was also seen in additional animals.

As this protocol offered no obvious improvement, the continuous infusion method described first was used for the experiments proper. However a second infusion pump holding a syringe containing PE at a higher concentration was already set up. This allowed the time between doses to be minimised, avoiding recovery of MABP between doses, and producing a smooth increase in MABP. As mentioned above (3.2.1), the intention was to repeat the PE infusion protocol within individual animals, so as to allow for a repeated measures experimental design. Therefore the reproducibility of the autoregulatory curve was assessed. As shown in the examples in Figure 19, in some animals the 2nd infusion produced a consistent 2nd autoregulatory curve (Figure 19a). In others, the response did not appear to reach the UL during the 2nd infusion (Figure 19b), or was shifted (Figures 19c and d), which would have altered interpretation of the UL. It was also observed that even the 1st PE infusion had an adverse effect on P_aO_2 at the higher doses (see Table 2). For these reasons, it was decided that a repeated measures design within animals was not possible and that comparisons would be made between groups of animals.

The initial fall in CBF seen with the first few increasing doses of PE (Figure 17a) raised the possibility that the induction of anaesthesia or surgery had caused a cerebral vasodilatation. Thus a further change was made to the protocol such that a series of 2-minute infusions of PE at 10µg.kg^{-1}.min^{-1} ('challenge' doses) were given before starting the infusion proper. It was hoped that the challenge doses would 'reset' the basal tone in the cerebral vasculature, and allow something closer to the expected autoregulatory relationship shown in Figure 17b. The effect of the 'challenge' doses on MABP and M RCBF are shown in Figures 20a & b respectively (n=8). The doses themselves caused an increase in MABP and decrease in M RCBF (data not shown). MABP then tended to recover back towards baseline levels between challenge doses (no significant difference between the baseline and recovery after each dose,

one-way ANOVA with post-hoc Dunnett's, F ratio=1.2, P=0.33), whilst M RCBF settled at a new, significantly lower baseline (paired t-test, baseline vs. CBF recovery value 1, P=0.0001). PE challenges were repeated until CBF settled at a similar value over three consecutive doses (one-way ANOVA with post-hoc Bonferroni showed no significant difference between the three CBF recovery values, F ratio=0.06, P=0.95). This usually required only three doses, but in some cases up to five were given. The PE infusion protocol was then carried out from this new baseline.

In a few of these experiments, a decrease in M RCBF, with increasing MABP caused by the PE infusion, was still observed over the range in which CBF is generally thought to be maintained by autoregulation. However, in the majority of experiments, this was not the case and the extent of this vasoconstriction appeared reduced. Therefore this variation to the protocol was used in all future experiments. In other words, all subsequent PE infusion data are presented with the post-challenge CBF as the baseline.

The data produced here were included in the Y control group data (n=17 successful experiments including those in group 2 and 3 below), and are presented in Chapter 4. However, an example of a single experiment using the final PE infusion protocol and analysed as described in 3.1.3 using dual-line linear regression analysis is shown in Figure 21.

The 'plateau' phase of the autoregulatory curve is shown in blue and the 'rising' phase, i.e. beyond the UL, is shown in red. This example clearly shows a much flatter plateau than in Figures 17-19, and the autoregulatory UL was exceeded and CBF rose at 178mmHg (calculated as the intersect of the two linear regression lines). Table 3 shows the Sy.x and r^2 values (indicators of goodness of fit) for each pair of linear regression lines selected as those with the best fit, and the resulting calculated UL, for the 8 successful experiments that used

challenge doses. The Sy.x values are low, indicating that the pairs of lines selected from the linear regression analyses had a good fit. It can also be seen that the PE challenge doses produced 'plateau' linear regression lines with low (0.3±0.08) r^2 values, indicating that they are flatter and therefore more representative of the expected data in the autoregulatory range. In contrast, the 'rising' linear regression lines had r^2 values closer to 1 (0.8±0.1), indicating that CBF rose with ABP above the UL. The mean ABP value at which the 'plateau' and 'rising' lines intersected, and therefore the UL, was 170±3.4mmHg.

In n=8 rats, FBF was also recorded during PE infusion, to assess hind limb skeletal muscle blood flow in parallel with CBF. Figure 22a shows that M FBF gradually increased with MABP up until around 170mmHg; coinciding with the mean UL value calculated from the values in Table 3. Beyond this pressure, MFBF fell. Femoral vascular resistance (FVR) showed an inverse relationship to FBF, initially decreasing before increasing beyond an ABP of ~170mmHg (Figure 22b).

3.3.2 Group 2: Vascular isolation had no effect on cerebral autoregulation or the UL

In 5 young rats, CBF was recorded bilaterally with the internal carotid artery vascularly isolated on the right (M RCBF), whilst the left carotid remained intact (M LCaBF) to control for any effect of vascular ligation on autoregulation. In these experiments, as shown in Figure 23a, basal MCBF was significantly higher on the intact, left side (1.2±0.04 vs 2.1±0.2ml·min^{-1}, paired t-test, P<0.0001). However, both the isolated (M RCBF) and intact (M LCaBF) carotid arteries showed the same response with respect to MABP. This is shown by a plot of the difference between the two sides (left - right) (Figure 23b). The difference between the two flow measurements was constant except when the UL was exceeded, at which point M LCaBF showed a trend to increase to a greater extent i.e. on the intact side, although this was

not significant (Δ0.9±0.07 vs. 1.4±0.3ml·min^{-1}, M RCBF vs M LCaBF, paired t-test, P=0.14). The ULs were not significantly different between the two sides; M RCBF: 168±4 vs. M LCaBF: 169±3mmHg (paired t-test, P=0.34).

At the end of the experiments in 3 of these rats, an Evans Blue solution was injected via the right common carotid artery, in the direction of the brain, in order to validate ligated carotid artery blood flow as an index of CBF. Figure 24 shows an example of the photos taken on examination of the rats' face, mouth and brain. A small amount of blue staining can be seen in the right eye, but there is little staining on the rest of the face (Figure 24a). Some blue staining was seen in the roof of the mouth and skin around the right side of the mouth and nostril, but little to no staining was seen in the tongue (Figure 24b). On removal of the skull, blue staining was clearly seen on the right side of the brain, as well as some colouration on the left (Figure 24c).

3.3.3 Group 3: Prone vs. supine position had no effect on cerebral autoregulation or the UL

4 young rats underwent the surgical set up described above (3.2.2), but were then placed prone into a stereotaxic frame. The PE infusion protocol was then carried out in order to assess any effect of postural position upon CA or the UL. Figure 25 shows the M RCBF autoregulatory response to increasing MABP in the prone position, as compared to the supine position shown in Figure 23a, indicating that this change in position had no effect on the data recorded. The mean UL in the prone position was 168±3mmHg, which was not significantly different from that seen in the group which were in a supine position (168±4, P=0.89, unpaired t-test).

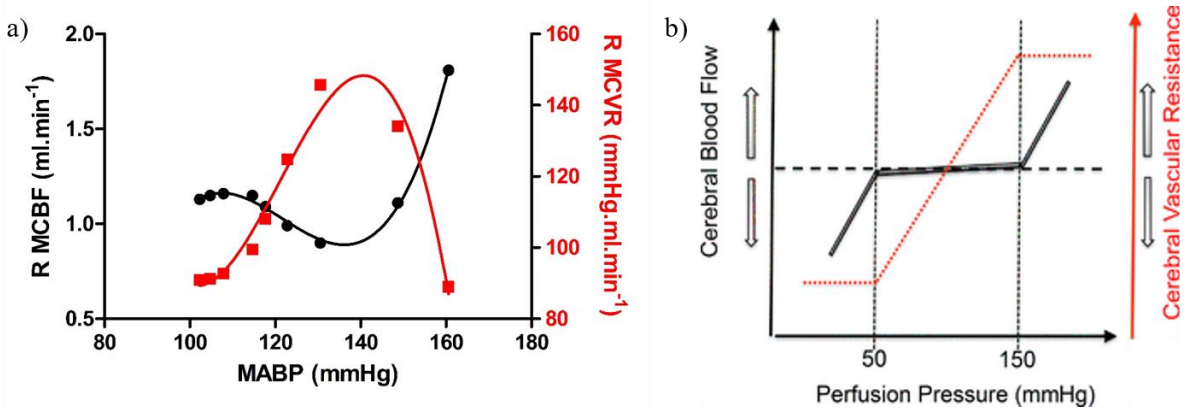

Figure 17: a) An example of an autoregulatory curve produced using a constant infusion of PE. As MABP was increased from ~100-140mmHg, a slight increase before a larger decrease in R MCBF was seen, suggesting a cerebral vasoconstriction. This was accompanied by a gradual increase in R MCVR. Above 140mmHg, R MCBF initially returned back towards baseline levels, before increasing as the UL was exceeded. R MCVR displayed an inverse relationship to CBF, decreasing to just below baseline. b) is a representation of the classical view of an autoregulatory curve adapted from Willie *et al* (2014), based on early data and description of cerebral autoregulation suggested by Lassen (1959). It shows a flat plateau of CBF across a wide range of ABPs, maintained by the changing CVR shown in red, before CBF falls or rises when the UL or LL is reached.

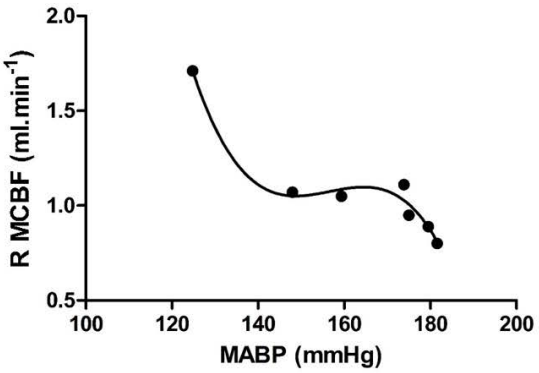

Figure 18: An example of the data generated when allowing recovery between each successive dose of PE to increase MABP. The apparent cerebral vasoconstriction resulting in a decrease in R MCBF was still seen using this protocol. In this example, this decrease in R MCBF persisted over the range of PE doses and the UL of autoregulation was not reached.

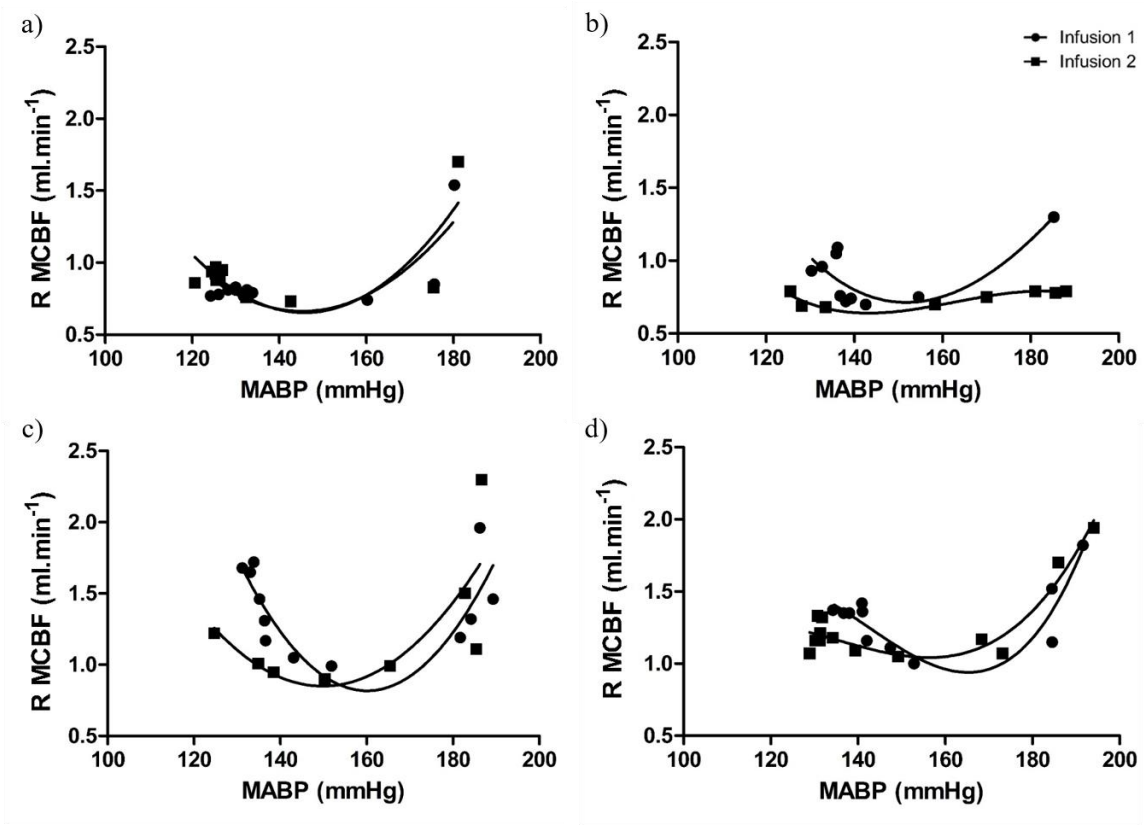

Figure 19: Four example graphs from experiments in which a 2nd PE infusion was attempted after recovery from the first. In a), the 2nd infusion was almost identical to the first, suggesting a reproducible protocol. b) shows an experiment in which the 2nd infusion produced similar MABP increases, but no increase in R MCBF i.e. an UL could not be identified. c) and d) are examples in which the 2nd infusion produced M RCBF data shifted compared to the 1st, whereby the UL appears to be reached at a different MABP.

	P_aO_2 (mmHg)	P_aCO_2 (mmHg)	pH
Basal	74±2.2	42±1.3	7.45±0.01
Highest PE dose	66±2.4 (*)	45±1.3 (*)	7.43±0.01 (*)

Table 2: The effect of the 1st PE infusion on arterial blood gasses and pH, in n=13 rats. P_aO_2 significantly decreased at the top dose of PE given compared to baseline (paired t-test, P=0.02). There was also a small but significant increase in P_aCO_2 (P=0.01) and decrease in pH (P=0.05).

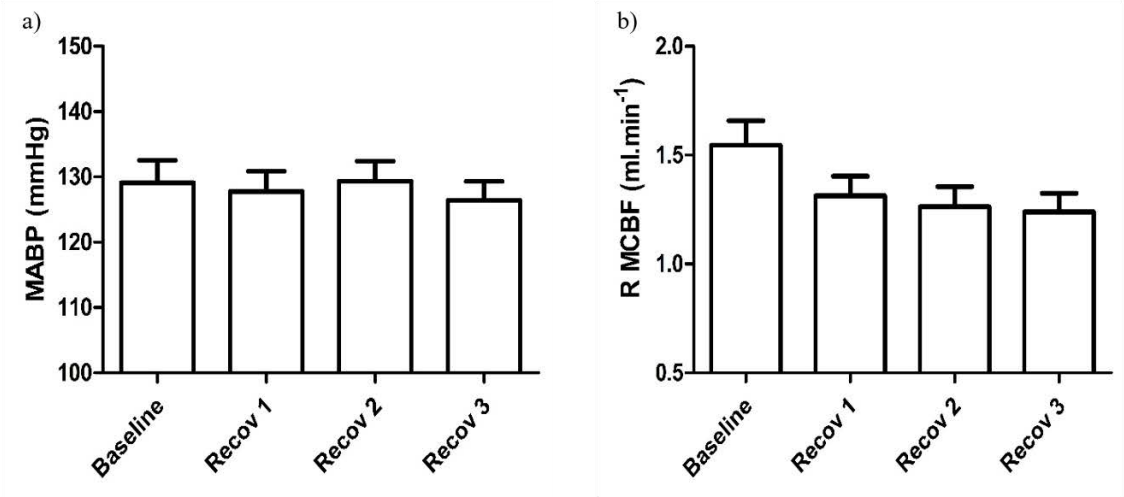

Figure 20: The effect of using 'challenge' doses of PE at 10µg.kg^{-1}min^{-1} on MABP (a) and R MCBF (b) in n=8 rats. MABP returned to baseline after each infusion, whilst R MCBF tended to settle at a new lower baseline. These doses were used in an attempt to reset the basal cerebral vascular tone, after observing an apparent vasoconstriction in previous experiments, over the range of MABP in which autoregulation of CBF would be expected.

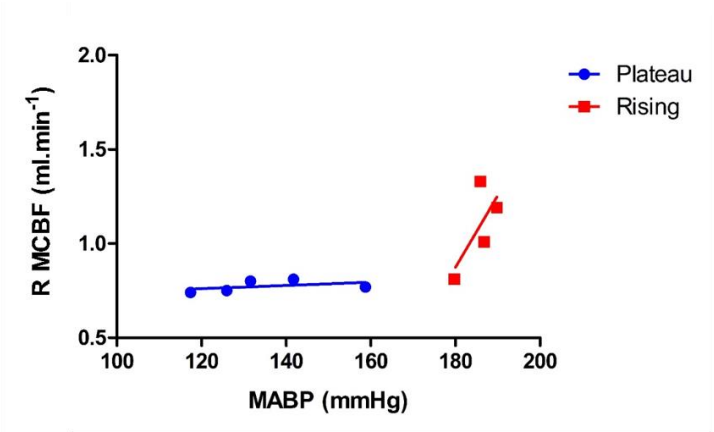

Figure 21: Data from a single experiment using 'challenge' doses of PE at 10µg.kg^{-1}min^{-1}, to achieve a steady basal CBF prior to infusing PE in increasing doses to investigate the UL of CA. A much flatter autoregulatory plateau was seen, in contrast to the apparent vasoconstriction seen previously. This graph also demonstrates use of dual-line linear regression analysis to split the data into 'plateau' and 'rising' phases, and allow calculation of the UL by determining the intersect of the two lines with the best fit. In this case the UL was calculated to be 178mmHg.

Experiment ID	Sy.x	r^2 (plateau & rising)	Intersect (mmHg)
14/12/12	0.09	0.84 & 1.00	164.2
14/1/13	0.22	0.20 & 0.51	178.4
15/1/13	0.12	0.22 & 1.00	169.2
16/1/13	0.28	0.03 & 0.99	161.3
25/1/13	0.03	0.31 & 1.00	174.8
28/1/13	0.14	0.29 & 1.00	152.5
29/1/13	0.63	0.30 & 0.24	176.7
30/1/13	0.39	0.40 & 0.69	180.4
Mean	0.24 ± 0.07	0.32 ± 0.08 & 0.8 ± 0.1	170 ± 3.4

Table 3: The Sy.x and r^2 values from the dual-line linear regression analysis of n=8 experiments in which PE challenge doses were used, and the calculated intersect values. The mean Sy.x value is low, indicating that the selected pairs of lines had a good fit. The mean r^2 value of the plateau lines was low (<1), whilst the rising line value was closer to 1.

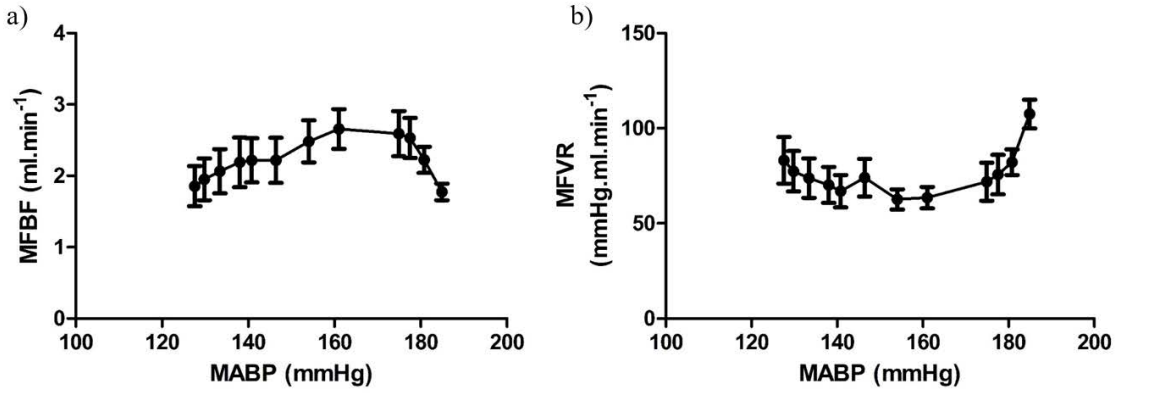

Figure 22: In n=8 rats, a Transonic flow probe was used to record mean femoral blood flow (MFBF), to assess hindlimb skeletal muscle blood flow in parallel with CBF. As PE was infused to increase MABP, (a) MFBF gradually increased, before decreasing from around 170mmHg. (b) Mean femoral vascular resistance (MFVR) showed an inverse relationship to MFBF, initially decreasing as MABP increased, before increasing from around 170mmHg.

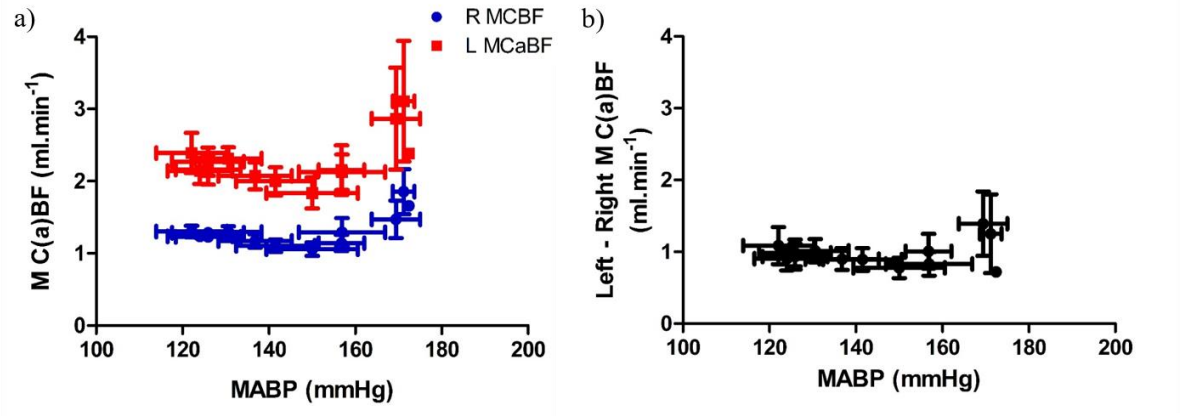

Figure 23: a) R MCBF was recorded from the right common carotid artery with branches ligated to vascularly isolate internal carotid flow (shown in blue), and from the left, intact carotid artery (L MCaBF – shown in red), during PE-induced increases in MABP, in n=5 rats. b) The difference between L MCaBF and R MCBF is also shown. Whilst basal L MCaBF was significantly higher than R MCBF, ligations carried out on the right side had no effect on autoregulatory behaviour, as both R MCBF and L MCaBF responded similarly as MABP was increased. The two calculated ULs were not significantly different. This is emphasised by the consistent difference between left and right shown in b), only showing a non-significant difference once CBF increased beyond the UL, indicating that L MCaBF increased to a greater extent.

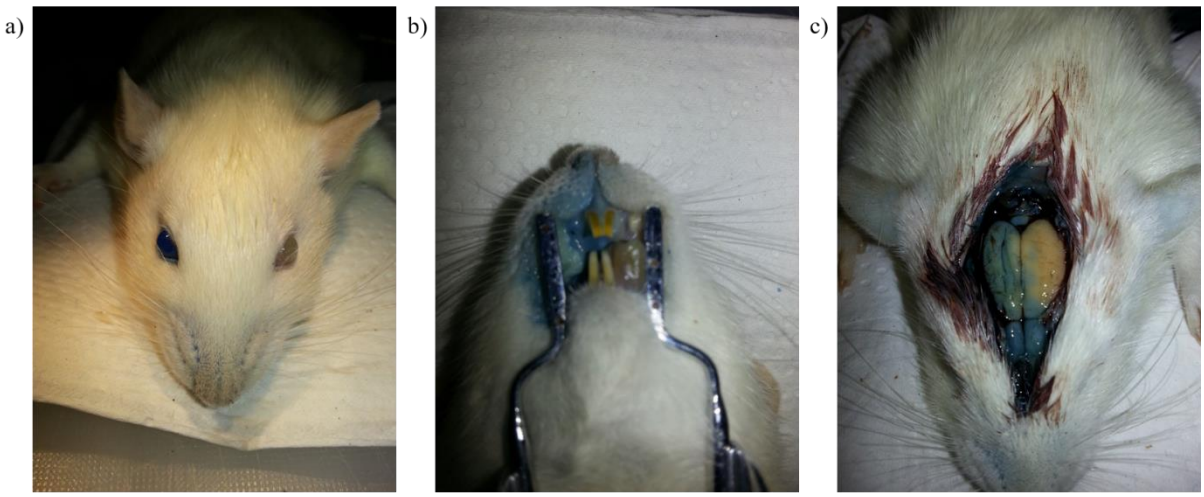

Figure 24: An example of the photos taken when Evans Blue solution was injected via the right common carotid artery, in the direction of the brain, in order to validate ligated carotid artery blood flow as an index of CBF. a) A small amount of staining was seen in the right eye, but little staining was seen on the rest of the face. b) Some staining was seen in the roof of the mouth and skin around the right side of the mouth and nostril, but no staining was seen in the tongue. c) Staining was clearly seen on the right side of the brain, as well as some colouration on the left.

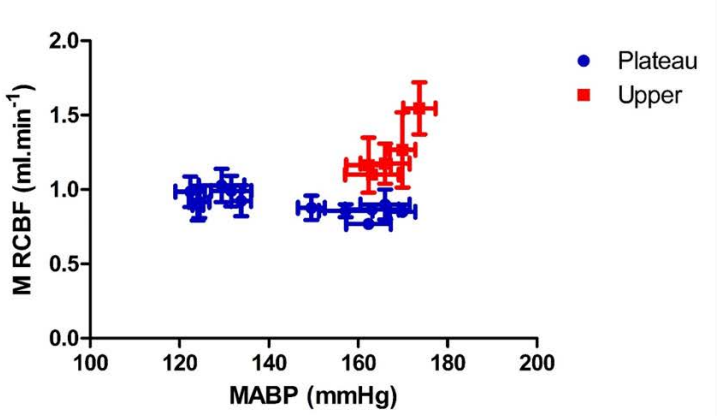

Figure 25: Group mean data from n=4 young rats placed prone in a stereotaxic frame. M RCBF (recorded from vascularly isolated right internal carotid arteries) showed similar autoregulatory behaviour with respect to increasing MABP, as that seen in animals in a supine position shown in Figure 23 a). The mean group UL, calculated by dual-line linear regression analysis of each data set, was 168±3mmHg, not significantly different from the M RCBF UL in Figure 23 a) (UL: 168±4mmHg, unpaired t-test, P>0.05).

3.4 Discussion

3.4.1 Method of cerebral blood flow measurement

In the present study, Transonic probes were used to measure CBF. They record the difference in transit times of ultrasonic waves intersecting the vessel both with and against the flow of blood, producing a measurement of volume flow (see section 1.3.2). By this means, carotid blood flow was used an index of CBF to allow the UL of autoregulation to be studied in anaesthetised rats. Basal CBF was 1.2±0.04ml·min^{-1} in the right common carotid artery with the internal carotid vascularly isolated. In the left common carotid, which was intact, basal CBF was 2.1±0.2ml·min^{-1} (after PE challenge doses in each case, see section 3.1). These data are similar to those reported in the literature. For example, Mutch *et al* (1989) measured rCBF using microspheres in Sprague-Dawley rats and reported a total CBF, calculated as a weighted mean of multiple regional measurements, of 1.8±0.2ml.g^{-1}min^{-1} relative to brain weight. The data collected in the present study were not normalised to weight of the rat or brain tissue, but the young rat brain weighs between 1.5-2g (based on observations in the current study and literature reports e.g. Ryzhavskii & Ivashkina, 1996). On the other hand, Craig & Martin (2012) reported a common carotid artery flow of ~2.6ml·min^{-1} in anaesthetised Wistar rats weighing 150-200g, which is slightly higher than the intact left carotid flow of the present study.

Using internal carotid blood flow, after ligation of all other common carotid branches, as an index of CBF was done previously by colleagues (Thomas & Marshall, 1994), who assessed the validity of this measure. They injected Evans Blue into the right common carotid artery towards the brain with both jugular veins occluded. The dye was seen in the ipsilateral cerebral hemisphere, and the cerebellum and rostral brainstem, but not in the skin or muscles of the cheek, or the tongue. Slight colouration of the right eye, nostril and the roof of the

mouth revealed the only contaminating flow, suggesting that internal carotid flow can be used in this way as a valid index of CBF, and mainly of the ipsilateral side of the forebrain. We repeated this method of validation, injecting Evans Blue dye via the right common carotid towards the brain and observed the resulting colouration (see 3.3.2). The images in Figure 24 show results similar to those described by Thomas & Marshall (1994), validating the surgical procedure for the recording of CBF for the study.

Vascular isolation of the internal carotid did not appear to effect autoregulatory behaviour or the UL when compared to recordings made in the contralateral intact carotid artery in the same animal, as shown by data from group 2 (Figure 23). The effect of postural position, prone or head raised, was also shown to have no effect on CA or the UL (Figure 25). The effect of posture may be more relevant when investigating cerebral autoregulation in humans, as moving from a supine, or even seated position, to standing, would be expected to induce a much larger change in cerebral perfusion pressure, due to the comparatively larger distance between the brain and heart (as cerebral arterial pressure is reduced due to the effects of gravity – see discussion in Zhang & Levine, 2007).

3.4.2 The use of PE to assess autoregulation and the UL

The use of PE infusion to increase ABP without causing cerebral vasoconstriction, and specifically to investigate the UL of autoregulation, is widely reported in the literature (see section 3.1.2.2). Therefore, in the present study, infusions of PE were given at doses of 0.1-60µg.kg^{-1}.min^{-1}, which increased ABP from a baseline of ~125 to ~180mmHg to produce autoregulatory curves. The doses of PE used were guided by studies using similar methods (section 3.1.2.2). The mean dose of PE used in group 1 was 17.7±2.4µg.kg^{-1}min^{-1}; this raised MABP by ~40mmHg which is in line with the literature. For example Drummond *et al* (1989)

found that 16.1±1.4µg.kg^{-1}min^{-1} was the mean optimum dose that needed to be infused to raise MABP gradually by 30-35mmHg above baseline in rats.

In the present study, cerebral vasoconstriction, i.e. a decrease in CBF and increase in CVR, occurred at the beginning of the infusion, often after an initial increase in CBF (e.g. Figure 17a). This has not been reported in the literature and was an unexpected result. As discussed in 3.1.2.2, Paternò *et al* (2000) used i.v. infusions of PE in anaesthetised Sprague-Dawley rats to increase MABP from a basal level of ~100mmHg to 130, 150, 170 and 200mHg. At the more moderate increases in pressure (130-150mmHg) they did report a *decrease* in pial arteriole diameter of 5-10% from a baseline diameter of 46±2µm. However, as flow was not determined, it is not known whether this was associated with a decrease in CBF, or with maintenance of total CBF i.e. autoregulation. Joshi *et al* (2000) reported similar results in humans when using the intracarotid ^{133}Xe injection technique with detector probes placed over the MCA. When PE was infused to increase MABP by ~20%, this was accompanied by an increase in CVR and a non-significant trend for CBF to decrease. They discussed this as a 'cerebral autoregulatory vasoconstriction', and it was unaffected by the sedative given to the subjects. Hence the vasoconstriction seen in the present study may represent normal autoregulatory function, which overcompensates during moderate increases in pressure, resulting in a decrease in CBF.

Mayhan & Heistad (1986) showed that the pressure in pial arterioles of the parietal cortex, roughly 40µm in diameter, is only around 50% of systemic arterial pressure, suggesting that the larger cerebral vessels account for at least 50% of CVR (see also Faraci & Heistad (1990), section 3.1.1.2). Therefore the vasoconstriction observed in proximal arterial vessels supplied by the carotid may represent a mechanism that protects the delicate downstream vessels,

which are more likely to be damaged by high pressure, and could potentially lead to haemorrhagic stroke (Faraci and Heistad, 1998).

The alternative possibility is that PE crosses the BBB and causes direct cerebral vasoconstriction. However, the literature suggests that this is not the case (see section 3.1.2.1). For example Drummond *et al* (1989), who used an autoradiographical method to determine local CBF, showed that PE-induced hypertension *improved* local CBF during ischemia induced by MCA occlusion in anaesthetised Sprague-Dawley rats. In the non-ischemic contralateral hemisphere, local CBF did not differ between the PE and control animals, suggesting that PE is not a direct cerebral vasoconstrictor. Hardebo *et al* (1979b) described the ability of extreme systemic hypertension to open the BBB enhancing the passage of monoamines, but the ABP values required to achieve this were >200mmHg when autoregulation is thought to be lost (see 1.2.1). Therefore leakage of PE through the BBB is unlikely to explain the current findings of cerebral vasoconstriction during the initial stages of PE infusion, when ABPs were below 170mmHg. Even if PE had entered the brain, adrenergic receptor density is low and so, as an α1-adrenoreceptor agonist, it would be relatively ineffective e.g. Bevan *et al* (1998), Oleson (1972) (see section 3.1.2.1).

Even after the relatively high challenge doses of PE were used in the present study to 'reset' basal CBF, initial increases in CBF followed by the previously discussed apparent cerebral vasoconstriction, were still observed at the lower doses during the PE infusion proper in some of the experiments. This occurred over the range in which autoregulation, and therefore no change in CBF, would be expected. Therefore it is pertinent to consider the mechanism of action of PE, which may offer some explanation for these observations. Richer *et al* (1987) showed, in pithed Sprague-Dawley rats, that lower doses of PE were associated with increased cardiac output and increased mesenteric and hind limb blood flow. At higher doses,

the cardiac output effect was lost, and increased resistance was seen in the mesenteric, hind limb and, to a lesser extent, renal vasculature. Interestingly, Brungardt *et al* (1974) showed that low doses of PE in dogs, was able to cause dilatation of femoral arteries, whilst constriction was seen at higher doses. This was attributed to PE interacting with β-receptors at low doses, confirmed by blockade with propranolol, and that binding to α-receptors occurred at higher doses, producing vasoconstriction. This could also explain the data from Richer *et al* (1987). Therefore the PE given in the present study may have increased flow (via β-mediated dilatation or by an increase in cardiac output) at lower doses, including in the arterial vessels downstream of the carotid artery. In response to an increase in MABP or flow, the cerebral circulation is known to constrict (in order to autoregulate). The carotid artery and downstream vessels are considered an extracranial extension of the cerebral circulation, and, if they behave similarly to the cerebral circulation, this could explain the constriction that followed the initial dilatation (e.g. Figure 17a).

There is also a potential for the anaesthesia and surgical procedure to have impaired cerebral autoregulation. Joshi *et al* (2003) reported that, in baboons, using isoflurane anaesthesia did not affect the ability to autoregulate in response to an increase in MABP evoked using PE; CVR increased and CBF remained constant. However, Werner *et al* (2005) showed that sevoflurane dose-dependently impaired CBF autoregulation (to decreases in MABP) in Sprague-Dawley rats. On the other hand, Strebel *et al* (1998) tested the effect of PE and noradrenaline on MCA and internal carotid blood flow velocity in humans under isoflurane or propofol (i.v.) anaesthesia. They observed no effect of either anaesthetic on the evoked vasoconstrictor response when the change in MABP was negated by a head-up position, suggesting no direct cerebral vasoconstriction (supporting the above discussion). However when MABP was allowed to change, they observed increases in blood flow velocity, implying

vasodilatation, to both vasoconstrictors under isoflurane anaesthesia, but not propofol. This suggests the inhalational anaesthetic may have affected CA. Therefore it is possible that the initial inhalation of isoflurane used in the present study for induction of anaesthesia, affected autoregulation. The isoflurane was quickly replaced with i.v. Alfaxan®, and the time elapsed during the surgery and stabilisation should have been sufficient for any effects to wear off (see methods 2.2). However the use of isoflurane may have contributed to the unexpected results.

The systemic hypoxia seen at the highest PE doses suggests that the infusion of this vasoconstrictor may have caused pulmonary vasoconstriction (Table 2). This has been demonstrated previously in dogs, both *in vivo* and *in vitro* (Ogawa *et al*, 2001) and was a factor that prevented the use of a repeated measures experimental design for the present study. It should be noted that the animals in most studies in which PE was used to increase ABP were mechanically ventilated and given supplemental O_2 to maintain normal blood gases (e.g. Drummond *et al*, 1989, Mutch *et al*, 1989, Stromberg *et al*, 1993, Ishikawa *et al*, 2009).

In summary, the methods tested in the present study allowed a protocol to be devised for continuous i.v. infusion of PE, increasing both rate and dose to achieve smooth, progressive increases in MABP, to produce autoregulatory curves that enabled calculation of the UL. This protocol was used subsequently throughout the studies described in this thesis.

3.4.3 Calculation of the autoregulatory upper limit

The experiments described here also resulted in a protocol which identified an UL of ~170mmHg (Figures 21, 23a & 25, Table 3); the MABP at which CBF was no longer maintained.

As discussed in sections 2.6 and 3.1.3, the method of calculation used to determine the UL of autoregulation in the present study was adapted from the technique used by Samsel & Schumacker (1988). This has also previously been used by colleagues Edmunds & Marshall (2001) to investigate the relationship between tissue O_2 delivery and consumption in hind limb muscle, and to define the critical O_2 delivery value at which O_2 consumption becomes directly dependent upon O_2 delivery. Essentially in both of these studies, the aim was to establish a mathematically justifiable and objective method for identifying the point of intersection of a relationship between two sets of biological data.

Such methodology has not been used before in the calculation of the UL in autoregulatory studies. Rather, most have used the point at which CBF rises by a certain percentage above the baseline level, or rises with no further increase in ABP (e.g. Sadoshima *et al* 1985, Zhang *et al*, 2009 - see section 3.1.3). Both techniques are rather subjective in terms of identifying a specific ABP value. However, finding the intersection of two linear regression lines ensured a more accurate determination of the pressure at which flow started to increase (e.g. Figure 21). The slope beyond the UL generally had an r^2 value of >0.5, showing that CBF had become related to MABP i.e. the UL had been exceeded (Table 3).

The ULs calculated in the present study, using the least squares method values quoted, compare favourably with the literature (further discussed in Chapter 4). For example Mayhan & Heistad (1986) induced acute hypertension up to 175mmHg in anaesthetised Sprague-Dawley rats and found that at this level there was an increase in pial venous pressure and BBB disruption (assessed by extravasation of FITC labelled-dextran), indicating the UL had been surpassed. This is consistent with the present value of ~170mmHg for the UL.

3.5 Conclusion

The experiments described here demonstrate that a gradual, PE-induced increase in MABP can be used to reliably assess the UL of CA in an anaesthetised rat model, but was not reproducible within experiments. PE was chosen due to the lack of reported direct cerebral vasoconstrictor activity, and due to its widespread use for similar studies. The PE was administered as a slow i.v. infusion, using a protocol shown to produce a smooth and progressive increase in MABP, and to allow investigation of the UL. The requirement to raise MABP to the level of >170mmHg to observe autoregulatory breakthrough provides support for the use of the anaesthetised rat model.

Gross CBF was measured at the level of the common carotid artery, with the internal carotid vascularly isolated. This was shown to be a valid index of CBF via the use of an Evans Blue infusion. The use of this invasive surgical approach to enable a reliable assessment of CBF lends further support to the use of an animal model.

The UL was identified by use of an adapted dual-line linear regression technique, which allowed for a mathematical and objective assessment, giving reproducible values.

CHAPTER 4: THE EFFECT OF AGEING ON THE CEREBRAL AUTOREGULATORY UPPER LIMIT

4.1 Introduction

4.1.1 The effects of ageing on vasculature

As described in the general introduction, CA is the mechanism by which CBF is maintained in the face of changes in ABP, and was first described by Lassen (1959). As ABP rises, cerebral vessels vasoconstrict in order to maintain CBF, and *vice versa*. There are two types of autoregulation; dynamic, which is the cerebrovascular response to rapid fluctuations in ABP (milliseconds to seconds), and static, the response to more prolonged and stable changes in ABP (seconds to minutes).

Also discussed in the introduction is that fact that the UK population is ageing, with over 11 million people aged 65 years or older (Age UK 2015). Prevalent with increasing age are a well-characterised number of changes in terms of cardiovascular function, although these do not appear at well-defined ages, or affect all individuals in the same way or to the same extent. With respect to vascular function, this includes an increase in arterial wall thickness, specifically intima-media thickness (Virmani *et al*, 1991), an increase in subendothelial collagen, a decrease in elastin and increased elastin break-down, and an increase in migration and proliferation of vascular smooth muscle cells into the intima (Hajdu *et al*, 1991). In combination, this results in reduced arterial distensibility i.e. increased stiffness (Roach & Burton, 1959, Hajdu *et al*, 1990), which contributes to increased total peripheral resistance and a tendency for an increased systolic and therefore pulse pressure. This increased pressure can further drive hypertrophy of the vessel wall and therefore cause a further increase in systemic pressure (Ferrari *et al*, 2003). Hypertension then predisposes for vascular damage,

including an increased risk of cerebrovascular events such as haemorrhage or stroke. In addition to these structural changes, there are also changes to the endothelium, including increased permeability and inflammation (Challah *et al*, 1997), decreased nitric oxide release (Taddei *et al*, 1995) and superoxide dismutase (SOD – a key antioxidant) activity (Kuzkaya *et al*, 2003), and reduced vasodilatation in response to β-adrenergic signalling (Kobayashi *et al* (1982). There is also thought to be a reduction in vascular sympathetic innervation density (Omar & Marshall, 2010b).

However it can be difficult to distinguish between the effects of ageing as compared to the effects of hypertension or other confounding age-related diseases such as atherosclerosis (Ferrari *et al*, 2003). Rats offer an excellent model for studying the effects of ageing alone, as they do not usually develop age-related hypertension or atherosclerosis (Chamiot-Clerc *et al*, 2001, Leong *et al*, 2015). Further, these vascular changes have clear implications for the mechanisms normally controlling blood flow, including cerebral blood flow, and as such use of a rat model offers an opportunity to study the effect of ageing on CA. These changes are discussed in more detail in specific relation to the cerebral circulation below.

4.1.2 Age-related changes in cerebral vasculature and cerebral blood flow

The cerebral vasculature undergoes age-related changes in structure, endothelial function, innervation density, and in oxidative stress levels.

4.1.2.1 Changes in cerebrovascular structure with ageing

For example, Cox (1977) studied the composition, mechanics and smooth muscle responses of segments of internal carotid arteries, from male rats aged 2, 12 and 24 months old. Myography was used to generate pressure-diameter curves, in the presence of noradrenaline to activate smooth muscle, and during metabolic inhibition to assess passive diameter

responses. Circumferential stress-strain (a function of pial pressure, diameter and wall thickness) and tangential elastic modulus vs stress curves (reflecting tissue stiffness) were calculated. The maximal active stress response was decreased with age, while the passive stress-strain curves were left-shifted, and passive tangential elastic modulus was also increased at some strain values. Staining for collagen and elastin showed a progressive increase in the collagen/elastin ratio with age. These data suggest a decrease in the distensibility of the carotid artery with age, and also that an increased passive responsiveness may compensate for the reduced smooth muscle response.

Increased wall thickness, collage/elastin ratio, and decreased distensibility have also been demonstrated in aged human vertebral and basilar arteries (Nagasawa *et al*, 1979), as well as decreased cross-sectional areas of smooth muscle, elastin and endothelium, and increased collagen/elastin ratio in pial arteries of aged rats (Hajdu *et al*, 1990).

4.1.2.2 Changes in the cerebrovascular endothelium with ageing

Ageing is associated with endothelial dysfunction in cerebral vessels, resulting in a disruption in the balance between endothelial vasodilator and vasoconstrictor substances.

Structurally, the number of endothelial mitochondria decrease (Burns *et al*, 1979), the capillary endothelium undergoes thinning (Topple *et al*, 1990), there is a decrease in endothelial area, and an increase in endothelial permeability, which may increase leakage across the BBB (Stewart *et al*, 1987).

Functionally, production of endothelial-mediators is decreased, due to an increase in oxidative stress, which can reduce synthesis of, and the vascular response to, NO. For example, Mayhan *et al* (1990) demonstrated that the response of cerebral arterioles to superfused ACh, which acts in an NO-dependent manner to cause vasodilatation, was reduced in aged (22-24 months)

compared to adult (6-8 months) rats. The arterioles vasodilated by 11% in the adult rats, but only 3% in the aged rats. This response was not restored in the aged rats by an i.v. dose of indomethacin, indicating that the reduced vasodilatation was not due to production of an opposing cyclooxygenase (COX) constrictor product. However other studies have shown a role for increased COX products in the reduced response to ACh in aged rat carotid artery (Denniss *et al*, 2011).

The observed reduction in response to vasodilators with age has been confirmed to be a result of endothelial dysfunction, as an age-related decrease in response to nitrovasodilators was not observed in endothelium-denuded cerebral arteries (Lee *et al*, 1987). Further, expression and activity of eNOS appears to be increased with age, as a possible compensatory mechanism for the decrease in response, which may be due to decreased synthesis, release or changes in cholinergic receptors (Strosznajder *et al*, 2004).

4.1.2.3 Increased oxidative stress with ageing

Oxidative stress is known to increase with ageing, and forms the basis for a theory of ageing, which says that accumulation of oxidative damage to cellular components, such as DNA, proteins and cell membranes, causes cell ageing and death (Harman, 1956).

Physiological production of free radicals such as superoxide (O_2^-), occurs during mitochondrial aerobic respiration (Matsuzaki *et al*, 2009). O_2^- can cause oxidative damage, and can also react to produce further free radicals such as peroxynitrite ($ONNO^-$), which is formed by a reaction with NO, and therefore also decreases NO bioavailability (Castro *et al*, 2011).

Oxidative damage is usually limited by endogenous antioxidants such as superoxide dismutase (SOD), and whilst some free radicals cause an increase in antioxidant level

(Matsuzaki *et al*, 2009), others can cause oxidative damage to the antioxidants themselves. Of particular interest to this study, free radicals can oxidize BH_4, a critical cofactor for the eNOS enzyme. This results in its uncoupling (Kuzkaya *et al*, 2003), and ultimately, production of OH^-, which has been linked to numerous cardiovascular diseases (Luo *et al*, 2014). Functionally, ageing, and the associated oxidative stress-induced damage, have been linked to a reduction in endothelium-dependent dilatation (EDD) (Eskurza *et al*, 2005).

4.1.2.4 Changes in cerebral Innervation density with ageing

The sympathetic and parasympathetic innervation of the cerebral vasculature has been shown to decline with ageing (Saba *et al*, 1984). A decrease in the intensity of immunofluorescent staining for, and the nerve fibre density of, noradrenergic nerves has been demonstrated in the MCA, PCA and internal carotid artery of aged rats (Cowen & Thrasivoulou, 1990). Further choline accumulation is decreased, and ChAT is increased, possibly as a compensatory mechanism, in large cerebral arteries, but not the pial arteries, of aged rats (Hamel *et al*, 1990).

Adrenergic and cholinergic receptors are also affected by ageing, with a decreased responsiveness and receptor density reported in α2-adrenoreceptors (Pan *et al*, 1986), β-adrenoreceptors (Kobayashi *et al*, 1982), and nicotinic ACh receptors (Nordberg *et al*, 1992). Further, catecholamine content and release from nerve terminals is also reduced with age (Daly *et al*, 1988), which may be driven in part by oxidative stress, as BH_4 is also a cofactor for tyrosine hydroxylase (see 4.1.2.3).

Functionally, it was shown that the blood flow response to stimulation of the cervical sympathetic trunks was decreased in aged rats compared to young. The decreases in CBF seen were abolished by an α-adrenergic antagonist, confirming an α-adrenoreceptor-mediated

vasoconstriction (Shiba *et al,* 2009). With regards to parasympathetic function, stimulation of an ACh-rich area of the basal forebrain, which causes cholinergic vasodilatation in young rats, produced no increase in CBF in aged rats (Uchida *et al*, 2000).

4.1.2.5 Basal CBF in aged subjects

The ageing-related changes described above, which include structural changes, decreased endothelial function, increased oxidative stress and reduced innervation of the cerebral vasculature, are likely to have implications for cerebrovascular tone and the control of basal CBF. As such, ageing is associated with a decrease in CBF and cerebral blood volume. For example, Amin-Hanjani *et al* (2015) used phase contrast quantitative magnetic resonance angiography (QMRA) to assess flow (in $ml \cdot min^{-1}$) in numerous proximal and distal cerebral arteries, as well as left and right anterior flow, posterior regional flow, and total CBF, in 325 healthy adult volunteers aged 18-84 years old. The volunteers had no history of cerebrovascular events or disease, cardiac or respiratory disease, and no untreated hypertension. They found that total CBF declined with age, equating to a $2.6ml \cdot min^{-1}$ decrease per year. When the volunteers were grouped into 3 age ranges, significant differences were seen for individual cerebral vessels, and total CBF, between the groups, being lowest in the oldest group (61-80 years).

Decreased CBF has also been demonstrated in rats. Berman *et al* (1988) showed that cortical blood flow was reduced in 24-month old rats, compared to 6 and 12 month old rats, and that this was associated with poorer performance in behavioural maze tasks. However, this age-related decrease in CBF is not always seen in animal models (Ohata *et al,* 1981, Takei *et al*, 1983).

As well as effects on basal CBF, ageing has also been shown to affect CBF responses. For example, myogenic responsiveness of segments of the MCA to pulsatile changes in intraluminal pressure, is blunted in aged mice (Springo *et al*, 2015).

Balbi *et al* (2015) used intravital microscopy over a cranial window in the right parietal cortex, and a Laser Doppler probe over the territory of the MCA, to assess the CBF and microcirculatory response to inhalation of 5 and 10% CO_2, in mice aged 6 weeks, 8 months and 12 months old. Whilst the increase in gross CBF to CO_2 was not different between the age groups, the CO_2 reactivity of the pial arterioles significantly decreased from 8 months of age, suggesting that age-related changes in vascular function may affect the microcirculation before the larger cerebral arteries.

Oudegeest-Sander *et al* (2014) assessed CO_2 reactivity and dynamic CA, in healthy volunteers aged 21-28, 65-69 and 74-86 years old. They recorded MCAv using a Transcranial Doppler probe, and frontal cortex oxygenation using NIRS. This was done during sit-stand manoeuvres to cause rapid fluctuations in ABP, and hyperventilation and inhalation of a gas mixture containing 7% CO_2. Basal MCAv decreased, and CVR increased with age, and the absolute changes in these measurements in response to dynamic CA and CO_2 were decreased. However, when the data was analysed as percentage changes from baseline, no difference was seen between the age groups.

Finally, neurovascular coupling; increases in CBF in the face of increased neural activity, is vital to maintain normal neuronal function, and has also been shown to be affected by ageing, and specifically by age-related oxidative stress. Toth *et al* (2014) showed that NO-mediated dilatation to whisker stimulation, a method to assess neurovascular coupling, was impaired in aged mice (24 months) compared to young (3 months). Resveratrol, a polyphenol thought to

possess anti-ageing and antioxidant properties, restored the response to whisker stimulation in aged mice. Age-related decline in neurovascular coupling has implications for decreased cortical function and increased risk of cognitive vascular diseases such as vascular dementia.

4.1.3 The effect of ageing on the LL of CA

Much research has been carried out into the effects of ageing on the cardiovascular system, basal CBF, CBF responses and neurovascular coupling, and dynamic CA, with the latter appearing to be relatively well maintained with ageing (see 1.4.7.2 and 4.1.2.5).

In terms of static CA, much of the research focus has been on the LL. This is due to the association between ABP falling below the LL, and falls and fainting. In elderly people, who are more prone to postural hypotension, this is significant due to the increased risk of serious injury or mortality associated with falls. 3 million people over the age of 65 have a fall each year, many of whom have previously had a stroke, which increases the risk of future falls. Falls account for the majority of emergency hospital admissions in the elderly, and often result in fractures or other injuries requiring ongoing care, generating significant costs for the NHS and social services (Later life in the UK fact sheet, 2015). Further, if CA at the LL is also less effective in the elderly, the risk of falls is further increased.

The LL has been shown to be affected by age. For example, in aged Wistar and Fischer-344 rats (14 and 23 months old), the LL of autoregulation, assessed by controlled haemorrhage to reduce ABP, was increased by ~20mmHg compared to young rats (Lartaud *et al*, 1993).

An increase in the LL has also been shown in aged SHRs (20 months old), who also showed an increased magnitude in the decrease in CBF beyond the LL (Fujishima *et al*, 1984).

4.1.4 The effect of ageing on the UL of CA

As well as the increased risk of falls, ageing is also associated with an increased risk of haemorrhage and stroke, which can both result in mental and physical disability, as well as a risk of mortality. As discussed above, the increased occurrence of falls with ageing is associated with an increase in the LL i.e. a reduced autoregulatory range and therefore reduced CBF tolerance to falls in ABP. Thus it is likely that ageing may also be associated with reduced effectiveness of cerebral blood vessels to respond to *increases* in ABP. A reduced tolerance at the UL may result in the transient increases in ABP that occur day-to-day, leading to cerebral hyperperfusion. This may lead to rupture of small cerebral vessels and disruption of the BBB, which becomes more fragile with ageing (Stewart *et al*, 1987), causing haemorrhagic injury.

Age-related changes at the top end of the autoregulatory curve are poorly understood. This can be partly explained by ethical concerns associated with the experimental design required to assess the UL. Raising the ABP to such high levels carries the risk of inducing a haemorrhagic stroke, limiting the applicability of studies in humans, especially in the elderly, who already have impaired CA at the LL, as well as the other age-related changes discussed above.

Therefore, studies using animals can offer an avenue for research into the effects of ageing on the UL, which, to our knowledge, has not been investigated, and is therefore the focus of the current study.

Experiments leading up to this project have been carried out in our lab. Omar & Marshall (2010b) recorded common carotid blood flow as an index of CBF, and infused noradrenaline to assess age-related changes in sympathetic responsiveness. ABP increased to 180mmHg in

mature (10-12 weeks) and middle-aged (42-44 weeks) rats, whilst it only increased to 150mmHg in juvenile (4-5 weeks) rats. CVC decreased in all rats, but to a greater extent in the mature and middle-aged rats, resulting in maintenance of CBF in juvenile rats, and a decrease in CBF in mature and middle-aged rats. The lack of CBF change in response to the achieved increase in ABP suggests efficient autoregulation in the juvenile rats. In the mature and middle-ages rats, CVC decreased beyond that required to maintain CBF, such that CBF fell. This suggests that autoregulation is not compromised in middle-aged rats, even when ABP was increased to 180mmHg, and that despite a reduced sympathetic innervation density in the middle-age rats, there is an active, sympathetically-mediated carotid vasoconstriction, that overcompensates for the increase in ABP. However, when L-NAME was given to inhibit NOS, which resulted in similar increases in basal ABP between the age groups, noradrenaline administration caused a larger increase in ABP, but no decrease in CVC in the middle-aged rats, resulting in an increase in CBF i.e. a failure of CA. This suggests that CA around the UL becomes dependent on NO by middle-age. Therefore age-related decreases in NO synthesis and endothelial responsiveness would cause further impairment of CA to high pressures.

It may be that the increased dependence on NO at the UL is contributed to by the reduced influence of sympathetic nerve fibres. As sympathetic nerves have been shown to play a role in the vasoconstriction seen during increases in ABP (Cassaglia *et al*, 2008), then increases in pressure may be more likely to reach the smaller cerebral arteries and the cerebral microcirculation, and the UL more likely to be exceeded, with ageing.

4.1.5 Aims and Hypotheses

The aim of this set of experiments was to assess the autoregulatory UL in young, male Wistar rats, under control conditions, using the PE infusion protocol developed in Chapter 3. Experiments were then repeated in older rats, to assess the effect of ageing on the autoregulatory control of CBF, and specifically on the UL. A secondary aim was to simultaneously record gross CBF and cortical blood flow (CoBF) during increases in ABP, in order to assess potential differences in the UL.

Our hypotheses were as follows:

- The UL would be lower in old rats compared to young, due to age-related degradation of normal control mechanisms. Therefore in old rats, CBF would increase more readily, increasing risk of BBB disruption and possibly haemorrhagic stroke.
- In young rats, the cortical UL would be higher than the gross UL, because CoBF will not increase until autoregulation by larger arterial vessels has achieved its maximum effect. In old rats, both the cortical and gross ULs will be lower than in the young, due to age-related degradation of normal control mechanisms.

4.2 Methods

4.2.1 Surgery

Surgery was carried out as described in 2.2. Briefly, anaesthesia was induced with 4% isoflurane in O_2 at 4 L min^{-1}. The left jugular vein was cannulated, and isoflurane anaesthesia was withdrawn and gradually replaced with i.v. Alfaxan® bolus doses (0.1ml boluses at 5$mg.ml^{-1}$), and then a maintenance infusion dose of 17-30 $mg.kg^{-1}.hour^{-1}$. The trachea was cannulated with a custom-made stainless steel T-piece cannula, to maintain a patent airway and supply oxygen if necessary. The left brachial artery was cannulated to take samples for blood gas analysis. The left femoral artery and vein were cannulated to record arterial blood pressure (ABP) and heart rate (HR), and for drug infusion respectively. All cannulae were filled with heparinised saline. The right common carotid artery was cleared distally up to its bifurcation. The external carotid, as well as occipital, facial and lingual branches were ligated, to achieve vascular isolation of the internal carotid artery and its distribution to the right side of the brain (as described by Thomas & Marshall, 1994). Blood flow was recorded through the common carotid artery as an index of gross CBF (n=25 young rats, n=12 old rats).

In n=8 young rats, and n=12 old rats, additional surgery was performed to record CoBF simultaneously with gross CBF. The animal was placed in a stereotaxic frame, and cranial thinning was carried out, leaving a layer through which cerebral vessels were visible. A Laser Speckle Contrast imager, mounted on a microstand at 10-15cm from the thinned bone, was used to image the dorsal surface of the right and left cortices, and record cortical tissue perfusion (perfusion units – PU). Data was recorded using a PowerLab and Labchart software (ADInstruments). CVR (=ABP/(Co)CBF) was continuously calculated during the experiment.

For further details of the equipment and data acquisition parameters used, see 2.3.

4.2.2 Stabilisation

Before the experiment began, equilibration was allowed until all variables were stable. A 20-min period of baseline was recorded, and blood gas samples were taken to check P_aO_2, P_aCO_2 and pH values. Blood samples were then taken every 5-10 minutes, in alignment with administration of each drug/increasing dose. If the blood gas values deviated from the mean, or breathing appeared laboured, the airway was aspirated. If P_aO_2 fell below the mean, supplemental O_2 was given. Close attention was paid to P_aCO_2 levels, due to high sensitivity of the cerebral circulation to changes in CO_2 (Willie *et al*, 2012). If P_aCO_2 levels rose above 45mmHg and could not be corrected, the data was discarded.

4.2.3 Experimental protocol

In 25 young rats (321±5g), and 12 old rats (820±32g), an infusion of PE was used to progressively increase MABP. Doses of 0.1–200µg.kg^{-1}.min^{-1} at 6-12ml.hr^{-1} were infused and around 2 minutes was allowed at each dose for the effects to stabilise. When the UL was reached, indicated by an increase in CBF, or CoBF (in a subgroup of 8 young rats, 322±8g, and in all 12 old rats), accompanied by a fall in CVR, with a rising or stable MABP, one further dose of PE was given before the infusion was stopped. Variables were then allowed to recover back to basal levels.

4.2.4 Data Analysis

Data was analysed as described in 2.7. Briefly, 60 second sections of LabChart data representing the baseline, the response to each drug, the baseline just prior to the start of the PE infusion, and the final minute of the response to each PE infusion step, were exported as a mean value for each variable, and opened in Excel for further analysis.

The analysis of the Laser Speckle data is described in detail in 2.7.2. Briefly, the data files were opened in MoorFLPI Full-Field Laser Perfusion Imager Review software, and ROIs representing an arterial vessel, venous vessel and capillary region were selected. The Flux data (given as PU) was compiled as graphs against time, and opened in Excel, to be aligned with the LabChart data. The imager review software was also used to generate videos containing averaged frames aligning with the selections from LabChart for the corresponding experiment. Lines intersecting clearly defined arterial vessels in the ROIs were added to generate a profile view of Flux (PU) against number of pixels, enabling vessel diameter to be determined. This was done for each averaged frame, to track cortical arterial diameter throughout an experimental protocol, and compare responses of different sized vessels.

4.2.5 Calculation of the UL

Autoregulatory curves were generated by plotting mean CBF, or right arterial, venous or capillary perfusion units (RA/RV/RCPU, with RCPU taken to represent CoBF), against MABP at each PE dose. Dual-line linear regression analysis (described by Samsel & Schumacker, 1988, and used previously in our laboratory by Edmunds & Marshall, 2001) was used to calculate the autoregulatory UL. The UL for each animal was defined as the intersection of the two regression lines with the best fit and the smallest standard deviation of residuals. A group mean UL was then calculated from the individual values. See 2.7.3 for more details.

4.2.6 Statistical analyses

All data are presented as the mean ± SEM. Graphs and statistics were generated using GraphPad Prism® 5. Data was analysed using t-tests (paired or unpaired as appropriate) and one-way ANOVAs with post-hoc Bonferroni. $P<0.05$ was taken as significant.

4.3 Results

4.3.1 Baseline characteristics of young vs. old rats

Baseline characteristics of the young and old control groups are shown in Table 4 and Figure 26. The old rats were significantly heavier than the young rats. They also tended to have higher brain weights, but these data are not shown as it was not collected consistently throughout the studies using the old rats. The old rats also had a significantly lower HR and P_aO_2, whilst MABP, P_aCO_2, HCT and pH were not different between the two groups. Mean basal CBF, measured from the right, vascularly isolated internal carotid artery, after the PE challenge doses described in 3.3.1, was significantly higher in old compared to young rats (2.4±0.3 vs. 1.2±0.1ml·min^{-1}, unpaired t-test; P<0.0001). Accordingly, calculated CVR was significantly lower in old compared to young rats (63±9 vs. 115±9mmHg·ml^{-1}·min, unpaired t-test; P=0.0007). However, when CBF and CVR were corrected per kg of body weight, CBF was significantly lower in the old rats (2.9±0.3 vs. 3.8±0.2 ml·min.kg^{-1}, unpaired t-test; P=0.04), but CVR was still significantly higher in young rats (363±31 vs. 78±12mmHg·ml^{-1}·min·kg^{-1}, unpaired t-test; P<0.0001).

In 50% of the old rats, a basal hypertension was seen when compared to young rats, and the rest of the old rats (148±2 vs. 127±2 vs. 107±6mmHg respectively, one-way ANOVA; F ratio =23.6, P<0.0001). However this did not translate to differences in any of the other basal parameters or in autoregulatory behaviour or the UL. Therefore data are presented as the whole n=12 old rat group.

4.3.2 Gross CBF and CVR data in young vs. old rats

Figure 27 shows a representative example of the raw traces from a control experiment in a young rat. As PE was infused, ABP gradually increased, but CBF was maintained by increasing CVR. In other words, CBF was effectively autoregulated against the increasing ABP. The point indicated by the dashed line is the UL; ABP continued to rise, but CVR decreased, and CBF increased, indicating a breakthrough of autoregulation.

Figure 28 a) shows the mean autoregulatory curve for the young control group (n=25). The blue 'plateau' portion of the curve shows CBF being relatively maintained between 1.1-1.3ml·min^{-1} despite an increase in MABP from ~125 to 160mmHg. The red 'rising' portion shows CBF increasing, indicating that the UL had been exceeded. The young mean UL (the point of autoregulatory breakthrough) was 168±2mmHg. This was calculated by performing dual-line linear regression analysis, as described in sections 2.7.3 and 3.1.3, for each individual experiment, and calculating the mean. The individual values ranged from 154 to 181mmHg, and the mean PE dose required to reach the UL was 23±3µg.kg^{-1}min^{-1}. Beyond the UL, CBF rose to a maximum of 2.3±0.1ml·min^{-1}. Overall, the increasing dose of PE had a significant effect on CBF, with many significant differences between the CBFs at PE doses between baseline-15µg.kg^{-1}min^{-1} and 45-150µg.kg^{-1}min^{-1} (one-way ANOVA; F ratio=5.1, P<0.0001, with post-hoc Bonferroni tests; P<0.05).

Figure 28 b) shows the changes in CVR with increasing MABP; CVR tended to increase from 115±9 to 160±11mmHg·ml^{-1}·min between the MABPs of 125 and ~160mmHg (slightly lower than the UL), corresponding with the relative maintenance of CBF. Beyond this, CVR tended to fall (and CBF rose), reaching a minimum of 102±5mmHg·ml^{-1}·min. There was an overall significant effect of the increasing dose of PE on CVR (one-way ANOVA; F ratio=2.9, P=0.001), although the only significant difference was seen between the 3 and 10µg.kg^{-1}min^{-1}

PE doses (post-hoc Bonferroni, $P<0.05$), equating to CVRs of 140±3 and 155±3mmHg·ml^{-1}·min.

Figure 28 c) shows the mean autoregulatory curve for the old control group (n=9). The plateau phase in old rats showed a greater fluctuation in CBF, between 1.9-2.3ml·min^{-1}, and was also over a wider range of ABPs, from ~130 to 175mmHg, compared to the young rats. The old control UL was calculated as 180±3mmHg, which was significantly higher than the young control UL (* unpaired t-test; P=0.0009). The individual values ranged from 176 to 191mmHg, and the mean PE dose required to reach the UL was 55±8 µg.kg^{-1}min^{-1}, significantly higher than the dose required in the young rats (unpaired t-test; $P<0.0001$).

The UL was less well defined in the old group. In most of the experiments, CBF tended to fluctuate as ABP increased, generally showing a trend to decrease during the plateau phase. Above the UL, CBF then increased from this new, lower value. As such, the maximum CBF reached beyond the UL was 2.4±0.3ml·min^{-1}, an increase of only ~0.2ml·min^{-1} compared to basal CBF. A two-way ANOVA comparing young and old CBF data revealed a significant effect of age (F ratio=87.3, $P<0.0001$), and of the increasing dose of PE (F ratio=2.9, P=0.0003), but no interaction between the two (F ratio=0.7, P=0.78).

Data from 3 old rats was not included in the analysis, as it was not possible to define an UL. Even after the maximum possible ABP was reached (191±4mmHg), such that increasing the dose of PE had no further effect on ABP, CBF did not increase, nor CVR decrease, in a manner that indicated breakthrough of autoregulation.

Figure 28 d) shows there was a similar pattern of CVR response in the old rats as the young rats (b). There was a trend for CVR to increase from 72±10 to 111±15mmHg·ml^{-1}·min as MABP increased from 130 to 175mmHg (slightly below the UL), suggesting autoregulatory

vasoconstriction to maintain CBF. Beyond this, there was a trend for CVR to decrease, reaching a minimum of 80± 8mmHg·ml^{-1}·min. However, overall, CVR did not change significantly with increasing PE dose in the old rats (one-way ANOVA; F ratio=1.1, P=0.4).

This supports the fact that the changes in CVR seen in the old rats appeared blunted compared to the young rats. A two-way ANOVA revealed a significant effect of age (F ratio=38.5, P<0.0001) and of PE dose (F ratio=2.2, P=0.006), but no significant interaction (F ratio=0.8, P=0.67). As such, the maximum CVR reached in the young rats was significantly higher than the CVR reached in old rats at the same PE dose (160±11 vs 93±15 mmHg·ml^{-1}·min, post-hoc Bonferroni; P<0.01).

4.3.3 Cortical CBF data and vessel diameters in young vs. old rats

4.3.3.1 Gross vs cortical autoregulatory curves and ULs

Figure 29 a) shows the same raw traces as in Figure 27, but with the corresponding mean Laser Speckle images, from the same young, control experiment, shown in Figure 29 b). The numbered labels indicate the points in the raw traces that align with the numbered, averaged images. As MABP increased, gross CBF was maintained, whilst the images showed a slight increase in cortical perfusion, as indicated by the increase in warm colours. The dashed line indicates the point where the UL was exceeded, beyond which both gross CBF and cortical perfusion increased. All variables then recovered to close to the baseline values.

Figure 30 shows the mean autoregulatory curves generated from the subgroup of 8 young rats in which (a) gross CBF and (b) cortical perfusion were measured simultaneously. The gross CBF autoregulatory curve was similar to that seen in Figure 28 a), and gave an UL of 168±4mmHg, which was not significantly different to the UL of the whole young group (168±2mmHg). In contrast, the plateau phase of the CoBF autoregulatory curve (taken from

the RCPU data), tended to slightly increase with MABP, before showing a larger increase indicative of exceeding the UL. The mean cortical UL was 170±4mmHg, which was slightly, but significantly higher than the gross UL (paired t-test, P=0.04).

Figure 30 c) shows the CoBF data from 9 old rats, which was recorded simultaneously with the gross CBF data shown in Figure 28 c). Similarly to the young group, during the plateau phase of the autoregulatory curve, CoBF tended to increase with MABP. This was seen to a greater extent in the old group, and as a result, there was a less well defined UL. The mean UL was calculated as 181±3mmHg, which was significantly higher than the young cortical UL (§ unpaired t-test, P=0.03), but was not significantly different to the old gross UL of 180±3mmHg (see Figure 28, † paired t-test, P=0.4).

4.3.3.2 Differences in autoregulation between gross CBF, RAPU, RCPU and RVPU

Figure 31 shows the ULs calculated from the gross CBF, and the cortical RA, RC and RVPU autoregulatory curves in the young rats. The ULs were 168±4, 169±4, 170±4 and 170±4mmHg respectively, showing a slight, but significant difference between the different vascular components (repeated measures ANOVA; F ratio=4.3, P=0.02), with significant differences between the gross and capillary, and gross and venous ULs. Figure 32 shows the corresponding gross and cortical RA, RC and RVPU ULs calculated in the old rats. The ULs were 180±3, 179±3, 181±3 and 180±2mmHg respectively, with no significant difference between these values (repeated measures ANOVA; F ratio=1.7, P=0.2).

When these data were compared between the young and old groups, the cortical ULs from each vessel type were significantly higher in the old rats (unpaired t-tests, RAPU; P=0.05, RCPU; P=0.03, and RVPU; P=0.05).

Figure 33 shows the slopes, taken from the dual-line linear regression analysis, of the plateau and rising phases of the a) gross, and b) cortical (RCPU) autoregulatory curves, in young and old rats. Slope values were analysed using two-way ANOVAs, with post-hoc Bonferroni tests, to compare the plateau and rising slopes, between and within the young and old groups, for the gross and cortical data separately.

For the gross data, there was a significant difference between the plateau and rising slopes, with the rising slopes being higher than the plateau slopes (F ratio=42.3, P<0.0001). There was a significant effect of age on the slope data (F ratio=12.4, P=0.0008), indicating that the plateau and rising slopes were not the same between the young and old groups. There was also a significant interaction between age, and the plateau and rising slope data (F ratio=13.6, P=0.01), indicating that the differences between the plateau and rising slopes was not the same between the young and old rats. Post-hoc Bonferroni tests showed that, although there was no significant difference between the young and old plateau slopes (P>0.05), the young rising slope was significantly higher than the old slope (P<0.001).

The same pattern of results was also seen for the cortical data; a significant difference between the plateau and rising slopes (F ratio=13.2, P=0.001), a significant effect of age (F ratio=7.6, P=0.01), and a significant interaction (F ratio=6.5, P=0.02). Post-hoc Bonferroni tests showed no significant difference between the young and old plateau slopes (P>0.05), but the young rising slope was significantly higher than the old slope (P<0.01).

4.3.3.3 Vessel diameter changes during autoregulation

Figure 34 shows an example of the vessel diameter data from a single, young control experiment, produced by adding intersecting lines across arterial and venous vessels in Laser Speckle images, to generate profiles of flux (PU) against pixel number. These data show that

vessel diameter, indicated by the width of the profile curves (number of pixels on the x axis), increased between baseline (a), and the UL (b), in both cortical arterioles and venules. Figure 32 a) shows the mean, cortical arterial diameter data, and b) the corresponding mean right arterial flux (RAPU) data for the subgroup of 8 young rats. As MABP increased, both cortical arterial diameter and perfusion showed a trend to slightly increase during the plateau phase. Beyond a MABP of ~170mmHg, both diameter and perfusion increased to a greater extent. A mean UL of 169±4mmHg was calculated from the linear regression analysis of the RAPU data, as shown in Figure 31.

Figures 35 c) and d) show the corresponding data from the group of 9 old rats. Cortical arterial diameter data (c), and (d) the corresponding mean right arterial flux (RAPU), both tended to increase across the range of MABPs. Consistent with the gross CBF and CoBF data, there was a less obvious separation into plateau and rising phases, although diameter and RAPU were seen to increase to a greater extent above 180mmHg. A mean UL of 179±3mmHg was calculated from the linear regression analysis of the RAPU data, as shown in Figure 32.

For both young and old rats, the arterial diameter data was split into two subgroups, those with a basal diameter of greater than or less than 200μm. In the young rats, when diameter vs MABP was plotted with respect to these subgroups, no difference was seen in the response to increasing MABP. There was also no significant difference between the RAPU ULs when they were compared with regards to the basal diameter of the artery the data was taken from (172±7 vs 160±4mmHg, unpaired t-test of >200 vs <200 μm; P=0.3). In the old rats, when diameter vs MABP was plotted with respect to these subgroups, the vessels >200μm in diameter appeared to undergo a larger increase in diameter beyond the UL. However, the mean change in diameter, from baseline to the diameter during the highest ABP, was not

significantly different between the two vessel groups (unpaired t-test; P=0.17). Further, the RAPU ULs were not different when analysed with respect to basal diameter (182±9 vs 180±3mmHg, unpaired t-test of >200 vs <200 μm; P=0.7).

Mean ± SEM	Young (n=25)	Old (n=12)	P value (unpaired t-test)
Body weight	321±5	820±32 *	< 0.0001
MABP	127±2	127±7	0.9
HR	417±7	350±7 *	< 0.0001
P_aO_2 (mmHg)	73±2	67±2 *	0.02
P_aCO_2 (mmHg)	43±1	43±1	0.9
pH	7.44±0.01	7.44±0.01	0.8
HCT (%)	39±1	37±1	0.09

Table 4: Baseline characteristics of young (n=25) and old (n=12) male Wistar rats from the control groups. Old rats were significantly heavier, had a significantly lower HR and lower P_aO_2. P_aCO_2, pH and HCT, and MABP were not significantly different between the 2 groups.

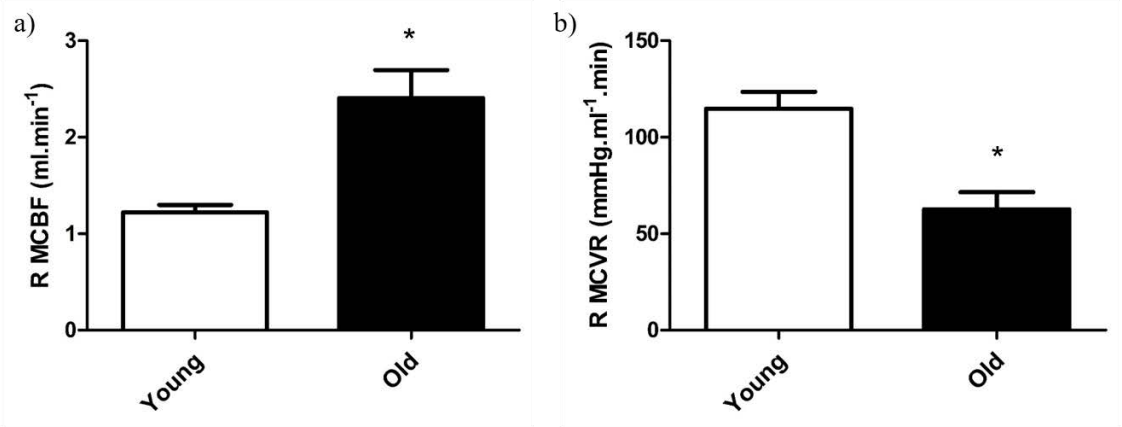

Figure 26: The old rat group (n=12) had significantly higher absolute baseline CBF (a) and lower CVR (b) compared with the young group (n=25, * unpaired t-tests, P<0.0001 and 0.0007 respectively).

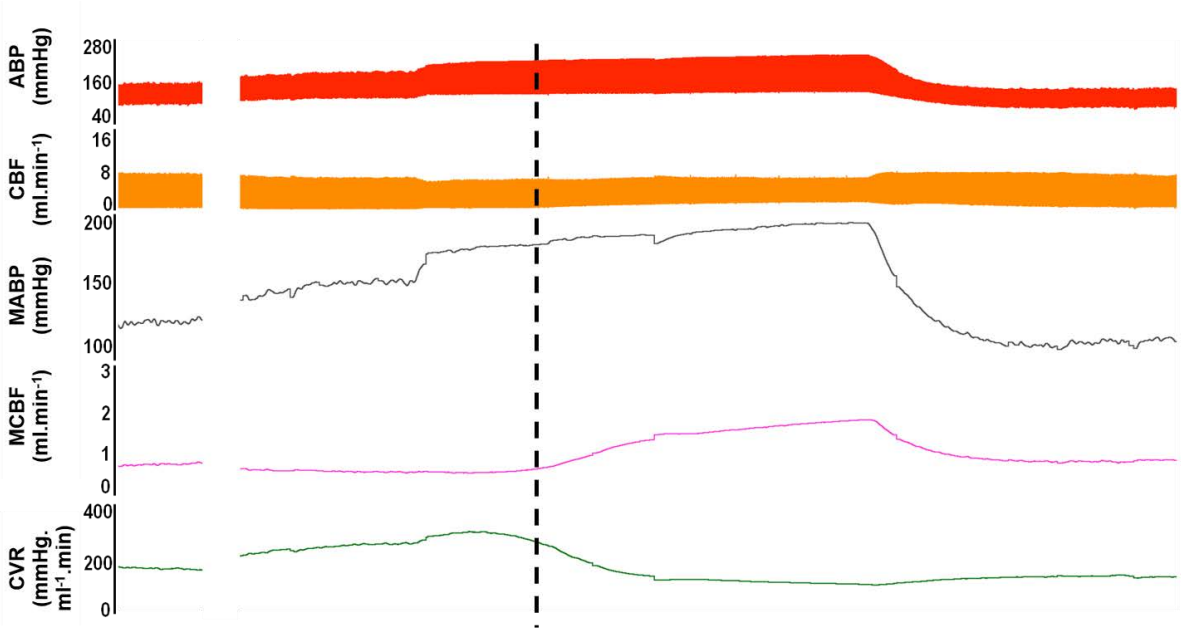

Figure 27: A representative raw trace from a control experiment in a young rat. ABP gradually increased, driven by continuous infusion of PE, which was matched with an increase in CVR to maintain CBF, demonstrating effective cerebral autoregulation. At the point indicated by the dashed line, ABP continued to rise but CVR began to fall, resulting in an increase in CBF, indicative of the UL being exceeded and subsequent autoregulatory breakthrough.

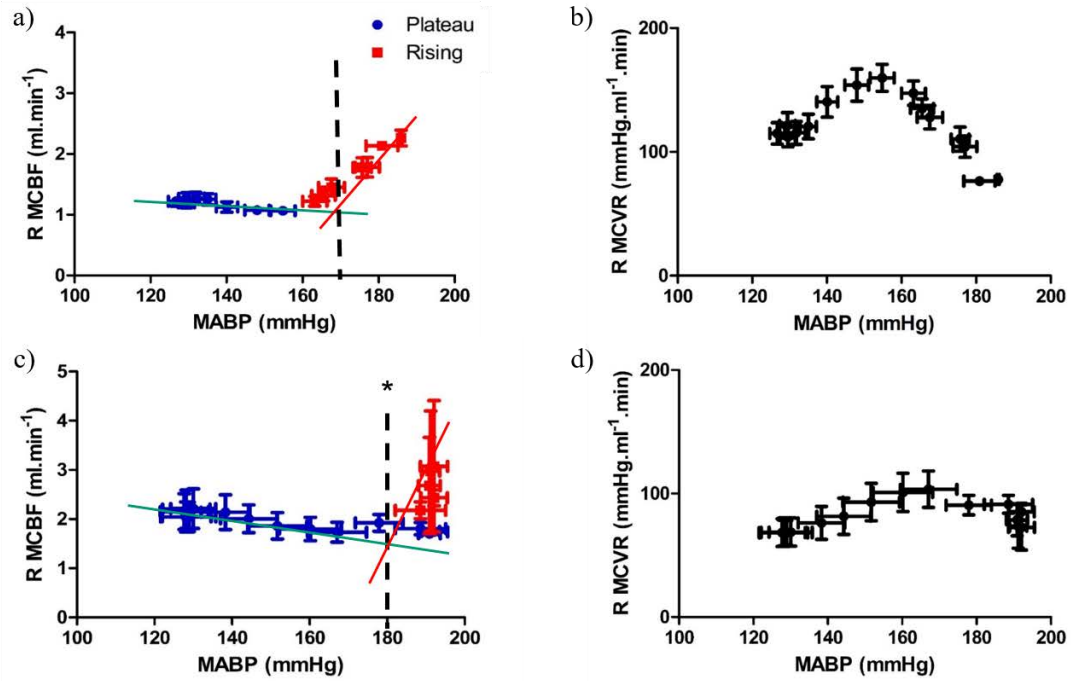

Figure 28: The mean CA curve generated in n=25 young (a) and n=9 old (c) male Wistar rats. Data shown is absolute R MCBF plotted against PE-induced increasing MABP (after PE challenge doses). The mean UL, calculated as the group mean of dual-line linear regression analysis for each experiment, was 168±2mmHg in the young rats, and was significantly higher at 180±3mmHg in the old rats (* P=0.0009, unpaired t-test). R MCVR showed a similar pattern of response in the young (b) and old (d) rats; an initial increase as MABP increased, demonstrating autoregulatory vasoconstriction to maintain CBF. Beyond the UL, CVR fell, resulting in the increase in CBF.

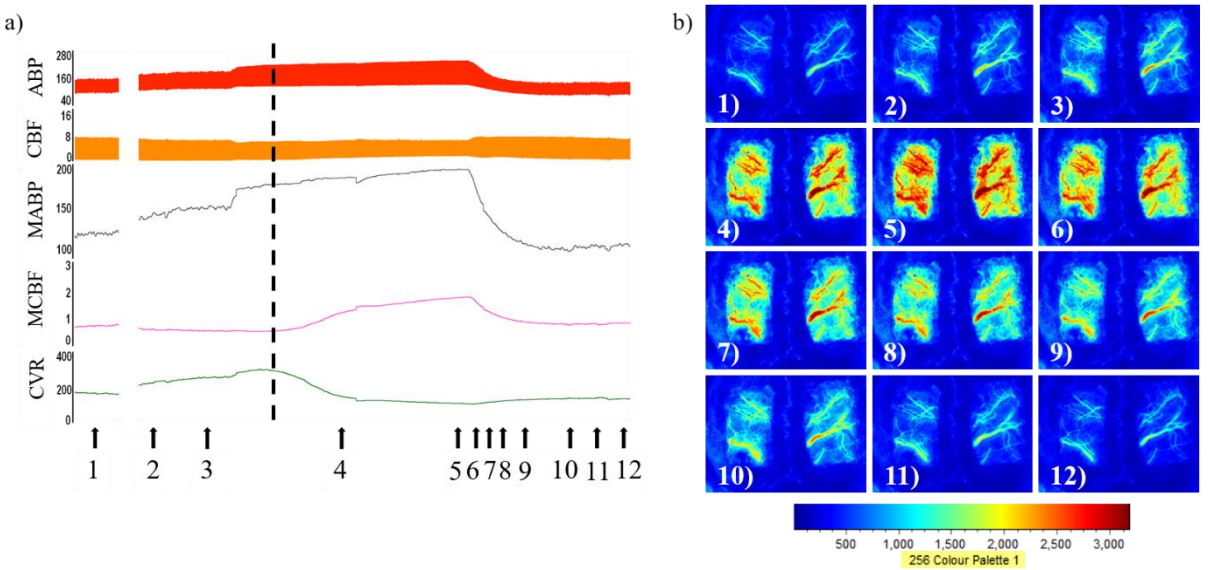

Figure 29: a) Raw traces as shown in Figure 27 and b) corresponding averaged Laser Speckle images, generated during a control experiment in a young rat. Blue to green colours indicate areas of low perfusion, and yellow to red colours indicate higher perfusion. The scale indicates the flux values associated with the colour range. The numbered labels indicate different stages of the experiment: 1) Baseline, 2-5) recordings during PE infusion, 6-12) recovery. The UL was exceeded at around the point indicated by the dashed line, after which MCBF and cortical blood flow increased (4-6).

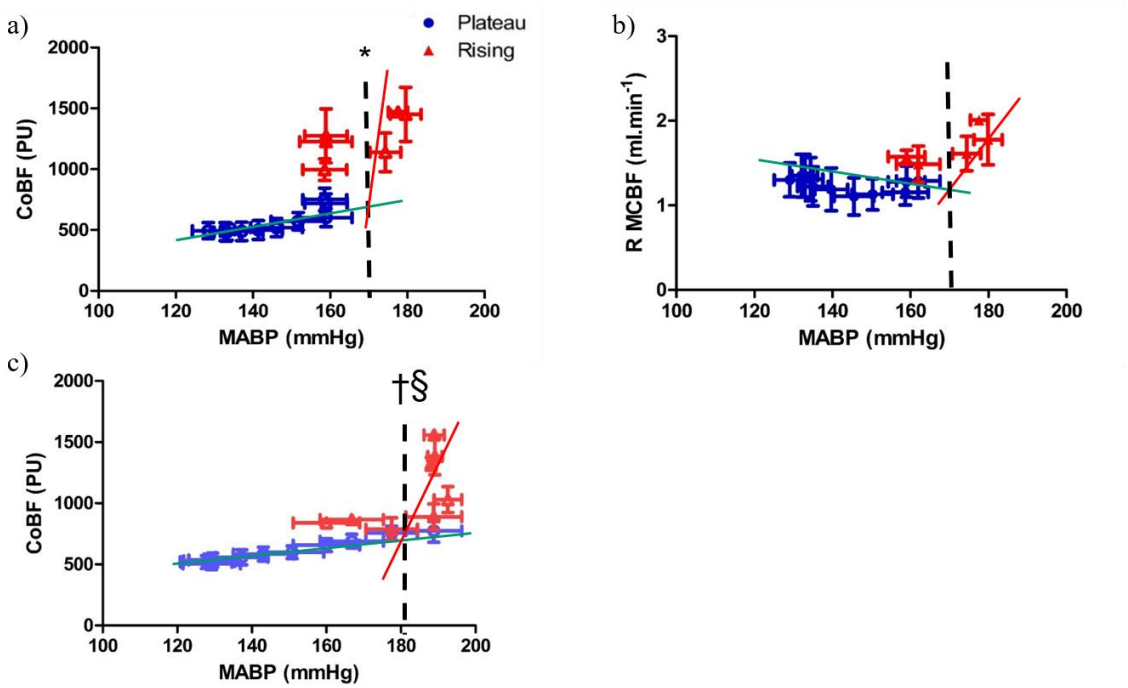

Figure 30: Data from n=8 young and n=9 old rats in which gross CBF and cortical blood flow (CoBF) were measured simultaneously during PE infusion. In young rats, a) CoBF showed a plateau until the UL of 170±4mmHg was reached, after which CoBF rose. b) Gross CBF was maintained up to the UL of 168±4mmHg, beyond which CBF rose. The young cortical UL was slightly, but significantly higher than the gross UL (* paired t-test, P=0.04). In old rats, c) as MABP increased, CoBF tended to gradually increase, before reaching the mean UL of 181±3mmHg, after which CoBF rose to a greater extent. The old cortical UL was significantly higher than the young cortical UL (§ unpaired t-test, P=0.03), but was not significantly different to the old gross UL of 180±3mmHg (see Figure 28, † paired t-test, P=0.4).

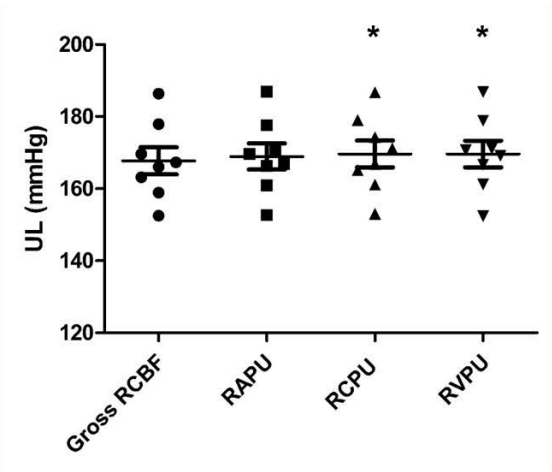

Figure 31: ULs calculated from flow probe and Laser Speckle imaging data from young rats, representing gross, RCBF, as well cortical arterial (RAPU), capillary (RCPU) and venous perfusion (RVPU). The ULs were 168±4, 169±4, 170±4 and 170±4mmHg respectively. A significant difference was seen between the 4 ULs (repeated measures ANOVA; P=0.02, post-hoc Bonferroni; * = significantly different vs gross CBF UL).

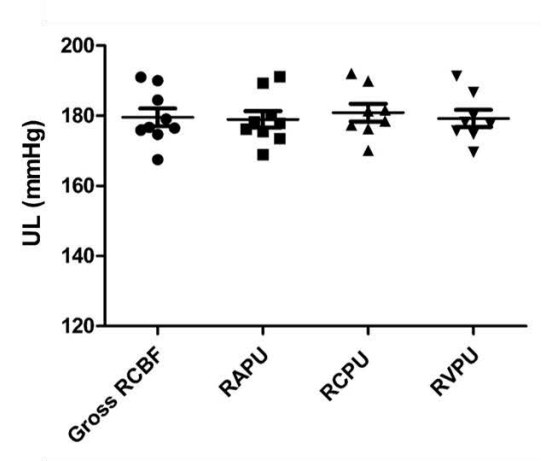

Figure 32: ULs calculated from flow probe and Laser Speckle imaging data from old rats, representing gross CBF, as well cortical arterial, capillary and venous perfusion in the old animals. The ULs were 180±3, 179±3, 181±3 and 180±2mmHg respectively. There was no significant difference between the 4 ULs (repeated measures ANOVA, P>0.05).

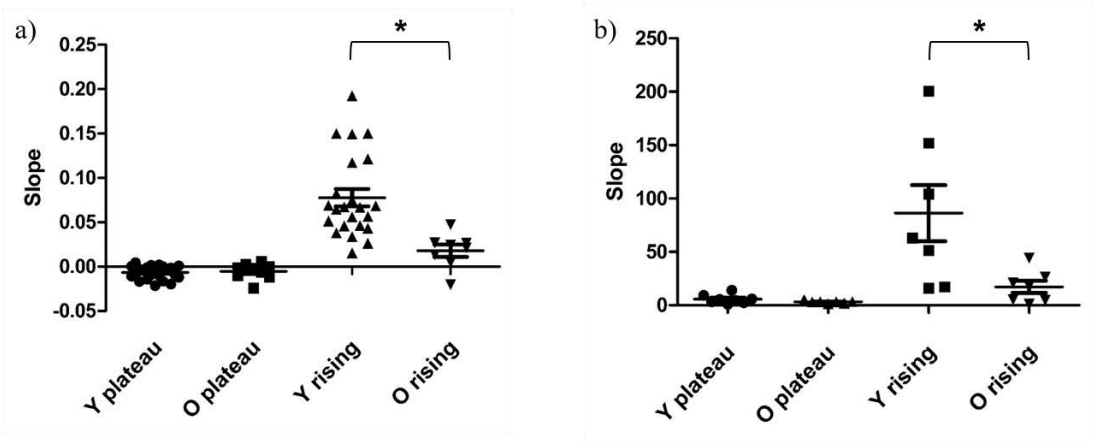

Figure 33: The slopes of the plateau and rising phases of the a) gross and b) cortical autoregulatory curves, in young (Y) and old (O) rats. Young and old plateau slopes were not significantly different for either gross or cortical data. The young rising slopes were significantly higher than the old for both gross and cortical data (two-way ANOVAs with post-hoc Bonferroni; * $P<0.001$ and $P<0.01$ respectively).

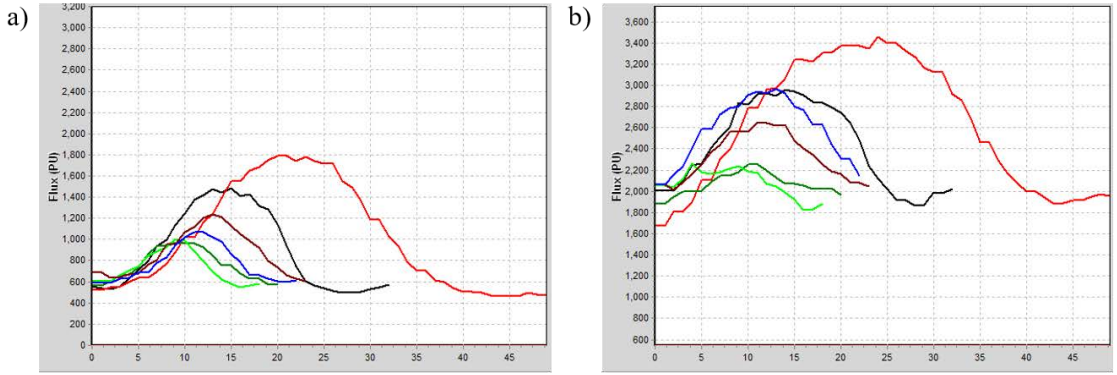

Figure 34: An example of the vessel diameter profiles generated in a single control experiment in a young rat. Each profile line represents a different vessel type (3 arteries and 3 veins), at a) baseline and b) the UL. The width of the profiles (represented along the x axis in pixels), as well as the flux values (in perfusion units), were increased at the UL compared to baseline, indicating an increase in vessel diameter and cortical blood flow beyond the UL.

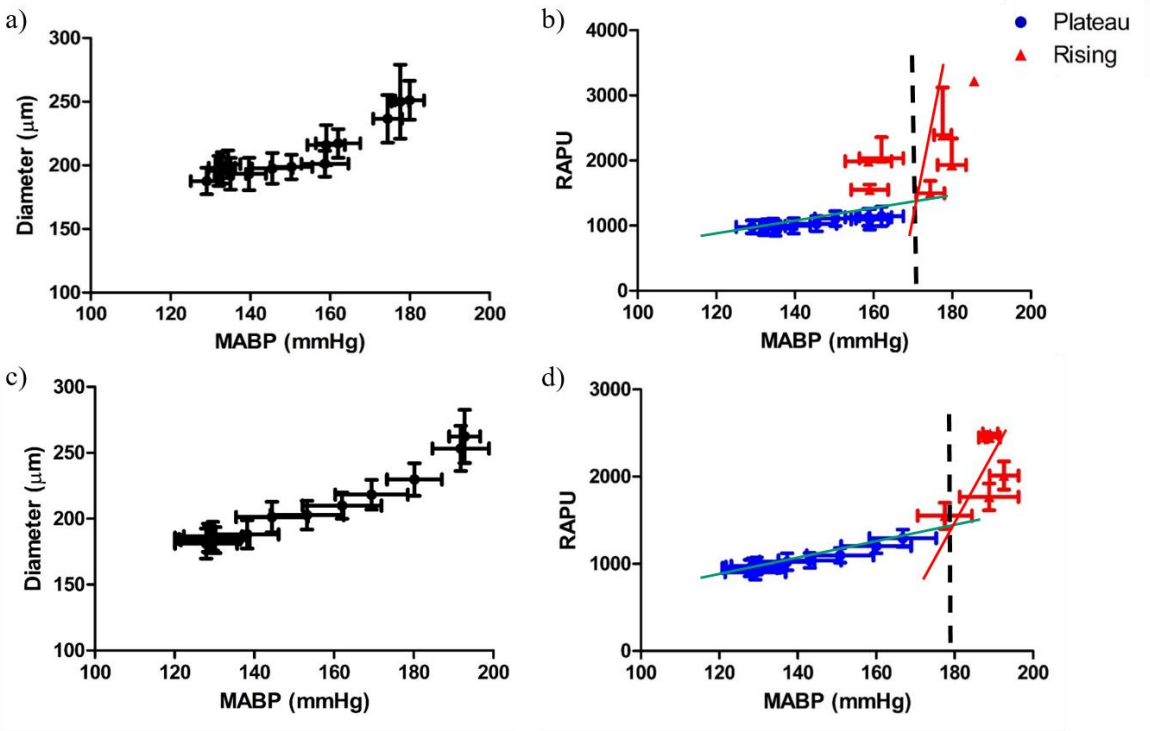

Figure 35: Graphs showing mean diameter and perfusion units in the cortical arterial vessels (RAPU), measured using Laser Speckle imaging. In young rats, as MABP increased, both (a) vessel diameter and (b) RAPU showed a slight increase up to 169±4mmHg, the group mean UL calculated from linear regression analysis, beyond which both diameter and RAPU increased to a greater extent, reflecting the increase in CBF. In the old rats, both (c) vessel diameter and (d) RAPU showed a more steady increase across the range of MABPs. A mean group UL of 179±3mmHg was calculated from the old RAPU data.

4.4 Discussion

4.4.1 Changes in cardiovascular baseline characteristics with ageing

The old rats had a significantly lower HR and P_aO_2 than the young rats. This is in contrast to what is generally reported in humans with ageing, where resting HR tends to increase due to decreased parasympathetic tone. For example, Parashar *et al* (2016) studied 3 groups of healthy volunteers, aged 25-45, 46-60, and 61-80 years old. They demonstrated a significantly decreased cardio-vagal HR response with ageing, assessed using the Valsalva manoeuvre, deep breathing, and moving from sitting to standing. They also showed that resting HR was significantly increased in the oldest group.

However, there is also some support in the literature for a decrease in HR with ageing. For example, both mean HR (Santos *et al*, 2013), and maximal HR in exercise have been shown to decrease with ageing, due to a combination of decreased intrinsic HR, and the β-adrenergic-dependent ability to increase HR during exercise (Christou & Seals 2008).

P_aO_2 (but not P_aCO_2) has also been shown to decrease gradually with age, from 95mmHg to 75mmHg between 20 and 70 years of age (Cerveri *et al*, 1995). This is due to age-related changes in pulmonary structure and perfusion, which cause a decline in gas exchange.

MABP and the other haematological parameters were not different between the two groups. Although hypertension is commonly reported to increase in incidence with advanced age (see 1.4), rat models of ageing are often used to avoid the confounding influence of hypertension (see 1.4.2). Therefore, even though a basal hypertension was seen in around half of the old rats, these rats did not display any further differences in the other basal parameters, the autoregulatory curves, or the UL.

Whilst absolute basal CBF was higher in the old rats, when CBF was corrected for body weight, it was significantly lower in the old rats compared to the young. It is generally agreed that CBF decreases with age in humans (e.g. Claus *et al*, 1998). The data in rats is more varied, with some studies showing a decrease (Berman *et al*, 1988), and others showing little or no change (Ohata *et al*, 1981). The fact that both absolute and corrected CVR were lower in the old rats is interesting. Arterial stiffness is known to increase with age, and in fact peripheral arterial stiffness, assessed by brachial-ankle pulse wave velocity, has been shown to positively correlate with CVR in subjects aged 67-92 years old (Robertson *et al*, 2010). It is possible that in this study, CVR, and absolute CBF, were affected by the higher anaesthetic dose and infusion rate required in the old rats. As discussed in 3.3.1, challenge doses of PE were used in order to 'reset' basal cerebrovascular tone, due to apparent vasoconstriction observed during the plateau phase of autoregulation. We hypothesised that basal tone may have been affected by the anaesthetic and surgical setup, and that this may have had a greater effect in the old rats.

4.4.2 The effect of ageing on CA and the UL

The 'plateau' portion of the autoregulatory curves, generated in both the young and old rats, did not demonstrate the classical, flat shape (see Figure 3) that is widely accepted in the literature. Rather CBF was seen to fluctuate, showing an initial increase, followed by a general trend to decrease towards the UL (Figures 28 a) & b)). As discussed in 3.4.2, this could be for a number of reasons:

- a direct cerebral vasoconstriction being caused by PE, which seems unlikely as PE is not thought to cross the BBB, and α-receptor density is low on cerebral vessels

- an effect of the anaesthetic/surgery, or of the initial low doses of PE, causing an vasodilatation, meaning that basal tone was lower at the start of the experiment
- an overcompensation in autoregulatory vasoconstriction to moderate increases in ABP, which may particularly occur in larger cranial and extracranial vessels, in a manner that is protective of the smaller, more fragile downstream vessels.

The 'rising' portions of the autoregulatory curves show that CBF increased beyond the UL in both young and old rats. The mean UL calculated for the young rats (168±2mmHg) is similar to data in the literature. For example, Hoffman *et al* (1991) saw effective autoregulation up to 170mmHg in both awake and anaesthetised rats, and Mayhan & Heistad (1986) saw an increase in pial vessel diameter and BBB disruption in rats when ABP was raised above 175mmHg. Paternò *et al* (2000) increased MABP in rats from a basal level of 100mmHg to 130, 150, 170 and 200mmHg. At the higher pressures of 170 and 200mmHg they saw large increases in pial artery diameter. Similarly, Kontos *et al* (1978) found that small arterial vessels (37-59μm) showed no change in diameter until ABP was raised to 170mmHg, at which point they dilated, whilst large vessels (117-174μm diameter) did not dilate until 190mmHg. The largest vessels (205-252 and 273-375μm) showed constriction even at minor increases in MABP, which was more pronounced as pressure was further increased, up to 170 and 200mmHg respectively. Increasing MABP beyond 200mmHg caused irreversible changes to pial arteriole diameter, which was still graded with vessel size. Based on pressure differences between the vascular beds studied, and measurement of CBF to calculate resistance in those cerebral vascular beds they did not directly study (see 1.2.2.4 for methods), they concluded that the responses they observed in the larger vessels were able to explain the maintenance of CBF between 100-170mmHg. Above this pressure range, forced dilatation of the pial arterioles began, which accounted for the increase in CBF above the UL. These data

agree well with the young UL in this study, and also provides evidence to suggest that larger cerebral arteries were responsible for the majority of pressure autoregulation observed.

However, it is difficult to make direct comparisons between the UL values generated in this study and the literature. This is because many studies use protocols that increase ABP in steps and therefore define the UL as a range, or state that it is simply beyond a pre-determined ABP value, whereas our use of dual-line linear regression analysis, and a continuous PE infusion, allows a more precise determination of the UL (see 3.1.2.2 and 3.1.1).

The UL was less easy to define in the old rats. The increase in CBF beyond the UL was lower, reflecting the general trend for CBF to decrease with age, and the PE dose required to reach the UL was higher, reflecting the higher UL, and also a potential decrease in α1-receptor sensitivity with age (McAdams & Waterfall 1986).

In contrast to our hypothesis, the UL was significantly higher in the old rats compared to the young (180±3mmHg vs 168±2mmHg). We postulated that the UL would be decreased in old rats, due to age-related declines in the normal mechanisms thought to contribute to cerebral autoregulation. To our knowledge, there is currently no literature on the UL in ageing with which we can compare our data. Therefore, this novel finding suggests that, despite reported age-related decreases in contributory mechanisms, such as disrupted NO-mediated tone and a reduced input by autonomic innervation, the autoregulatory range is actually increased with age. This may be due to changes in cerebral vessel structure that are known to occur with ageing, subsequently causing reduced distensibility (see 1.4.3.2). For example, Hajdu *et al* (1990) showed in pial arterioles from aged rats (24-27 months old), that the collagen/elastin ratio, and functional vessel stiffness were both increased compared to young rats (9-12 months). Stiffer, less elastic cerebral vessels may be able to withstand higher ABPs before a

forced dilatation would occur. This is supported by the fact that, in 3 old rats, the UL was not reached, even at ABPs of 191±4mmHg.

CVR significantly increased during the plateau phase of autoregulation in both young and old rats, corresponding with the relative maintenance of CBF despite increasing ABP. The maximum CVR reached in the old rats was significantly lower than that seen in the young rats, but there was no significant difference when the change in CVR (from baseline to the maximum) was analysed. If the raised UL in old rats is explained by increased cerebral arterial stiffness, it could also have reasonably been expected for the old rats to have a higher CVR. Similarly to the high, absolute basal CBF seen in the old rats, this corresponding low CVR may be an artefact of the anaesthetic and/or surgery.

Regarding CVR at the UL, it appears that CVR began to decrease prior to the increase in CBF, in both young and old rats. As the fall in CVR preceded the increase in CBF, rather than occurring as a mathematical result of it, and also as CVR fell despite the fact that ABP was often still increasing, these findings suggest an active dilatation, as opposed to a passive, forced dilatation. This idea of an active vasodilatation beyond the UL has been proposed by another group; Talman & Dragon, who carried out a series of experiments in which removal of cerebral neural inputs and sources of NO was shown to extend the autoregulatory curve, abolishing the UL, and suggesting an active mechanism was driving the increase in CBF.

For example, when rats underwent sinoaortic denervation to disrupt the baroreflex, an infusion of PE to increase ABP up to ~185mmHg did not result in autoregulatory breakthrough, whereas intact rats demonstrated an increase in CBF above ~155mmHg. This result was unaffected by bilateral sympathetic denervation, and so could not be explained by an increase in sympathetic nerve activity (Talman *et al*, 1994). Central disruption of the

baroreflex pathway had similar effects. Inhibition of the NTS in rats, by injection of lidocaine, caused ABP to rise to ~185mmHg, which was matched by infusion of PE in an intact, control group. In the intact group, a large increase in CBF and decrease in CVR was seen at the top ABP. However, the group in which the baroreflex pathway had been disrupted showed a significantly smaller increase in CBF, and no change in CVR from that seen at the maximum ABP. This suggests that whilst the intact group underwent an active dilatation beyond the UL, the baroreflex-disrupted group had no active vasodilatation, but rather a smaller, forced increase in CBF (Talman & Dragon, 2002).

If the increase in CBF above the UL is an active process, it is presumably physiologically important, and may represent a safety pressure release mechanism, which could be intrinsically linked with the baroreflex pathway. The existence of two distinct sets of baroreceptor fibres has been discussed by Andresen & Kunze (1994), the classical A-type fibres that respond within the range of 40-120mmHg, with a regular discharge that reflects the pulsatile waves of ABP, and the C-type fibres, which respond over a higher range of 60 to >200mmHg, and have a more irregular discharge pattern. It would be the latter set of 'high-pressure baroreceptors' that would be actively responding at ABPs around the UL identified in the young rats in the current study.

The raised UL seen in the old rats in the current study, raises the possibility of an impairment, or resetting of the baroreceptor threshold or range, in ageing. Ferrari *et al* (1991) investigated the effect of ageing on the baroreceptor reflex, and found that aged rats (75-90 weeks old) showed a significant reduction in the bradycardic and tachycardic HR responses (-42% and -45% respectively), as well as a significant impairment in the initial pressor responses at 3 seconds (-63%) and 6 seconds (-54%), when compared to young rats (5-6 and 12-16 weeks old).

Thoren *et al* (1983) showed that the threshold for the C-type baroreceptor fibres was shifted from ~140mmHg to ~163mmHg in aged rats between 16- and 32-weeks of age, although this was only seen in SHR rats, whilst control WKY rats showed no baroreceptor resetting. However, if as hypothesised, the resetting is linked to structural changes, such as increased collagen and stiffening of the arterial vessel wall, which are seen in normal ageing, this would also be expected to be seen in the otherwise healthy, aged WKY rats >32 weeks.

If cerebral vessels were to continue to vasoconstrict above 170mmHg, the constriction could become excessive and lead to tissue ischaemia, and vascular and endothelial damage. If the vessels did eventually undergo a forced dilatation, the large pressure increase seen by the downstream vessels could be more likely to cause haemorrhagic bleeding. Therefore an active dilatation at the UL may in fact be a protective, pressure-release mechanism, and a raised UL, as seen in the old rats, may predispose to an increased risk of experiencing a cerebrovascular event.

4.4.3 Differences in the UL across the cerebrovascular bed: The effect of ageing

The experiments in which gross and cortical CBF were recorded simultaneously, enabled CA and the UL to be assessed at different levels of the cerebrovascular bed. In young rats, the ULs calculated for the different vascular components were slightly, but significantly different from one another. The UL showed a tendency to increase as vessel size decreased, with the UL calculated for gross CBF, cortical RA, RC and RVPU being 168±4, 169±4, 170±4 and 170±4mmHg respectively, with significant differences between the gross and capillary, and gross and venous ULs. These data are in agreement with our hypothesis that the cortical UL would be higher than the gross UL in young rats, and suggests that the smaller, cortical arterial vessels are protected from high ABPs by the larger, downstream vessels, and even the

extracranial carotid artery. Thus, the reason that the cortical arteries and arterioles/capillaries (represented by RA and RCPU) had higher ULs than the larger vessels (gross CBF), was that they were not exposed to the increased ABP until autoregulation in the larger arteries had reached maximum effect. Despite this, when autoregulatory curves and the ULs were analysed with respect to the cortical arterial diameter data, no difference was seen between the vessels with a basal diameter of > or < 200µm, in either the young or old rats.

However, there is support for different autoregulatory behaviour in vessels of different sizes in the literature. As discussed above, Kontos *et al* (1978) visualised pial vessels using cranial windows in anaesthetised cats, and measured vessel diameter responses to hypertension. They categorised the vessels into 4 diameter groups: 37-59, 117-174, 205-252 and 273-375µm. The 2 smallest vessel groups showed no change in diameter until ABP reached 170 and 190mmHg respectively, above which they dilated with pressure. In contrast, the 205-252 and 273-375µm diameter vessels showed significant constriction with even minor changes in ABP. The constriction was greater as pressure increased, with diameter reaching its minimum at 160-170mmHg, and the vessels remained constricted at pressures of up to 200mmHg. This suggests that constriction of the larger cerebral vessels fully explains the maintenance of CBF between 100-170mmHg, and protects the smaller vessels from exposure to changes in pressure, as they showed no change in diameter until ABPs near or above the gross UL seen in the current study. However it does also suggest that the smallest vessels have the lowest ULs, in contrast with the higher ULs seen in the current study.

The reason for the lack of difference in behaviour between the two vessel diameter groups in the current study may be due to the method used. Diameter was not assessed by direct measurement of the vessels, but by adding intersecting lines to Laser Speckle images of the vessels. Diameter was then determined manually by analysing the profile curves, and

therefore should not be taken to represent exact diameter values. The vessels analysed were also not as small in diameter as the smallest vessels in the study by Kontos *et al* (1978), and so we may not have detected any differences that were in fact present.

The ULs in the old rats were not significantly different between the different cerebral vascular components, but were still significantly higher than the corresponding young ULs. This suggests that the protective mechanism present in the young rats, by which the larger vessels protect the smaller, downstream vessels, is not present in older animals. A study by Balbi *et al* (2015) offers some support for these data. They carried out a study in mice, in an attempt to define the age at which dysfunction of the cerebral vessels, and therefore compromised neurovascular coupling, begins. They used intravital microscopy and a Laser Doppler probe, to assess the pial microcirculation in response to a CO_2 challenge or stimulation of the forepaw, in 6 week, 8 month and 12 month old mice. They found no global CBF changes in mice up to 12 months of age, but they did see a reduction in CO_2 reactivity and neurovascular coupling from the age of 8 months. This suggests that age-related cerebrovascular dysfunction is not seen across all cerebral vessels in parallel, but may affect the pial microcirculation before any global CBF changes are seen, at least in mice. If the smaller arteries in the old rats in the current study had also developed age-related dysfunction before the larger vessels, this may underlie the apparent loss of protection of the small arteries by the larger ones. It does not, however, explain the consistently raised UL in comparison to the young rats. As discussed above, this may be due to structural changes causing increased arterial stiffness, or due to a resetting of high-pressure baroreceptors.

4.4.4 Differences in autoregulatory behaviour across the cerebrovascular bed: The effect of ageing

Analysis of the dual-line linear regression slopes fitted to the plateau and rising phases of the gross and cortical (RCPU) autoregulatory curves, and of cortical vessel diameter, allowed for a comparison of autoregulatory behaviour across the cerebrovascular bed, as well as between young and old rats. In line with the increase in CBF and CoBF seen above the UL, the slopes of the rising phases were positive, and arterial diameter also increased beyond the UL, indicating a breakthrough of autoregulation. The values of the rising slopes also tended to be higher than those of the plateau phases, representing the relative maintenance of CBF during the plateau phase. This difference between the plateau and rising phase was more obvious for the young rats, reaching significance for the young cortical data. Further, the slope of the young rising phase was significantly higher than the corresponding old slope, for both the gross and cortical data. Consistent with this, the cortical arterial diameter data in old rats tended to increase across the range of MABPs, resulting in a less obvious separation into the two phases, and a less easily identifiable UL.

These data suggest a blunted response in the old rats, which may be important if the hypothesis of an active dilatation beyond the UL is correct, as it would suggest an age-related dysfunction in this autoregulatory behaviour.

In line with the tendency for gross CBF to decrease during the plateau phase, the slopes of this phase tended to be negative for the gross data. CoBF tended to increase during the plateau phase, and accordingly the slopes were positive for the cortical data. Further, cortical arterial diameter also showed a trend to slightly increase during the plateau phase. The possible reasons for the negative slope seen for the gross CBF data has been discussed in section 4.4.2. Regarding the contrasting positive slopes seen for the cortical data, Lucas *et al* (2010) have

reported similar findings. When they raised ABP using PE infusions in healthy volunteers, they found that MCA velocity was positively correlated with MABP, and suggested that this 'pressure-passive' response was in fact representative of normal CA.

4.5 Conclusion

In contrast to our 1st hypothesis, the UL in the old rats was significantly raised compared to the young rats, which may be due to increased arterial stiffness with age. The significant fall in CVR before the UL in young rats, suggests an active dilatation rather than a passive increase in CBF. This may be physiologically important, representing a safety pressure release mechanism. This was significantly blunted in old animals, which supports the idea of increased arterial stiffness pushing the UL to higher ABPs.

In agreement with our 2nd hypothesis, the cortical UL was significantly higher than the gross UL in young rats. This suggests that larger cerebral vessels, and even extra-cranial vessels, respond at lower ABPs than the smaller, cortical arterial vessels, in a protective autoregulatory manner. In old rats, this potentially protective difference between gross and cortical ULs appears to be lost, which could increase the risk of haemorrhagic stroke.

CHAPTER 5: THE ROLE OF NITRIC OXIDE AT THE CEREBRAL AUTOREGULATORY UPPER LIMIT, AND CHANGES WITH AGEING

5.1 Introduction

As described in 1.3.4, nitric oxide (NO) is a short-lived, gaseous molecule, and an important transmitter in vertebrates. It is generated by the constitutive endothelial and neuronal nitric oxide synthase enzymes (eNOS and nNOS) found in endothelial cells, autonomic 'nitrergic' nerves and neurons, and requires the substrate L-arginine, oxygen and cofactors including BH_4. NO is involved in signalling pathways that result in vasodilatation and increased blood flow. With specific reference to CA, NO derived from endothelial, nerve fibre and neuronal sources (Moncada *et al*, 1991, Toda and Okamura *et al*, 2003, Bhardwaj *et al*, 2000), has been shown to play a key role in a number of relevant areas. These include in the maintenance of cerebrovascular tone and basal CBF, the cerebrovascular response to hypercapnia and hypoxia, and in mediating vasodilatation to maintain CBF when ABP falls (i.e. at the LL of CA). It is therefore reasonable to hypothesise that NO may also play a role in CA when ABP rises. As ageing has been shown to be associated with a decreased NO bioavailability, due to oxidative stress, as well as impaired endothelial function (see 1.4.4), any role played by NO in CA is likely to be impaired with ageing.

5.1.1 The role of NO in CBF regulation

As discussed in 1.3.4.1, NO has been implicated in setting basal cerebrovascular tone, and therefore in controlling basal CBF. For example, Faraci *et al* (1990) used a cranial window preparation to study diameter responses in the basilar artery of anaesthetised rats. Topical application of L-NMMA caused the basilar artery to constrict, an effect that was abolished by application of L-Arginine. Application of ACh caused the vessel to dilate, a response which

was inhibited by L-NMMA. In turn, L-Arginine was shown to prevent the L-NMMA-mediated inhibition of the response to ACh. This set of experiments provided evidence for a role of NO, synthesised from L-Arginine, in controlling basal tone of the basilar artery, and further, that the response to ACh is also mediated by NO.

Joshi *et al* (2000) performed a similar study in humans, and observed that intracarotid infusion of L-NMMA to inhibit NOS caused an increase in ABP and decrease in CBF. This was reversed by L-Arginine infusion, and the effect on CBF was not reproduced by using PE to mimic the increase in ABP.

In addition, nNOS-derived NO had also been shown to play a role in maintenance of basal CBF, as i.p. injection of the nNOS-specific inhibitor 7-NI decreased basal CBF without altering ABP in conscious rats (Montecot *et al*, 1997).

Daneshtalab and Smeda (2010) used immunohistochemistry to detect the NOS isoforms present on MCAs from WKY SHRsp rats, and observed that all three isoforms (eNOS, nNOS and iNOS) were expressed in the endothelium. There was also nNOS, and small amounts of iNOS, in the adventitial and smooth muscle cells. Before stroke had occurred in these rats, they studied isolated MCAs using pressure myography, and used a Laser Doppler probe to assess CBF in the region of the MCA. Through a combination of NOS inhibitors, NO scavengers, altering levels of available cofactors, and removal of the endothelium, they concluded that NO from eNOS and nNOS, but not iNOS, caused a decrease in the basal tone in isolated MCAs, and an increase in CBF.

As well as NO synthesised at the cellular level in cerebral vessels, Okamura *et al* (2002) hypothesised that the cerebral vasculature receives innervation from non-adrenergic, non-cholinergic nerves, and that NO is the main neurotransmitter (see section 1.3.4.1).

5.1.1.1 Role of NO in chemoregulation of CBF

In addition to contributing to basal CBF, the main role for NO in the regulation of CBF is thought to be in chemoregulation, i.e. the response to changes in P_aCO_2 and O_2.

Smith *et al* (1997) measured CoCBF using a Laser Doppler probe in anaesthetised, artificially ventilated rats. The rats received either saline (control), L-NAME (20mg.kg^{-1}, i.v.), or 7-NI (40mg.kg^{-1}, i.p.). They were then exposed to hypercapnia, by inhalation of 5% CO_2. Compared to the control group, where hypercapnia increased cortical CBF by ~70%, L-NAME caused a 25% decrease in cortical flow, and hypercapnia in the presence of L-NAME caused only a ~36% increase. 7-NI caused a smaller, 14% decrease in cortical flow, and hypercapnia caused only a ~38% increase, which was not significantly different to the effect of L-NAME. They concluded that nNOS-derived NO appears to be important for hypercapnic vasodilatation, and that eNOS-derived NO does not contribute.

Lavi *et al* (2006) studied CO_2 vasoreactivity in patients with endothelial dysfunction in comparison to healthy volunteers. They analysed the slope of CBF velocity, against the end-tidal CO_2 seen during normocapnia, hyperventilation and inhalation of 5% CO_2, and found that the patient group had an impaired CO_2 vasoreactivity compared with controls. This impairment was reduced by infusion of SNP, indicating an NO-dependent mechanism.

5.1.1.2 The role of NO in CA

Most studies that investigate the role of NO in pressure CA, tend to focus on its contribution to the CBF response to decreases in ABP, particularly in dynamic CA, and at the LL (see 1.3.4.2). For example, White *et al* (2000) inhibited NOS using a bolus, followed by an infusion, of L-NMMA (i.v.) in healthy volunteers. They assessed dynamic CA to sudden falls in ABP, by inflating and suddenly deflating thigh cuffs, and measured MCA velocity using a

transcranial Doppler probe. They analysed the rate of rise in MCAv against the falls in ABP, to calculate an autoregulatory index; where a value of 0 represents velocity changing in parallel with ABP, and a 9 represents no change in velocity with ABP. The bolus dose of L-NMMA caused the autoregulatory index to fall from ~4.6 to 3.9, whilst the subsequent infusion of L-NMMA saw some recovery of the index back to 4.3. These data suggest that NO plays a role in dynamic CA, and that NOS inhibition reduces the speed of dynamic CA response.

On the other hand, some studies have shown that NO has no influence on dynamic CA. Zhang *et al* (2003) measured MCAv using a transcranial Doppler in healthy volunteers. They assessed dynamic CA using transfer function analysis of beat-to-beat changes in ABP and velocity, when in a supine position, and during head-up tilt, in the presence and absence of L-NMMA. They found no differences in transfer function analysis between the 4 conditions, suggesting that NO does not play a role in dynamic CA. However, L-NMMA did not decrease basal CBF velocity in this study, although it did cause a 10mmHg increase in ABP, and therefore the dose may have been insufficient to see the full effect of removal of basal NO.

Jones *et al* (1999) investigated the role of NO at the LL of CA. They inhibited NOS at the cortical level, by application of L-NA for either 105 or 35 minutes directly into a cranial window in rats, and measured cortical CBF using a Laser Doppler probe. ABP was decreased using controlled haemorrhage, and the LL identified as the point at which the slope of CBF vs ABP changed, indicating a decrease in CBF. NOS inhibition significantly increased the LL of CA from ~75 to ~90mmHg after 105 minutes. However, this increase in the LL was not seen after 35 minutes, suggesting that the L-NA may have only had its effect by inhibiting an eNOS source of NO. However, Bauser-Heaton & Bohlen (2007) showed that nNOS was also important. They decreased ABP using controlled haemorrhage in rats, and measured an

increase in cerebral NO concentration, using an NO electrode via a cranial window. This increase in NO was reduced by nNOS inhibition.

The role of NO in static, pressure CA, and at the UL, has not been widely studied. Lavi *et al* (2006) gave increasing doses of PE to raise ABP in healthy subjects, and a patient group with endothelial dysfunction. They saw no difference in pressure-regulation between the two groups, suggesting that impaired endothelial NO release did not affect pressure autoregulation. However the ABP changes induced were only roughly 5-20mmHg above basal ABP, and so no inferences can be made about the UL.

5.1.2 The effect of ageing on NO

As discussed in 1.4.4, ageing is associated with changes in endothelial structure, such as decreased endothelial cell area, and increased permeability (Stewart *et al*, 1987), as well as functional changes, such as impaired synthesis and release of NO, and other vasoactive substances. These changes would therefore be expected to impair any role of NO in CA with ageing.

5.1.2.1 Impaired release and response to NO with age

As discussed in 1.4.4.2, ageing is generally associated with a decrease in the release of, and response to, vasoactive substances. The response to endothelial vasodilatory substances such as NO, are typically impaired (e.g. Mayhan *et al,* 1990), and this may (Heymes *et al,* 2000) or may not (Eisenach *et al,* 2014) be associated with an increase in constricting substances, tipping the normal balance to an increasingly vasoconstricted state.

In our lab we have demonstrated that application of graded doses of adenosine to open carotid artery preparations, caused a graded release of NO, as measured by an NO sensor. This release was attenuated in rats aged 44-48 weeks old, compared to young, adult rats aged 10-12 weeks

old, suggesting that even at an age equivalent to early middle-age in humans, evoked NO release from the endothelium was reduced.

5.1.2.2 Impaired NO synthesis with age

As well as impaired responses to NO, there is also evidence for age-related changes in NO synthesis and NOS expression (see 1.4.4.3). Typically, NOS mRNA and activity is seen to increase with age, but NOS protein levels are reduced, suggesting age-related impairment in translation (e.g. Strosznajder *et al*, 2004). In terms of NO synthesis, there is evidence for both an increase (McCann *et al*, 1998) and decrease (Yamada & Nabeshima, 1998) in NO levels with age.

Yoon *et al* (2010) investigated NO synthesis by eNOS in young and old cultures of human endothelial cells. They measured NO production by detection of nitrite, and eNOS protein expression levels and phosphorylation status using ELISA, Western blot and immunoprecipitation. They found that NO production significantly decreased with age of the cells. This NO production was inhibited by the non-selective NOS inhibitor L-NIO, but was unaffected by the iNOS-selective inhibitor 1400W, suggesting that the source of the NO was eNOS. They also showed that levels of eNOS protein decreased with age, as did the levels of active, phosphorylated eNOS. Further, levels of the inhibitory regulatory protein calveolin-1 were increased with age, whilst the levels of the activating regulatory proteins Akt and Hsp90 were decreased. Similar age-related changes were also seen for the binding between these regulatory proteins and eNOS.

5.1.2.3 Ageing and oxidative stress: implications for NO

As discussed in 1.4.5, oxidative stress, a well-known marker of ageing associated with increased levels of harmful free radicals, has implications for the synthesis and bioavailability of NO. The NOS cofactor BH_4 is known to be damaged by free radicals, leading to eNOS uncoupling and decreased NO production (Kuzkaya *et al*, 2003). Further, uncoupled NOS produces O_2^-, adding to the environment of oxidative stress (Luo *et al*, 2014).

Functionally, Eskurza *et al* (2005) found that endothelium-dependent dilatation (EDD), assessed by measuring the flow-mediated dilatation in response to brachial artery occlusion, was significantly impaired in aged, sedentary subjects. However, a single, oral dose of BH_4 was able to restore this response close to that seen in a young control group.

Mayhan *et al* (2008) measured pial arterial diameter via a cranial window in rats. Application of ACh caused an eNOS-dependent dilatation, reflected by an increase in vessel diameter, which was reduced in magnitude in aged vs. young rats. However, application of various antioxidants increased the dilatation seen in the aged rats.

5.1.3 Aims and Hypotheses

Little research has addressed the role of NO in regulating CBF to increases in ABP, or at the UL of CA, in either young or aged subjects. Therefore the aim of this set of experiments was to investigate the role of NO, from both endothelial and neuronal sources, in setting the basal cerebrovascular tone from which autoregulatory constriction occurs, as well as in CA when ABP rises, and at the UL. Further, as ageing, and the related increase in oxidative stress, is associated with impaired endothelial function, including a reduced NO synthesis, release, and NO-mediated vasodilatation, it is likely that any role played by NO in CA is diminished with ageing.

Our hypotheses were as follows:

- Inhibition of nNOS-derived NO, by either SMTC or 7-NI, would decrease the UL in young rats compared to that seen in control conditions, indicating the importance of neuronal NO-mediated vascular tone in the control of CBF. Removal of a tonic vasodilatory influence would leave the vessels more constricted, hence reducing the range for subsequent autoregulatory vasoconstriction if ABP rises.
- Inhibition of both eNOS and nNOS by L-NAME would have a greater effect than inhibition of nNOS alone i.e. the UL would be lowered further compared to control.
- NOS inhibition would have no effect on the UL in old rats, due to impaired endothelium-dependent vasodilatation, and a reduced NO bioavailability, associated with ageing.

5.2 Methods

5.2.1 Surgery

Surgery was carried out as described in 2.2. Anaesthesia was induced with 4% isoflurane in O_2 at 4 L min^{-1}. The left jugular vein was cannulated, and isoflurane anaesthesia was withdrawn and gradually replaced with i.v. Alfaxan® bolus doses (0.1ml boluses at 5mg.ml^{-1}), and then a maintenance infusion dose of 17-30 mg.kg^{-1}.$hour^{-1}$. The trachea was cannulated with a custom-made stainless steel T-piece cannula, to maintain a patent airway and supply oxygen if necessary. The left brachial artery was cannulated to take samples for blood gas analysis. The left femoral artery and vein were cannulated to record arterial blood pressure (ABP) and heart rate (HR), and for drug infusion respectively. All cannulae were filled with heparinised saline. The right common carotid artery was cleared distally up to its bifurcation. The external carotid, as well as occipital, facial and lingual branches were ligated, to achieve vascular isolation of the internal carotid artery and its distribution to the right side of the brain (as described by Thomas & Marshall, 1994). Blood flow was recorded through the common carotid artery as an index of gross CBF.

Of the L-NAME group, n=8 young rats, and all of the old rats underwent additional surgery to record CoBF simultaneously with gross CBF. The animal was placed in a stereotaxic frame, and cranial thinning was carried out, leaving a layer through which cerebral vessels were visible. A Laser Speckle Contrast imager, mounted on a microstand at 10-15cm from the thinned bone, was used to image the dorsal surface of the right and left cortices, and record cortical tissue perfusion (perfusion units – PU). Data was recorded using a PowerLab and Labchart software (ADInstruments). CVR (=ABP/C(o)BF) was continuously calculated during the experiment.

For further details of the equipment and data acquisition parameters used, see 2.3.

5.2.2 Stabilisation

Before the experiment began, equilibration was allowed until all variables were stable. A 20-min period of baseline was recorded, and blood gas samples were taken to check P_aO_2, P_aCO_2 and pH values. Blood samples were then taken every 5-10 minutes, in alignment with administration of each drug/increasing dose. If the blood gas values deviated from the mean, or breathing appeared laboured, the airway was aspirated. If P_aO_2 fell below the mean, supplemental O_2 was given. Close attention was paid to P_aCO_2 levels, due to high sensitivity of the cerebral circulation to changes in CO_2 (Willie *et al*, 2012). If P_aCO_2 levels rose above 45mmHg and could not be corrected, the data was discarded.

5.2.3 Experimental protocol

5.2.3.1 Non-selective inhibition of NOS

A single dose of L-NAME (10mg.kg^{-1} i.v.) was given to non-selectively inhibit NOS, in n=16 young (330±7g) and n=7 old (786±26g) rats. A bolus dose of ACh (10µg.kg^{-1} i.v.) was given before and after L-NAME to assess its effectiveness in blocking NO-mediated dilatation.

5.2.3.2 Selective inhibition of nNOS

In n=10 (319±9g), and n=16 (317±4g) young rats, a single dose of 7-Nitroindazole (7-NI dissolved in DMSO (final concentration of 1%), 25mg.kg^{-1} i.p.) or S-Methyl-L-Thiocitrulline (SMTC, 0.56mg.kg^{-1} i.v.) respectively, were given to selectively inhibit nNOS. A bolus dose of ACh (10µg.kg^{-1} i.v.) was given before and after each drug to assess its effectiveness in blocking NO-mediated dilatation.

Following NOS inhibition, by either L-NAME, 7-NI or SMTC, an infusion of PE was used to progressively increase MABP. Doses of 0.1–200µg.kg^{-1}.min^{-1} at 6-12ml.hr^{-1} were infused and around 2 minutes was allowed at each dose for the effects to stabilise. When the UL was reached, indicated by an increase in CBF, or CoBF (in a subgroup of 8 young rats, 328±13g, and in all 7 old rats), accompanied by a fall in CVR, with a rising or stable MABP, one further dose of PE was given before the infusion was stopped. Variables were then allowed to recover back to basal levels.

5.2.4 Data Analysis

Data was analysed as described in 2.7. Briefly, 60 second sections of LabChart data representing the baseline, the final minute of the response to each NOS inhibitor, just prior to the start of the PE infusion, and of each PE infusion step, were exported as a mean value for each variable, and opened in Excel for further analysis. For the responses to ACh bolus, 5 seconds of data was exported, representing the peak of the response.

The analysis of the Laser Speckle data is described in detail in 2.7.2. Briefly, the data files were opened in MoorFLPI Full-Field Laser Perfusion Imager Review software, and ROIs representing an arterial vessel, venous vessel and capillary region were selected. The Flux data (given as PU) was compiled as graphs against time, and opened in Excel, to be aligned with the LabChart data.

5.2.5 Calculation of the UL

Autoregulatory curves were generated by plotting mean CBF, or right arterial, venous or capillary perfusion units (RA/RV/RCPU, with RCPU taken to represent CoBF), against MABP at each PE dose. Dual-line linear regression analysis (described by Samsel & Schumacker, 1988, and used previously in our laboratory by Edmunds & Marshall, 2001) was

used to calculate the autoregulatory UL. The UL for each animal was defined as the intersection of the two regression lines with the best fit and the smallest standard deviation of residuals. A group mean UL was then calculated from the individual values. See 2.7.3 for more details.

5.2.6 Statistical analyses

All data are presented as the mean ± SEM. Graphs and statistics were generated using GraphPad Prism® 5. Data was analysed using t-tests (paired or unpaired as appropriate) and one-way ANOVAs with post-hoc Bonferroni. $P<0.05$ was taken as significant.

5.3 Results

5.3.1 Baseline characteristics of young vs. old rats

Baseline characteristics of the young and old L-NAME groups are shown in Table 5. Similar to the control groups in Chapter 4, the old rats in this study were significantly heavier than the young rats. However, in comparison, they had a lower ABP, HR and HCT vs young, whilst P_aO_2, P_aCO_2 and pH were not different between the two groups.

The old rats also had a significantly higher mean, basal CBF (2.4±0.3 vs. 1.4±0.1ml·min^{-1}, unpaired t-test; P=0.002), and calculated CVR was significantly lower in old compared to young rats (54±6 vs. 109±13mmHg·ml^{-1}·min, unpaired t-test; P=0.01).

When CBF and CVR were corrected per kg of body weight, CBF was not different between the young and old rats (3.0±0.3 vs. 4.2±0.4ml·min·kg^{-1}, unpaired t-test; P=0.09), but CVR was still significantly higher in young rats (331±29 vs. 68±7mmHg·ml^{-1}·min·kg^{-1}, unpaired t-test; P=0.0004). These baseline characteristics are not significantly different from the control groups, enabling comparison between the control and NOS inhibition data to assess the role of NO.

5.3.2 The effect of NOS inhibition in young vs. old rats

5.3.2.1 Basal effects of NOS inhibition

Figure 36 shows the effect of the ACh bolus, before and after infusion of L-NAME to inhibit NOS, on MABP (a & b), CBF (c & d) and CVR (e & f), in young and old rats respectively. The data are shown as the change from the immediately preceding baseline (i.e. ACh = ACh – baseline, L-NAME = L-NAME – recovery from ACh, ACh + L-NAME = ACh + L-NAME – L-NAME). The data within in each age group was analysed by one-way ANOVA with post-

hoc Bonferroni, for each parameter measured (results described as significant gave $P<0.05$ in the post-hoc tests). Comparisons between young and old were made using unpaired t-tests.

In the young rats, ACh caused a significant decrease in ABP, but no significant changes in CBF or CVR, although CBF tended to increase and CVR to decrease. In old rats, ACh also caused a significant decrease in ABP, but no significant change in CBF or CVR, although there was a trend for both CBF and CVR to decrease.

L-NAME significantly increased ABP in young rats, and significantly decreased CBF and increased CVR in both young and old rats. L-NAME did not significantly change ABP in the old rats although there was a trend for ABP to increase. The effect on CBF was larger in old animals (unpaired t-test; $P=0.03$).

In young rats, the second bolus of ACh, in the presence of L-NAME, produced the same pattern of response as the first ACh bolus. The decrease in ABP and increase in CBF were significantly larger than that seen with ACh alone. Both ABP and CVR also decreased significantly compared to the preceding baseline. In old rats, ABP significantly decreased, and CBF now showed a significant increase compared to the preceding baseline. CVR did not significantly change, but did show a trend to decrease. None of the changes seen were significantly different to ACh alone.

5.3.2.2 Effects of NOS inhibition on CA and the UL

Figure 37 shows the mean autoregulatory curves and corresponding changes in CVR, generated in young and old rats after L-NAME. Figure 37 a) shows that, in n=4 young rats, CBF autoregulation was seen as in control experiments. CBF was maintained between ~0.3-0.4ml·min^{-1} during the plateau phase, shown in blue. Beyond the UL, CBF rose significantly, from 0.4±0.02 to 0.8±0.1ml·min^{-1} (paired t-test; $P=0.04$). The gross UL after L-NAME was

significantly higher than control (187±2mmHg vs 168±2mmHg, unpaired t-test; P=0.0002). Figure 37 b) shows that CVR increased from 354±20 to 601±117mmHg·ml^{-1}·min (paired t-test; P=0.01) between the MABPs of 140 and ~180mmHg (slightly lower than the UL), corresponding with the maintenance of CBF during the plateau phase. Beyond this, CVR tended to fall (and CBF rose), reaching a minimum of 254±42mmHg·ml^{-1}·min, although this was not significantly lower than baseline (paired t-test; P=0.07). Figure 37 c) shows that in n=12 young rats, CBF was maintained between ~0.2-0.4ml·min^{-1}, even when ABP was raised to 186±3mmHg. This maximum ABP was significantly higher than the control UL (paired t-test; P<0.0001). Figure 37 d) shows that, in these rats where the UL was not reached, CVR increased significantly, and remained raised.

Figure 37 e) shows that, in n=7 old rats, CBF was maintained between ~0.8-0.5ml·min^{-1}, and no UL was seen even when ABP was raised up to a maximum of 199±5mmHg. This maximum ABP was significantly higher than both the old control UL (unpaired t-test; P=0.003) and the young L-NAME UL/maximum ABP (unpaired t-test; P=0.01). Figure 37 f) shows that, in the old rats where the UL was not reached, CVR increased significantly, and remained raised.

Figure 38 shows the autoregulatory curves generated in experiments in which gross CBF and cortical perfusion (CoBF) were measured simultaneously in a) young (n=8) and b) old (n=7) rats. Unlike the gross CBF data shown in Figure 37, CoBF showed a slight increase with MABP, and no UL was reached in either young or old animals at the maximal ABPs stated above.

Figure 39 shows the ULs, or in those experiments where an UL was not reached, the top ABP achieved, for the young and old rats after infusion of L-NAME. The ULs from the control

experiments (chapter 4) were included for reference. The values were as follows; 168±2, 180±3, 187±2 and 199±5mmHg, for the young control, old control, young L-NAME and old L-NAME groups respectively. One-way ANOVA with post-hoc Bonferroni revealed a significant difference between most of the values ($P<0.0001$). The only groups of data that were not significantly different from one another, were the old control and young L-NAME values.

5.3.3 The effect of nNOS inhibition in young rats

5.3.3.1 Basal effects of nNOS inhibition

Figure 40 shows the effect of the ACh bolus, before and after infusion of either SMTC (n=10), or 7-NI (n=16) to inhibit nNOS, on MABP (a & b), CBF (c & d) and CVR (e & f) in young rats. The data are shown as the change from the immediately preceding baseline. The data within each of the nNOS inhibitor groups was analysed by one-way ANOVA with post-hoc Bonferroni, for each parameter measured. Comparisons between the two groups, and with the L-NAME data described above, were made using unpaired t-tests.

In the SMTC group, ACh caused a significant decrease in ABP, a non-significant trend for CBF to increase, and a significant decrease in CVR. SMTC significantly increased ABP, showed a trend for CBF to decrease, and significantly increased CVR. The decrease in CBF to SMTC was significantly smaller than the decrease caused by L-NAME. The response to the second bolus of ACh, in the presence of SMTC, was similar to those seen with ACh alone, except that the decrease in ABP was significantly bigger.

In the 7-NI group, ACh caused the same pattern of responses as the SMTC group, a significant decrease in ABP, an increase in CBF, and a significant decrease in CVR.

7-NI caused a small increase in ABP, which was significantly smaller than the effect of SMTC and L-NAME. It also caused a significant decrease in CBF, and significant increase in CVR. The second bolus of ACh, in the presence of 7-NI, produced the same effects as the first bolus.

5.3.3.2 Effects of nNOS inhibition on CA and the UL

Figure 41 shows the mean autoregulatory curves and corresponding changes in CVR, generated in young rats after SMTC. Figure 41 a) shows that, in n=8 young rats, CBF autoregulation was seen as in control experiments. CBF showed some fluctuation between ~0.8-1.4ml·min^{-1} during the plateau phase, shown in blue. Beyond the UL, CBF rose significantly (shown in red) to 1.9±0.1ml·min^{-1} (paired t-test vs. baseline; P=0.003). The gross UL after SMTC was not significantly higher than control (171±2mmHg vs. 168±2mmHg, unpaired t-test; P=0.14).

Figure 41 b) shows that CVR increased from 108±13 to 161±10mmHg·ml^{-1}·min (paired t-test; P=0.02) between the MABPs of 120 and ~160mmHg (slightly lower than the UL), corresponding with the maintenance of CBF during the plateau phase. Beyond this, CVR fell (and CBF rose), reaching a minimum of 101±7mmHg·ml^{-1}·min, not significantly different from baseline. Figure 41 c) shows that in the other n=8 young rats, CBF was maintained between ~1-1.2ml·min^{-1}, even when ABP was raised to 169±3mmHg. This maximum achievable ABP was not significantly different to the control UL. Figure 37 d) shows that, in these rats where the UL was not reached, CVR increased significantly, and remained raised.

Figure 42 shows the mean autoregulatory curves and corresponding changes in CVR, generated in young rats after 7-NI. Figure 42 a) shows that, in n=5 rats, CBF autoregulation was seen as in control experiments. CBF was maintained between ~0.8-1ml·min^{-1} during the

plateau phase (shown in blue). Beyond the UL, CBF rose significantly (shown in red) to 1.6±0.1ml·min^{-1} (paired t-test vs baseline; P=0.002). The gross UL after 7-NI was significantly higher than control (174±7mmHg vs. 168±2mmHg, unpaired t-test; P=0.05).

Figure 42 b) shows that CVR increased from 155±9 to 199±31mmHg·ml^{-1}·min (paired t-test; P=0.15) between the MABPs of 120 and ~170mmHg (slightly lower than the UL), corresponding with the maintenance of CBF during the plateau phase. Beyond this, CVR fell (and CBF rose), reaching a minimum of 120±12mmHg·ml^{-1}·min, not significantly different from baseline (paired t-test; P=0.053). Figure 42 c) shows that in the other n=5 rats, CBF was maintained between ~0.6-0.9ml·min^{-1}, even when ABP was raised to 174±2mmHg. This was the maximum ABP that could be reached in the group, and was not significantly different to the control UL. Figure 42 d) shows that, in these rats where the UL was not reached, CVR increased significantly, and remained raised.

Figure 43 shows the ULs, or in those experiments where an UL was not reached, the top ABP achieved, for the young rats after infusion of SMTC or 7-NI. The ULs from the control experiments (chapter 4) and young L-NAME experiments were included for reference. The values were as follows; 168±2, 170±2, 174±2 and 187±2mmHg, for the young control, SMTC, 7-NI and L-NAME groups respectively. One-way ANOVA with post-hoc Bonferroni revealed a significant difference between L-NAME and each of the other three values (P<0.0001).

Mean ± SEM	Young (n=16)	Old (n=7)	P value (unpaired t-test)
Body weight	330±7	786±26	<0.0001*
MABP	133±2	120±7	0.03*
HR	424±7	380±11	0.004*
P_aO_2 (mmHg)	72±2.4	75±2.9	0.45
P_aCO_2 (mmHg)	43±1.6	42±2.3	0.82
pH	7.44±0.01	7.44±0.02	0.9
HCT (%)	38±0.6	35±0.7	0.006*

Table 5: Baseline characteristics of young (n=16) and old (n=7) male Wistar rats in the L-NAME groups. Old rats were significantly heavier, had a significantly lower MABP, HR and HCT. P_aO_2, P_aCO_2 and pH were not significantly different between the 2 groups.

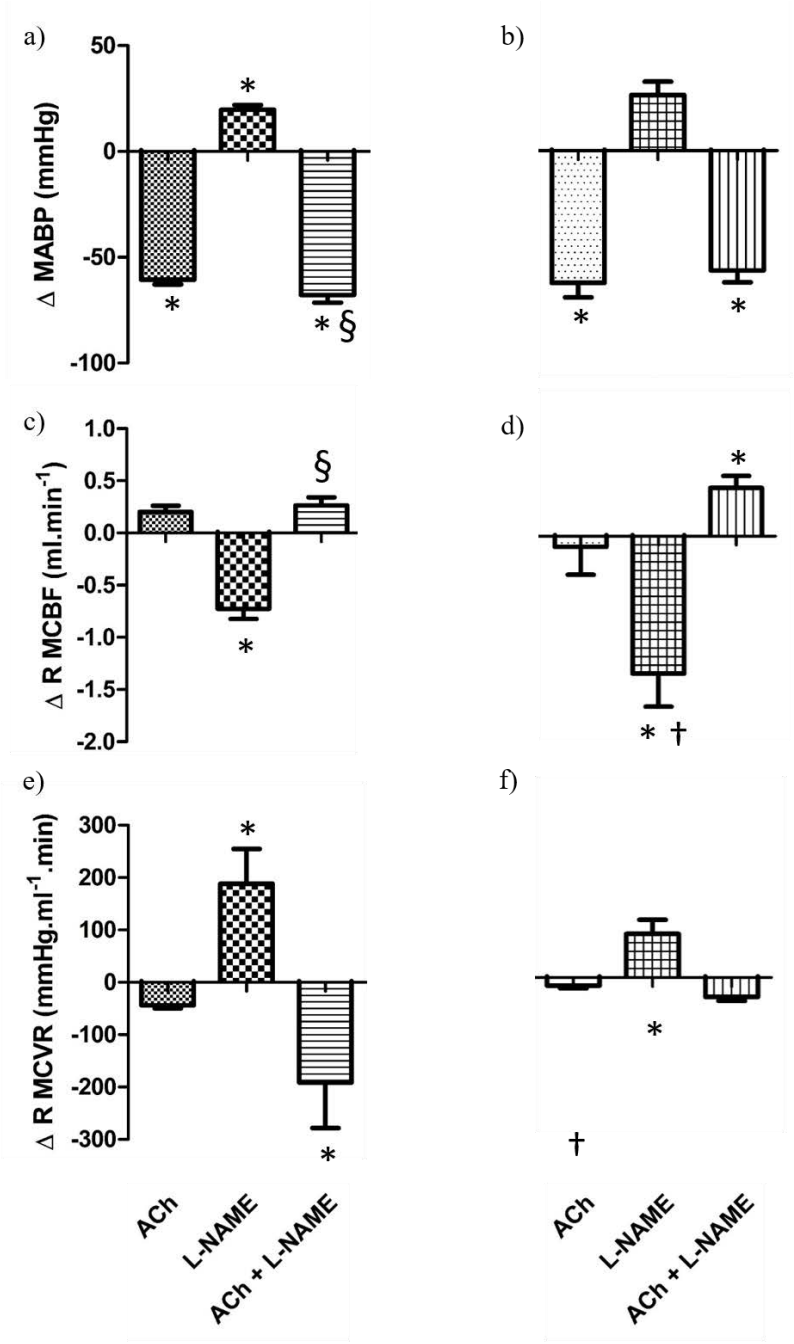

Figure 36: The effect of i.v. ACh (10 µg.kg^{-1}), before and after L-NAME (10mg.kg^{-1}) on a & b) MABP, c & d) R MCBF and e & f) R MCVR (plotted as change from the preceding baseline), in young (left column) and old (right column) animals respectively. One-way ANOVAs; * = significant difference vs preceding baseline, § = significant difference between the ACh bolus before and after L-NAME. Unpaired t-test; † = significant difference between young & old.

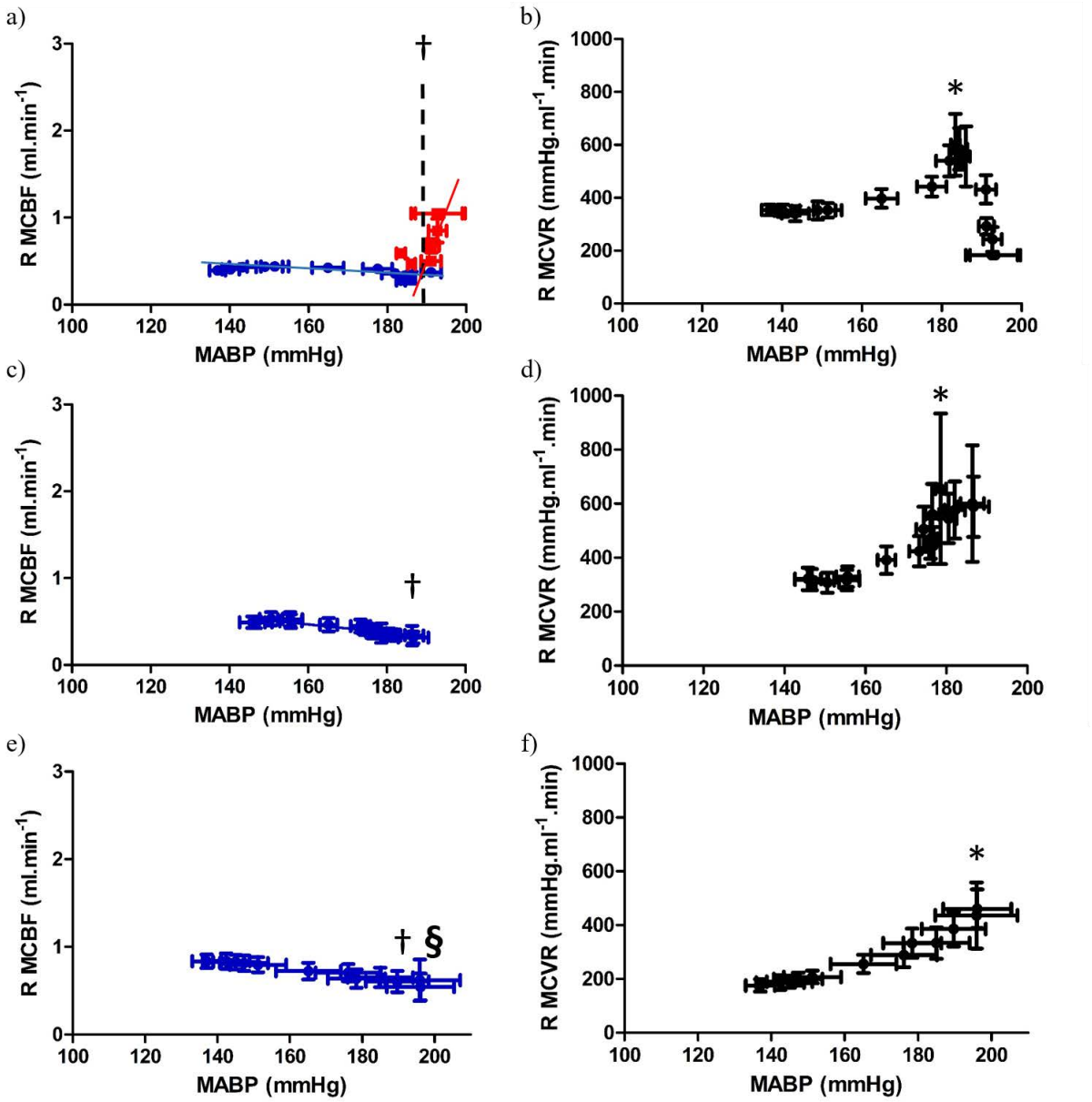

Figure 37: The mean cerebral autoregulatory curves generated in young (n=16) and old (n=7) male Wistar rats, after L-NAME. Data shown is absolute M RCBF (a, c & e) and CVR (b, d & f) during PE-induced increases in MABP. a) and b) show the data from n=4 young rats in which an UL, shown by the dashed line, could be calculated. c) and d) show the data from the remaining n=12 young rats, and e) and f) the old rats, in which an UL was not reached. Paired or unpaired t-tests; † = significantly higher than control UL (chapter 4), § = significantly higher than young L-NAME value, * = significantly higher than baseline CVR.

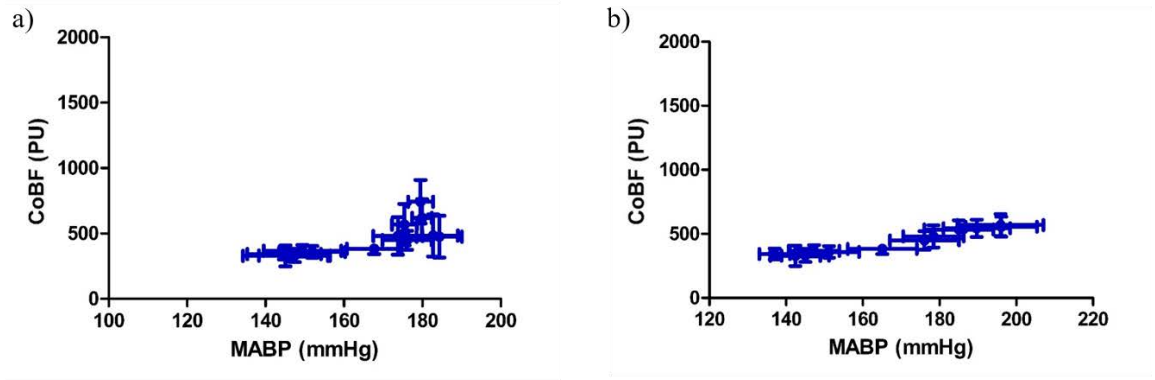

Figure 38: Changes in CoBF during PE-induced increases in ABP, after L-NAME, in a) young (n=8) and b) old rats (n=7). No clear UL was reached after NOS inhibition, even when ABP was raised to the maximum possible values (~190 and 200mmHg in the young and old rats respectively).

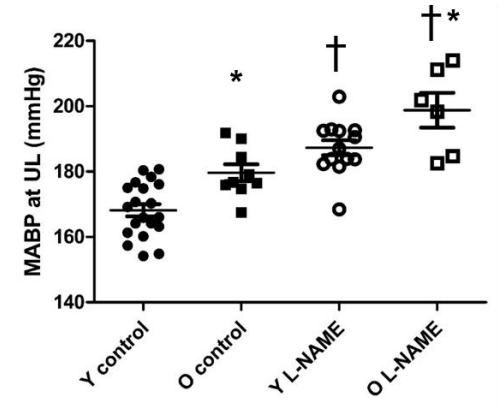

Figure 39: Gross ULs from the young and old control groups (chapter 4), and the UL or top ABP reached in young and old rats after L-NAME. The values seen after L-NAME were significantly higher than the equivalent control values, for both the young and old rats. In addition, the old values were significantly higher than the young values, for both the control and L-NAME experiments (one-way ANOVA; $P<0.0001$, post-hoc Bonferroni; † = significantly different vs. control, * = significantly different vs. young).

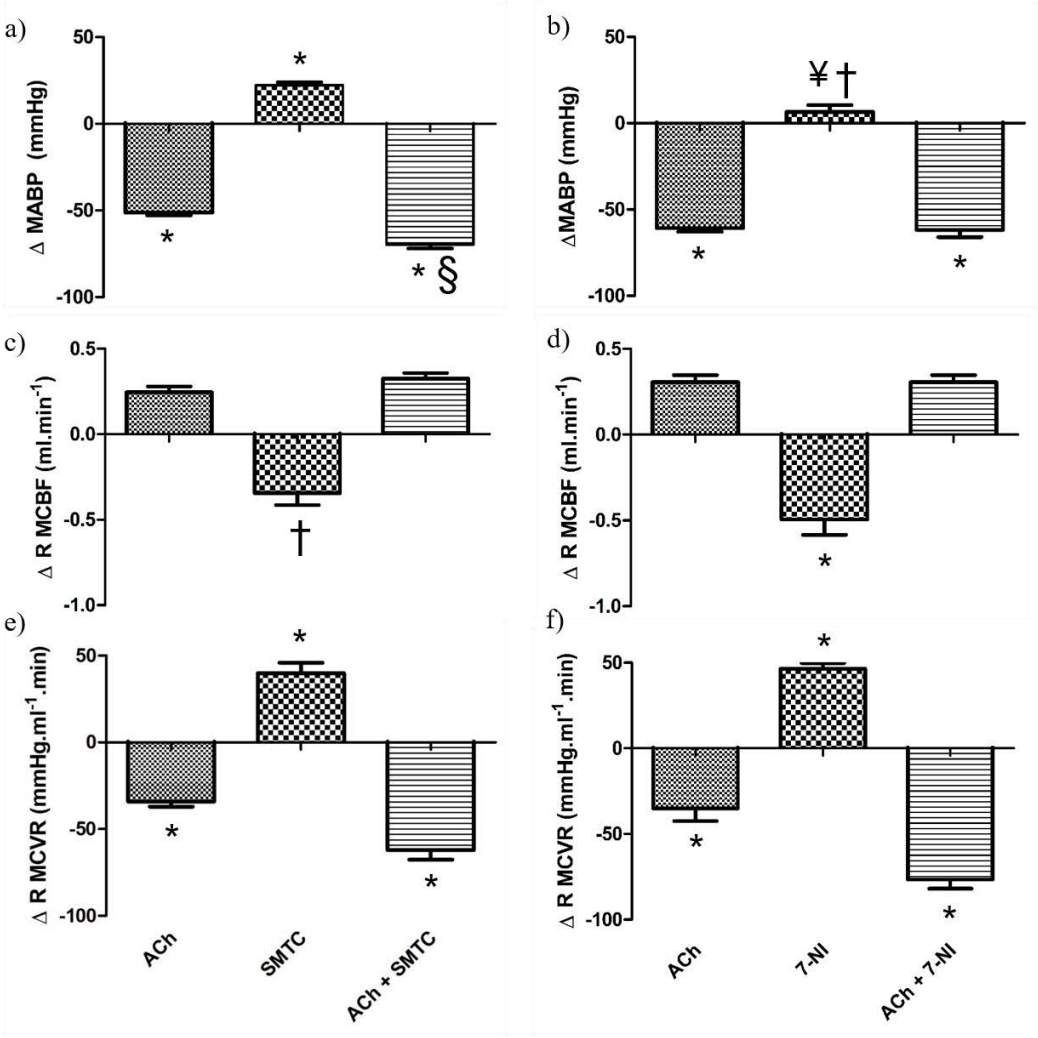

Figure 40: The effect of i.v. ACh (10 µg.kg^{-1}), before and after SMTC (0.56mg.kg^{-1}, left column) or 7-NI (25mg.kg^{-1}, right column) on a & b) MABP, c & d) R MCBF and e & f) R MCVR (plotted as change from the preceding baseline), in young animals. One-way ANOVAs; * = significant difference vs preceding baseline, § = significant difference between the ACh bolus before and after nNOS inhibition, ¥ or † (marked on the 7-NI graphs in the right column) = significantly different to the equivalent response with SMTC or L-NAME respectively.

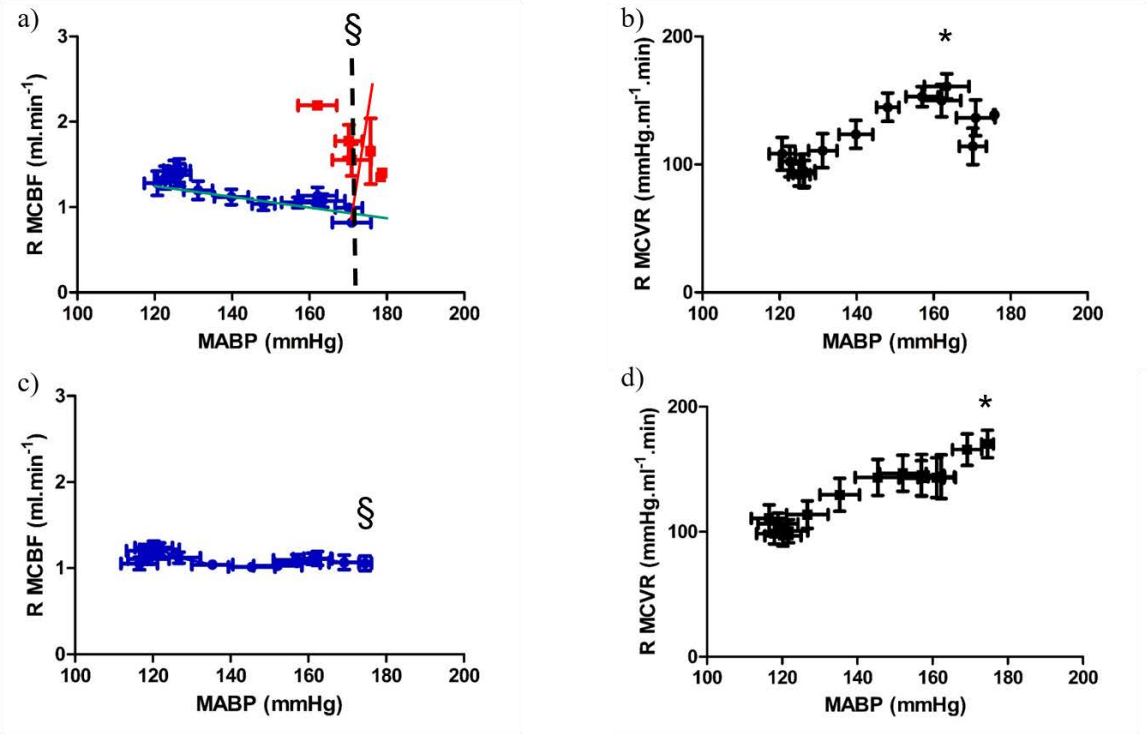

Figure 41: The mean CA curves generated in young rats after SMTC (n=16). Data shown is absolute R MCBF (a & c) and R MCVR (b & d) during PE-induced increases in MABP. a) and b) show the data from n=8 young rats in which an UL, shown by the dashed line, could be calculated. c) and d) show the data from the remaining n=8 young rats in which an UL was not reached. Unpaired t-test; § = significantly different to the L-NAME value. Paired t-test; * = significantly higher than baseline CVR.

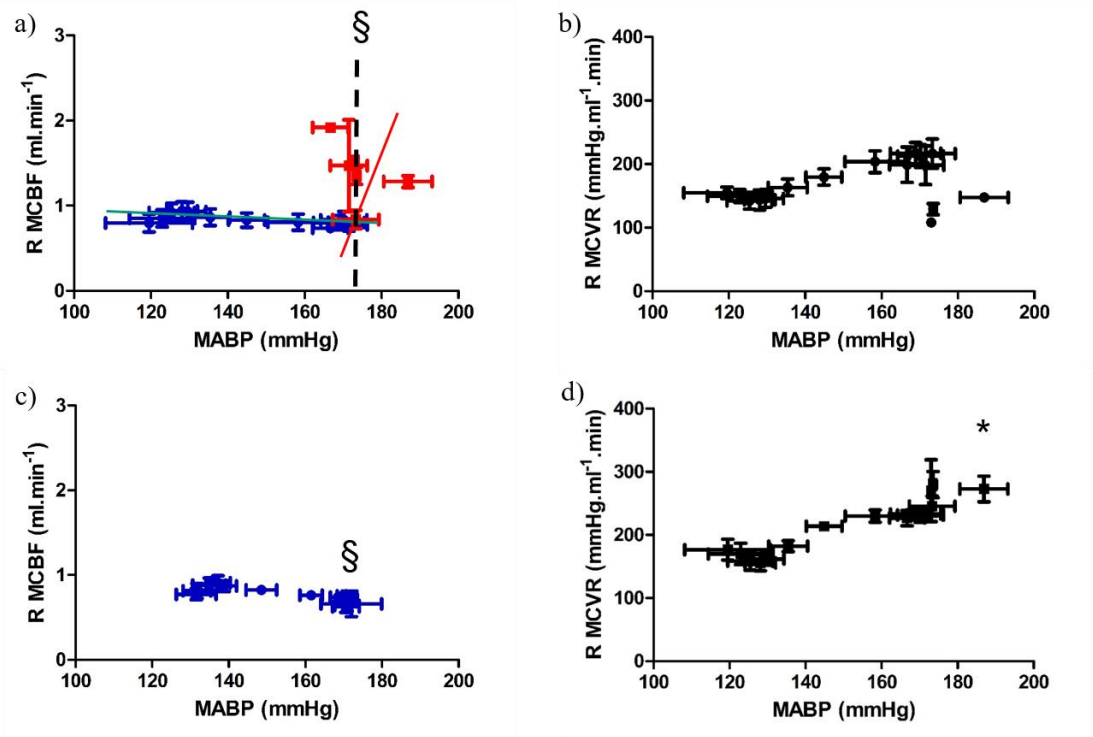

Figure 42: The mean cerebral autoregulatory curves generated in young rats after 7-NI (n=10). Data shown is absolute R MCBF (a & c) and R MCVR (b & d) during PE-induced increases in MABP. a) and b) show the data from n=5 young rats in which an UL, shown by the dashed line, could be calculated. c) and d) show the data from the remaining n=5 rats in which an UL was not reached. Paired or unpaired t-tests; § = significantly different to the L-NAME value, * = significantly higher than baseline CVR.

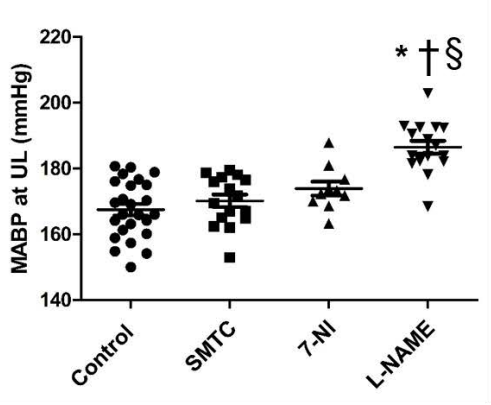

Figure 43: Gross ULs from the young control group (chapter 4), and the UL or top ABP reached in young rats after SMTC, 7-NI or L-NAME (one-way ANOVA; $P<0.0001$, post-hoc Bonferroni; * = significantly different vs. control, § = significantly different vs. SMTC, † = significantly different vs. 7-NI).

5.4 Discussion

The typical changes in baseline cardiovascular parameters with ageing are discussed in 4.4.1. The baseline values seen in these experiments were not significantly different from the control groups of the same age, enabling comparisons to be made. In both the control groups, and the current NOS inhibition groups, absolute CBF was significantly higher in the old rats. However, in contrast to the data in control groups, where CBF corrected for body weight was lower in the old rats, in agreement with the literature (see 4.4.1), in the NOS inhibition groups there was no significant difference in corrected basal CBF between the young and old rats. The reason for this is not known; there was no significant differences between the control and NOS inhibition groups of the same age, in body weight (unpaired t-tests of control vs NOS inhibition; young; P=0.3 and old; P=0.4), or basal CBF (unpaired t-tests; young; P=0.3, and old; P=0.9).

5.4.1 The role of NO in basal CBF, CA and the UL: The effect of ageing

5.4.1.1 Basal effect of NOS inhibition

The basal effects of using L-NAME, used to non-selectively inhibit NOS, were suggestive of a cerebral, NO-mediated tone being present in both young and old rats, as basal ABP increased, yet CBF decreased and CVR increased in both groups (Figure 36). This agrees well with the literature, for example Faraci *et al* (1990) observed a decrease in basilar artery diameter of young, anaesthetised rats when L-NMMA was applied topically via a cranial window. Fernandez *et al* (1993) showed that, in conscious goats, an i.v. bolus dose of L-NAME caused a 20% increase in ABP, a 40% decrease in CBF, and a 115% increase in CVR, supporting the idea of an NO-mediated input in basal cerebrovascular tone.

In the current study, the L-NAME-induced change in CBF was larger in the older animals; this may have been an artefact of the higher absolute CBF seen in the old rats, or may reflect an increased role for NO in maintaining basal CBF with age. As discussed in 1.4.4 and 5.1.2, ageing is generally associated with a decrease in responsiveness to vasoactive substances such as NO, as well as alterations in its synthesis and release. For example, Omar & Marshall (2010a) demonstrated that the ability of adenosine to invoke NO release from the endothelium of the carotid artery was attenuated in middle-aged (42-44 weeks), vs mature (10-12 weeks) Wistar rats.

Further, Omar & Marshall (2010b) investigated the effect of L-NAME in juvenile (4-5 weeks old), mature (10-12 weeks old) and middle-aged (42-44 weeks old) rats, on the carotid blood flow response to infusion of noradrenaline. L-NAME itself induced an increase in ABP, and a decreased HR, CVC, and CBF in all ages. When calculated as a percentage change from baseline, the decreases in CVC and CBF were greater in the mature and middle-aged rats compared to the juvenile rats, suggesting a greater tonic influence of NO in the carotid artery of aged rats, and agreeing with the current data.

In the current study, bolus doses of ACh were given before and after the L-NAME infusion, to assess the effectiveness of the NOS inhibition. NO is widely accepted as the mediator of the vasodilatory effect of ACh. For example, in the study discussed above by Faraci *et al* (1990), when they applied ACh via a cranial window, they saw a dilatation of the basilar arteries, a response which was inhibited by L-NMMA. Therefore the current observation that the response to ACh in the presence of L-NAME was unaffected, or even potentiated, was surprising. However, other endothelium-dependent, NO-independent vasodilatory factors that mediate the action of ACh have been proposed, particularly in the cerebral vessels

(Rosenblum, 1992). This may be an eicosanoid-pathway, or involve an undefined EDHF substance (Peterson *et al*, 2011).

Of particular interest in the responses to ACh, was the fact that in the old rats, ACh alone induced a small decrease in CBF, which was associated with a decrease in ABP, and a decrease in CVR that was significantly smaller than the equivalent in the young rats. After infusion of L-NAME in old rats, CBF increased in response to ACh, and both the CBF and CVR responses were increased in magnitude.

Similar results were seen in the study by Omar & Marshall (2010a) discussed above. When adenosine was infused to induce NO release *in vivo*, ABP decreased to 60mmHg, and CVC and CBF increased in adult rats. However, in the middle-aged rats, CVC increased to a lesser extent, and CBF decreased in half of the rats, suggesting either a failure in autoregulation, or a shift in the autoregulatory range, such that the LL was exceeded.

When the adenosine infusion was repeated after L-NAME, the responses in adult rats were blunted, which is in contrast with the current data, and suggests a dependence on NO. However, in agreement with the current data, the CVC response in middle-aged rats was unchanged, and CBF increased. This may again be explained by an increased LL in middle-aged rats, such that the increase in ABP caused by L-NAME shifted the ABP back into the autoregulatory range. The authors also suggested that the LL could have become dependent on NO with age, such that basal NO-mediated tone in middle-aged rats limited the ability to autoregulate to falls in ABP (Omar and Marshall, 2010a).

5.4.1.2 CA and the autoregulatory UL after NOS inhibition

In contrast to our hypotheses regarding the effect of non-selective inhibition of eNOS and nNOS by L-NAME, the UL of CA was significantly raised in both young and old rats

compared to the respective controls (Figure 39). In fact, in half of the young group, and the whole old group, an UL was not reached, despite increasing the ABP to the maximum possible value. This was seen for both gross CBF (Figure 37) and CoBF (Figure 38).

There are few studies in the literature which attempt to address the effect of NO at the UL, in either young or old subjects. However, Daneshtalab and Smeda (2010) assessed CBF in anaesthetised WKY SHRsp rats prior to stroke, using a Laser Doppler probe in the region of the MCA. They increased MABP via abdominal compression and PE infusion, and assessed CA. This was done before and during NOS inhibition with L-NAME (40 mg/kg, i.v.). Before L-NAME, CBF showed a trend to slightly increase up to an ABP of ~200mmHg, after which a large increase in CBF was seen. This 'control' UL before L-NAME was higher than the control UL reported in chapter 4, which may have been due to use of a rat strain that is predisposed to hypertension. When L-NAME was present, the trend for CBF to increase was reduced, and they were unable to raise the ABP using PE to a point at which the UL was reached, which agrees well with the current study. Interestingly, post-stroke rats lost the ability to autoregulate, showing almost linear increases in CBF with ABP, and no clear UL. This was unaffected by infusion of L-NAME, suggesting that the impairment of CA was possibly contributed to by a loss of basal NO-mediated tone.

Similar data has also been reported by Euser and Cipolla (2007), who studied the role of NO in the effect of pregnancy and preeclampsia on CA. They increased ABP using PE, and measured CBF using a Laser Doppler probe, in pregnant and non-pregnant rats, either with or without pre-treatment with L-NAME. In agreement with our study, NOS inhibition significantly increased the UL, such that breakthrough was not seen until ABPs >200mmHg, in both groups.

In terms of an explanation for the raised ULs and/or extended autoregulatory range, some evidence can be drawn from the study by Omar & Marshall (2010b) discussed above, in which L-NAME was infused to assess its effect on the CBF response to noradrenaline. In mature rats, CBF decreased with noradrenaline alone, but this was reduced to a non-significant decrease in the presence of L-NAME. It is possible that removal of a tonic influence of NO allowed an increased input from myogenic mechanisms and/or sympathetic vasoconstrictor fibres in response to the increased ABP, which could explain the results seen in the young rats in the current study. In middle-aged rats, L-NAME + noradrenaline produced a much larger increase in ABP, and an increase in CBF, with no associated change in CVC, indicating that the UL of autoregulation was exceeded. This is in contrast to a decrease in CBF seen with noradrenaline alone. This suggests that, in middle-aged rats, the sympathetic vasoconstrictor influence is decreased, potentially due to the concurrently observed decrease in innervation density, such that the tonic dilator influence of NO, on both ABP and carotid blood flow, helps to prevent autoregulatory breakthrough.

Alternatively, as discussed in 1.3.4.2 and 4.4.2, the work carried out by the research group of Talman and Dragon offers a different explanation. When they inhibited NOS with L-NA prior to increasing MABP with PE in anaesthetised rats, the UL was not reached even at ABPs of > 185mmHg. No increase in CBF was seen, and CVR was maintained at its maximum level, which agrees with the current results. In contrast, the rats that did not receive L-NA showed an increase in CBF, and a decrease in CVR, indicative of breakthrough. This indicated a dependence on NO at the UL, such that breakthrough did not occur when NOS was inhibited. They suggested that NO was responsible for the breakthrough of autoregulation at the UL i.e. that it is an active vasodilatation (Talman & Dragon, 1995). This agrees well with the

majority of the experiments in the current study, in which no increase in CBF, or decrease in CVR, was seen at maximal ABPs.

As discussed in 4.4.2, the changes seen in CVR at the UL are significant, as CVR falling prior to the increase in CBF, as well as in spite of ABP continuing to increase, could be taken to indicate an active, vasodilatory mechanism. The loss of this change in CVR in the majority of the current experiments, in both young and old, when NOS was inhibited, therefore strongly suggests that the potentially active increase in CBF above the UL is NO-mediated.

Further, Talman *et al* (2000) also showed that the proposed nitrergic innervation of the cerebral vasculature, which consists of fibres that originate from the parasympathetic pterygopalatine ganglion, and use NO as a neurotransmitter to induce cerebral vasodilatation (see 1.3.3.2), are also implicated at the UL. Bilateral sectioning of these parasympathetic nerves before ABP was increased using PE, resulted in attenuation of the increase in CBF, and decrease in CVR, at the UL, when compared with that seen in intact control animals. This offers further support for an active, NO-mediated vasodilatation beyond the UL, which may involve activation of such nitrergic nerves.

Regarding the effect of ageing on the role of NO in CA, the increase in the UL caused by NOS inhibition in the young rats, and the comparative increase in UL seen in the old animals, was approximately 20mmHg for both age groups. Therefore there does not appear to be any additional effect of ageing.

5.4.2 The role of nNOS-derived NO in CA and at the UL in young rats

5.4.2.1 Basal effect of nNOS inhibition

The nNOS inhibitors SMTC and 7-NI were used to assess the contribution of nNOS-mediated NO to basal CBF in young rats. SMTC caused significant increases in ABP and CVR, and a strong trend for CBF to decrease (although this was slightly, but significantly smaller than the change in CBF caused by L-NAME). 7-NI caused a significantly smaller increase in ABP (compared to SMTC and L-NAME), but significantly increased CVR and decreased CBF (Figure 40). These basal effects of SMTC and 7-NI were suggestive that NO derived from nNOS contributes significantly to NO-mediated cerebrovascular tone in young rats, as L-NAME, which non-selectively inhibits both eNOS and nNOS, did not have a consistently, significantly larger effect.

There is evidence in the literature to show that nNOS-derived NO is important in the control of basal vascular tone. For example, application of 7-NI has been shown to decrease basal CBF in both awake (Montecot *et al*, 1997) and anaesthetised rats (Hudetz *et al*, 1998). Gotoh *et al (*2001) investigated the increase in CBF caused by stimulation of the vibrissae in conscious rats. Administration of L-NAME or 7-NI caused a decrease in basal CBF, and also reduced the increase in CBF in response to stimulation. Hudetz *et al* (1998) used intravital microscopy to study the response of cerebral capillaries to hypoxia, and assessed the role of nNOS-derived NO in the response. Hypoxia increased red cell velocity (an index of CBF) by 34% in control rats. Pre-treatment with 7-NI reduced baseline red cell velocity by 12%, and reversed the response in hypoxia, to produce an 8% decrease in red cell velocity, indicating its importance in both basal CBF and the response to hypoxia.

Regarding SMTC, Seddon *et al* (2008), studied the effect of infusion of SMTC on basal forearm blood flow (FBF) in healthy subjects. SMTC caused a dose-dependent decrease in

basal FBF. Infusion of L-NMMA was able to produce similar decreases in FBF, but required a much higher dose to achieve it. In agreement with our data, these results suggest that nNOS-derived NO plays an important role in vascular tone. Further, Seddon *et al* showed that, when ACh was given to induce endothelium-dependent vasodilatation, only L-NMMA was effective in inhibiting the response, suggesting that eNOS-derived NO becomes more important in stimulated responses.

This lends support to our data showing the effect of ACh before and after SMTC or 7-NI (Figure 40). The control responses to ACh were not significantly different between the two drug groups, or in comparison to that seen in the young rats before L-NAME. In addition, the response to ACh was not reduced by 7-NI or SMTC, and in fact the increase in ABP seen during ACh+SMTC was significantly increased, agreeing with the lack of a role for nNOS-derived NO in ACh-stimulated vasodilatation.

5.4.2.2 CA and the autoregulatory UL after nNOS inhibition

Figures 41 and 42 show the effect of nNOS-specific inhibition by SMTC and 7-NI respectively, on the gross CBF and CVR autoregulatory curves in young rats. In contrast to our hypothesis, other than significantly reducing the basal CBF from which autoregulation occurred, inhibition of nNOS-derived NO slightly, but not significantly, increased the ULs compared to the control ULs (Figure 43). This suggests that nNOS-derived NO does not play a role in CA at the UL.

In terms of the literature, there is little evidence on the role of nNOS-derived NO at the UL. It has been shown that non-specific NOS inhibition by L-NNA, suffused directly onto the cortex for 105 minutes via a cranial window in rats, increases the LL of autoregulation. This effect was not seen when suffusion was only carried out for 35 minutes, suggesting that time was

required for diffusion to the source of the NO i.e. eNOS in the vascular wall (Jones *et al*, 1999), which agrees with the suggestion of the current data, that nNOS-derived NO plays little role in stimulated CBF responses, such as to ACh or increases in ABP.

Bauser-Heaton and Bohlen (2007) showed that when ABP was decreased, NO levels in Sprague-Dawley rat cerebral arterioles was increased *in vivo*. Inhibition of nNOS using N4S, an NMDA receptor antagonist, abolished this increase in NO, whereas it had no effect on flow-mediated dilatation, which is typically thought to be mediated by eNOS-derived NO. This suggested that nNOS was the dominant source of NO during hypotension i.e. near the LL. Further, the same group found that NO concentration, and vessel diameter, increased in rat cortical arterioles when periarteriolar pO_2 was reduced. When nNOS was inhibited, the previously seen increase in NO was reduced, supporting the idea that nNOS-derived NO plays a major role in increasing vessel diameter during decreases in ABP/pO_2.

However, similarly to the L-NAME data, half of the young rats from each group in the present study showed no breakthrough of autoregulation, despite increasing the ABP to the maximum possible value (maximum ABP data was included in the ULs for each group). Accordingly in these experiments, CVR increased as ABP increased, and remained significantly raised compared to baseline.

As mentioned above, Talman *et al* (2000) demonstrated that removal of the nitrergic innervation input to the cerebral vasculature attenuated, but did not abolish, the normal increase in CBF, and decrease in CVR, seen beyond the UL. This may offer an explanation for the current experiments were no UL was reached after nNOS inhibition, as activation of such nitrergic nerves, which presumably provide nNOS-derived NO to the cerebral vasculature, may play a partial role in the hypothesised active vasodilatation beyond the UL.

In addition, removal of a tonic, nNOS-mediated vasodilatory influence, may have uncovered an increased input from myogenic vasoconstriction and/or sympathetic vasoconstriction in response to increases in ABP, increasing the subsequent autoregulatory range towards the UL (Omar & Marshall (2010b), see 5.1.4.2).

As the effect of nNOS inhibition on the gross CBF ULs was not significant compared to control, this was not investigated further in Laser Speckle imaging experiments, or in old animals.

5.5 Conclusion

In contrast to our hypotheses, inhibition of nNOS-derived NO, by SMTC or 7-NI, did not significantly change the UL in young rats compared to that seen in control experiments (chapter 4). nNOS-derived NO was, however, shown to be important, if not the main vasodilatory input controlling basal CBF.

Inhibition of both eNOS and nNOS using L-NAME did have a greater effect than inhibition of nNOS alone on the UL in young rats. However, this was not in the direction we hypothesised, i.e. the UL was significantly raised, or not reached, compared to control. This may reflect an increase in the relative input by myogenic or sympathetic vasoconstriction, after removal of an NO-mediated tone. Alternatively, and in line with the CVR responses observed at the UL in the control experiments, and evidence from a body of work by Talman and Dragon, this may reflect that the increase in CBF beyond the UL is an active, NO-mediated dilatation. As discussed in 4.4.2, this may be a physiologically relevant, safety mechanism, dissipating the build-up of pressure and preventing potentially greater damage (ischaemic, or haemorrhagic) that may be caused by continuing to vasoconstrict in response to rising ABP.

NOS inhibition also increased the UL in old rats, despite evidence in the literature for age-related impairments in endothelium-dependent vasodilatation, and reduced NO bioavailability. However, if the hypothesis of CBF increasing above the UL as a protective mechanism is correct, the fact that the UL is raised in old rats under control conditions, and abolished in NOS inhibited experiments, in old rats, may actually put them at increased risk of cerebrovascular damage.

CHAPTER 6: THE ROLE OF CEREBROVASCULAR AUTONOMIC INNERVATION ON THE CEREBRAL AUTOREGULATORY UPPER LIMIT, AND CHANGES WITH AGEING

6.1 Introduction

6.1.1 The role of autonomic innervation in the control of CBF and CA

As discussed in 1.3.3, the cerebral circulation is known to be autonomically innervated. Sympathetic vasoconstrictor fibres from the superior cervical ganglion (SCG) have been shown to supply rich, unilateral innervation to the cerebral vessels (Arbab *et al*, 1986). They use noradrenaline as the main neurotransmitter, although the co-transmitter NPY has also been detected (Edvinsson *et al*, 1987). Parasympathetic vasodilator fibres arise primarily from the pterygopalatine ganglia (PPG, also known as the sphenopalatine ganglia), and are generally cholinergic (Walters *et al*, 1986). However the extent of the role of autonomic innervation in the control of CBF is controversial and is mostly accepted to be minimal.

6.1.1.2 The role of sympathetic innervation in the control of CBF and CA

Heistad *et al* (1978) performed sympathetic denervation at the level of the SCG in monkeys and cats, and found that it had no effect on basal CBF. Similarly, Sadoshima *et al* (1986) performed a bilateral sympathetic denervation at the SCG in anaesthetised WKY, and SH rats, and saw no change in basal ABP or CBF.

However, stimulation at the level of the SCG did significantly decrease CBF in monkeys, and during acute, severe hypertension, the effect of sympathetic stimulation was augmented in cats and dogs, protecting the BBB from disruption (Heistad *et al*, 1978).

In healthy human subjects, sympathetic ganglionic blockade with trimethaphan has been shown to decrease ABP, and decrease MCAv, as assessed using a Transcranial Doppler probe. When ABP was corrected by an infusion of PE, the decrease in MCAv was still seen, suggesting the existence of a sympathetically-mediated, tonic input to maintain basal CBF (Zhang *et al*, 2002).

Further, a study by Tuor (1992) demonstrated that stimulation of the SCG, during acute hypertension induced by angiotensin II, caused a rightward shift in the autoregulatory curve in anaesthetised rats. This had the effect of raising the UL and protecting the cerebral circulation against increases in pressure.

This supports the idea that sympathetic vasoconstriction may contribute to the apparently significant role of extracranial and large cerebral arteries in the maintenance of a constant CBF, and protection of more fragile, downstream arteries from exposure to higher pressures (Warnert *et al*, 2016).

Kontos *et al* (1978) showed that the large, cerebral surface vessels, between the Circle of Willis and the pial arteries, were almost solely responsible for the autoregulatory vasoconstriction seen between 120-160mmHg (see 4.4.2). The same group also found that vessels of this size were also responsive to cervical sympathetic stimulation and topical application of noradrenaline, in contrast to smaller pial arteries (Wei *et al,* 1975).

This concept of a sympathetically-mediated autoregulatory vasoconstriction is supported by a study by Cassaglia *et al* (2008), who measured sympathetic nerve activity in the SCG in anaesthetised lambs, during pharmacological or mechanical increases in arterial pressure. They saw that sympathetic nerve activity increased in response to large increases in ABP. However, when hypotension was induced by infusion of SNP, there was no associated change

in sympathetic nerve activity. This study therefore provided evidence for a vasoconstriction mediated by cerebral sympathetic innervation, which they hypothesised could contribute to the maintenance of a constant CBF during rises in ABP i.e. autoregulation. Regarding the role of sympathetic innervation at the UL, Sadoshima *et al* (1986) performed a bilateral sympathetic denervation in anaesthetised rats, and then infused PE i.v. to increase ABP. They found that the UL of CA was significantly lowered after removal of sympathetic input.

From these studies, sympathetic innervation may or may not play a role in determining basal cerebrovascular tone, but does appear to provide cerebral vasoconstriction that responds to, and protects the cerebral circulation against, rises in ABP, making it potentially important at the UL.

6.1.1.3 The role of parasympathetic innervation in the control of CBF and CA

There is limited evidence on the role of parasympathetic innervation in controlling CBF and CA. Ishii *et al* (2014) stimulated the lingual nerve to study parasympathetic cerebral vasodilatation, measured from the internal carotid artery using an ultrasonic flow probe, and the parietal cortex using Laser Speckle imaging. They observed an increase in internal carotid flow in response to stimulation, which was significantly reduced by ACh receptor antagonists. In terms of involvement in CA, Morita *et al* (1995) measured CoBF using a Laser Doppler probe over the parietal cortex, as ABP was decreased by controlled withdrawal of blood. This was carried out in sham and bilaterally parasympathetically denervated rats. The LL limit of CA was seen to be shifted to a higher ABP in the denervated rats, suggesting a role for parasympathetic innervation during decreases in ABP.

As well as the classical cholinergic, parasympathetic innervation, there is also evidence for non-adrenergic, non-cholinergic innervation of cerebral vasculature, that uses NO as its main

neurotransmitter (Okamura *et al*, 2002). Evidence for this includes the fact that the vasodilatation caused by transmural stimulation of the perivascular nerves in the walls of cerebral artery strips, can be inhibited by L-NMMA (Toda & Okamura 1990). As discussed in 1.3.4.1, it has been proposed that a source of these so called nitrergic nerves may be the PPG. Talman & Dragon (2000) transected the parasympathetic nerves projecting from the PPG in anaesthetised rats, and measured CoBF using a Laser Doppler probe over the parietal cortex. When they gave PE to gradually increase ABP, they found that parasympathetic denervation prevented the UL from being reached, suggesting that breakthrough of autoregulation is an active dilatation, which is dependent upon cerebral parasympathetic innervation. In conjunction with their previous work, which showed that NOS inhibition (Talman & Dragon 1995, see 1.3.4.2), and baroreflex disruption (Talman *et al*, 1994) also attenuated the UL, they hypothesised that release of NO from these parasympathetic nerves was therefore involved in the increase in CBF beyond the UL.

6.1.2 The effect of ageing on cerebral autonomic innervation

As discussed in 1.4.6.1, ageing has been shown to be associated with a decrease in noradrenergic (sympathetic) innervation density. For example a decrease has been seen on vessels in, and branching from, the circle of Willis in rats (Mione *et al*, 1988).

Omar & Marshall (2010b) have shown that glyoxylic acid staining for sympathetic innervation in cerebral arteries from rats, decreases with age, even by 42-44 weeks (see Figure 8). However, resting sympathetic nerve activity seems to be well maintained with ageing, or to even increase in humans (Iwase *et al*, 1991) and rats (Ito *et al*, 1986).

Decreases in adrenoreceptor density (Pan *et al*, 1986), and catecholamine content and release from nerve terminals have also been shown to occur with ageing (Daly *et al*, 1988). Further,

catecholamine synthesis, in common with NO synthesis, relies on the cofactor BH_4 which is known to be affected by age-related oxidative stress damage.

Changes in cholinergic innervation and receptor density appear to show regional differences with ageing. Accumulation of choline decreases by 25%, and ChAT increases by 187% in the major cerebral arteries of 22 month old rats, whilst the same markers in the small pial arteries revealed no age-related change (Hamel *et al*, 1990). Further, cholinergic muscarinic and nicotinic receptors were found to be decreased in the cortex, but increased in the thalamus with age (Nordberg *et al*, 1992).

Functionally, the implications for decreased sympathetic and parasympathetic function in ageing on CA and the UL, have not been widely studied. Hervonen *et al* (1990) measured the cortical CBF response to stimulation of cervical sympathetic trunks in adult (4-6 months) and aged (28-32 months) anaesthetised rats, and saw frequency-dependent changes in CBF, which were unaffected by age. However, Shiba *et al* (2009) similarly stimulated the cervical sympathetic trunks, and measured olfactory bulb blood flow. They saw that the decrease in flow caused by stimulation in aged rats (18-21 months), was attenuated compared to young rats (4-6 months).

Uchida *et al* (2000) stimulated an area of the basal forebrain rich in acetylcholine and ChAT and saw an increase in cortical CBF in both young adult rats (4-7 months) and old rats (24-25 months). However, in very old (32-42 months) rats, the response was significantly attenuated.

6.1.3 Aims and hypotheses

Considering the evidence for the role of cerebral autonomic innervation in the control of CBF, as well as the relative lack of specific investigation into its role in CA, this area warrants investigation. Further, as ageing has been shown to be associated with decreased autonomic innervation density and function, it is reasonable to expect that any role for such neural input in CA during adulthood, may be impaired in ageing.

Therefore the focus of this chapter was to investigate the effect of sympathetic and parasympathetic stimulation, and the effect of removal of sympathetic input on basal CBF, autoregulatory curves during increases in ABP, and on the UL. Further, the effect of ageing on these responses was investigated.

Our hypotheses were as follows:

- Unilateral stimulation of the SCG would cause a frequency-dependent decrease in ipsilateral CBF, demonstrating a sympathetically-mediated vasoconstriction. This would be inhibited by the α-adrenoreceptor antagonist phentolamine, indicating a role for sympathetic control of CBF in young rats.
- Unilateral SCG stimulation in old rats would cause a frequency-dependent decrease in CBF, which is reduced in magnitude compared to young rats, reflecting age-related decline in sympathetic input.
- Both uni- and bilateral sympathectomy (SympX) would increase basal (ipsilateral) CBF, indicating a basal sympathetic tone in young rats.
- Both uni- and bilateral SympX would decrease the UL in young rats, due to removal of tonic sympathetic input, as well as a reduced ability of the cerebral vessels to vasoconstrict in response to increases in ABP.

- SympX would have a reduced effect on the UL in old rats. Noradrenaline synthesis and vascular sympathetic innervation density would already be reduced with ageing, due to increased oxidative stress, and age-related decline in sympathetic input.
- Unilateral stimulation of the PPG would cause an increase in ipsilateral CBF in young rats, demonstrating a parasympathetically-mediated cerebral vasodilatation. The magnitude of this increase in CBF would be reduced in old compared to young rats, reflecting age-related alterations in parasympathetic input.

6.2 Methods

6.2.1 Surgery

Surgery was carried out as described in 2.2. Briefly, anaesthesia was induced with 4% isoflurane in O_2 at 4 L min^{-1}. The left jugular vein was cannulated, and isoflurane anaesthesia was withdrawn and gradually replaced with i.v. Alfaxan® bolus doses (0.1ml boluses at 5$mg.ml^{-1}$), and then a maintenance infusion dose of 17-30 $mg.kg^{-1}.hour^{-1}$. The trachea was cannulated with a custom-made stainless steel T-piece cannula, to maintain a patent airway and supply oxygen if necessary. The left brachial artery was cannulated to take samples for blood gas analysis. The left femoral artery and vein were cannulated to record arterial blood pressure (ABP) and heart rate (HR), and for drug infusion respectively. All cannulae were filled with heparinised saline. Bilaterally, the common carotid arteries were cleared distally up to their bifurcation. The external carotid, as well as occipital, facial and lingual branches were ligated, to achieve vascular isolation of the internal carotid artery and its distribution to the brain (as described by Thomas & Marshall, 1994). Blood flow was recorded through the common carotid arteries as an index of gross CBF, allowing for direct comparison between right (R) and left (L) CBF when performing surgical sympathectomy or stimulation.

6.2.1.1 Sympathetic stimulation and sympathectomy

The vascular isolation of the carotid artery was carried out at the level of the SCG; after the facial and lingual branches of the common carotid artery were isolated and ligated, they were carefully cut to free the common carotid artery for lateral retraction. This allowed visualisation of the SCG, which lies on top of the carotid bifurcation. The internal carotid artery was identified and the SCG was carefully dissected free of its borders with the common and internal carotid arteries. A suture was threaded around the SCG to allow for easy access

later in the protocol. This approach was developed with guidance from the study by Savastano *et al* (2010).

6.2.1.2 Parasympathetic stimulation

For parasympathetic stimulation, the right PPG was isolated using a supraorbital surgical approach, guided by a study by Talman *et al* (2007). Briefly, an incision was made over the zygomatic arch to expose the bone. A small length of the bone was removed, and the masseter muscle and lacrimal glands were retracted, enabling location of the trigeminal nerve, which was also retracted or sectioned. The PPG could be located just behind the maxillary arm of the trigeminal nerve, allowing placement of electrodes around the ganglion.

6.2.2 Stabilisation

Before the experiment began, equilibration was allowed until all variables were stable. A 20-min period of baseline was recorded, and blood gas samples were taken to check P_aO_2, P_aCO_2 and pH values. Blood samples were then taken periodically throughout the stimulation protocols, and after administration of each drug. If the blood gas values deviated from the mean, or breathing appeared laboured, the airway was aspirated. If P_aO_2 fell below the mean, supplemental O_2 was given. Close attention was paid to P_aCO_2 levels, due to high sensitivity of the cerebral circulation to changes in CO_2 (Willie *et al*, 2012). If P_aCO_2 levels rose above 45mmHg and could not be corrected, the data was discarded.

6.2.3 Experimental protocol

6.2.3.1 Sympathetic stimulation

Stimulation of the SCG was used to assess the role of sympathetic innervation in the control of cerebral vascular tone. In n=7 young (328±10g), and n=9 old (733±25g) rats, electrodes,

handmade using Teflon-insulated, 0.125mm annealed silver wire (Advent Ltd), within PP10 polyethylene tubing (Portex), were placed around the right SCG, so that the exposed tips were in contact with the ganglion, but not with each other. The SCG was then stimulated at 1, 3, 5, 10, 30 and 50Hz for 5 seconds, at between 1-2V, using the PowerLab stimulator panel, and the effects on (R and/or L) CBF and CVR, ABP and HR were recorded. In n=4 of these young rats, and all of the old rats, this was repeated after 10mg.kg^{-1} i.v. phentolamine (non-selective α-adrenergic antagonist), to assess the involvement of α-adrenoreceptor-mediated signalling pathways, i.e. sympathetic innervation.

6.2.3.2 Unilateral sympathectomy

Sympathectomy was used to assess the role of sympathetic innervation in both basal cerebral vascular tone, and at the UL of autoregulation. In n=8 young rats (327±9g), after recording of baseline parameters (R and L MCBF, MCVR, MABP, HR), flow probes (and other equipment if necessary) were removed to allow access to the SCG. Unilateral sympathectomy (uni sympX) was performed by isolating the R SCG away from surrounding vessels with forceps, guided by the previously placed suture, before carefully cutting though the structure. It was ensured that no nerve connections remained before replacing the flow probes and recording the effect of unilateral sympathectomy on the various parameters at baseline, and then during PE infusion (0.1-200μg.kg^{-1}.min^{-1}) to reach the UL.

6.2.3.3 Bilateral sympathectomy

The bilateral sympathectomy protocol was carried out as detailed above (section 2.2.2) in n=9 young (314±9g) and n=10 (804±34g) old rats, except both the R and L SCG were sectioned in randomised order.

6.2.3.4 Parasympathetic stimulation

Stimulation of the PPG was used to assess the role of parasympathetic innervation in the control of cerebral vascular tone. In n=7 young (311±6g), and n=8 old (875±56g) rats, electrodes, handmade using Teflon-insulated, 0.125mm annealed silver wire (Advent Ltd), within PP10 polyethylene tubing (Portex), were placed around the right PPG, so that the exposed tips were in contact with the ganglion, but not with each other. The PPG was then stimulated at 3, 10, 30 and 60Hz, at 2-4V, for 90 seconds (Suzuki *et al*, 1990), using the PowerLab stimulator panel, and the effects on R MCBF and MCVC, MABP and HR were recorded. This was repeated after 10mg.kg^{-1} i.v. L-NAME, to assess the involvement of NO in mediating parasympathetic vasodilatation.

6.2.4 Data analysis

Data were analysed as described in 2.7. Briefly, 60 second sections of LabChart data representing the baseline, the response to each drug or intervention (e.g. SympX), the baseline just prior to the start of the PE infusion, and the final minute of the response to each PE infusion step, were exported as a mean value for each variable, and opened in Excel for further analysis. Sympathetic stimulation at each frequency only lasted for 5 seconds, and so the whole 5 seconds of data was exported for each response. Parasympathetic stimulation was carried out for 90 seconds at each frequency, and so the final 60 seconds of each response was exported.

6.2.5 Calculation of the UL

Autoregulatory curves were generated by plotting mean CBF, against MABP at each PE dose. Dual-line linear regression analysis (described by Samsel & Schumacker, 1988, and used previously in our laboratory by Edmunds & Marshall, 2001) was used to calculate the

autoregulatory UL. The UL for each animal was defined as the intersection of the two regression lines with the best fit and the smallest standard deviation of residuals. A group mean UL was then calculated from the individual values. See 2.7.3 for more details.

6.2.6 Statistical analyses

All data are presented as the mean ± SEM. Graphs and statistics were generated using GraphPad Prism® 5. Data were analysed using paired or unpaired t-tests, and one-way or two-way (repeated measures as appropriate) ANOVAs with post-hoc Bonferroni or Dunnett's. $P<0.05$ was taken as significant.

6.3 Results

6.3.1 Baseline characteristics

Table 6 shows the baseline characteristics of the young and old rats. This is a combination of data from the sympathetic stimulation, bi sympX and parasympathetic stimulation experiments. These are presented together as HR and blood gas data was not collected for every experiment. There was no significant difference in basal MABP, or blood gas data between the young and old rats, but HR was significantly lower in the old rats. Similarly to the control and NOS inhibition groups, the old rats were significantly heavier than the young rats (see Table 6), and had a higher absolute CBF (1.9±0.1 vs 2.9±0.2 ml·min^{-1}, unpaired t-test; P<0.0001), which became significantly lower when corrected for body weight.

One-way ANOVAs, with post-hoc Bonferroni tests to assess the changes in the parameters between each stimulation frequency, showed that, in both young and old rats, sympathetic stimulation had no significant effect on MABP (one-way ANOVAs; F ratio=0.6, P=0.8, and F ratio=0.3, P=0.9 respectively) or HR (one-way ANOVAs; F ratio=1.3, P=0.3 and F ratio=1.5, P=0.2 respectively). Therefore these data are not shown.

6.3.2 Sympathetic stimulation

Figure 44 shows the effect of stimulation of the ipsilateral SCG on R MCBF, as absolute data in a) n=7 young rats, and b) n=9 old rats. For both age groups, absolute CBF showed a graded decrease in response to stimulation of increasing frequency. The absolute MCBF seen at each frequency was significantly different to baseline for the young rats. For old rats, the same was true except for the stimulation at 1Hz, which was not significantly different to baseline (repeated measures ANOVAs; P<0.0001, with post-hoc Dunnett's).

In n=4 young animals, LCBF was recorded simultaneously (data not shown). There was no clear pattern of response in absolute L MCBF to contralateral SCG stimulation at any frequency (repeated measures ANOVA with post-hoc Dunnett's test: P=0.16), although when plotted as Δ L MCBF, there was a trend for a small, but non-significant, graded response.

In n=5 of the young, and all of the old rats, the stimulation protocol was repeated in the presence of phentolamine. Figure 45 shows the effect of phentolamine on baseline MABP, HR, CBF and CVR, as the difference between the baseline and the phentolamine value. In young rats, the basal CBF was significantly decreased by phentolamine (paired t-test, P=0.001 (a)). CVR was decreased, however this was not significant (paired t-test, P=0.2 (b)). MABP was significantly decreased compared to baseline (paired t-test, P=0.003 (c)), but there was no significant effect on HR (paired t-test, P=0.7 (d)). In old rats, the basal CBF was significantly decreased by phentolamine (paired t-test, P<0.0001 (a)), as was CVR (paired t-test, P=0.03 (b)) and MABP, compared to baseline (paired t-test, P=0.0001 (c)), but there was no significant effect on HR (paired t-test, P=0.1 (d)). There were no significant differences in the effect of phentolamine between the young and old rats.

Two-way ANOVAs were used to assess the effect of stimulation frequency, and phentolamine or age, on CBF, and any interaction between the two. Figure 46 a) shows that, in young rats, stimulation frequency had a significant effect on the Δ CBF (P=0.003) phentolamine significantly reduced the effect of stimulation upon the Δ CBF (P<0.0001), and there was no interaction between stimulation frequency and phentolamine (P=0.4), i.e. there was still a trend towards a frequency-dependent effect of stimulation on CBF in the presence of phentolamine. Figure 46 b) shows that, in old rats, stimulation frequency had a significant effect on the Δ CBF (P=0.005). Phentolamine significantly reduced the effect of stimulation upon the Δ CBF (P<0.0001). There was no interaction between stimulation frequency and

phentolamine (P=0.2). However, no frequency-dependent trend for CBF to decrease was apparent after phentolamine in the old rats. When a two-way ANOVA was used to compare the Δ CBF in young vs old rats, there was a significant effect of frequency on the Δ CBF (P=0.0005). Age significantly decreased the effect of stimulation on the Δ CBF (P=0.04), but there was no interaction between the two (P=0.9), i.e. there was still a significant effect of frequency in both the young and old rats.

Δ CVR showed an inverse relationship to the Δ CBF. In young rats, there was a frequency-dependent increase in CVR in response to stimulation (two-way ANOVA; P= 0.003, data not shown). Phentolamine significantly decreased the CVR response to stimulation (P=0.006), but there was no interaction between the two factors (P=0.3), indicating that a frequency-dependent relationship was still apparent in the presence of phentolamine. In old rats, the pattern of CVR responses was similar. There was a trend for a frequency-dependent increase in response to stimulation (P=0.06). Phentolamine significantly decreased the response to stimulation (P=0.0003), and there was no interaction between the two factors (P=0.9).

As a non-significant trend for a frequency-dependent effect of stimulation was maintained after phentolamine in young rats, but not old rats, this was investigated further by analysing the proportion of the CBF response to stimulation that was lost after phentolamine. Figure 47 shows the magnitude of the phentolamine-dependent response, expressed as a % of the control response. A two-way ANOVA showed no significant effect of frequency (P=0.5), but did show a significant effect of age (P<0.0001), reflecting fact that the old rats consistently lost a larger proportion of their response to phentolamine. There was no interaction between frequency and age (P=0.4).

6.3.3 Unilateral sympathectomy

8 young animals underwent a unilateral sympathectomy (uni sympX) at the level of the right SCG. Figure 48 shows the effect on baseline R and L MCBF (a) and CVR (b). There was no significant difference between R and L MCBF or CVR at baseline. Right uni sympX significantly increased R CBF, but had no effect on L CBF (one-way repeated measures ANOVA with post-hoc Bonferroni; $P<0.0001$ (a)). This correlated with a corresponding significant decrease in R CVR after uni sympX, but no change in L CVR (one-way repeated measures ANOVA with post-hoc Bonferroni; $P<0.0001$ (b)). There was no effect of uni sympX on MABP or HR (paired t-tests vs baseline, data not shown).

After the effects on basal parameters were recorded, the effect of uni sympX on the UL of autoregulation was investigated (n=7). Figure 49 a) shows the group mean autoregulatory curve (R MCBF vs MABP) generated after uni sympX. Figure 49 b) shows the correlating changes in CVR, which reached a maximum value significantly higher than baseline (unpaired t-test; $P=0.005$). The mean UL after uni sympX (indicated by the black dashed line) was slightly, but not significantly higher vs the control UL (174±2mmHg vs 168±2mmHg, unpaired t-test; $P=0.06$). Beyond the UL, CVR fell and CBF increased, but not significantly vs. baseline or the maximum CVR respectively. Interestingly, L MCBF, L MCVR and the L UL data was almost identical to that seen on the right, despite the uni sympX being carried out on the right only (data not shown).

6.3.4 Bilateral sympathectomy

In n=9 young and n=10 old rats, the sympathectomy protocol was repeated as in the above experiments, however both the R and L SCG were cut (in randomised order), resulting in a bilateral sympathectomy (bi sympX). Figure 50 shows the effect on baseline R MCBF and

CVR. Bi sympX tended to increase CBF, and decrease CVR in both young and old rats. A one-way ANOVA gave a P value of 0.004, however the post-hoc Bonferroni did not reveal any significant differences between the baseline and sympX values. There was no significant effect of bi sympX on MABP or HR in young or old rats (paired t-tests vs baseline, data not shown).

The effect of bi sympX on the autoregulatory UL was then investigated in n=7 young rats, and n=9 old rats. Figure 51 a) shows the group R MCBF vs MABP autoregulatory curve, and b) the R MCVR response generated after bi sympX in young rats. As MABP was increased, R MCVR increased significantly (unpaired t-test; $P<0.0001$), and R MCBF tended to decrease. The mean UL after bi sympX was significantly increased to 178±3mmHg (unpaired t-test; $P=0.01$ vs control UL). Figure 51 c) shows the group R MCBF vs MABP autoregulatory curve, and d) the R MCVR response generated after bi sympX in n=4 old rats. As MABP was increased, R MCVR increased significantly (unpaired t-test; $P<0.0001$), and R MCBF tended to decrease. The mean UL after bi sympX was significantly increased to 190±3mmHg (unpaired t-test; $P=0.03$ vs control UL). In n=5 rats, no UL was reached, even at the maximum achievable ABP of 194±3mmHg.

Figure 52 shows the ULs generated after uni- and bilateral sympathectomy, in young and old rats, as well as the relevant control ULs (Chapter 4) for reference. The ULs were 168±2, 174±2, 178±3, 180±3 and 190±3mmHg respectively. A one-way ANOVA gave $P<0.0001$, however a post-hoc Bonferroni only found a significant difference between the young and old control ULs.

6.3.5 Parasympathetic stimulation

General observation of the parasympathetic stimulation data shows that young rats displayed a clear, frequency-dependent, graded increase in CBF. In contrast, the old rats reached a maximum increase in CBF at 10Hz, before the response decreased. L-NAME significantly reduced the CBF and CVC responses, but had no effect on ABP in young rats. In old rats, L-NAME significantly reduced the CBF response, but had no effect on CVC. There was a trend for the ABP response to be reduced (P=0.08).

Figures 53 a & b) show the Δ CBF, c & d) the Δ CVC, and e & f) the Δ MABP caused by parasympathetic stimulation of the PPG, before and after infusion of L-NAME, in both young and old rats. CVC was used here rather than CVR, due to its better representation of a vasodilatation. Plotting CVR would produce the inverse of the CVC graphs. The basal effects of L-NAME were not shown here, as they are already described in detail in Chapter 5.

Two-way ANOVAs were used to assess the effect of stimulation frequency, and L-NAME or age, on CBF, and any interaction between the two. Figure 53 a) shows that, in young rats, PPS stimulation increased CBF, with the increasing stimulation frequency having a significant effect on the Δ CBF ($P<0.0001$). L-NAME significantly reduced the effect of stimulation upon the Δ CBF (P=0.0001). There was no interaction between stimulation frequency and L-NAME (P=0.08).

Figure 53 b) shows that PPG stimulation also increases CBF in old rats, and that increasing stimulation frequency had a significant effect on the Δ CBF ($P<0.0001$), although this was not graded in the same way as the response seen in the young rats. L-NAME significantly reduced the effect of stimulation upon the Δ CBF (P=0.0025), and there was a significant interaction

between stimulation frequency and L-NAME (P=0.005), indicating that the frequency-dependent response was lost in old rats after L-NAME.

Figure 53 c) shows that, in young rats, CVC showed a similar pattern of responses as seen for CBF. Frequency (P<0.0001) and L-NAME (P<0.0001) had significant effects, whereas there was no interaction (P=0.09). In contrast, in Figure 53 d), old rats showed a significant effect of frequency (P=0.001), but not of L-NAME (P=0.5), and there was a significant interaction (P=0.003). Figures 53 d) and e) both showed a significant effect of frequency on ABP (P=0.02, P<0.0001), but no significant effect of L-NAME (P=0.2, P=0.08) or interaction (P=0.5, P=0.7), for young or old respectively. Additionally, two-way ANOVAs to assess the effects of frequency and age, revealed a significant effect of age on the ΔCVC (P=0.04) and ΔABP (P=0.03), but not on ΔCBF (P=0.6).

Mean ± SEM	Young (n=24)	Old (n=25)	P value (unpaired t-test)
Body weight	319±9	818±30	<0.0001*
MABP	122±2	128±3	0.09
HR	422±7	389±7	0.002*
P_aO_2 (mmHg)	71±1	74±2	0.15
P_aCO_2 (mmHg)	41±1	40±1	0.7
pH	7.42±0.01	744±0.01	0.3
HCT (%)	37±0.8	37±0.8	0.8

Table 6: Baseline characteristics of young (n=24) and old (n=25) male Wistar rats in the autonomic stimulation and bilateral sympathectomy groups. Old rats were significantly heavier, and had a significantly lower HR. MABP, P_aO_2, P_aCO_2, pH and HCT were not significantly different between the 2 groups.

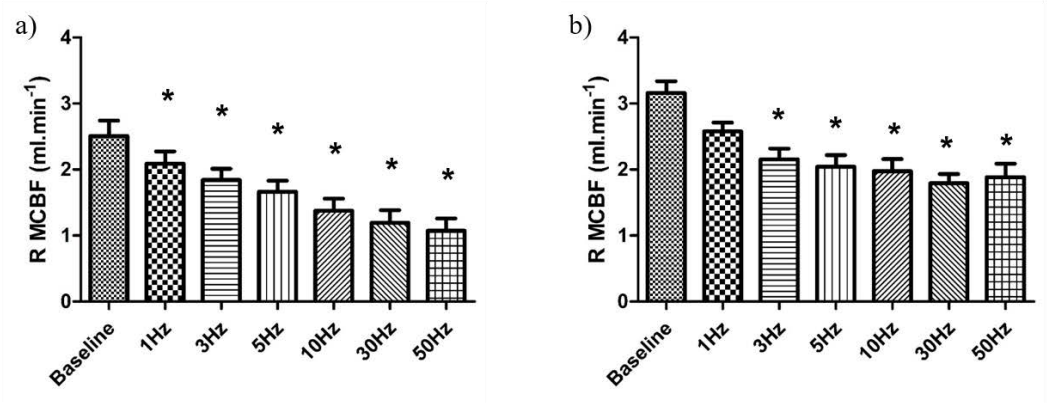

Figure 44: The absolute R MCBF response to ipsilateral SCG stimulation of increasing frequency in a) young and b) old rats. CBF decreased in a frequency-dependent manner in both young and old rats, although the response in the old rats was less clearly graded. Repeated measures ANOVAs; P<0.0001, post-hoc Dunnett's; * = significant difference vs the relevant baseline.

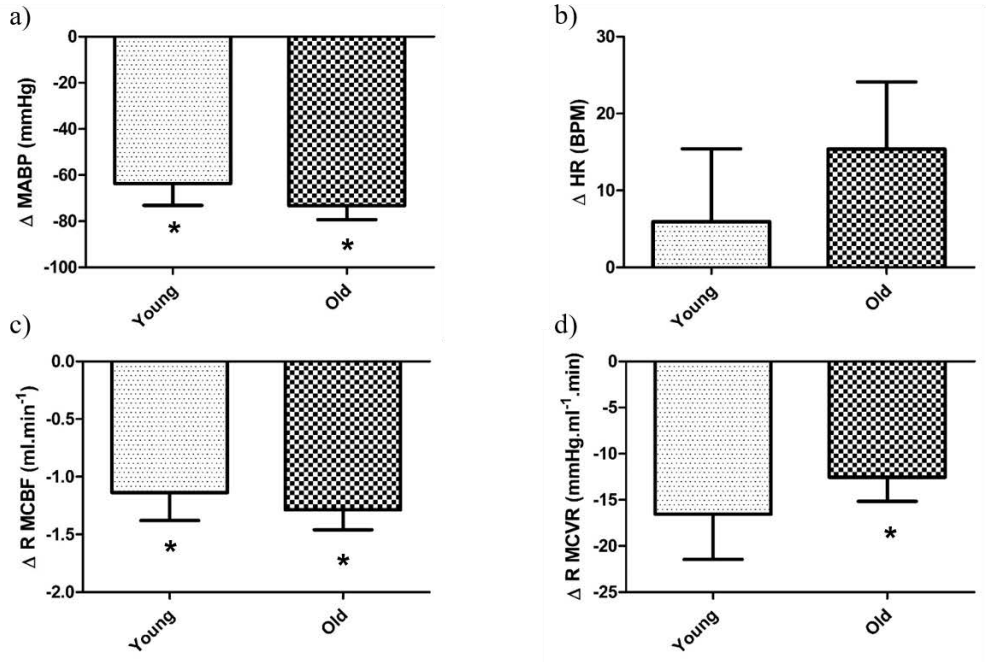

Figure 45: The effect of phentolamine on baseline a) MABP, b) HR, c) R MCBF and d) R MCVR, in young and old rats, shown as the change from baseline. Phentolamine significantly decreased ABP and CBF in both young and old rats. It also tended to increase HR and decrease CVR, with the latter being significant in the old rats. Paired t-tests; * = significant difference vs baseline.

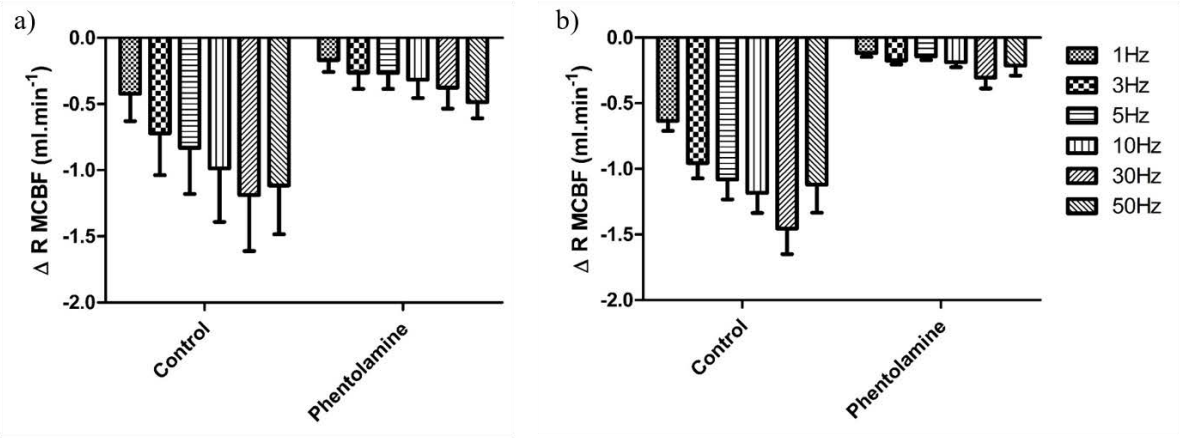

Figure 46: The change in CBF (from baseline) with SCG stimulation in a) young and b) old rats, before and after phentolamine. Two-way ANOVAs: significant frequency-dependent decrease in CBF in both young (P=0.003) and old (P=0.005) rats, and a significant effect of phentolamine on the response in stimulation in both young and old (P<0.0001) rats. There was no interaction between frequency and phentolamine in young (P=0.4) or old rats (P=0.2).

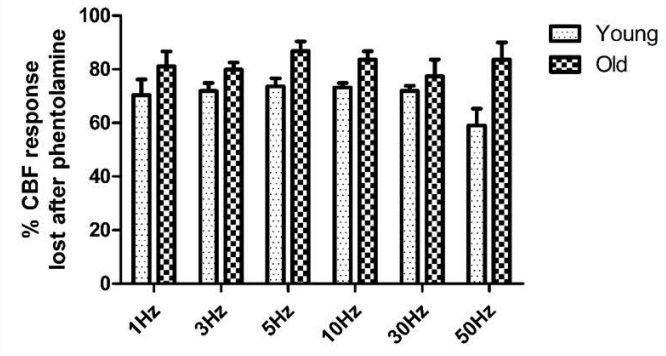

Figure 47: The reduction in the CBF response to SCG stimulation caused by phentolamine, plotted as a % of the control response in young and old rats. A two-way ANOVA showed there was no significant effect of frequency on the % CBF response (P=0.5), but there was a significant effect of age (P<0.0001). There was no interaction between frequency and age (P=0.4).

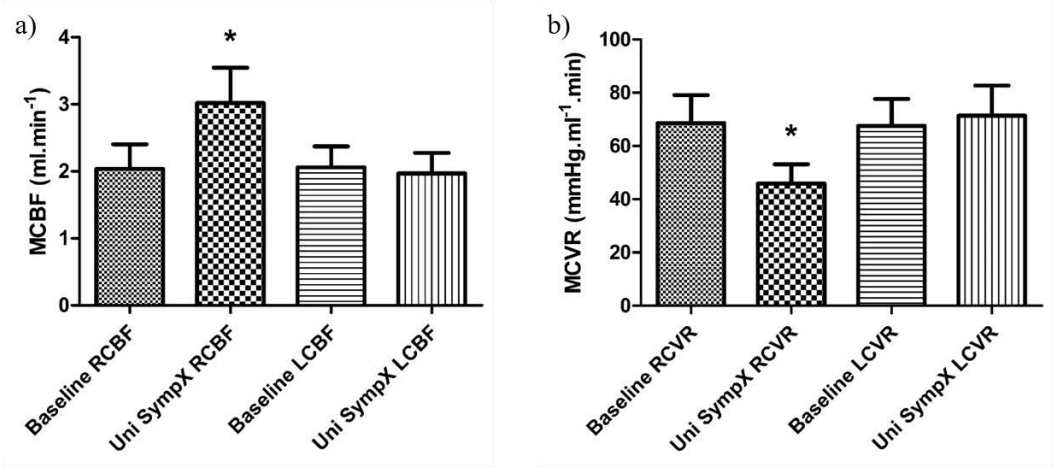

Figure 48: The basal effects of a right, unilateral sympathectomy, on a) R and L MCBF and b) MCVR. R MCBF significantly increased, but there was no change in L MCBF (repeated measures ANOVA; $P < 0.0001$, with post-hoc Bonferroni; *). R MCVR significantly decreased, but there was no change in L MCVR (repeated measures ANOVA; $P<0.0001$, with post-hoc Bonferroni; *).

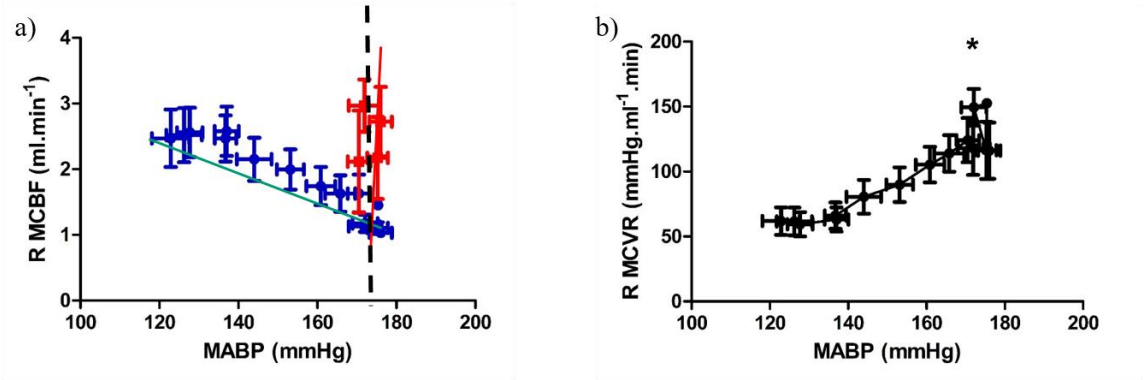

Figure 49: a) shows the R MCBF vs MABP autoregulatory curve and b) the corresponding changes in R MCVR, generated after right unilateral sympathectomy. The UL was 174±2mmHg, which was not significantly different to the control UL of 168±2mmHg (unpaired t-test; $P=0.06$). * = maximum CVR significantly higher than baseline (unpaired t-test; $P=0.005$).

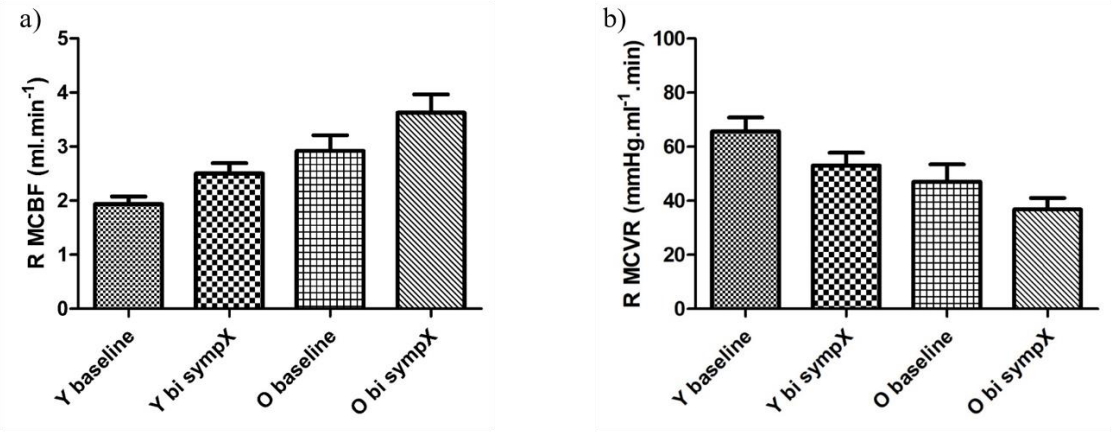

Figure 50: The basal effects of a bilateral sympathectomy, on a) right MCBF and b) right MCVR, in young (Y) and old (O) rats. RCBF increased from baseline, in both Y and O rats (one-way ANOVA; P =0.0004). RCVR decreased from baseline, in both Y and O rats (one-way ANOVA; P=0.004). Post-hoc Bonferroni revealed no significant difference between the individual columns.

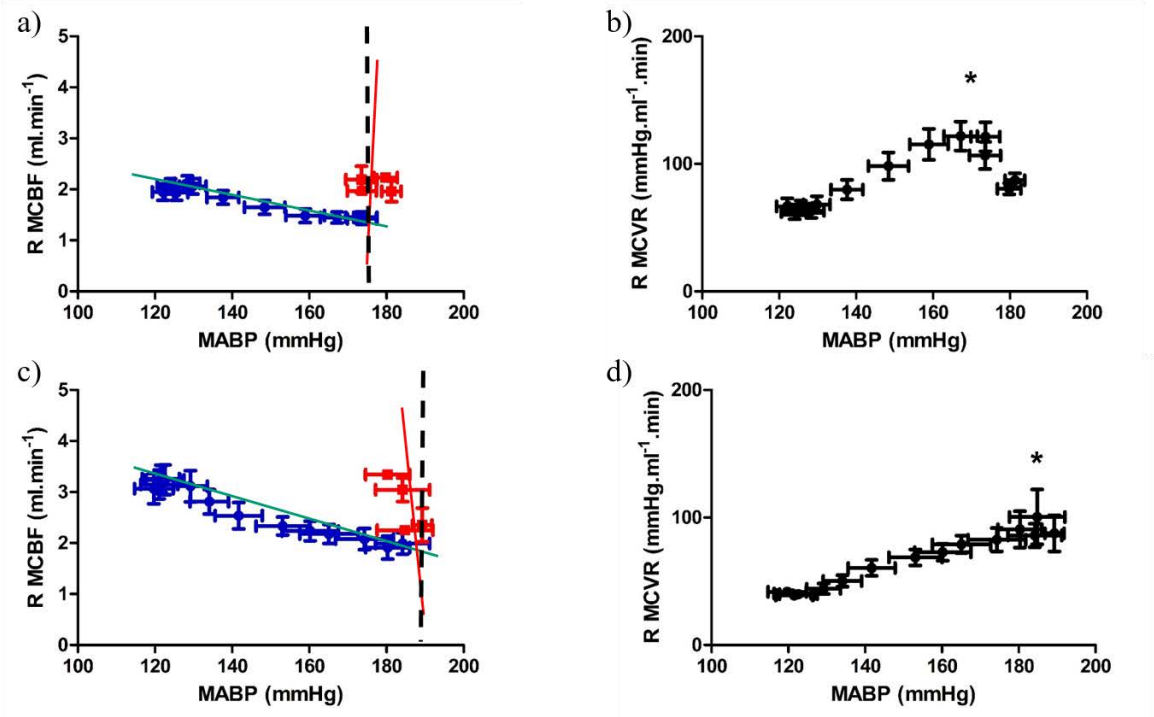

Figure 51: a) shows the R MCBF vs MABP autoregulatory curve and b) the corresponding changes in R MCVR in young rats after bilateral sympathectomy. c) and d) shows the equivalent graphs for the old rats. The UL for the young rats was 178±3mmHg, and for the old rats was 190±3mmHg. In n=5 of the old rats, no UL was seen. Unpaired t-test; * = maximum CVR significantly higher than baseline (P<0.0001).

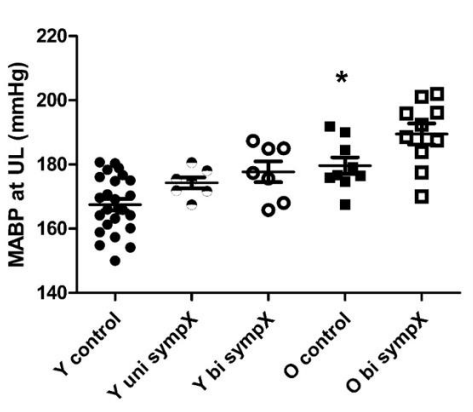

Figure 52: The ULs generated after uni- and bilateral sympathectomy, in young (Y) and old (O) rats. The control ULs (Chapter 4) have been added for reference. The ULs were 168±2, 174±2, 178±3, 180±3 and 190±3mmHg respectively. One-way ANOVA; P<0.0001, post-hoc Bonferroni; * = significantly different from relative control.

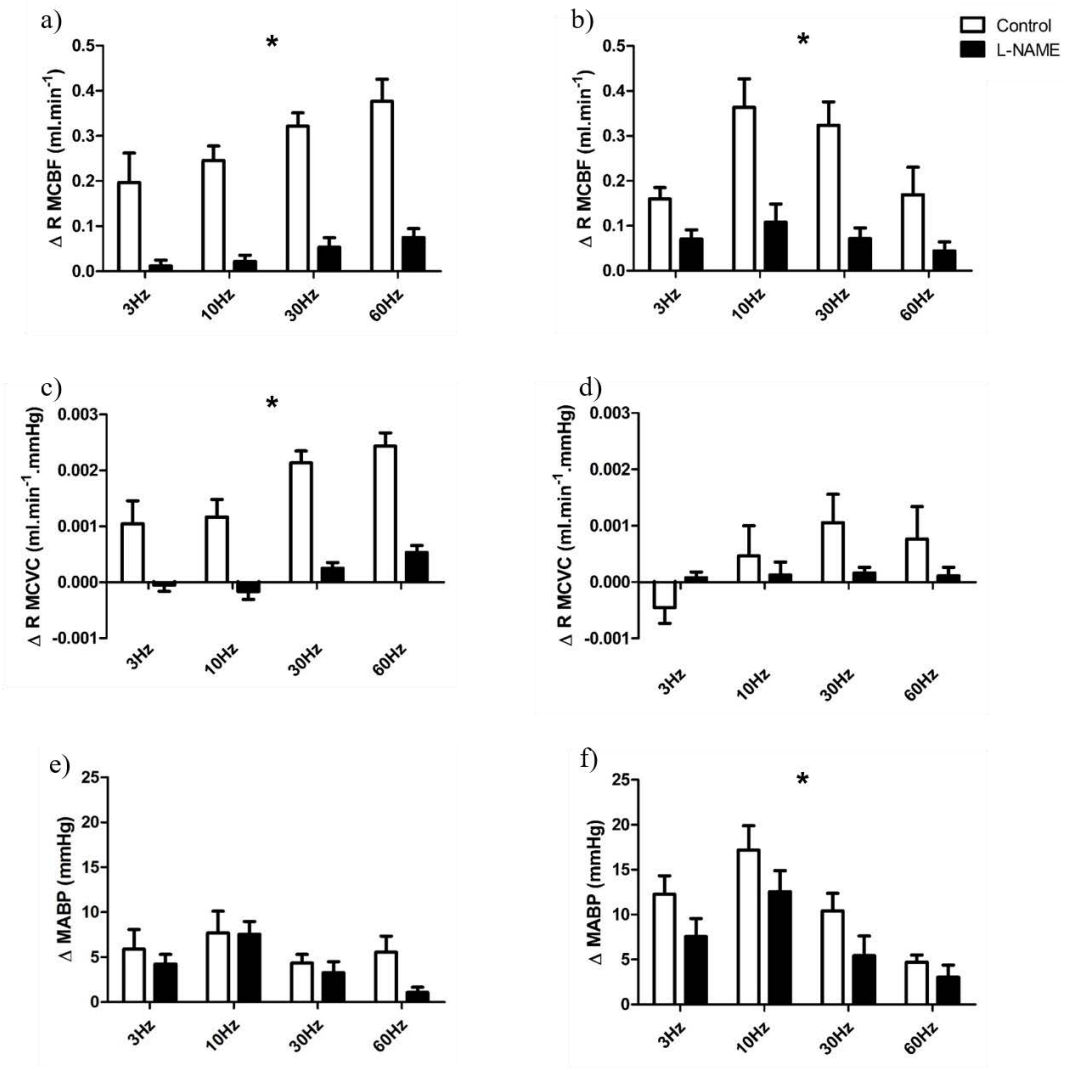

Figure 53: The effect of stimulation of the pterygopalatine ganglion on a & b) CBF, c & d) CVC and e & f) ABP, before and after L-NAME, in young (left column) vs old (right column) rats. Young rats showed a graded increase in CBF and CVC, with no significant changes in ABP. Old rats showed a reduced CBF and CVC response, which was associated with significant changes in ABP. L-NAME significantly reduced the CBF and CVC response in young, and the CBF and ABP response in old (two-way ANOVAs; *. See results).

6.4 Discussion

6.4.1 The effect of sympathetic stimulation on CBF and changes with ageing

When the SCG was electrically stimulated in rats in the current study, there was a frequency-dependent decrease in CBF seen in both young and old rats, suggesting that the sympathetic innervation of the cerebral vessels can contribute to the control of cerebrovascular tone, and is unaffected by age. This agrees well with some studies in the literature, such as Heistad *et al* (1978), who also showed a decrease in basal CBF in response to SCG stimulation. Further, the decrease in CBF was only seen ipsilaterally, agreeing with evidence to suggest that the pattern of innervation is mainly ipsilateral (Arbab *et al*, 1986). However the response in old rats did not become significant until a higher frequency stimulation, suggesting a possible decrease in sensitivity to sympathetic stimulation with ageing.

Phentolamine was given to assess the role of α-adrenoreceptor transmission in the effects of sympathetic stimulation. Basally, phentolamine caused a significant decrease in MABP and CVR in both young and old rats, in agreement with removal of a tonic vasoconstriction that may contribute to regulation of ABP. However, CBF also significantly decreased, when an increase in CBF might have been expected (e.g. as seen by Edvinsson *et al*, 1978). The reason for this could be that the decrease in ABP was sufficient to surpass the LL of CA, or that CA is actually more pressure-passive than the traditional models propose. There was no significant difference in the effects of phentolamine between the young and old rats, suggesting that basal sympathetic input was not affected by ageing.

The change in CBF in response to stimulation after phentolamine was significantly reduced in both young and old rats, such that in old rats, the frequency-dependent pattern of response was no longer apparent. In contrast, there was still a graded, frequency-dependent decrease in CBF in the young rats. Further analysis of this, by looking at the percentage of the CBF

response to stimulation that was lost in the presence of phentolamine, revealed that there was a larger effect of phentolamine on the responses in the old rats. Macarthur *et al* (2007) found that increased oxidative stress associated with the SHR strain, caused a decrease in NO bioavailability, which in turn caused an attenuation of the normal negative modulation of noradrenaline release by NO. This led to an increase in noradrenaline spill over, and a relative decrease in the contribution of the co-transmitter NPY. It may be the case that, in our old rats, an increase in oxidative stress has diminished the NO-mediated regulation of noradrenaline release, and reduced the NPY contribution, therefore increasing the effect of phentolamine on the CBF response to sympathetic stimulation.

Macarthur *et al* acutely applied the antioxidant N-acetylcysteine (NAC) to their mesenteric artery preparation from SHRs, and observed a decrease in noradrenaline release, and increase in NPY release. This effect of NAC was reversed by L-NAME, confirming that the mechanism of action by which noradrenaline release was increased, was via increasing NO bioavailability.

In order to address this, we carried out a mini study in which stimulation of the SCG was carried out in old rats, before and after administration of NAC (150mg.kg^{-1} i.p., n=3). NAC caused a ~20mmHg decrease in MABP, a ~0.9ml·min^{-1} decrease in CBF, and a ~5mmHg·ml^{-1}·min increase in CVR. However none of these changes were significant. When stimulation was repeated in the presence of NAC, a two-way ANOVA revealed a significant effect of NAC on the graded CBF response. The frequency dependence of the control responses were lost, and the magnitude of the decreases in CBF to stimulation were increased compared to those seen in the presence of phentolamine. This did not reach significance, but could be an area for future research.

6.4.2 The effect of sympathectomy on CBF, CA and the UL

Unilateral and bilateral sympathectomies (uni/bi sympX) at the level of the SCG were carried out in young rats. Uni sympX significantly increased baseline CBF and decreased CVR, only on the ipsilateral side. This agrees again with the finding of SCG stimulation only changed CBF on the ipsilateral side, and reports in the literature that the cerebral sympathetic innervation pattern was primarily ipsilateral. A basal effect of sympX is not widely reported in the literature. James *et al* (1969) sectioned the cervical sympathetic nerve in anaesthetised baboons, and saw an increase in CBF. However several other papers have reported that sympX has no effect at baseline (e.g. Heistad *et al* (1978), Sadoshima *et al* (1986)). However the data in the current study suggests that there is a sympathetically-mediated, basal cerebrovascular tone.

When PE was infused to assess the UL after uni sympX, a negative slope was seen during the plateau phase, such that CBF decreased as ABP increased. This may reflect the loss of the input that helps to maintain CBF when ABP increases, agreeing with the findings by Cassaglia *et al* (2008) that sympathetic nerve activity increases as ABP rises. Therefore, the large vasoconstriction seen in the absence of sympathetic input could be reflective of an increased contribution of the myogenic response.

The increase in CBF at the UL appears to be a steeper slope than that seen in the control experiments (chapter 4), although CBF did not increase significantly above the baseline value. The CVR response towards the UL also appears to be different to the control responses, in the absence of sympathetic input. A well-defined pattern of CVR falling before CBF increased at the UL was seen in chapters 4 and 5, which had added to the hypothesis of the increase in CBF being an active dilatation. Here, CVR continues to increase up to the UL. These

observations suggest that sympathetic nerve activity may therefore also play a role in this hypothesised, safety pressure release mechanism (see 4.4.2).

Bilateral sympX, which was carried out in both young and old rats, showed a similar pattern of basal effects as uni sympX, although they did not achieve significance when analysed using a one-way ANOVA.

When PE was infused to assess the UL after bilateral sympX, similar to uni sympX, a decrease in CBF was seen during the plateau phase of autoregulation. The increase in CBF above the UL was small, and typically did not reach above the baseline value. In fact, in half of the old rats, autoregulatory breakthrough was not seen, even when ABP was increased to the maximum possible value. Further, particularly in the old rats, the CVR response also appeared different to control, with CVR falling at, or above the UL, rather than preceding it.

When the ULs or top ABP achieved were compared for each group (young control, young uni sympX, young bi sympX, old control and old bi sympX), there was a trend for the UL to increase, graded with the 'severity' of the experimental condition (one-way ANOVA; $P<0.0001$).

6.4.3 The effect of parasympathetic stimulation on CBF

When the PPG was stimulated to assess parasympathetic, vasodilatory input to the cerebral vasculature, a frequency-dependent increase in CBF was seen in both young and old rats, although this was more obvious in the young rats. The old rats were seen to reach their maximum increase in CBF at a stimulation of 10Hz, beyond which, the increase in CBF to higher frequencies was reduced in size. This could suggest a change in the sensitivity of old rats to parasympathetic stimulation.

A parasympathetically-mediated increase in CBF agrees with reports in the literature, for example Levi *et al* (2012) carried out stimulation of the PPG for 3 hours a day, for 4 days after inducing cerebral ischaemia in anaesthetised rats. They reported an intensity- and duration-dependent vasodilatation and increase in CBF in both ischaemic and sham-operated rats. In the ischaemic rats, PPG stimulation also attenuated some of the damage; the ischaemic lesion was partly reperfused, BBB dysfunction decreased and some cortical functions were restored.

When L-NAME was given prior to PPG stimulation in the current study, the CBF and CVC responses seen in the young animals were significantly reduced, as were the CBF and ABP results in old rats. This suggests that stimulation of the PPG is causing an NO-mediated, cerebral vasodilatation. This is in agreement with reports in the literature that have studied this so called nitrergic cerebral innervation. For example Talman *et al* (2007) stimulated the PPG and saw a ~40% increase in CBF.

Additionally, two-way ANOVAs to compare the effect of frequency and age on the responses between young and old, revealed a significant effect of age on CVC and ABP. This suggests that the response to parasympathetic stimulation is blunted with ageing. This could have implications for the hypothesis of an active, NO-mediated dilatation at the UL, in which these nerves are implicated, in that this mechanism appears to be decreased with ageing.

6.5 Conclusion

In agreement with our 1st hypothesis, unilateral stimulation of the SCG did induce a frequency-dependent decrease in ipsilateral CBF, demonstrating a sympathetically-mediated vasoconstriction in young rats. The α-adrenoreceptor antagonist phentolamine, reduced the response to SCG stimulation, indicating an adrenergic, sympathetically-mediated cerebrovascular tone.

However, in contrast with our second hypothesis, unilateral SCG stimulation caused a frequency-dependent decrease in CBF in old rats, the magnitude of which was not significantly different to the response seen in young rats. However, statistical analysis did reveal a significant effect of age on the frequency response to stimulation. The old rats also appeared to have an altered sensitivity to stimulation. These findings may reflect age-related decline in sympathetic input.

In agreement with our 3rd hypothesis, uni- and bilateral sympX increased basal (ipsilateral) CBF, indicating a basal sympathetic tone in young rats. However the bilateral data did not reach significance.

In contrast to our 4th hypothesis, unilateral sympX had no significant effect on the UL in young rats, but did show a trend to increase it. Further, bilateral sympX significantly increased the UL in young rats. This may reflect the removal of tonic sympathetic input allowing the myogenic constrictor response to play a larger role in CA, constricting to a higher ABP. It may also support a role for the sympathetic cerebral innervation in controlling the UL as a safety mechanism, such that, when continuing to constrict in response to increasing ABP may be more damaging than allowing CBF to increase, an active vasodilatation occurs to release the pressure.

In contrast to our 5th hypothesis, bilateral sympX had a greater effect on the UL in old rats, significantly increasing it to levels higher than seen in the other groups. As discussed above, if the UL is an active dilatation that the sympathetic nerves are involved in, the higher control UL and higher UL after sympX, may actually reflect a blunting of this safety mechanism, increasing risk of cerebrovascular damage in old rats.

In agreement with our final hypothesis, unilateral stimulation of the PPG did cause an increase in ipsilateral CBF in young rats, demonstrating a parasympathetically-mediated cerebral vasodilatation. However, while the magnitude of this increase in CBF was not reduced in old compared to young rats, there was a significant effect of age on the frequency-dependent increases in CBF. Further, the old rats did not display a graded response as seen in the young rats, and also demonstrated an altered sensitivity to the stimulation. This may reflect an age-related alteration in parasympathetic input, which would have implications for any role these nerves play in the hypothesised, active-vasodilatation at the UL. In addition, the increase in CBF induced by PPG stimulation was significantly decreased by L-NAME in young and old rats, confirming that at least a portion of the cerebral vasodilatation is NO-mediated.

CHAPTER 7: GENERAL DISCUSSION

CA is the mechanism by which the cerebral vasculature is able to preserve a constant CBF in the face of changes in ABP. As ABP rises or falls, cerebral arterial vessels constrict or dilate, driving a change in cerebral vascular resistance. These adaptations in cerebral vessel calibre therefore enable cerebral blood flow to be maintained. When the autoregulatory capacity of the cerebral vessels are exceeded, CBF either rises or falls, at points called the upper and lower limits respectively (see Figure 3).

The aim of this thesis was to elucidate the mechanisms involved in CA to increases in ABP, and at the UL. Specifically, we aimed to develop a method for reliable assessment of CA in an anaesthetised rat model, and then to investigate the roles of NO- and sympathetically-mediated vascular tone. We aimed to do this by concurrently studying both gross CBF, assessed by measuring flow in the internal carotid artery, and CoBF, by imaging red blood cell flux in the cortex. Further, as it was hypothesised that these mechanisms would be impaired with advanced age, a secondary aim was to investigate the effect of ageing on CA and the UL.

Our hypotheses were:

- The control UL would be lower in old rats compared to young, due to age-related degradation of normal control mechanisms. Further, the cortical UL would be increased compared to the gross UL, due to reported protective mechanisms by larger cerebral vessels, preventing smaller, downstream vessels from being exposed to high blood pressures.

- NOS inhibition would decrease the UL in young rats, due to removal of a tonic vasodilatory influence. NOS inhibition would have a reduced effect on the UL in old rats, due to age-related decrease in NO bioavailability.
- Stimulation of the autonomic innervation of cerebral vasculature would alter basal CBF in young rats. The magnitude of this response would be reduced in old rats, due to an age-related decline in innervation and function.
- Removal of the autonomic innervation to the cerebral vasculature would alter basal CBF, and the UL, in young rats, due to removal of a vasoactive input. The magnitude of this effect would be reduced in old rats, due to an age-related decline in innervation and function.

7.1 The cerebral autoregulatory UL is increased with ageing

In contrast to our 1st hypothesis, the control UL in old rats was significantly raised compared to the control UL in young rats (168±2mmHg vs. 180±3mmHg, unpaired t-test; P=0.0009). This may be explained by an increased arterial stiffness associated with age, which is known to occur in conjunction with structural and functional vessel changes, or an increased contribution by myogenic mechanisms.

Before the UL was reached in young rats, there was a significant fall in CVR, which was suggestive of an active vasodilatation, rather than a passive increase in CBF, being responsible for the breakthrough of autoregulation. This may therefore be a physiologically relevant mechanism, in the form of a safety pressure release mechanism, protecting the circulation from exposure to large increases in pressure/flow if the vessels were forcibly dilated, or ischaemia if they continued to vasoconstrict. As this change in CVR was seen to be

significantly blunted in old animals, this lends support for the hypothesis of an increased arterial stiffness pushing the UL to higher ABPs.

However, in agreement with our 1st hypothesis, the cortical UL was significantly higher than the gross UL in young rats, supporting the idea that larger cerebral vessels, and even extra-cranial vessels, show CA at lower ABPs than cortical arterial vessels, such that smaller, downstream arterioles are protected from increases in ABP. In old rats, this potentially protective difference between gross and cortical ULs was lost, which could predispose the older rats to an increased risk of haemorrhagic stroke.

7.2 Inhibition of NOS raises or abolishes the UL

In contrast to the 2nd hypothesis, inhibition of nNOS-derived NO, by SMTC or 7-NI, did not significantly change the UL in young rats compared to the control ULs (168±2mmHg vs. 171±2mmHg, unpaired t-test; P=0.14, and vs 174±7mmHg, unpaired t-test; P=0.05). Further, inhibition of eNOS and nNOS-derived NO using L-NAME, significantly increased the UL compared to young rats (168±2mmHg vs. 187±2mmHg, unpaired t-test; P=0.0002).

This may reflect an increase in the relative input by myogenic or sympathetic vasoconstriction, after removal of an NO-mediated tone. Alternatively, this also supports the idea that the increase in CBF beyond the UL is an active, NO-mediated dilatation. An active dilatation may be a physiologically relevant, safety mechanism, which acts to dissipate the build-up of pressure, and prevent ischaemia and damage that may be caused by continuing to vasoconstrict in response to rising ABP.

In further contrast to our hypothesis, NOS inhibition also increased the UL in old rats, such that autoregulatory breakthrough was not seen. Therefore if the increase in CBF above the UL

is a protective mechanism, the raised UL in old control experiments, and abolishment of the UL in old NOS inhibition experiments, may actually increase risk of cerebrovascular damage.

7.3 Sympathetic stimulation decreases CBF and sympathectomy raises the UL

In agreement with our 3rd hypothesis, unilateral sympathetic stimulation induced a frequency-dependent decrease in ipsilateral CBF, demonstrating a sympathetically-mediated vasoconstriction in young rats.

In contrast with our second hypothesis, unilateral sympathetic stimulation caused a similar frequency-dependent decrease in CBF in old rats. However, there was a significant effect of age on the frequency response to stimulation, and a change in sensitivity to stimulation in old rats which may reflect an age-related decline in sympathetic input.

In agreement with our 4th hypothesis, uni- and bilateral sympX increased basal, ipsilateral CBF, indicating a basal sympathetic tone in young rats. In contrast to the hypothesis, unilateral sympX had no effect on the UL, but showed a trend to increase it (168±2mmHg vs 174±2mmHg, unpaired t-test; P=0.06). Further, bilateral sympX significantly increased the UL in young rats (168±2mmHg vs 178±3mmHg, unpaired t-test; P=0.01).

This suggests that removal of a tonic sympathetic input increases the relative contribution of the myogenic constrictor response in CA. It may also suggest that sympathetic cerebral nerves are involved in the safety mechanism at the UL, as continuing to constrict to increasing ABP may increase risk of damage and ischaemia. It is possible that sympathetic vasoconstriction constricts up to the UL, and then receives a signal to stop, allowing an active vasodilatation to occur to release the pressure.

In further contrast to our hypothesis, bilateral sympX also raised the UL in old rats (180±3mmHg vs 190±3mmHg, unpaired t-test; P=0.03). As discussed above, if the UL is an active dilatation involving the cerebral sympathetic nerves, the raised ULs seen with ageing, may reflect an attenuated safety mechanism, increasing risk of cerebrovascular damage.

The role of parasympathetic nerves in CA at the UL did not originally form part of our hypotheses. However, the data seen in the other experimental groups suggested that parasympathetic dilatation, particularly by nitrergic nerve fibres, may be important at the UL. In agreement with this, unilateral stimulation of the PPG increased ipsilateral CBF in young rats, demonstrating a parasympathetically-mediated cerebral vasodilatation, which was also seen in old rats. However, statistical analysis did reveal a significant effect of age on the frequency-dependent decreases in CBF, and further there was an altered pattern of response and sensitivity to stimulation seen in the old rats. This may indicate an altered parasympathetic input in old rats, which could affect any role these nerves play in the hypothesised, active-vasodilatation at the UL.

7.4 New working hypothesis for control of cerebral autoregulation and the UL

The studies by Talman *et al* (1995, 2007) have demonstrated that NOS inhibition extends CA, such that the UL was not reached. They demonstrated the same effect after sectioning the parasympathetic input to the cerebral vasculature (Talman *et al*, 2000). Further, when they stimulated the PPG, they observed a cerebral vasodilatation (2007), and suggested that cerebral parasympathetic innervation provides a tonic dilator influence. This is supported by the observation that cerebral vasoconstriction is seen when the PPG is removed (Boysen *et al*, 2009). The same group suggested a role for the arterial baroreflex pathway in autoregulation, as sinoaortic denervation (1994) or central disruption at the nucleus tractus solitarius (NTS)

(2002) extended the CA range, such that autoregulatory breakthrough was not seen. They hypothesised that an increase in sympathetic activity after baroreceptor denervation, or after NOS inhibition, may explain the increase in the UL. However, bilateral removal of the SCG had no further effect on autoregulation (1994).

They subsequently demonstrated an anatomical pathway which links the baroreceptor signalling pathway to the preganglionic parasympathetic nerves, via direct projections at the NTS. The postganglionic parasympathetic neurons leaving the PPG, have been shown to project to and innervate the cerebral vasculature (Agassandian *et al*, 2003).

Based on these findings, they hypothesised that the increase in CBF seen beyond the UL is an active, NO-mediated vasodilatation, and that this NO is released from the parasympathetic, nitrergic fibres projecting from the PPG. The link between the baroreflex pathway and the parasympathetic fibres that are associated with dilatation at the UL, provides an anatomical link between the UL and systemic ABP, potentially a specific subset of C-type baroreceptor fibres, which are maximally activated at ABPs close to the UL (Andresen and Kunze, 1994).

Further linking the literature outlined here, with the data generated in this thesis, specifically that both NOS inhibition and sympX were seen to extend the autoregulatory range, is evidence for a close apposition between sympathetic and parasympathetic, nitrergic nerve terminals in the cerebral arteries (Lee, 1981). Chang *et al* (2012) investigated this close apposition in the BA of rats and found that sympathetic nerve activation, by stimulation of the SCG, was able to cause a parasympathetic, nitrergic vasodilatation. This was mediated by noradrenaline, released from the sympathetic terminals, binding with β_2-adrenoreceptors on the close by parasympathetic nerves, and modulating the release of NO.

Therefore we propose that a similar arrangement may exist throughout the cerebral circulation. During increases in ABP, sympathetic activity may dominate the autoregulatory plateau of autoregulation to maintain CBF. When ABP nears the UL, a parasympathetically-mediated cerebral dilatation is induced, producing the increase in CBF at the UL. This would mean that, in the current data, the normal autoregulatory breakthrough seen in the young control experiments is NO-mediated, and the raised UL associated with an increase in CBF, seen in some of the NOS inhibition and sympX experiments, could be a passive dilatation, at the point where myogenic vasoconstriction is overcome. This point which may not always be reached, explaining the lack of autoregulatory breakthrough in some of our experiments.

The hypothesised switch between sympathetic vasoconstriction, and parasympathetic vasodilatation, producing the increase in CBF at the UL, may be linked to the ABP at which the high pressure baroreceptors are maximally activated, and via their connection with the preganglionic parasympathetic nerves that innervate the cerebral vessels. Removal of either the cerebral sympathetic innervation, or the ability of the parasympathetic nerves to cause an NO-mediated dilatation, would therefore result in the autoregulatory range being extended. This new working hypothesis is represented in Figure 54.

7.5 Limitations and potential future experiments

One of the major limitations of the current study is the issue around the use of PE to assess CA, and the apparent contradiction this presents with the use of phentolamine to assess the role of sympathetic stimulation on CBF. The main argument in favour of using PE in this study is the fact that it is not thought to cross the BBB, and that α-adrenoreceptor density on the smooth muscle of cerebral vessels is low. As such, PE was used in an attempt to increase ABP by causing peripheral vasoconstriction, without any direct constriction of the cerebral

vessels, therefore avoiding any confounding effects on CBF data, or the CA curves (see section 3.1.2.2).

However, the α-adrenoreceptor antagonist phentolamine significantly decreased the effect of sympathetic stimulation on CBF, confirming a successful blockade of α-adrenoreceptors, and a reduction in a sympathetically-mediated cerebral vasoconstriction. As phentolamine is not thought to cross the BBB, this suggests that the adrenoreceptors are positioned lumenally in the cerebral vessels, and therefore that PE should also have had an effect on CBF. As described in 3.3.1, a decrease in CBF was often seen when the initial doses of PE were infused. It was hypothesised that this might represent a cerebral vasoconstriction beyond that required to maintain a constant CBF, but still reflected autoregulatory behaviour. However, this may also reflect a direct vasoconstriction caused by PE.

A second limitation of this study is the fact that only male rats were used. While this is standard in many scientific studies, it is not representative of the population. It is also highly significant to the current study, due to the strong link between sex and stroke. Women have an increased lifetime risk of stroke, and it is the 3rd leading cause of death in women (Howe & McCullough, 2015).

Future work to extend the current findings and address the limitations could include repeating the studies using female rats to assess any sex differences. Any differences seen in female rats may be linked to the increased risk of stroke observed in women. In addition, to investigate the new working hypothesis, studies recording sympathetic (SCG) and parasympathetic (PPG) nerve activity, during increases in ABP to reach the UL, could shed light on whether the increase in CBF beyond the UL is an active process. This could be carried out in

combination with other interventions, such as baroreflex denervation, sympX or NOS inhibition.

In addition, further experiments could be designed to elucidate the effect of ageing on the mechanisms outlined, potentially in rats of a more advanced age, and could also be extended to disease models, such as animals predisposed to hypertension and stroke.

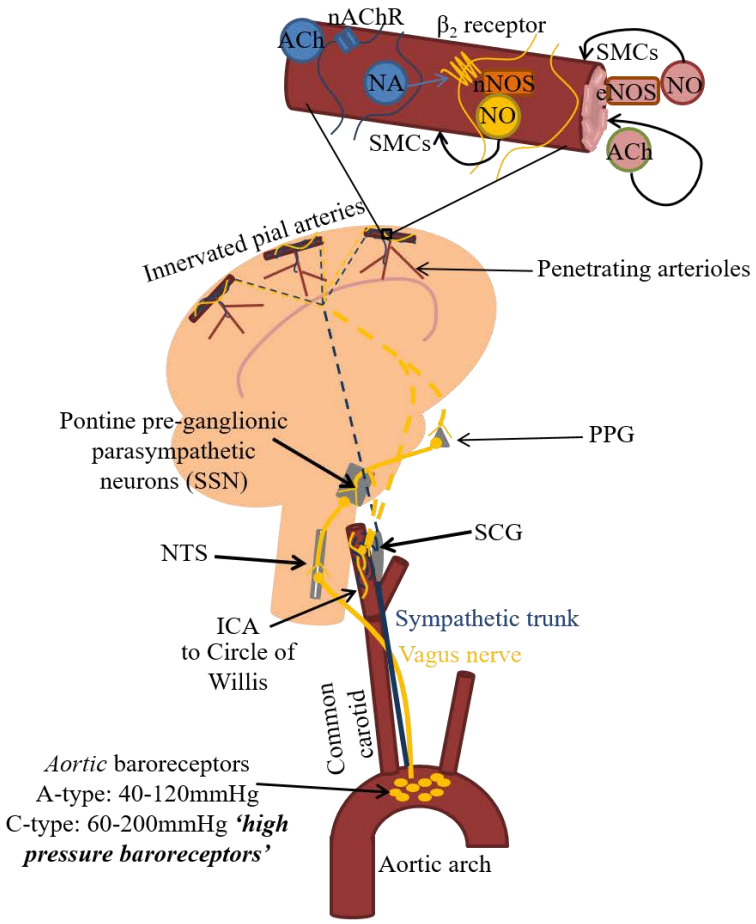

Figure 54: This diagram highlights the components involved in our new working hypothesis. It proposes that coordinated responses between cerebral sympathetic and parasympathetic innervation, enable CBF to be maintained as ABP rises, until the point at which activation of high pressure baroreceptors occurs. A signalling pathway then induces a cerebral vasodilatation, seen as the UL, which may actually be a protective, pressure-release mechanism. See 7.4 for more details.

REFERENCES

Age UK, 2015. Later life in the United Kingdom. , (October), pp.1–34. Available at: http://www.ageuk.org.uk/Documents/EN-GB/Factsheets/Later_Life_UK_factsheet.pdf?dtrk=true.

Alderton, W.K., Cooper, C.E. & Knowles, R.G., 2001. Nitric oxide synthases: structure, function and inhibition. *Biochem J*, 357(Pt 3), pp.593–615. Available at: http://www.ncbi.nlm.nih.gov/pubmed/11463332.

Amin-Hanjani, S. et al., 2015. Effect of age and vascular anatomy on blood flow in major cerebral vessels. *J Cereb Blood Flow Metab*, 35(2), pp.312–318. Available at: http://www.nature.com/doifinder/10.1038/jcbfm.2014.203.

Amrani, M. et al., 1996. Ageing is associated with reduced basal and stimulated release of nitric oxide by the coronary endothelium. *Acta Physiol Scand*, 157(1), pp.79–84. Available at: http://www.ncbi.nlm.nih.gov/pubmed/8735657.

Andresen, M.C. & Kunze, D.L., 1994. Nucleus tractus solitarius--gateway to neural circulatory control. *Annu Rev Physiol*, 56, pp.93–116. Available at: http://www.ncbi.nlm.nih.gov/pubmed/7912060.

Araujo, D.M. et al., 1990. Effects of aging on nicotinic and muscarinic autoreceptor function in the rat brain: relationship to presynaptic cholinergic markers and binding sites. *The Journal of Neuroscience*, 10(9), pp.3069–3078. Available at: http://www.jneurosci.org/content/10/9/3069.abstract.

Ayajiki, K. et al., 2001. Relatively selective neuronal nitric oxide synthase inhibition by 7-nitroindazole in monkey isolated cerebral arteries. *Eur J Pharmacol*, 423(2–3), pp.179–

183. Available at: http://www.ncbi.nlm.nih.gov/entrez/query.fcgi?cmd=Retrieve&db=PubMed&dopt=Citation&list_uids=11448483%5Cnhttp://www.sciencedirect.com/science/article/pii/S0014299901010688.

Balbi, M. et al., 2015. Dysfunction of mouse cerebral arteries during early aging. *J Cereb Blood Flow Metab*, 35(9), pp.1445–1453. Available at: http://www.nature.com/doifinder/10.1038/jcbfm.2015.107.

Barcroft, H., Basnayake, V., Cobbold, A.F., Cunningham, D.J.C., Jukes, M.G.M. & Young, I.M., 1957. Response to noradrenaline in man. *J Physiol*, (137), pp.365–373.

Baron, J.C. et al., 1982. Noninvasive Measurement of Blood Flow, Oxygen Consumption, and Glucose Utilization in the Same Brain Regions in Man by Positron Emission Tomography : Concise Communication. *Medicine*, 23(5), pp.391–399.

Baumbach, G.L. & Heistad, D.D., 1985. Regional, segmental, and temporal heterogeneity of cerebral vascular autoregulation. *Annals of Biomedical Engineering*, 13(3–4), pp.303–310.

Bauser-Heaton, H.D. & Bohlen, H.G., 2007. Cerebral microvascular dilation during hypotension and decreased oxygen tension: a role for nNOS. *Am J Physiol Heart Circ Physiol*, 293(4), pp.H2193-201. Available at: http://www.ncbi.nlm.nih.gov/pubmed/17630350 [Accessed May 6, 2014].

Bayliss, W.M., 1902. On the local reactions of the arterial wall to changes of internal pressure. *J Physiol*, 28, pp.220–231.

Berman, R.F., Goldman, H. & Altman, H.J., 1988. Age-related changes in regional cerebral

blood flow and behavior in Sprague-Dawley rats. *Neurobiology of Aging*, 9(5–6), pp.691–696.

Bevan, J.A., Duckles, S.P. & Lee, T.J.F., 1975. Histamine potentiation of nerve- and drug-induced responses of a rabbit cerebral artery. *Circulation Research*, 36, pp.647–653.

Bevan, R.D. et al., 1998. Weakness of Sympathetic Neural Control of Human Pial. *Stroke*, (29), pp.212–221.

Biesold, D. et al., 1989. Stimulation of the nucleus basalis of Meynert increases cerebral cortical blood flow in rats. *Neurosci Lett*, 98, pp.39–44.

Bishop, C.C. et al., 1986. Transcranial Doppler measurement of middle cerebral artery blood flow velocity: a validation study. *Stroke*, 17(5), pp.913–915.

Borton, M. & Docherty, J.R., 1989. The effects of ageing on neuronal uptake of noradrenaline in the rat. *Naunyn-Schmiedeberg's Archives of Pharmacology*, 340(2), pp.139–143.

Bredt, D.S., Hwang, P.M. & Snyder, S.H., 1990. Localization of nitric oxide synthase indicating a neural role for nitric oxide. *Nature*, 347(6295), pp.768–770.

Brennan, K.C., Beltran-Parrazal, L., Lopez-Valdes, H.E., Theriot, J., Toga, A.W. and Charles, A.C., 2007. Distinct vascular conduction with cortical spreading depression. *Headache*, 97, pp.4143–4151.

Brungardt, J.M., Swan, K.G. & Reynolds, D.G., 1974. Adrenergic mechanisms in canine hindlimb circulation. *Cardiovascular Research*, 8, pp.423–429.

Bryan, R.M. et al., 2001. Effects of luminal shear stress on cerebral arteries and arterioles. *Am J Physiol Heart Circ Physiol*, 280(5), pp.H2011–H2022.

Burns, A. and & Tyrrell, P., 1992. Association of age with regional cerebral oxygen utilization: a positron emission tomography study. *Age and Ageing*, 21(5), pp.316–320.

Burns, E.M. et al., 1979. Thinning of capillary walls and declining numbers of endothelial mitochondria in the cerebral cortex of the aging primate, Macaca nemestrina. *J Gerentol*, 34(5), pp.642–650.

Cassaglia, P.A., Griffiths, R.I. & Walker, A.M., 2008. Sympathetic nerve activity in the superior cervical ganglia increases in response to imposed increases in arterial pressure. *Am J Physiol Regul Integr Comp Physiol*, 294(4), pp.R1255-61. Available at: http://www.ncbi.nlm.nih.gov/pubmed/18216142 [Accessed May 6, 2014].

Castro, L., Demicheli, V., Tortora, V. and Radi, R., 2011. Mitochondrial protein tyrosine nitration. *Free Radical Research*, 45(1), pp.37–52.

Cerveri, I. et al., 1995. Reference values of arterial oxygen tension in the middle-aged and elderly. *American Journal of Respiratory and Critical Care Medicine*, 152(3), pp.934–941.

Chalimoniuk, M. & Strosznajder, J.B., 1998. Aging modulates nitric oxide synthesis and cGMP levels in hippocampus and cerebellum. Effects of amyloid beta peptide. *Molecular and Chemical Neuropathology*, 35(1–3), pp.77–95.

Challah, M. et al., 1997. Circulating and cellular markers of endothelial dysfunction with aging in rats. *Am J Physiol*, 273(4 Pt 2), pp.H1941-8. Available at: http://www.ncbi.nlm.nih.gov/pubmed/9362264.

Chamiot-Clerc, P., Renaud, J.F. & Safar, M.E., 2001. Pulse pressure, aortic reactivity, and endothelium dysfunction in old hypertensive rats. *Hypertension*, 37, pp.313–321.

de Champlain, J. et al., 1976. Circulating catecholamine levels in human and experimental hypertension. *Circ Res*, 38(2), pp.109–114.

Chédotal, A. et al., 1994. Distinct choline acetyltransferase (ChAT) and vasoactive intestinal polypeptide (VIP) bipolar neurons project to local blood vessels in the rat cerebral cortex. *Brain Research*, 646(2), pp.181–193.

Christou, D.D. & Seals, D.R., 2008. Decreased maximal heart rate with aging is related to reduced beta-adrenergic responsiveness but is largely explained by a reduction in intrinsic heart rate. *J Appl Physiol*, 105(1), pp.24–29.

Cipolla, M.J., 2009. *The Cerebral Circulation*, San Rafael (CA): Morgan & Claypool Life Sciences. Available at: https://www.ncbi.nlm.nih.gov/books/NBK53081/.

Claus, J.J. et al., 1998. Regional Cerebral Blood Flow and Cerebrovascular Risk Factors in the Elderly Population. *Neurobiology of Aging*, 19(1), pp.57–64.

Coney, A.M. & Marshall, J.M., 1998. Role of adenosine and its receptors in the vasodilatation induced in the cerebral cortex of the rat by systemic hypoxia. *J Physiol*, 509.2, pp.507–518.

Cowen, T. & Thrasivoulou, C., 1990. Cerebrovascular nerves in old rats show reduced accumulation of 5-hydroxytryptamine and loss of nerve fibres. *Brain Research*, 513(2), pp.237–243.

Cox, R.H., 1977. Effects of age on the mechanical properties of rat carotid artery. *Am J Physiol*, 233(2), pp.H256-63.

Craig, J. & Martin, W., 2012. Dominance of flow-mediated constriction over flow-mediated dilatation in the rat carotid artery. *British Journal of Pharmacology*, 167, pp.527–536.

Csati, A. et al., 2012. Distribution of vasoactive intestinal peptide, pituitary adenylate cyclase-activating peptide, nitric oxide synthase, and their receptors in human and rat sphenopalatine ganglion. *Neuroscience*, 202(158), pp.158–168. Available at: http://dx.doi.org/10.1016/j.neuroscience.2011.10.055.

Czynski, A.J. et al., 2013. Cerebral autoregulation is minimally influenced by the superior cervical ganglion in two-week-old lambs, and absent in preterm lambs immediately following delivery. *PLoS ONE*, 8(12).

Daly, R.N., Goldberg, P.B. & Roberts, J., 1988. Effects of age on neurotransmission at the cardiac sympathetic neuroeffector junction. *The Journal of Pharmacology and Experimental Therapeutics*, 245(3), pp.798–803.

Dauphin, F. & Hamel, E., 1990. Muscarinic receptor subtype mediating vasodilation in feline middle cerebral artery exhibits M3 pharmacology. *Eur J Pharmacol*, 178(2), pp.203–213.

Delp, M.D. et al., 2008. Ageing diminishes endothelium-dependent vasodilatation and tetrahydrobiopterin content in rat skeletal muscle arterioles. *J Physiol*, 586(4), pp.1161–1168. Available at: http://doi.wiley.com/10.1113/jphysiol.2007.147686 [Accessed April 11, 2017].

Denison, A.B. & Green, H.D., 1956. Absence of vasomotor responses to epinephrine and arterenol in an isolated intracranial circulation. *Circ Res*, 4(5), pp.565–573.

Denniss, S.G., Levy, A.S. & Rush, J.W.E., 2011. Effects of glutathione-depleting drug buthionine sulfoximine and aging on activity of endothelium-derived relaxing and contracting factors in carotid artery of Sprague-Dawley rats. *Journal of Cardiovascular Pharmacology*, 58(3), pp.272–283.

Deveci, D. & Egginton, S., 1999. Development of the Fluorescent Microsphere Technique for Quantifying Regional Blood Flow in Small Animals. *Exp Physiol*, 84, pp.615–630.

Donahue, S., Zeman, W. & Watanabe, I., 1967. Alterations of basement membranes of cerebral capillaries. *Journal of Neuropathology and Experimental Neurology*, 26(3), pp.397–411.

Drummond, J.C. et al., 1989. Phenylephrine-induced hypertension reduces ischemia following middle cerebral artery occlusion in rats. *Stroke*, 20(11), pp.1538–44. Available at: http://www.ncbi.nlm.nih.gov/pubmed/2815189 [Accessed September 29, 2015].

Dunn, L., 2002. Raised intracranial pressure. *Journal of Neurology, Neurosurgery & Psychiatry*, 2(3), pp.i23–i27. Available at: http://discovery.ucl.ac.uk/172546/.

Edmunds, N.J. & Marshall, J.M., 2001. Vasodilatation, oxygen delivery and oxygen consumption in rat hindlimb during systemic hypoxia: roles of nitric oxide. *J Physiol*, 532.1, pp.251–259.

Edvinsson, L. et al., 1978. Effect of exogenous noradrenaline on local cerebral blood flow after osmotic opening of the blood-brain barrier in the rat. *J Physiol*, 274, pp.149–56.

Edvinsson, L. & Owman, C., 1977. Sympathetic innervation and adrenergic receptors in intraparenchymal cerebral arterioles of baboon. *Acta Physiol Scand*, 452, pp.57–59.

Eisenach, J.H. et al., 2014. Cyclo-oxygenase-2 inhibition and endothelium-dependent vasodilation in younger vs. older healthy adults. *British Journal of Clinical Pharmacology*, 78(4), pp.815–823.

Endres, M. et al., 2011. Primary prevention of stroke: blood pressure, lipids, and heart failure. *European Heart Journal*, 32(5), pp.545–52. Available at:

http://www.ncbi.nlm.nih.gov/pubmed/21285072 [Accessed May 6, 2014].

Eskurza, I. et al., 2005. Tetrahydrobiopterin augments endothelium-dependent dilatation in sedentary but not in habitually exercising older adults. *J Physiol*, 5683, pp.1057–1065.

Euser, A.G., Bullinger, L. & Cipolla, M.J., 2008. Magnesium sulphate treatment decreases blood-brain barrier permeability during acute hypertension in pregnant rats. *Exp Physiol*, 93(2), pp.254–61. Available at: http://www.ncbi.nlm.nih.gov/pubmed/17933863 [Accessed May 6, 2014].

Euser, A.G. & Cipolla, M.J., 2007. Cerebral blood flow autoregulation and edema formation during pregnancy in anesthetized rats. *Hypertension*, 49(2), pp.334–40. Available at: http://www.ncbi.nlm.nih.gov/pubmed/17200432 [Accessed May 6, 2014].

Faraci, F.M., 1990. Role of nitric oxide in regulation of basilar artery tone in vivo. *Am J Physiol Heart Circ Physiol*, 259(4), pp.H1216-1221. Available at: http://ajpheart.physiology.org/content/259/4/H1216 [Accessed December 8, 2016].

Faraci, F.M. & Heistad, D.D., 1990. Regulation of large cerebral arteries and cerebral microvascular pressure. *Circ Res*, 66(1), pp.8–17.

Feldman, M.L. & Dowd, C., 1975. Loss of dendritic spines in aging cerebral cortex. *Anatomy and Embryology*, 148(3), pp.279–301.

Ferrari, A.U. et al., 1991. Differential effects of aging on the heart rate and blood pressure influences of arterial baroreceptors in awake rats. *Journal of Hypertension*, 9(7), pp.615–621.

Ferrari, A.U., Radaelli, A. & Centola, M., 2003. Invited review: aging and the cardiovascular system. *J Appl Physiol*, 95(6), pp.2591–2597.

Filosa, J.A. & Iddings, J.A., 2013. Astrocyte regulation of cerebral vascular tone Astrocyte regulation of cerebral vascular tone. *Am J Physiol Heart Circ Physiol*, 305(June), pp.H609–H619.

Fleg, J.L. et al., 1995. Impact of age on the cardiovascular response to dynamic upright exercise in healthy men and women. *J Appl Physiol*, 78(3), pp.890–900.

Florence, V.M. & Bevan, J.A., 1979. Biochemical determinations of cholinergic innervation in cerebral arteries. *Circ Res*, 45(2), pp.212–8. Available at: http://www.ncbi.nlm.nih.gov/pubmed/445705.

Fog, M., 1938. The Relationship Between the Blood Pressure and the Tonic Regulation of the Pial Arteries. *Journal of Neurology and Psychiatry*, 1, pp.187–197.

Folkow, B. & Svanborg, A., 1993. Physiology of cardiovascular aging. *Physiol Rev*, 73(4), pp.725–764. Available at: http://physrev.physiology.org/content/73/4/725 [Accessed January 3, 2017].

Fujishima, M. et al., 1984. Autoregulation of cerebral blood flow in young and aged spontaneously hypertensive rats (SHR). *Gerontology*, 30(1), pp.30–36.

Gebremedhin, D., Yamaura, K. & Harder, D.R., 2008. Role of 20-HETE in the hypoxia-induced activation of Ca2+-activated K+ channel currents in rat cerebral arterial muscle cells. *Am J Physiol Heart Circ Physiol*, 294(1), pp.H107–H120.

Gerstenblith, G. et al., 1977. Echocardiographic assessment of a normal aging population. *Circulation*, 56, p.273–278.

Geurts, L.J. et al., 2018. Vascular reactivity in small cerebral perforating arteries with 7 T phase contrast MRI – A proof of concept study. *NeuroImage*, 172(February), pp.470–

477. Available at: https://doi.org/10.1016/j.neuroimage.2018.01.055.

Greenfield, J.C. & Tindall, G.T., 1965. Effect of Acute Increase in Intracranial Pressure on Blood Flow in the Internal Carotid Artery of Man. *Journal of Clinical Investigation*, 44(8), pp.1343–1351.

Gross, P.M. et al., 1979. Cerebral vascular responses to physiological stimulation of sympathetic pathways in cats. *Circ Res*, 44(2), pp.288–294. Available at: http://circres.ahajournals.org/cgi/doi/10.1161/01.RES.44.2.288 [Accessed May 6, 2014].

Hajdu, M.A. et al., 1990. Effects of aging on mechanics and composition of cerebral arterioles in rats. *Circ Res*, 66(6), pp.1747–1754.

Hamel, E. et al., 1990. Selective age-related changes in neuronal markers and smooth muscle reactivity in cerebrovascular beds of Fischer 344 rats. *Neurobiology of Aging*, 11(6), pp.631–639.

Hamner, J.W. & Tan, C.O., 2014. Relative contributions of sympathetic, cholinergic, and myogenic mechanisms to cerebral autoregulation. *Stroke*, 45(6), pp.1771–1777.

Hara, H., Hamill, G.S. & Jacobowitz, D.M., 1985. Origin of cholinergic nerves to the rat major cerebral arteries: coexistence with vasoactive intestinal polypeptide. *Brain Research Bulletin*, 14(2), pp.179–188.

Hardebo, J.E., Edvinsson, L., et al., 1979. Histofluorescence study on monoamine entry into the brain before and after opening of the blood-brain barrier by various mechanisms. *Acta Neuropathologica*, 47(2), pp.145–50. Available at: http://www.ncbi.nlm.nih.gov/pubmed/38622 [Accessed September 29, 2015].

Hardebo, J.E., Falck, B., et al., 1979. Studies on the enzymatic blood-brain barrier:

quantitative measurements of DOPA decarboxylase in the wall of microvessels as related to the parenchyma in various CNS regions. *Acta Physiol Scand*, 105(4), pp.453–460.

Harder, D.R., 1984. Pressure-dependent membrane depolarization in cat middle cerebral artery. *Circ Res*, 55(2), pp.197–202. Available at: http://www.ncbi.nlm.nih.gov/entrez/query.fcgi?cmd=Retrieve&db=PubMed&dopt=Citation&list_uids=6744529.

Harder, D.R. & Madden, J.A., 1985. Cellular mechanism of force development in cat middle cerebral artery by reduced PCO2. *Pflugers Archiv: Eur J Physiol*, 403(4), pp.402–406.

Harman, D., 1956. Aging: A Theory Based on Free Radical and Radiation Chemistry. *Journal of Gerontology*, 11(3), pp.298–300.

Harper, A.M. & Bell, R.A., 1963. The effect of metabolic acidosis and alkalosis on the blood flow through the cerebral cortex. *Journal of Neurology, Neurosurgery & Psychiatry*, 26(22), pp.341–4.

Heistad, D.D. et al., 1977. Effect of sympathetic nerve stimulation on cerebral blood flow andon large cerebral arteries of dogs. *Circulation research*, 41(3), pp.342–350. Available at: http://eutils.ncbi.nlm.nih.gov/entrez/eutils/elink.fcgi?dbfrom=pubmed&id=3945523&retmode=ref&cmd=prlinks%5Cnpapers3://publication/doi/10.1203/00006450-198602000-00007.

Heistad, D.D. & Kontos, H.A., 2011. Cerebral Circulation. In *Comprehensive Physiology*. John Wiley & Sons, Inc., pp. 137–182. Available at: http://dx.doi.org/10.1002/cphy.cp020305.

Heistad, D.D. & Marcus, M.L., 1979. Effect of sympathetic stimulation on permeability of the blood-brain barrier to albumin during acute hypertension in cats. *Circ Res*, 45(3), pp.331–338.

Heistad, D.D. & Marcus, M.L., 1978. Evidence that neural mechanisms do not have important effects on cerebral blood flow. *Circ Res*, 42(3), pp.295–302.

Heistad, D.D., Marcus, M.L. & Gross, P.M., 1978. Effects of sympathetic nerves on cerebral vessels in dog, cat, and monkey. *Am J Physiol Heart Circ Physiol*, 235(5), p.H544 LP-H552. Available at: http://ajpheart.physiology.org/content/235/5/H544.abstract.

Hervonen, A. et al., 1990. Responses of cortical cerebral blood flow produced by stimulation of cervical sympathetic trunks are well maintained in aged rats. *Neuroscience Letters*, 120, pp.55–57.

Heymes, C. et al., 2000. Cyclo-oxygenase-1 and -2 contribution to endothelial dysfunction in ageing. *British Journal of Pharmacology*, 131(4), pp.804–810.

Hill, C.E. et al., 1986. Sympathetic innervation and excitability of arterioles originating from the rat middle cerebral artery. *J Physiol*, (371), pp.305–316.

Hoedt-Rasmussen, K., Sveinsdottir, E. and Lassen, N.A., 1966. Regional Cerebral Blood Flow in Man Determined by Intra-arterial Injection of Radioactive Inert Gas. *Circ Res*, 18, pp.237–247.

Hoffman, W.E. et al., 1991. Cerebral autoregulation in awake versus isoflurane-anesthetized rats. *Anesthesia and Analgesia*, 73(6), pp.753–757. Available at: http://www.ncbi.nlm.nih.gov/pubmed/1952176.

Horsfield, M.A. et al., 2013. Regional Differences in Dynamic Cerebral Autoregulation in the

Healthy Brain Assessed by Magnetic Resonance Imaging. *PLoS ONE*, 8(4), pp.2–8.

Howe, M.D. & McCullough, L.D., 2015. Prevention and management of stroke in women. *Expert Review of Cardiovascular Therapy*, 13(4), pp.403–415. Available at: https://doi.org/10.1586/14779072.2015.1020300.

Iadecola, C., 1992. Does nitric oxide mediate the increases in cerebral blood flow elicited by hypercapnia? *Proc Natl Acad Sci USA*, 89(9), pp.3913–3916.

Ishii, H., Sato, T. & Izumi, H., 2014. Parasympathetic reflex vasodilation in the cerebral hemodynamics of rats. *J Comp Physiol B: Biochemical, Systemic, and Environmental Physiology*, 184(3), pp.385–399.

Ishikawa, S. et al., 2009. Phenylephrine ameliorates cerebral cytotoxic edema and reduces cerebral infarction volume in a rat model of complete unilateral carotid artery occlusion with severe hypotension. *Anesthesia and Analgesia*, 108(5), pp.1631–7. Available at: http://www.ncbi.nlm.nih.gov/pubmed/19372348 [Accessed September 29, 2015].

Ito, K. et al., 1986. Increases in adrenal catecholamine secretion and adrenal sympathetic nerve unitary activities with aging in rats. *Neurosci Lett*, 69(3), pp.263–268.

Iwase, S. et al., 1991. Age-related changes of sympathetic outflow to muscles in humans. *Journal of Gerontology*, 46(1), pp.M1-5.

James, I.. M., Millar, R.. A. & Purves, M.J., 1969. Observations on the control of cerebral blood flow in the sheep fetus and newborn lamb. *Circ Res*, 25(6), pp.651–67. Available at: http://www.ncbi.nlm.nih.gov/pubmed/5364642.

Jansen, G.F.A. et al., 2000. Cerebral Autoregulation in Subjects Adapted and Not Adapted to High Altitude. *Stroke*, 31, pp.2314–2318.

Jendzjowsky, N.G. et al., 2014. Acute tetrahydrobiopterin supplementation attenuates sympathetic vasoconstrictor responsiveness in resting and contracting skeletal muscle of healthy rats. *Physiol Rep*, 2(10), p.e12164.

Jesko, H., Chalimoniuk, M. & Strosznajder, J.B., 2003. Activation of constitutive nitric oxide synthase(s) and absence of inducible isoform in aged rat brain. *Neurochemistry International*, 42(4), pp.315–322.

Jobsis, F.F., 1977. Noninvasive monitoring of cerebral oxygenation and myocardial oxygen sufficiency and circulatory parameters. *Science*, 198, pp.1264–1267.

Jones, S.C. et al., 1999. Cortical NOS inhibition raises the lower limit of cerebral blood flow-arterial pressure autoregulation Cortical NOS inhibition raises the lower limit of cerebral blood flow-arterial pressure autoregulation. *Am J Physiol Heart Circ Physiol*, (276), pp.H1253-1262.

Jordan, J. et al., 2000. Interaction of carbon dioxide and sympathetic nervous system activity in the regulation of cerebral perfusion in humans. *Hypertension*, 36(3), pp.383–388.

Joshi, S. et al., 2003. Despite in vitro increase in cyclic guanosine monophosphate concentrations, intracarotid nitroprusside fails to augment cerebral blood flow of healthy baboons. *Anesthesiology*, 98(2), pp.412–419.

Joshi, S. et al., 2000. Intracarotid infusion of the nitric oxide synthase inhibitor, L-NMMA, modestly decreases cerebral blood flow in human subjects. *Anesthesiology*, 93(3), pp.699–707. Available at: http://www.ncbi.nlm.nih.gov/pubmed/10969303.

Jung, J., Na, C. & Huh, Y., 2012. Alterations in nitric oxide synthase in the aged CNS. *Oxidative Medicine and Cellular Longevity*, pp.1–7.

Kapatos, G., Hirayama, K. & Hasegawa, H., 1992. Tetrahydrobiopterin turnover in cultured rat sympathetic neurons: developmental profile, pharmacologic sensitivity, and relationship to norepinephrine synthesis. *Journal of Neurochemistry*, 59(6), pp.2048–2055.

Kawai, Y. & Ohhashi, T., 1986. Histochemical studies of the adrenergic innervation of canine cerebral arteries. *Journal of the Autonomic Nervous System*, 15(2), pp.103–108.

Kazmi, S.M.S. et al., 2015. Expanding applications, accuracy, and interpretation of laser speckle contrast imaging of cerebral blood flow. *J Cereb Blood Flow Metab*, 35(7), pp.1076–1084. Available at: http://www.nature.com/doifinder/10.1038/jcbfm.2015.84.

Kety, S.S. & Schmidt, C.F., 1948. The nitrous oxide method for the quantitative determination of cerebral blood flow in man; theory, procedure and normal values. *The Journal of Clinical Investigation*, 27(4), pp.476–483.

Kobayashi, H. et al., 1982. Effect of age on beta-adrenergic receptors on cerebral microvessels. *Brain Research*, 244(2), pp.374–377.

Koller, A. & Toth, P., 2012. Contribution of Flow-Dependent Vasomotor Mechanisms to the Autoregulation of Cerebral Blood Flow. *Journal of Vascular Research*, 49, pp.375–389.

Kontos, H.A. et al., 1978. Responses of cerebral arteries and arterioles to acute hypotension and hypertension. *Am J Physiol*, 234, pp.H371–H383.

Kontos, H.A., Raper, A.J. & Patterson, J.L., 1977. Analysis of vasoactivity of local pH, PCO2 and bicarbonate on pial vessels. *Stroke*, 8(3), pp.358–360.

Kopincová, J., Púzserová, A. & Bernátová, I., 2011. Biochemical aspects of nitric oxide synthase feedback regulation by nitric oxide. *Interdisciplinary Toxicology*, 4(2), pp.63–

68. Available at: http://www.ncbi.nlm.nih.gov/pmc/articles/PMC3131676/.

Korkushko, O. V et al., 1991. Autonomic control of cardiac chronotropic function in man as a function of age: assessment by power spectral analysis of heart rate variability. *Journal of the Autonomic Nervous System*, 32(3), pp.191–198.

Kuzkaya, N. et al., 2003. Interactions of peroxynitrite, tetrahydrobiopterin, ascorbic acid, and thiols: Implications for uncoupling endothelial nitric-oxide synthase. *Journal of Biological Chemistry*, 278(25), pp.22546–22554.

Lakatta, E. G. and Levy, D., 2003. Arterial and Cardiac Aging: Major Shareholders in Cardiovascular Disease Enterprises: Part I: Aging Arteries: A "Set Up" for Vascular Disease. *Circulation*, 107(1), pp.139–146. Available at: http://circ.ahajournals.org/cgi/doi/10.1161/01.CIR.0000048892.83521.58.

Lartaud, I. et al., 1993. In vivo cerebrovascular reactivity in Wistar and Fischer 344 rat strains during aging. *Am J Physiol Heart Circ Physiol*, 264(3), p.H851 LP-H858. Available at: http://ajpheart.physiology.org/content/264/3/H851.abstract.

Lassen, N.A., 1959. Cerebral blood flow and oxygen consumption in man. *Physiol Revs*, 39(2), pp.183–238.

Lee, T.J., Shirasaki, Y. & Nickols, G.A., 1987. Altered endothelial modulation of vascular tone in aging and hypertension. *Blood Vessels*, 24(3), pp.132–136.

Leenders, K.L. et al., 1990. Cerebral blood flow, blood volume and oxygen utilization. Normal values and effect of age. *Brain: A Journal of Neurology*, 113.1, pp.27–47.

Leong, X.F., Ng, C.Y. & Jaarin, K., 2015. Animal Models in Cardiovascular Research: Hypertension and Atherosclerosis. *BioMed Research International*, 2015(ii).

Lincoln, J., 1995. Innervation of cerebral arteries by nerves containing 5-hydroxytryptamine and noradrenaline. *Pharmacology & Therapeutics*, 68(3), pp.473–501.

London, E.D. et al., 1981. Local cerebral glucose utilization during development and aging of the Fischer-344 rat. *Journal of Neurochemistry*, 37(1), pp.217–221.

Loutzenhiser, R. et al., 1990. H(+)-induced vasodilation of rat aorta is mediated by alterations in intracellular calcium sequestration. *Circ Res*, 67(2), pp.426–439. Available at: http://circres.ahajournals.org/cgi/doi/10.1161/01.RES.67.2.426.

Lucas, S.J.E. et al., 2010. Influence of Changes in Blood Pressure on Cerebral Perfusion and Oxygenation. *Hypertension*, 55, pp.698–705.

Luff, S.E. & McLachlan, E.M., 1989. Frequency of neuromuscular junctions on arteries of different dimensions in the rabbit, guinea pig and rat. *Blood Vessels*, 26(2), pp.95–106.

Luo, S. et al., 2014. Molecular mechanisms of endothelial NO synthase uncoupling. *Current Pharmaceutical Design*, 20(22), pp.3548–53. Available at: http://www.ncbi.nlm.nih.gov/pubmed/24180388.

Madsen, P.L. et al., 1993. Average Blood-Flow and Oxygen-Uptake in the Human Brain During Resting Wakefulness - a Critical-Appraisal of the Kety-Schmidt Technique. *J Cereb Blood Flow Metab*, 13(4), pp.646–655.

Markus, H.S., 1999. Transcranial Doppler ultrasound. *J Neurol Neurosurg Psychiatry*, 67, pp.135–137.

Matsuzaki, S. et al., 2009. Regulated Production of Free Radicals by the Mitochondrial Electron Transport Chain: Cardiac Ischemic Preconditioning. *Adv Drug Deliv Rev*, 61(14), pp.1324–1331.

Mayhan, W.G. et al., 2008. Age-Related Alterations in Reactivity of Cerebral Arterioles : Role of Oxidative Stress. *Microcirculation*, 15, pp.225–236.

Mayhan, W.G. et al., 1990. Effects of aging on responses of cerebral arterioles. *Am J Physiol*, 258(4 Pt 2), pp.H1138-43. Available at: http://www.ncbi.nlm.nih.gov/pubmed/2109940.

Mayhan, W.G. & Heistad, D.D., 1986. Role of veins and cerebral venous pressure in disruption of the blood-brain barrier. *Circ Res*, 59(2), pp.216–220.

McAdams, R.P. & Waterfall, J.F., 1986. The effect of age on the sensitivity of pre- and postsynaptic alpha-adrenoceptors to agonists and antagonists in the rat. *Naunyn-Schmiedeberg's Archives of Pharmacology*, 334(4), pp.430–435.

McCann, S.M. et al., 1998. The nitric oxide hypothesis of aging. *Experimental Gerontology*, 33(7–8), pp.813–826.

McGeer, E.G. et al., 1971. Aging and brain enzymes. *Experimental Gerontology*, 6(6), pp.391–396.

Mchedlishvili, G., 1980. Physiological mechanisms controlling cerebral blood flow. *Stroke*, 11(3), pp.240–248. Available at: http://stroke.ahajournals.org/cgi/doi/10.1161/01.STR.11.3.240 [Accessed May 6, 2014].

McLean, M.R., Goldberg, P.B. & Roberts, J., 1983. An ultrastructural study of the effects of age on sympathetic innervation and atrial tissue in the rat. *Journal of Molecular and Cellular Cardiology*, 15(2), pp.75–92.

Minami, Y. et al., 1994. Projections of nitric oxide synthase-containing fibers from the sphenopalatine ganglion to cerebral arteries in the rat. *Neuroscience*, 60(3), pp.745–759.

Mione, M.C. et al., 1988. An increase in the expression of neuropeptidergic vasodilator, but

not vasoconstrictor, cerebrovascular nerves in aging rats. *Brain Research*, 460, pp.103–113.

Modin, A., Weitzberg, E. & Lundberg, J.M., 1994. Nitric oxide regulates peptide release from parasympathetic nerves and vascular reactivity to vasoactive intestinal polypeptide in vivo. *Eur J Pharmacol*, 261(1–2), pp.185–197.

Mokri, B., 2001. The Monro-Kellie hypothesis: applications in CSF volume depletion. *Neurology*, 56(12), pp.1746–1748.

Montécot, C. et al., 1997. Nitric oxide of neuronal origin is involved in cerebral blood flow increase during seizures induced by kainate. *J Cereb Blood Flow Metab*, 17(1), pp.94–9.

Morita, Y., Hardebo, J.E. & Bouskela, E., 1995. Influence of cerebrovascular sympathetic, parasympathetic, and sensory nerves on autoregulation and spontaneous vasomotion. *Acta Physiologica Scandinavica*, 154(2), pp.121–130.

Muir, E.R. et al., 2014. Quantitative Cerebral Blood Flow Measurements Using MRI. *Methods Mol Biol.*, 1135, pp.205–211. Available at: http://link.springer.com/10.1007/978-1-4939-0320-7.

Mulvany, M.J. & Halpern, W., 1977. Contractile properties of small arterial resistance vessels in spontaneously hypertensive and normotensive rats. *Circ Res*, 41(1), pp.19–26.

Mutch, W.A.C., Malo, L.A. and Ringaert, K.R.A., 1989. Phenylephrine increases regional cerebral blood flow following hemorrhage during isoflurane-oxygen anesthesia. *Anesthesiology*, 70, pp.276–279.

Nagasawa, S. et al., 1979. Mechanical properties of human cerebral arteries. Part 1: Effects of age and vascular smooth muscle activation. *Surgical Neurology*, 12(4), pp.297–304.

Nagatsu, T. & Nagatsu, I., 2016. Tyrosine hydroxylase (TH), its cofactor tetrahydrobiopterin (BH4), other catecholamine-related enzymes, and their human genes in relation to the drug and gene therapies of Parkinson's disease (PD): historical overview and future prospects. *Journal of Neural Transmission*, 123(11), pp.1255–1278.

New, D.I. et al., 2003. Cerebral artery responses to pressure and flow in uremic hypertensive and spontaneously hypertensive rats. *Am J Physiol Heart Circ Physiol*, 284(4), pp.H1212–H1216.

Nielsen, K.C. & Owman, C., 1967. Adrenergic innervation of pial arteries related to the circle of Willis in the cat. *Brain Research*, 6(4), pp.773–6. Available at: http://www.ncbi.nlm.nih.gov/pubmed/6080228.

Nordberg, A., Alafuzoff, I. & Winblad, B., 1992. Nicotinic and muscarinic subtypes in the human brain: changes with aging and dementia. *Journal of Neuroscience Research*, 31(1), pp.103–111.

Numan, T. et al., 2014. Static autoregulation in humans: a review and reanalysis. *Medical Engineering & Physics*, 36(11), pp.1487–1495. Available at: http://dx.doi.org/10.1016/j.medengphy.2014.08.001.

O'Leary, D.H. et al., 1999. Carotid-Artery Intima and Media Thickness As a Risk Factor for Myocardial Infarction and Stroke in Older Adults. *New England Journal of Medicine*, 340, pp.14–22.

Ogawa, K. et al., 2001. Propofol Potentiates Phenylephrine-induced Contraction via Cyclooxygenase Inhibition in Pulmonary Artery Smooth Muscle. *Anesthesiology*, 94(5), pp.833–839.

Ogoh, S. et al., 2015. Blood flow in internal carotid and vertebral arteries during graded lower body negative pressure in humans. *Exp Physiol*, 100(3), pp.259–266. Available at: http://doi.wiley.com/10.1113/expphysiol.2014.083964.

Ogoh, S. et al., 2011. The effect of phenylephrine on arterial and venous cerebral blood flow in healthy subjects. *Clin Physiol Funct Imaging*, 31, pp.445–451.

Ohata, M. et al., 1981. Regional cerebral blood flow during development and ageing of the rat brain. *Brain*, 104(2), pp.319–32. Available at: http://www.ncbi.nlm.nih.gov/pubmed/7237097.

Okamura, T. et al., 2002. Pharmacology and Physiology of Perivascular Nerves Regulating Vascular Function: Neurogenic Cerebral Vasodilation Mediated by Nitric Oxide. *Japanese Journal of Physiology*, 38, pp.32–38.

Omar, N.M. & Marshall, J.M., 2010a. Age-related changes in carotid vascular responses to adenosine and nitric oxide in the rat: in vitro and in vivo studies. *J Appl Physiol*, 109, pp.305–313.

Omar, N.M. & Marshall, J.M., 2010b. Age-related changes in the sympathetic innervation of cerebral vessels and in carotid vascular responses to norepinephrine in the rat: in vitro and in vivo studies. *J Appl Physiol*, 109, pp.314–322.

Oudegeest-Sander, M.H. et al., 2014. Assessment of dynamic cerebral autoregulation and cerebrovascular CO2 reactivity in ageing by measurements of cerebral blood flow and cortical oxygenation. *Exp Physiol*, 99(3), pp.586–98.

Owen-Reece, H. et al., 1996. Use of near infrared spectroscopy to estimate cerebral blood flow in conscious and anaesthetized adult subjects. *British Journal of Anaesthesia*, 76(1),

pp.43–48.

Oxenham, H. & Sharpe, N., 2003. Cardiovascular aging and heart failure. *European Journal of Heart Failure*, 5(4), pp.427–434.

Pan, H.Y. et al., 1986. Decline in beta adrenergic receptor-mediated vascular relaxation with aging in man. *The Journal of Pharmacology and Experimental Therapeutics*, 239(3), pp.802–807.

Parashar, R. et al., 2016. Age related changes in autonomic functions. *Journal of Clinical and Diagnostic Research*, 10(3), pp.CC11-CC15.

Partanen, M. et al., 1985. Indices of neurotransmitter synthesis and release in aging sympathetic nervous system. *Neurobiology of Aging*, 6(3), pp.227–232.

Paterno, R., Faraci, F.M. & Heistad, D.D., 1994. Age-related changes in release of endothelium-derived relaxing factor from the carotid artery. *Stroke*, 25(12), pp.2452–2457.

Paternò, R., Heistad, D.D. & Faraci, F.M., 2000. Potassium channels modulate cerebral autoregulation during acute hypertension Potassium channels modulate cerebral autoregulation during acute hypertension. *Am J Physiol Heart Circ Physiol*, 278, pp.H2003–H2007.

Paulson, O.B., Strandgaard, S. & Edvinsson, L., 1990. Cerebral autoregulation. *Cerebrovascular and Brain Metabolism Reviews*, 2(2), pp.161–92. Available at: http://www.ncbi.nlm.nih.gov/pubmed/2201348.

Perry, B.G. et al., 2014. The effect of hypercapnia on static cerebral autoregulation. *Physiological Reports*, 2(6), pp.e12059–e12059. Available at:

http://www.ncbi.nlm.nih.gov/pubmed/24973333 [Accessed March 12, 2017].

Poller, U. et al., 1997. Age-dependent changes in cardiac muscarinic receptor function in healthy volunteers. *Journal of the American College of Cardiology*, 29(1), pp.187–193.

Poon, H.F. et al., 2004. Free Radicals: Key to Brain Aging and Heme Oxygenase as a Cellular Response to Oxidative Stress. *The Journals of Gerontology Series A: Biological Sciences and Medical Sciences*, 59(5), pp.M478–M493. Available at: http://biomedgerontology.oxfordjournals.org/content/59/5/M478.full#sec-23.

Purkayastha, S. et al., 2013. α1-Adrenergic receptor control of the cerebral vasculature in humans at rest and during exercise. *Experimental physiology*, 98(2), pp.451–61. Available at: http://www.ncbi.nlm.nih.gov/pubmed/23024369.

Pyke, K.E. & Tschakovsky, M.E., 2005. The relationship between shear stress and flow-mediated dilatation: implications for the assessment of endothelial function. *The Journal of physiology*, 568(Pt 2), pp.357–69. Available at: http://www.pubmedcentral.nih.gov/articlerender.fcgi?artid=1474741&tool=pmcentrez&rendertype=abstract.

Querido, J.S. et al., 2013. Dynamic cerebral autoregulation during and following acute hypoxia: role of carbon dioxide. *Journal of Applied Physiology*, 114(9), pp.1183–90. Available at: http://www.ncbi.nlm.nih.gov/pubmed/23471947.

Raichle, M. E. and Plum, F., 1972. Hyperventilation and Cerebral Blood Flow. *Stroke*, (3), pp.566–575.

Reese, T.S. & Karnovsky, M.J., 1967. Fine structural localizatin of blood-brain barrier to exogenous peroxidase. *J Cell Biol*, 34(20), pp.207–217.

Richer, C. et al., 1987. Systemic and regional hemodynamic characterization of alpha-1 and alpha-2 adrenoceptor agonists in pithed rats. *Journal of Pharmacology and Experimental Therapeutics*, 240(3), p.944 LP-953. Available at: http://jpet.aspetjournals.org/content/240/3/944.abstract.

Roach, M.R. & Burton, A.C., 1959. The effect of age on the elasticity of human iliac arteries. *Canadian journal of biochemistry and physiology*, 37(4), pp.557–570.

Robertson, A.D., Tessmer, C.F. & Hughson, R.L., 2010. Association between arterial stiffness and cerebrovascular resistance in the elderly. *J Hum Hypertens*, 24(3), pp.190–196. Available at: http://www.ncbi.nlm.nih.gov/pubmed/19571826%5Cnhttp://www.nature.com/jhh/journal/v24/n3/pdf/jhh200956a.pdf.

Ryzhavskii, B.Y. & Ivashkina, S.I., 1996. Relationship between litter size and the development of the rat brain during the suckling period. *Bulletin of Experimental Biology and Medicine*, 121(5), pp.526–528. Available at: http://dx.doi.org/10.1007/BF02446958.

Saba, H. et al., 1984. Reduction in noradrenergic perivascular nerve density in the left and right cerebral arteries of old rabbits. *Journal of Cerebral Blood Flow and Metabolism*, 4, pp.284–289.

Sadoshima, S., Fujii, K., Yao, H., Kusuda, K. Ibayashi, S. and Fujishima, M., 1986. Regional Cerebral Blood Flow Autoregulation in Normotensive and Spontaneously Hypertensive Rats: Effects of Sympathetic Denervation. *Stroke*, (17), pp.981–984.

Sadoshima, S. et al., 1985. Upper limit of cerebral autoregulation during development of hypertension in spontaneously hypertensive rats--effect of sympathetic denervation.

Stroke, 16(3), pp.477–481.

Saka, O., McGuire, a. & Wolfe, C., 2008. Cost of stroke in the United Kingdom. *Age and Ageing*, 38(1), pp.27–32. Available at: http://www.ageing.oxfordjournals.org/cgi/doi/10.1093/ageing/afn281.

Samsel, R.W. & Schumacker, P.T., 1988. Determination of the critical O2 delivery from experimental data: sensitivity to error. *J Appl Physiol*, 64(5), pp.2074–2082. Available at: http://jap.physiology.org/content/64/5/2074 [Accessed January 8, 2017].

Santhanam, A.V.R., D'Uscio, L.V. & Katusic, Z.S., 2014. Erythropoietin increases bioavailability of tetrahydrobiopterin and protects cerebral microvasculature against oxidative stress induced by eNOS uncoupling. *J Neurochem*, 131(4), pp.521–529.

Santhanam, L. et al., 2007. Inducible NO synthase-dependent S-nitrosylation and activation of arginase1 contribute to age-related endothelial dysfunction. *Circ Res*, 101, pp.692–702.

Santos, M.A.A. et al., 2013. Does the Aging Process Significantly Modify the Mean Heart Rate? *Arquivos Brasileiros de Cardiologia*, 101, pp.388–398. Available at: http://www.gnresearch.org/doi/10.5935/abc.20130188.

Sengupta, P., 2013. The Laboratory Rat: Relating Its Age With Human's. *International Journal of Preventive Medicine*, 4(6), pp.624–630. Available at: http://www.ncbi.nlm.nih.gov/pmc/articles/PMC3733029/.

Shaw, B.H. et al., 2015. Cardiovascular responses to orthostasis and their association with falls in older adults. *BMC Geriatrics*, 15(1), p.174. Available at: http://www.biomedcentral.com/1471-2318/15/174.

Shiba, K. et al., 2009. Sympathetic neural regulation of olfactory bulb blood flow in adult and

aged rats. *Autonomic Neuroscience: Basic and Clinical*, 147(1–2), pp.75–79.

Siles, E. et al., 2002. Age-related changes of the nitric oxide system in the rat brain. *Brain Research*, 956, pp.385–392. Available at: www.elsevier.com.

Singer, J.R. & Crooks, L.E., 1983. Nuclear magnetic resonance blood flow measurements in the human brain. *Science*, 221(4611), pp.654–656.

Smeda, J.S., VanVliet, B.N. & King, S.R., 1999. Stroke-prone spontaneously hypertensive rats lose their ability to auto-regulate cerebral blood flow prior to stroke. *Journal of Hypertension*, 17(12 Pt 1), pp.1697–1705.

Sorond, F.A. et al., 2010. Cerebrovascular hemodynamics, gait, and falls in an elderly population: MOBILIZE Boston Study. *Neurology*, 74(20), pp.1627–1633.

Springo, Z. et al., 2015. Aging impairs myogenic adaptation to pulsatile pressure in mouse cerebral arteries. *J Cereb Blood Flow Metab*, 35(4), pp.527–530. Available at: http://www.nature.com/doifinder/10.1038/jcbfm.2014.256.

Stewart, P.A. et al., 1987. Analysis of Blood-Brain Barrier in the Aging Human Ultrastructure. *Microvascular Research*, 282, pp.270–282.

Stout, R.W. et al., 2001. Transcutaneous blood gas monitoring in the rat. *Comparative Medicine*, 51(6), pp.524–33. Available at: http://www.ncbi.nlm.nih.gov/pubmed/21244487.

Strebel, S.P. et al., 1998. The Impact of Systemic Vasoconstrictors on the Cerebral Circulation of Anesthetized Patients. *Survey of Anesthesiology*, 43(2), p.79. Available at: http://www.mendeley.com/catalog/impact-systemic-vasoconstrictors-cerebral-circulation-anesthetized-patients/ [Accessed September 29, 2015].

Stromberg, C., Naveri, L. & Saavedra, J.M., 1993. Nonpeptide Angiotensin AT1 and AT2 Receptor Ligands Modulate the Upper Limit of Cerebral Blood Flow Autoregulation in Rats. *J Cereb Blood Flow Metab*, 13, pp.298–303.

Strosznajder, J.B. et al., 2004. Age-related alteration of activity and gene expression of endothelial nitric oxide synthase in different parts of the brain in rats. *Neurosci Lett*, 370(2–3), pp.175–179. Available at: http://www.ncbi.nlm.nih.gov/entrez/query.fcgi?cmd=Retrieve&db=PubMed&dopt=Citation&list_uids=15488318.

Taddei, S. et al., 1995. Aging and Endothelial Function in Normotensive Subjects and Patients With Essential Hypertension. *Circulation*, 91(7), p.1981 LP-1987. Available at: http://circ.ahajournals.org/content/91/7/1981.abstract.

Takei, H. et al., 1983. Cerebral blood flow and oxidative metabolism in conscious Fischer-344 rats of different ages. *Journal of Neurochemistry*, 40(3), pp.801–805.

Talman, W.T. & Dragon, D.N., 2002. Inhibiting the nucleus tractus solitarii extends cerebrovascular autoregulation during hypertension. *Brain Research*, 931, pp.92–95.

Talman, W.T. & Dragon, D.N., 1995. Inhibition of nitric oxide synthesis extends cerebrovascular autoregulation during hypertension. *Brain Research*, 672(1–2), pp.48–54. Available at: http://www.ncbi.nlm.nih.gov/pubmed/7749753.

Talman, W.T. & Dragon, D.N., 2000. Parasympathetic nerves influence cerebral blood flow during hypertension in rat. *Brain Research*, 873(1), pp.145–8. Available at: http://www.ncbi.nlm.nih.gov/pubmed/10915822.

Talman, W.T., Dragon, D.N. & Ohta, H., 1994. Baroreflexes influence autoregulation of

cerebral blood flow during hypertension. *Am J Physiol*, 267(3 Part 2), pp.H1183–H1189.

Tan, C.O., 2012. Defining the characteristic relationship between arterial pressure and cerebral flow. *J Appl Physiol (1985)*, 113(8), pp.1194–1200. Available at: http://www.ncbi.nlm.nih.gov/pubmed/22961266.

Tan, C.O., Hamner, J.W. & Taylor, J.A., 2013. The role of myogenic mechanisms in human cerebrovascular regulation. *J Physiol*, 20, pp.5095–5105.

Thomas, T. & Marshall, J.M., 1994. Interdependence of respiratory and cardiovascular changes induced by systemic hypoxia in the rat: the roles of adenosine. *J Physiol*, 480(3), pp.627–636.

Thompson, B.G. et al., 1996. Nitric oxide mediation of chemoregulation but not autoregulation of cerebral blood flow in primates. *Journal of Neurosurgery*, 84(1), pp.71–8. Available at: http://thejns.org/doi/abs/10.3171/jns.1996.84.1.0071 [Accessed December 12, 2016].

Tiecks, F.P. et al., 1995. Comparison of static and dynamic cerebral autoregulation measurements. *Stroke*, 26(6), pp.1014–1019.

Toda, N. et al., 2000. Cerebral vasodilatation induced by stimulation of the pterygopalatine ganglion and greater petrosal nerve in anesthetized monkeys. *Neuroscience*, 96(2), pp.393–398.

Toda, N., 1988. Hemolysate inhibits cerebral artery relaxation. *J Cereb Blood Flow Metab*, 8(1), pp.46–53. Available at: http://www.ncbi.nlm.nih.gov/entrez/query.fcgi?cmd=Retrieve&db=PubMed&dopt=Citation&list_uids=2448322.

Toda, N., Ayajiki, K. & Okamura, T., 2009. Cerebral blood flow regulation by nitric oxide: Recent advances. *Pharmacological Reviews*, 61(1), pp.62–97.

Toda, N., Ayajiki, K. & Okamura, T., 1993. Neural mechanism underlying basilar arterial constriction by intracisternal L-NNA in anesthetized dogs. *Am J Physiol*, 265(1 Pt 2), pp.H103-7. Available at: http://www.ncbi.nlm.nih.gov/entrez/query.fcgi?cmd=Retrieve&db=PubMed&dopt=Citation&list_uids=8342620.

Toda, N. & Okamura, T., 1990. Modification by L-NMMA of the response to nerve stimulation in isolated dog mesenteric and cerebral arteries. *Japanese Journal of Physiology*, (52), pp.170–173.

Topple, A., Fifkova, E. & Cullen-Dockstader, K., 1990. Effect of age on blood vessels and neurovascular appositions in the rat dentate fascia. *Neurobiology of Aging*, 11(4), pp.371–380.

Toth, P. et al., 2014. Resveratrol treatment rescues neurovascular coupling in aged mice: role of improved cerebromicrovascular endothelial function and downregulation of NADPH oxidase. *Am J Physiol Heart Circ Physiol*, 306(3), pp.H299-308. Available at: http://ajpheart.physiology.org/content/ajpheart/306/3/H299.full.pdf.

Toyoda, K. et al., 1997. Effect of aging on regulation of brain stem circulation during hypotension. *J Cereb Blood Flow Metab*, 17, pp.680–685.

Tsai, S.H. et al., 1985. Retrograde localization of the innervation of the middle cerebral artery with horseradish peroxidase in cats. *Neurosurgery*, 16(4), pp.463–467.

Tuor, U.I., 1992. Acute hypertension and sympathetic stimulation: local heterogeneous

changes in cerebral blood flow. *Am J Physiol Heart Circ Physiol*, 263(2). Available at: http://ajpheart.physiology.org/content/263/2/H511.long [Accessed April 4, 2017].

Uchida, S. et al., 1997. Effect of stimulation of nicotinic cholinergic receptors on cortical cerebral blood flow and changes in the effect during aging in anesthetized rats. *Neuroscience Letters*, 228(3), pp.203–206.

Uchida, S. et al., 2000. Effects of age on cholinergic vasodilation of cortical cerebral blood vessels in rats. *Neuroscience Letters*, 294(2), pp.109–112.

Venkataraman, K., Khurana, S. & Tai, T., 2013. Oxidative Stress in Aging-Matters of the Heart and Mind. *International Journal of Molecular Sciences*, 14(9), pp.17897–17925. Available at: http://www.mdpi.com/1422-0067/14/9/17897/.

Virmani, R. et al., 1991. Effect of aging on aortic morphology in populations with high and low prevalence of hypertension and atherosclerosis. Comparison between occidental and Chinese communities. *The American Journal of Pathology*, 139(5), pp.1119–29. Available at: http://www.pubmedcentral.nih.gov/articlerender.fcgi?artid=1886332&tool=pmcentrez&rendertype=abstract.

Wagner, B.P. et al., 2011. Rapid Assessment of Cerebral Autoregulation by Near-Infrared Spectroscopy and a Single Dose of Phenylephrine. *Pediatric Research*, 69(5), pp.436–441.

Warnert, E.A.H. et al., 2016. The major cerebral arteries proximal to the Circle of Willis contribute to cerebrovascular resistance in humans. *J Cereb Blood Flow Metab*, 36(8), pp.1384–1395.

Webb, R.C. & Inscho, E.W., 2005. Age-related changes in the cardiovascular system. In L. M. Prisant, ed. *Clinical Hypertension and Vascular Diseases: Hypertension in the Elderly*. Totowa, NJ: Humana Press Inc., pp. 11–21.

Weiss, B., Greenberg, L. & Cantor, E., 1979. Age-related alterations in the development of adrenergic denervation supersensitivity. In *Fed Proc*. pp. 1915–1921.

Werner-Felmayer, G., Golderer, G. & Werner, E.R., 2002. Tetrahydrobiopterin biosynthesis, utilization and pharmacological effects. *Current Drug Metabolism*, 3(2), pp.159–173.

Werner, C. et al., 2005. Sevoflurane Impairs Cerebral Blood Flow Autoregulation in Rats: Reversal by Nonselective Nitric Oxide Synthase Inhibition. *Anesthesia and Analgesia*, 101, pp.509–516.

White, R.P., Vallance, P. & Markus, H.S., 2000. Effect of inhibition of nitric oxide synthase on dynamic cerebral autoregulation in humans. *Clinical Science*, 99(6), pp.555–60. Available at: http://www.ncbi.nlm.nih.gov/pubmed/11099400.

Willie, C.K. et al., 2014. Integrative regulation of human brain blood flow. *J Physiol*, 592 (Pt 5), pp.841–59. Available at: http://www.pubmedcentral.nih.gov/articlerender.fcgi?artid=3948549&tool=pmcentrez&rendertype=abstract.

Willie, C.K. et al., 2012. Regional brain blood flow in man during acute changes in arterial blood gases. *J Physiol*, 590(Pt 14), pp.3261–75. Available at: http://www.pubmedcentral.nih.gov/articlerender.fcgi?artid=3459041&tool=pmcentrez&rendertype=abstract [Accessed May 6, 2014].

Yam, A.T. et al., 2005. Cerebral autoregulation and ageing. *Journal of Clinical Neuroscience*,

12(6), pp.643–646.

Yamada, K. & Nabeshima, T., 1998. Changes in NMDA receptor/nitric oxide signaling pathway in the brain with aging. *Microscopy Research and Technique*, 43(1), pp.68–74.

Yamada, M. et al., 2001. Cholinergic dilation of cerebral blood vessels is abolished in M(5) muscarinic acetylcholine receptor knockout mice. *Proc Natl Acad Sci USA*, 98(24), pp.14096–101. Available at: http://www.ncbi.nlm.nih.gov/pubmed/11707605%5Cnhttp://www.pubmedcentral.nih.gov/articlerender.fcgi?artid=PMC61174.

Yoshida, K. et al., 1993. Nitric oxide synthase-immunoreactive nerve fibers in dog cerebral and peripheral arteries. *Brain Research*, 629(1), pp.67–72.

Yoshida, K., Okamura, T. & Toda, N., 1994. Histological and functional studies on the nitroxidergic nerve innervating monkey cerebral, mesenteric and temporal arteries. *Jpn J Pharmacol*, 65(4), pp.351–359. Available at: http://www.ncbi.nlm.nih.gov/entrez/query.fcgi?cmd=Retrieve&db=PubMed&dopt=Citation&list_uids=7527469.

Zhang, R. et al., 2002. Autonomic Neural Control of Dynamic Cerebral Autoregulation in Humans. *Circulation*, 106, pp.1814–1820.

Zhang, R., Behbehani, K. & Levine, B.D., 2009. Dynamic pressure – flow relationship of the cerebral circulation during acute increase in arterial pressure. *J Physiol*, 11, pp.2567–2577.

Zhang, R. & Levine, B.D., 2007. Autonomic ganglionic blockade does not prevent reduction in cerebral blood flow velocity during orthostasis in humans. *Stroke*, (38), pp.1238–

1244.

Ziegler, M.G., Lake, C.R. & Kopin, I.J., 1976. Plasma noradrenaline increases with age. *Nature*, 261(5558), pp.333–335.